5-2003

Surface Interactions of Mercury on Gold Foil Electrodes in Electrodeposition and Stripping and ; An Investigation of Free Thiolate Ions from Metal-Thiolate Chalcogenides

Charles Martin Watson

SURFACE INTERACTIONS OF MERCURY ON GOLD FOIL ELECTRODES IN ELECTRODEPOSITION AND STRIPPING AND; AN INVESTIGATION OF FREE THIOLATE IONS FROM METAL–THIOLATE CHALCOGENIDES

By

Charles Martin Watson

B.S. Chemistry, Montana State University, 1990

(in Chemistry)

A THESIS

Submitted in Partial Fulfillment of the

Requirements for the Degree of

Doctor of Philosophy

(in Chemistry)

The Graduate School

The University of Maine

May, 2003

Advisory Committee:

Mitchell R.M. Bruce,	Associate Professor of Chemistry, Advisor
Alice E. Bruce,	Associate Professor of Chemistry
François G. Amar,	Associate Professor of Chemistry
Brian G. Frederick,	Assistant Professor of Chemistry
Touradj Solouki,	Assistant Professor of Chemistry
Daniel J. Dwyer,	Professor of Chemistry, Vice Provost for Research: New Mexico State University

LIBRARY RIGHTS STATEMENT

In presenting this thesis in partial fulfillment of the requirements for an advanced degree at The University of Maine, I agree that the Library shall make it freely available for inspection. I further agree that permission for "fair use" copying of this thesis for scholarly purposes may be granted by the Librarian. It is understood that any copying of publication of this thesis for financial gain shall not be allowed without my written permission.

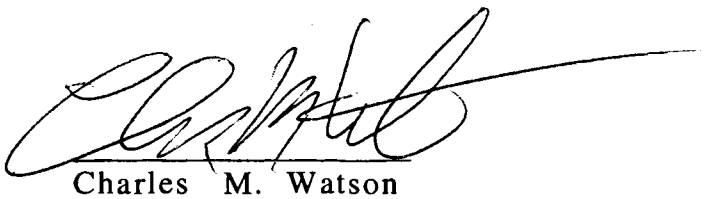

Charles M. Watson May 16, 2003

PART I: SURFACE INTERACTIONS OF MERCURY ON GOLD FOIL ELECTRODES IN ELECTRODEPOSITION AND STRIPPING
PART II: INVESTIGATION OF FREE THIOLATE IONS FROM METAL-THIOLATE CHALCOGENIDES

By Charles Martin Watson

Thesis Advisor: Dr. Mitchell R.M. Bruce

An Abstract of the Thesis Presented
In Partial Fulfillment of the Requirements for the
Degree of Doctor of Philosophy
(in Chemistry)
May, 2003

Mercury, a highly toxic metal, whose environmental concentration magnifies with ascension of the food chain, is monitored in our waters, food and air. Monitoring mercury is generally done by sample collection, transport to the laboratory; followed by: digestion of the sample, separation of the mercury and detection of the mercury: mostly by cold vapor atomic absorption or, cold vapor atomic fluorescence. These monitoring methods, preclude, routine, in-the-field mercury determination.

New analytical techniques have been proposed for in the field determination of mercury. They consist of mercury adsorption onto a sensor or electrode and measuring how much is there either as the adsorbate or, as the analate being removed from the detection device. Many employ gold as an accumulation substrate because of its affinity for mercury. One group of proposed techniques, requires that mercury be reduced electrochemically onto a gold electrode and then removed by anodic current oxidation. The determination of mercury is made from measurements of: the current, or the frequency shift of a surface acoustic wave due to the mass of the accumulated mercury.

Our research focused on the electrodepositon and stripping of mercury on gold foil electrodes. We demonstrated by x-ray photoelectron spectroscopy that electrodeposited mercury cannot be completely removed by electrochemical stripping and that with many repetitive deposition and stripping cycles, there is a progressive accumulation of mercury on the gold electrodes which continues to manifest even in mercury free electrolyte solution. The latter was demonstrated by linear sweep voltammetry and temperature programmed desorption of the accumulated mercury.

Mercury's toxicity is based on its formation of relatively non-polar complexes and its high affinity for thiol and sulfide functional groups (i.e. the amino acid cysteine). Our electrochemical and conductivity studies of nine metal-thiolate chalcogenides indicated that some form free thiolate ions at high concentrations rather than low ones.

DEDICATION

This Doctoral Thesis is dedicated to:

Armelle, Lucinda and Abbegael;

Mom, Chuck and John;

Dr. Craig

ACKNOWLEDGEMENTS

In completion of this Doctoral Program in Chemistry at The University of Maine, Charles M. Watson has several people to thank:

Dr. Mitchell R. M. Bruce for his effervescent enthusiasm for science and experimentation and his energy and drive to get it right.

Dr. Alice E. Bruce for her calmness and gentle guidance to the more productive path.

Dr. Daniel J. Dwyer for his unwavering support of the research and its exposition.

Dr. Brian G. Frederick for his willingness to join the project, late in the game, and his gentle leading through the simple modeling of the mercury gold surface amalgam.

Dr. François G. Amar for his steadfast participation in the thesis, especially thinking about possibility of forming solvated clusters of mercury during deposition.

Dr. Touradj Solouki for his active participation in the surface depth profiling and willingness to join the project in its final stages.

Dr. Jeffrey C. Andle and the Biode Corp. for their initiation and support of the first 2 years of the thesis work through their DOE Grant: DOE-FG02-94ER81717.

Mike Handley and Tiffany Lindstrom of the Water Research Institute for their assistance and permission to use their mercury analysis laboratory.

Dr. Robert J. Lad and Dr. David Frankel for their continued support of this project and their acceptance to have mercury experiments run at LASST.

Dr. Brian Green who made it possible for Charles to come to the University of Maine

Scott Delcourt and Dottie Poisson of the Graduate School for their positivity and flexibility in allowing Charles to come back and complete this thesis.

TABLE OF CONTENTS

Chapter

LIST OF FIGURES

LIST OF TABLES

CHAPTER I

The History, Toxicology, Biological Cycle and Determination of Mercury and Mercury Compounds

History

Mercury, one of the seven metals of antiquity,[♦] has been found in tombs dating back to 1500 and 1600 BC. Pliny, the Roman chronicler, outlined purification techniques by squeezing it through leather and also noted that it was poisonous. Mercury was widely used because of its ability to dissolve silver and gold (amalgamation) and was the basis of many plating technologies. Mercury's symbol is Hg from hydragyrum, liquid silver. Mercury is the only metal which is liquid at room temperature.[1]

Mercury rarely occurs as a mineral in nature. The chief ore is cinnabar (HgS). Spain and Italy produce about 50% of the world's supply of the metal. The metal is

[♦] The first six metals of antiquity and their dates of exploitation are: Gold (6000 BC), Copper (4200 BC), Silver (4000 BC), Lead (3500 BC), Tin (1750 BC), Iron (1500 BC).

obtained by heating cinnabar in a current of air and by condensing the vapor. In 315 B.C., Dioscorides mentions recovery of hydragyros by distillation, stating " An iron bowl containing cinnabar is put into an earthenware container and sealed with clay. It is then set on a fire and the soot which sticks to the cover is quicksilver". Methods changed little until the 18th century. In the ancient art of alchemy, mercury, sulfur, and salt were the Earth's three principle substances. The Hindu word for alchemy is "Rasasiddhi", meaning "knowledge of mercury." Believing that mercury was at the core of all metals, alchemists supposed that gold, silver, copper, tin, lead and iron were all mixtures of mercury and other substances. While alchemists in different cultures had different beliefs, one of the central themes to European alchemy was the belief that the correct combination of mercury and other ingredients would yield riches of gold.[1, 2]

The line between alchemy and medicine was not always clear. In 2nd century China, the study of mercury centered on a search for an elixir of life to confer longevity or immortality. The prominent Chinese alchemist Ko Hung, who lived in the 4th century, believed that man is what he eats, and so by eating gold he could attain perfection. Yet, he reasoned, a true believer was likely to be poor, and so it was necessary to find a substitute for the precious metal. This, in his estimation, could be accomplished by making gold from cinnabar. Ko Hung's other uses for cinnabar included smearing it on the feet to enable a person to walk on water, placing it over a doorway to ward off thieves, and combining it with raspberry juice to enable elderly men to beget children.[1, 3]

The felt hat industry has been traced to the mid-17th century in France, and it was probably introduced into England some time around 1830. Eventually the use of solutions

of mercuric nitrate was widespread in the felt industry, and mercury poisoning became endemic. Danbury, Connecticut, an important center of America's hat-making industry until men's hats went out of fashion in the 1960s, developed its own reputation for madness. Regionally, the "Danbury shakes" were a commonly recognized series of ailments. On December 1, 1941 the United States Public Health Service banned the use of mercury in the felt industry in this country. Although it has been suggested that the expression "mad as a hatter" and the character portrayed in Lewis Carroll's Alice in Wonderland may have origins other than mercurialism among hatters, few can resist making this apocryphal analogy.[1]

There are many metals more precious than mercury; but, there are none with greater allure and fascination. Mercury is both water and metal alike, wet but dry, fleeting yet heavy.[4] Mercury's charm certainly lies in seemingly uniqueness of its physical characteristics. Is there any other substance of old the could so captivate a child. As a metal, mercury is a rather poor conductor of heat, as compared and a fair conductor of electricity. The main uses for mercury in the United States are in chemical production (particularly chlorine/caustic manufacture), electrical and electronic components, dental amalgams and until the 1990's, in batteries and paints.[5] A significant portion of the developing world still uses mercury in the smelting of gold.[6] The U.S. consumption of mercury dropped from 1209 MT (metric tons) in 1989 to 346 MT in 1997 and worldwide production for the same time periods went from 7000 to 2900 MT.[5, 6]

Toxicology

Mercury was used as a medicine over 2000 years ago in India, China, and Asia Minor. In the Middle Ages, the medicinal use of mercury was widely accepted, particularly for the treatment of syphilis. In the eighteenth and nineteenth centuries, the application of mercury compounds expanded to being used as diuretic and in antiseptic agents. Mercury's toxicity from both medicinal uses and occupational causes have been recognized and described since the Middle Ages. The phrase "a night with Venus followed by a life with Mercury" described the toxic effects of mercury for the treatment of syphilis..[7] Of the many modern epidemics of mercury poisonings, the most notorious included: the Minamata disease, from methyl mercury released into the ocean from a chlor/alkali plant in Japan; acrodynia, from calomel teething powder;[8] erethism, in the hatting industry (the "mad hatter syndrome" from mercuric nitrate);[9] overdoses, from mercuric bichloride antiseptic and diuretic agents,[10] and toxicity, from methylmercury-treated grain seeds used for feed and flour in Iraq.[11] Despite all these epidemics, mercury exposures and toxicities persist.[12]

The various mercury compounds can be divided, by their pathophysiological characteristics, into three groups: elemental, inorganic (Hg(I) and Hg(II) species) and organic mercury compounds (considered Hg(0) by the medical literature). There are numerous sources for potential mercury exposures and some of these are listed in Table 1.1.

Table 1.1: Potential Sources of Mercury Exposure

Elemental	Inorganic	Organic
Batteries	Acetaldehyde production	Bactericides
Barometers, Thermometers	Cosmetics	Embalming processes
Coal Power Plants	Disinfectants	Seeds
Paints, Ceramics	Dyes	Fungicides
Chloralkali production	Explosives	Insecticide manufacturing
Dental amalgams	Fur processing, Taxidermy	Paper manufacturing
Electroplating	Herbal medicines	Seafoods
Fluorescent lights	Leather tanning	Seed dressing
Gold and silver extraction	Paints	Wood preservatives
Mining	Stool fixatives	
Waste incineration	Vinyl chloride production	
Paper pulp manufacturing		
Photography		
Traditional remedies		
Mercury vapor lamps		

Toxicokinetics:

The primary route of exposure to elemental mercury is through inhalation of the vapors. Despite its relatively low vapor pressure at room temperature (1.85 μTorr)[13], toxic air concentrations can be readily achieved in an enclosed environment (air saturation of 20 mg/m3)[♣] Elemental mercury is readily absorbed by the alveoli and passes in the blood to the various tissues. In the red blood cells and tissues, elemental mercury is mostly oxidized into inorganic mercury (Hg(II)) by catalase enzymes.[14] This

[♣] The recommended safety level of mercury are: Threshold Limit Value (TLV®) 0.05 mg/m3 from the American Conference of Governmental and Industrial Hygenists (ACGIH), Minimal Risk Level (MRL) of 0.2 μg/m3 for chronic exposure from the Agency for Toxic Substances and Disease Registry (ATSDR) and the Environmental Protection Agency (EPA) has set a limit of 2 parts of mercury per billion parts of drinking water (2 μg/L) and is recommending 144 parts of mercury per trillion parts of lake and stream water (144 ng/L). www.atsdr.cdc.gov/toxprofiles/phs46.html.

inorganic mercury, is extremely irritating to the gastrointestinal tract, and approximately 7–15% may be absorbed through the damaged mucosa. Inorganic mercury accumulates in the proximal renal tubules, where it predisposes to acute renal failure.[15] Inorganic mercury is primarily eliminated in the feces and the urine with an approximate half-life of 40–60 days. Organic mercury is readily absorbed from the gastrointestinal tract (up to 90–95 per cent). Long-chain alkyl mercury compounds are rapidly converted rapidly to the inorganic forms; whereas, the short-chain compounds like dimethyl and diethylmercury are stable and readily diffuse throughout all tissues, including the blood-brain barrier, directly causing CNS toxicity and congenital CNS toxicity from in utero exposure. Organic mercury compounds are eliminated in the feces after acetylation or conjugation in the liver with a half-life of 70 days.[8, 9]

Pathophysiology:

The pathophysiology of mercury toxicity is predominantly related to its covalent binding to thiol groups of different cellular enzymes interrupting cellular metabolism and function. Mercury also has an affinity to bind to carboxyl, amide, amine, and phosphoryl groups of enzymes, which contributes to its toxicity.[10] The most vulnerable organ is the central nervous system (CNS), but the renal system and the pulmonary system are also susceptible to the toxic effects of mercury. More specific mechanisms for CNS toxicity are postulated to include effects on calcium homeostasis, membrane functions, protein synthesis, phosphorylation/dephosphorylation, and the generation of free radicals.[16] Toxicities and clinical manifestations are related to a number of factors: the form of the mercury, the route, the concentration, and the duration of the exposure. These clinical manifestations are summarized in Table 1.2 below.

Table 1.2: Clinical Manifestations of Mercury Poisoning[17]

Organ System	Type of Mercury		
	Elemental	**Inorganic♦**	**Organic**
Neurologic	Tremor		Tremor
	Encephalopathy *		Encephalopathy
	Erethism (shyness, emotional lability, nervousness, insomnia, memory problems, inability to concentrate) Irritability, Hypotonia		Erethism
	Peripheral neuropathy, acrodynia		Paresthesias, Dysarthria
	Dysarthria		Ataxia, Tunnel vision, Hearing impairment, Spasticity,
			Congenital neuro encephalopathy: Mental retardation, Micrognathia, Microcephaly, Blindness, Chorea
Gastrointestinal		Vomiting, Hematemesis, Abdominal pain, Intestinal abscess, Proctitis/colitis	
Renal	Proteinuria	Acute failure	
Cardiopulmonary	Pneumonitis	Cardiovascular collapse	
Dermal	Allergic dermatitis, Cheilitis, Gingivitis, Stomatitis, Excessive salivation, Rash with desquamation of hands/feet		
Systemic	Diaphoresis, Fever,		
Immunologic	Splenomegaly		

♦ Chronic inorganic mercury toxicity is similar to chronic elemental mercury toxicity.
* Acute elemental mercury inhalation.

Elemental Mercury

The two organs most vulnerable to elemental mercury inhalation are the lungs and the brain; the blood-brain barrier is readily penetrated. Elemental mercury ingestion is considered benign because systemic absorption is unlikely.[9] The exceptions are in patients with intestinal problems such as diverticulosis, fistula formation, or obstruction, where mercury may be trapped or retained in the gastrointestinal tract for a prolonged period of time. This allows bacteria to convert the elemental form into organic mercury which can be systemically absorbed.[2, 18] Aspiration of elemental mercury, however, may cause a severe pneumonitis and even result in respiratory failure.[19] Subcutaneous injections (mercury thermometer accidents) of elementary mercury may also allow continuous absorption leading to chronic toxicity and possible sequestration in the lungs causing both acute and chronic toxicity.[20]

Acute toxicity from inhalation of concentrated mercury vapor can cause acute bronchitis, bronchiolitis, and pneumonitis. Clinical manifestations that may include: cough, fever and chills, dyspnea, metallic taste, and headaches. Severe cases may progress into hypoxia with respiratory failure, acute encephalopathy and seizures.[21] Metallic mercury aspiration,[13] subcutaneous or intravenous injections can lead to a severe pneumonitis and embolization of the pulmonary vasculature,[22] which may lead to hypoxia. With sufficient systemic absorption, acute renal toxicity manifested by proteinuria, nephrotic syndrome, and acute renal failure may occur.[9]

Prolonged or chronic exposure to mercury vapor manifest as the classic features of mercury toxicity: tremors (intentional fine tremors with coarse shakes), oral cavity lesions (gingivitis, stomatitis, cheilitis), rash, salivation, headaches, diaphoresis, and

erethism. Erethism is a constellation of signs and symptoms, including shyness, emotional lability, nervousness, insomnia, memory problems, and inability to concentrate. Peripheral sensorimotor neuropathy, dysarthria, and parkinsonian symptoms are frequently associated with chronic elementary mercury toxicity.[9]

Inorganic Mercury

Acute inorganic mercury ingestion should be considered extremely serious and potentially life-threatening. Previously, mercuric bichloride (tablets) was commonly used as a disinfectant and was readily available. Numerous fatalities were reported in suicidal ingestions.[5] Because of the corrosive effects of inorganic mercury, nausea and vomiting are almost universal in significant ingestions. Abdominal pain and hematemesis from esophageal and gastric erosions are common. Acute oliguric or anuric renal failure rapidly ensues in these patients. The renal dysfunction may manifest initially as proteinuria and nephrotic syndrome.[9] Shock with cardiovascular collapse is the primary cause of death.[5, 23]

Chronic ingestion of inorganic mercury will lead to signs and symptoms similar to those from chronic exposure to elemental mercury. These manifestations were documented in the hatting and furring industry, where the primary route of exposure was from the inhalation of mercuric nitrate used for the limping of furs.[3] Although the full spectrum of chronic inorganic toxicity is less commonly seen in the modern workplace, subclinical peripheral nerve conduction and neuropsychiatric abnormalities have been documented in workers.[24]

Acrodynia (pink disease), initially described in 1920, is characterized by pink, swollen hands and feet; desquamation; evanescent rashes; with burning, painful extremities in young children. Other symptoms included: photophobia, hypotonia, insomnia, and apathy alternating with irritability. During the 1930s and 40s, over 500 children died from pink disease in England and Wales as a result of using calomel teething powder.[2] Acrodynia has been rarely described in older children and adults. With the discontinuation of calomel teething powder, acrodynia is extremely uncommon now. There are occasional reports of acrodynia from other forms of mercury exposures, such as exposures to elemental mercury vapors and organic mercury (dermal absorption from diapers disinfected with phenyl mercury and respiratory absorption from phenyl mercuric acetate in latex paint).[3, 25]

Organic Mercury

The clinical toxicity from organic mercury differs depending on whether exposure was to short-chain or long-chain compounds. The long-chain compounds such as phenyl mercury and methoxyethylmercury cause toxicity similar to that seen in chronic inorganic mercury toxicity. The classic short-chain compounds include dimethylmercury, the etiologic agent for Minamata disease, and diethylmercury. The toxicity from short-chain organic mercury is limited to the CNS except at the highest doses.[9] The symptoms of organic mercury toxicity consist of tremor; ataxia; dysarthria; paresthesias of the hands, feet, and mouth; visual field constriction; erethism; and spasticity.[2, 8, 9, 26]

Prenatal methyl mercury exposure has much more diffuse and widespread effects than exposure in adults. First, dimethylmercury readily crosses the placenta and achieves a higher level in the cord blood than in the maternal circulation. Second,

dimethylmercury inhibits brain cell division and migration, perhaps related to its effects on the polymerization of microtubules.[27] Prenatal exposure to methyl mercury can result in severe congenital abnormalities such as micrognathia and neuroencephalopathy (microcephaly, mental retardation, blindness, and symmetric motor deficits).[23b]

Laboratory Analysis:

The laboratory evaluation of mercury toxicity should include a complete blood count, serum electrolytes, renal function tests, and urinalysis. Although only the renal function tests and urinalysis are expected to be abnormal in mercury toxicity (elevated creatinine and proteinuria), other laboratory studies may be helpful to differentiate other etiologies. For acute ingestion of inorganic mercury, blood type and cross should be performed because of potential gastrointestinal tract hemorrhage and perforation. Because mercury is radiopaque, appropriate radiographs can detect the recent ingestion of elemental mercury. A chest radiograph may demonstrate aspirated mercury, or mercury sequestered in the heart and lungs from intravenous mercury injection (perhaps resulting from an accident with a mercury thermometer). Soft-tissue radiographs can show mercury injected subcutaneously.[17a, c]

Blood and urine assays for mercury are used to detect mercury exposures. Both whole blood and 24-hour urine mercury levels can detect inorganic mercury and elemental mercury exposure. Whole blood assays can detect recent exposures. The 24-hour urine mercury concentration may reflect both recent exposure and continued renal elimination of tissue burden. A spot urine level test can be used for emergency evaluation, but a 24-hour urine collection should be arranged as soon as possible. Normal blood concentration is less than 10–20 μg/L and urine concentration is less than 20 μg/L;

however, the correlation between mercury levels and toxicity varies considerably. In general, a blood level greater than 35 μg/L or a urine level greater than 100 μg/L will necessitate therapy.[17] To monitor organic mercury exposure, whole blood analysis should be used because organic mercury is concentrated in the erythrocytes. Because mercury levels are not readily available, empirical therapy should be instituted in patients suspected to have significant acute exposure or symptoms of toxicity.[8]

Other types of diagnostic tests have been used to monitor mercury exposure, usually in occupational settings. Elevation of *N*-acetylglucosaminidase (NAG) and ß-galactosidase (lysosomal enzymes in the renal tubular cells) can be used as sensitive but nonspecific detectors for mercury toxicity in patients with chronic inorganic mercury exposure. X-ray fluorescence technique can detect mercury in the wrist and temporal bones. Hair analysis for mercury can detect past exposure but is not routinely used because of the potential for environmental contamination.[9]

Treatment:

The treatment for mercury toxicity (outlined in Table 1.3 below) depends on the type, duration and mode of exposure. Gastrointestinal decontamination should be implemented for recent acute inorganic and organic mercury ingestions, because of significant systemic absorption and potential toxicity. In patients with numerous vomiting episodes, the need for additional decontamination must be individualized, depending on the amount and the time of the ingestion and the symptoms. Despite the corrosiveness of inorganic mercury and the potential risk for perforation, the benefit of gastrointestinal decontamination still outweighs the risk. Lavage with a small orogastric or nasogastric tube using milk or egg white, sources of thiol groups, may be adequate for liquid or

powder forms of mercury. Whole bowel irrigation with polyethylene glycol should be considered for any significant mercury ingestion. The need for whole bowel irrigation and the duration and effectiveness of the procedure may be determined by examining abdominal radiographs for radiopaque material. For accidental elemental mercury ingestion, decontamination is not necessary because systemic absorption does not occur in normal gastrointestinal tracts. In patients with intestinal obstruction or ileus (nonmotile bowel), elemental mercury from ruptured Cantor tubes or similar devices should be removed by suction. Similarly, mercury injected subcutaneously should be removed surgically to prevent systemic absorption.[9, 17, 22]

The primary treatment involves chelation to remove mercury from the body. All chelating agents for mercury contain thiol groups, which bind mercury. Dimercaprol (BAL) and *d*-penicillamine have previously been the primary chelators, but the newer water-soluble BAL derivatives and meso-2,3-dimercaptosuccinic acid (DMSA) are more effective. BAL should be used in patients with renal dysfunction because approximately 50 per cent is excreted in the bile. However, BAL is not recommended for organic mercury toxicity because of animal studies demonstrating an increase in CNS mercury level due to redistribution by BAL.[28] Furthermore, DMSA is recommended for therapy in patients with normal renal function because it is a better chelator.[21, 29] In patients with renal failure, extracorporeal regional complexing hemodialysis has also effectively removed mercury. In cases of poisoning with inorganic and organic mercury, patients were hemodialyzed while DMSA was infused into the arterial line; effective removal of the DMSA-mercury complex was then achieved.[30]

Table 1.3: Treatment Essentials for Mercury Poisoning[9, 17, 21]

Decontamination	• Lavage early (within 2 hr) for ingestion of inorganic and organic mercury with milk or egg white added to the lavage fluid • Whole bowel irrigation when mercury is identifiable in the abdominal radiograph
Chelation	Initiate on history of acute exposure, do not wait for pending levels.
1. *Initial therapy*	Meso-2,3-dimercaptosuccinic acid (DMSA) for all forms of mercury toxicity 10 mg/kg/dose, tid po for 5 days, then bid for 14 days (2 week hiatus recommended for repeated cycles)
or	• BAL for inorganic and elemental mercury toxicity * 3–5 mg/kg intermuscularly (IM), every 4 hours for 2 days, then 2.5–3 mg/kg IM every 6 hours for 2 days, then 2.5–3 mg/kg IM every 12 hours for 1–3 days • Consider switching to an oral agent (DMSA or *d*-penicillamine) when more prolonged therapy is required
2. *Alternative therapy:*	• *d*-Penicillamine† for inorganic and elemental mercury toxicity *adults:* 250 mg orally four times a day for 1–2 weeks; *children:* 20–30 mg/kg/day (1000 mg maximum) in 4 equally divided doses for 1–2 weeks. •repeat course of treatment should be separated by 3–5 days (adults and children).
End point for chelation should be guided by symptoms and mercury levels, e.g., stop chelation when urine mercury level measured 1 week after chelation remains in the normal range, less than 20 μg/L	

* Ineffective against organic mercury toxicity; may increase the CNS mercury levels.
† *d*-Penicillamine is contraindicated in renal failure because elimination is exclusively via the kidneys.

Biocycle

Mercury exists in many different physical and chemical forms in the environment. It is the interconversions between these species that mediate its distribution patterns and biogeochemical cycling. The atmosphere is considered the dominant pathway for the delivery of inorganic Hg to aquatic ecosystems.[31] In the atmosphere, mercury exists predominantly as gaseous elemental mercury Hg(0) and as Hg(II) adsorbed onto particulate surfaces(Hg_p) or as reactive gas $Hg(II)_g$. Gaseous Hg(0) comprises 97-99% of the total mercury found in the atmosphere and has a residence time on the order of 1 year.[31, 32] The remaining 1-3% is comprised of Hg(II) and Hg_p, with residence times on the order of days to weeks.[32] The atmospheric oxidation of Hg(0) to Hg(II) is thought to principally to occur via ozone.[33] Other atmospheric oxidizers playing a role are: HClO, HSO_3 and $OH^{\bullet}$.[34] Some of the atmospheric Hg(II) is reduced back to Hg(0) by SO_3, or photoreduction of $Hg(OH)_2$.[34a] These various species of mercury in the atmosphere originate from natural processes (25-30%) and anthropogenic activities (60-75%).[31b]

Natural or background sources of atmospheric mercury, mainly as Hg(0), include emissions from volcanoes, soils, vegetation, and the ocean. Estimates of the pre-industrial (pre 1850) mercury flux is 8 Mmol a year.[31b] These estimates are based on mercury concentrations in Antartic ice core samples and the current models of environmental mercury cycling. The modern total environmental mercury flux is 25 Mmol per year. The pre-industrial and modern global mercury cycling are depicted in figures 1.1 and 1.2, respectively. The chemistry of the interconversion between the various mercury species in both air and water will be discussed later.

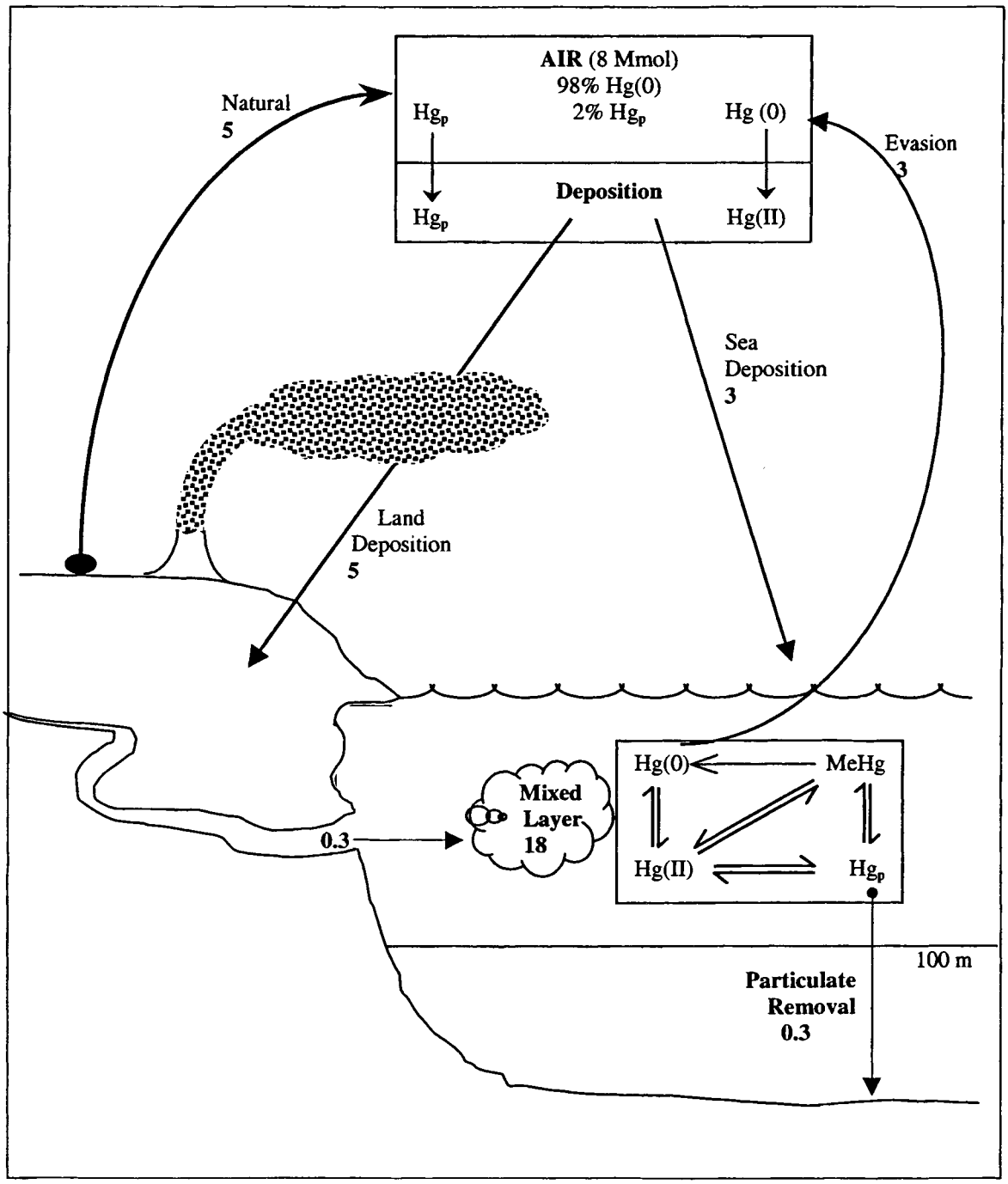

Figure 1.1: Yearly pre-industrial global mercury flux: numbers are in Mmol Hg.[31b]

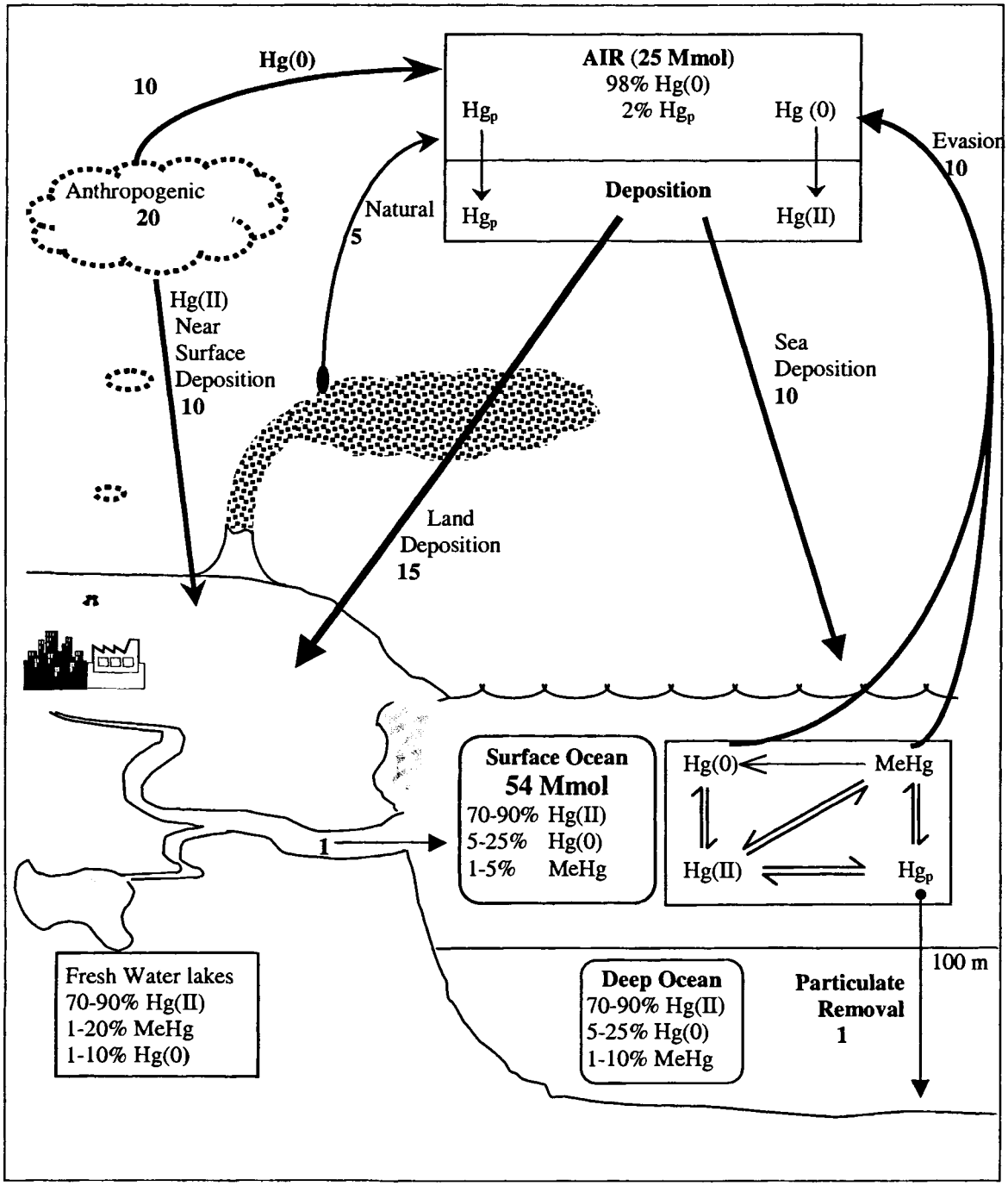

Figure 1.2: Yearly global mercury flux: numbers are in Mmol Hg.[31b, 35]

As depicted in figures 1.1 and 1.2, most of the mercury coming out of the atmosphere is in the form of dissolved Hg(II). The other significant pathway is the deposition of mercury adsorbed onto aerosols, this constitutes most of the "near surface Hg(II) deposition".[31b, 35] The atmospheric elemental mercury Hg(0) can travel 10,000 km, remain suspended in the air for a year or more and is not a significant portion of the mercury returning to earth.[32, 34b, 36] The mercury in the ocean surfaces continually undergoes oxidation and reduction. Both elemental and dimethylmercury diffuse out of the oceans and lakes. The solubility of mercury in water is very low and natural waters tend to be supersaturated with mercury as compared to the air above them.[37] This supersaturation is highest in the summer months when the photoreduction of Hg(II) to Hg(0) is at its highest.[38] Within the water systems mercury is found in many different forms. These water systems can be divided into surface (oxic), deep (anoxic) and the sediment layers. Figure 1.3 depicts the mercury speciation and bioaccumulation pathways for natural "uncontaminated" water. The partitioning of mercury between dissolved, colloidal and particulate varies widely spatially, seasonally and with the depth of the water column. Much of this variation depends upon on phytoplankton and bacteria.[39] The principal inorganic aqueous mercury species are: elemental mercury Hg(0), which is volatile but considered unreactive; Hg(II) bound to dissolved organic carbon (humic acids); $HgCl^+$, $HgCl_2$, $Hg(OH)_2$; HgClOH. The principal organic species are: MeHgCl, MeHgOH, Me_2Hg, Et_2Hg. In the deep anoxic waters the complexation is believed to be dominated by sulfide and bisulfide compounds. The principal compounds are humic Hg(II), HgS_2H, $Hg(SH)_2$ and MeHg as either the chloride in seawater or hydroxide in freshwater.[39a, 40] It is felt that much of the mercury in sediment is HgS.

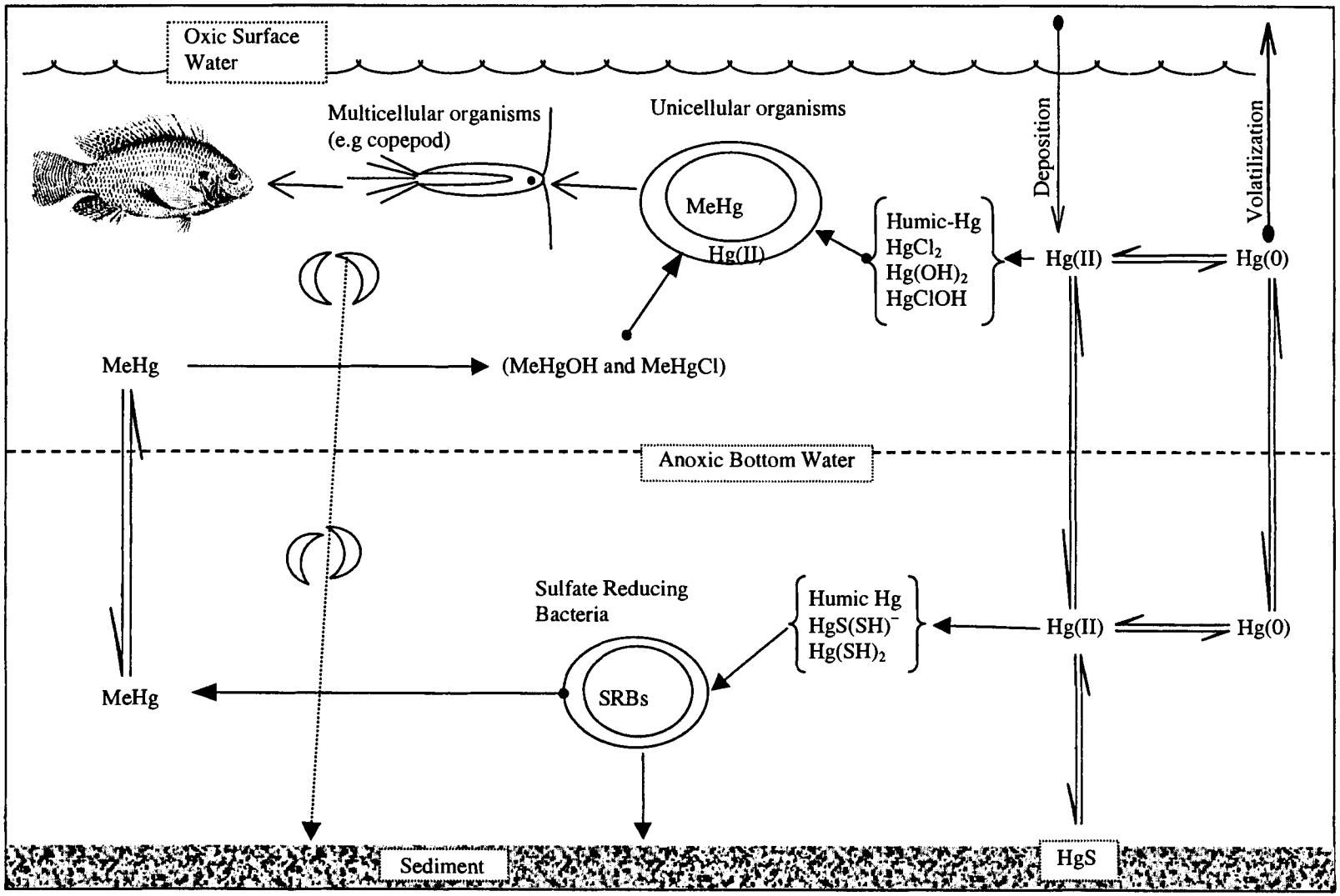

Figure 1.3: Aquatic cycle of mercury in natural waters.[38, 41]

To be methylated by sulfate-reducing bacteria, or to enter the aquatic food chain, mercury must be first transported across the lipid cell membrane. Most metals enter cells by leaking through the membrane transporter proteins of other physiologic ions. However, mercury, except for at high concentrations, appears to diffuse through the cell membrane. Mercury compounds are able to do this because they are relatively non-polar. Lipid solubility is generally quantified by the octanol-water partition coefficient (K_{OW}), which correlates a compound's relative solubility in these two solvents. Very hydrophillic compounds are near zero and very hydrophobic compounds up to several million.[42] Mercuric Chloride has a K_{OW} of 3.3 and diffuses readily across cell membranes; whereas $Hg(OH)_2$ has a K_{OW} of 0.5 and diffused much more slowly across cell membranes. It has been widely theorized that sulfate-reducing bacteria are responsible for the bulk of mercury methylation that occurs in natural waters.[43] This has recently been backed up with laboratory studies where the bacteria *Desulfovibrio Desulfricans* produces large quantities of methylmercury.[44]

Many trace metals are efficiently accumulated in planktonic bacteria and microalgae; but, most are not biomagnified. An understanding of mercury's bioaccumulation can be had by the comparison of Hg(0), Hg(II) and Me_2Hg with MeHg. The first three are not biomagnified; whereas the latter is.[45] Hg(0) and Me_2Hg are not bioaccumulated because they are non-reactive and they diffuse out of bacterial cells as easily as they diffused in. This does not hold true for

higher order organisms where it has been shown that Hg(0) is oxidized by catalase and H_2O_2 in red blood cells and in the brain; but, this is much further up the food chain.[46] The difference between Hg(II), chiefly as $HgCl_2$, and MgHgCl is more subtle. Both have similar diffusion rates across the cell membranes and both are reactive with cellular components; however, Hg(II) binds to cell membrane proteins and MeHgCl becomes associated with cellular components within the cell.[45] Laboratory studies showed that the transfer of MeHgCl from marine diatoms to a copepod was four times greater than for Hg(II).[45a] The copepod ingests the diatoms and consume the soluble cytoplasm and discard the insoluble membrane. Thus the accumulation and magnification of MeHg begins. In higher organisms (fish) MeHgCl is assimilated from the intestine more readily than Hg(II).[47] The results of the preference of MeHgCl over Hg(II) is that the average percentage of total mercury that is MeHg goes from 10% in the water column, 15% in phytoplankton, 30% in zooplankton and 95% in fish.[45b]

Determination of Environmental Mercury

The toxicity, global circulation and bioaccumulation of mercury and mercury compounds necessitate that analytical methods for the detection and monitoring of environmental mercury be developed. In consideration of federal requirements and recommendations for safe drinking water levels and natural water sources, mercury detection methods for environmental samples be capable of detecting mercury at part per billion (ppb: μg/L, ng/g) and part per trillion (ppt: ng/L, pg/g) concentrations. Research has shown that in aquatic environments where mercury concentrations are low or sub ppt levels, the mercury concentration in fish ranges from 0.5 to 2 parts per million (ppm). Most of this mercury is methylmercury.[48] There are a myriad of analytical techniques for determining mercury concentrations in water, soil, air and biological samples. A comparison of these and procedures is given below in Tables 1.5 and 1.6.

Most of the analytical techniques for determining mercury levels, in environmental samples, follow the same roadmap: sample preparation, separation of mercury from the sample and mercury detection. Along with determining the total mercury concentration for various environmental sources, it is desirable to determine whether the mercury is in the elemental, inorganic (usually Hg(II) species) or organic form (usually dimethylmercury or methylmercury chloride). Table 1.4 gives a description of the various analytical techniques and procedures that are used in the determination of environmental mercury.

Table 1.4a: Analytical Procedures for Mercury Detection: Sample Preparation

Technique	Explanation
Homogenization (Hom.)	Grinding and or blending of solid samples to prepare them for chemical extraction procedures. Care must be taken not to loose volatile Hg(0) species.
Digestion (Dig.)	Chemical digestion of biological materials to allow for the mercury to be accessed for chemical manipulation and detection. Examples: • 1:2.5 (v/v) H_2SO_4 97%, HNO_3 71% at 90°C (total Hg) • saturated KOH/MeOH extraction (organomercurials)[49] • microwave heating of the acid solution[50]
Oxidation (Ox.)	Chemical process of oxidizing all mercury species to Hg(II) to prevent evaporation and allow for chemical reduction to a single species for extraction and detection. Examples: • 0.5 % KBr/$KBRO_3$/HCL [51](EPA standard reagent)[52] • Hot H_2SO_4 / HNO_3 will both destroy organic matter and oxidize Hg(0) to Hg(II).
Reduction (Red.)	Reduction Hg(II) from the oxidation step to Hg(0) usually with $NaBH_4$ or $SnCl_2$. Often hydroxylamine (NH_2OH) is used first to quench the oxidizing agent.[54]
Derivatization (Der)	Chemically altering the mercury compounds to facilitate speciation. Generally adding an alkyl group to Hg(II) and Hg(I) species. Source for incomplete mercury detection, since unreacted mercury will not be detected. Examples: • $NaHEt_4$ at pH 4.5[53] $HgCl_2 + 2\ NaHEt_4 \rightarrow Et_2Hg$ $MeHgCl + NaHEt_4 \rightarrow MeHgEt$

Table 1.4b: Analytical Techniques for Mercury Detection: Mercury Separation

Technique	Explanation
Amalgamation (Am)	Process for collecting and concentrating Hg(0) from gas purging stream. Gold is most common material as a wire gauze, plate, film or coated onto beads or sand. Also used are Ag, Pt, Pt/Au and Pd. Mercury is desorbed by heating.[54]
Carbotrap (Cbt)	Graphitized carbon black column that absorbs gas phase mercury species which are then thermally desorbed.
Column Chromatography (CC)	Liquid chromatography to separate organic mercury species after the sample preparation phase.[55]
Cryogenic Packed Column (CryPC)	A GC column is immersed in liquid nitrogen to trap and concentrate volatilized mercury species which are then separated upon warming.[49b]
Extraction (Ext)	Laboratory of solvent extraction sometimes two step process. Examples: • CCl_4 solvent extraction (for Me_2Hg from digested sample)[56] • (Benzene or toluene) / cysteine solvent extraction (for Me_2Hg and MeHgCl from digested sample)[57]
Gas Chromatography (GC)	For separation of organic mercury compounds after derivatization.[55b]
High Pressure Liquid Chromatography (HPLC)	For separation of organic mercurials in normal phase with removal of organomercury halides in reverse phase mode.[56, 58]
Purge	Process of bubbling a gas through a sample solution, after digestion to remove volatile mercury compounds.

Table 1.4c: Analytical Techniques for Mercury Detection: Mercury Detection

Technique	Explanation
Anodic Stripping Voltammetry (ASV)	Potential applied to an electrode causing the oxidation of the mercury from the surface as Hg(II). Also called Potentiometric Stripping Voltammetry. The anodic current is plotted vs. the applied potential. There can be various wave forms for the voltage steps (e.g. DPASV, SWASV, LSV).
Atomic Absorption (AA)	The absorption of at 253.7 nm, Hg(0) in a noble gas atmosphere, is measured in a traditional flame atomic absorption spectrometer.[59] Problems of water droplet contamination have been noted.[60]
Bioluminescence (BL)	Gentically engineered *Escherichia Coli* grown on agar plates can detect the bioavailability of Hg(II) laden materials by inducing the expression of Luciferase. The light emission intensity corresponds to the Hg(II) concentration.[61]
Cold Vapor Atomic Absorption (CVAA)	Hg(0) species are purged in noble gas stream and the absorption at 253.7 nm is measured.[62] Water and organic vapors can interfere with absorption.[60]
Cold Vapor Atomic Fluorescence (CVAF)	Hg(0) in a noble gas stream is irradiated at 253.7 nm and the fluorescence at the same wavelength is measured, improving detection limits over AA techniques. This is the detection method of choice by the EPA.[52]
Constant Current Stripping Voltammetry (CCSV)	A potential is applied to the working electrode such that the anodic current remains at a fixed value. A plot of potential vs. time is made. There is improved resolution of anodic stripping peaks compared to ASV techniques. [63]
Enzymtic Inhibition (EI)	Mercury inhibition of enzymatic activity is measured as the chemical activity of end products. [64]
Inductively Coupled Plasma Atomic Emission Spectroscopy (ICP-AES)	An Ar plasma ionizes Hg(0), in He gas stream, to Hg^+ and the spectral emission at 194.227 nm, is measured. This emission has fewer absorbance interferences from water vapor and other gasses. [65]

Table 1.4c cont.: Analytical Techniques for Mercury Detection: Mercury Detection

Technique	Explanation
Inductively Coupled Plasma Atomic Emission Spectroscopy (ICP-AES)	An Ar plasma ionizes Hg(0), in He gas stream, to Hg^+ and this is analyzed in a mass spectrometer. Preconcentration improves detection limits as or 30% of Hg(0) is ionized.[54b]
Ion Selective Electrode (ISE)	A solid state electolyte Ag8Hg2S2I6 detects mercury in Flow Injection Analysis procedures.[66]
Optochemical Sensing (OCS)	Organomercury complexation reactions induce color change in organic dyes. Examples • 2-(5-amino-3, 4-dicyano-2H-pyrol-2-ylidene)-1,1,2-tricyanoethanide changes from violet to blue.[67]
Piezoresonance (Pzr)	Coated (usually gold) piezoelectric crystals have a resonance frequency that is changes proportionally to adsorbed mass.[68]
Pneumoamperometric Oxidation (PAO)	Hg(0) in solution is volatilized through a gas permeable gold electrode held at an oxidizing potential where the peak current is proportional to the solution concentrion.[69]
Potentiometric Stripping Voltammetry (PSV)	See Anodic Stripping Voltammetry
Radiochemical Neutron Activation (RNA)	Samples are irradiated in a thermal neutron flux and after a period of decay gamma ray emission at 77.4 keV (197 Hg) and 279.2 keV 9203 Hg) can be measured. Se peak correction must be made for the 279.2 keV peak.[70]
Surface Acoustic Wave (SAW)	The resonance frequency of a SAW varies as a function of mercury interaction with the surface, either as a mass effect of a change in the nature of the solution. [64b, 68b,c, 71]
Thin Film Conductivity (TFD)	The adsorption and subsequent amalgamation of Hg(0) on gold increases the electrical resistance of a thin gold film.[72]
Thin Film Reflectivity (TFR)	An optically thin layer of gold is vapor deposited on the end of an optical fiber. The amount of return reflectance is measured as a function of Hg(0) vapor concentration.[73]

Each analytical method reported in the literature has its own merits and drawbacks. No one technique is the best for every situation. Appropriate comparison parameters for the analytical methods are: detection limits, reliability (precision and accuracy), complexity, cost, and possible interferences. Detection limits are usually reported as 3 times the standard deviation of concentration measurements or have also been reported as the lowest detection limit from known concentrations. The reliability factor comes in the measurement of certified standards. Complexity of the procedure is quite subjective; but, one has to consider the number of different steps, material transfers etc. Each step has the potential for losing part of the analyte sample. The cost is rarely reported; but, can be inferred from the type of equipment used. Possible interferences are usually looked at after a particular analytical technique has been proven to be reliable on simple solutions. Interferences can be other analates that may inhibit the measurements or environmental factors (e.g. chloride ion concentration, dissolved organic matter, water vapor) that impede of alter the measurement. Rarely are all facets of the analytical technique completely delineated in the literature reports.

The mercury detection modalities fall into two main categories: the determination of total mercury in a sample or, distinguishing between the types of mercury compounds present. The latter can vary from the determination of all inorganic vs. all other mercury species to the total speciation of all the major mercury compound groups. These groups being: elemental mercury, Hg(0); pure inorganic mercury, Hg(II); mixed alkyl mercurous compounds, RHgX (e.g. MeHgCl); and organomercury compounds, RHgR′ (e.g. Me_2Hg: usually in nature R = R′ = Me). Table 1.5 lists a representative sample of analytical techniques that were developed to detect total mercury and Table 1.6 lists techniques that

distinguish between different classes or mercury compounds. It should also be remembered, that these different mercury compounds are found in a variety of environmental sources from: plant and animal species, sediments, water systems, the atmosphere, industrial wastes, etc.

Total Mercury:

For most "in the laboratory" analytical techniques, the determination of total mercury generally requires sample digestion to liberate mercury within the sample matrix, allowing for separation and or chemical modification. This is followed by chemical oxidation to completely transform all mercury species to Hg(II): example given as Equation 1.1. Equation 1.2 is an example of the follow-up step which is the reduction of the Hg(II) to Hg(0): usually with stannous chloride (Sn(II)) in an acid environment. The Hg(0) is then purged from the sample solution, with nitrogen, argon or air, and either collected and analyzed, or simply analyzed.

$$R_2Hg \,/\, RHgX \,/\, Hg(I) \xrightarrow[\text{oxidation}]{} Hg(II) \qquad (1.1)$$

$$Hg(II) + Sn(II) \xrightarrow[3\%\ HCL]{} Hg(0) + Sn(IV) \qquad (1.2)$$

The "in the field" techniques for determining total mercury (most data taken in the laboratory) are for the most part electrochemical techniques, where mercury is reduced onto an electrode and measured by any one of the electrochemical stripping procedures featured in Table 1.4c. Other methods for on site determination of total mercury are also found in Table 1.5. Gas phase mercury detection usually involves adsorption of mercury onto a gold surface followed by thermal desorption with pyrolysis and detection by atomic absorption of atomic fluorescence techniques. A sampling of these techniques and others are also found in Table 1.5.

Table 1.5: Analytical Methods for Determining Total Mercury			
Sample Preparation	**Mercury Separation**	**Detection (Limit)**	**Comments**
Samp: rock, metal, soil Dig.: Hom. → H_2SO_4 / HNO_3 90 °C Red.: NH_2OH → $SnCl_2$	Sep.: Air purge Conc.:none	CVAA (1 ng/g)	Pub: 1968 Ref [74] • One of first to use CVAA
Samp: urine Dig.: none Red.: $NaBH_4$	Sep.: air purge Conc.: none	ETAA (1-2 ng/mL)	Pub: 1975 Ref. [75]
Samp: water, waste water Dig.: none Red.: $NaBH_4$ (in the field)	Sep.: air purge Conc.: Au	He de plasma emission (0.5 ng/L)	Pub: 1980 Ref. [76] • Hg separation and concentration done onsite.
Samp: water, waste water Dig.: none Red.: $NaBH_4$	Sep.: air purge Conc.: Au (in the field)	CVAA (1.0 ng/g)	Pub: 1988 Ref. [77]
Samp: fish Dig.: hot conc. H_2SO_4/HNO_3 Ox..: 0.2 M $KBr/KBrO_3/HCl$ Red.: Sn(II)	Sep.: He purge Conc.: Au	CVAF (1.0 ng/g)	Pub: 1989 Ref. [78] • First use of CVAF, improved detection limits
Samp: fresh water, urine Dig./ Ox.: microwave 90°C, $KBr/KBrO_3/HCl$ Red.: $NaBH_4$	Sep.: Ar purge Conc.: Au	CVAA (10 ng/L)	Pub: 1992 Ref. [50]
Samp: seawater, sediments, sewage Dig.: hot conc. H_2SO_4/HNO_3 Ox.: 0.2 M $KBr/KBrO_3/HCl$ Red.: NH_2OH → Sn(II)	Sep.: N_2 purge Conc.: Au	CVAA (0.1 ng/L)	Pub: 1983 Ref. [51]

Table 1.5 cont.: Analytical Methods for Determining Total Mercury			
Sample Preparation	**Mercury Separation**	**Detection (Limit)**	**Comments**
Samp: freash water Dig.: H_2SO_4/HNO_3 60 °C Ox.: $KMnO_4/K_2S_2O_8$ Red.: $NH_2OH \rightarrow Sn(II)$	Sep.: N_2 purge Conc.: Au	CVAA (20 ng/L)	Pub: 1989 Ref. [79]
Samp: fresh water Dig.: none Red.: Sn(II)/HCl Ox.: 0.16M $HNO_3/KmnO_4$	Sep.: air purge after Sn(II) reductions Conc.: none	CVAA (1 ng/L)	Pub: 1975 Ref. [80] • Selective reduction of Hg(II) and RHgX with Sn(II) with air purge to remove Hg(0), remaing sample to
Samp: seawater, fresh water Dig.: none Red.: Sn(II)/ HCl	Sep.: N_2 purge Conc.: Au	CVAA (42 ng/L)	Pub: 1981 Ref. [81] • Selective reduction of Hg(II) and RHgX with Sn(II) with air purge, remaing sample to determing R_2Hg.
Samp: water, biological solids Dig: water none, acid heating Ox: BrCl Red: Sn(II)	Sep.: N2 purge Conc: gold sand	CVAFS, reverse flow (70 pg/L, water) (1 ng/g, solids)	Pub: 1994 Ref.[82] • Blanks for DL from repetitive sample purge • 1% Hg retention after >100 pg
Samp: water Dig: acid heating Ox: BrCl Red: Sn(II)	Sep.: N2 purge Conc: gold gauze	AAS (2 ng/L)	Pub: 1993 Ref.[84] • Au amalgamation increased sensitivity 200% • DW blank registered 2 ng/L (considered LOD), carryover not ruled
Samp: laboratory Hg(II) Dig: none Ox: none Red: Sn(II)	Sep.: Ar purge Conc: AuPt gauze	ICP-AES (0.76 ng/L)	Pub: 1997 Ref.[85] ICP-AES uses spectral line free at 194.227 nm that is free from absorption by organic and water vapors or contamination from

Table 1.5 cont.: Analytical Methods for Determining Total Mercury			
Sample Preparation	**Mercury Separation**	**Detection (Limit)**	**Comments**
Samp: laboratory Hg(II) Dig: none, Ox: none Red: Electrochemical on Au Red.: $NH_2OH \rightarrow Sn(II)$	Sep.: none Conc: direct Au amalgamation	DPASV (20 pg/L)	Pub: 1976 Ref.[87] • Low detection limits based on linear deposition time plots vs. Hg(II) concentration. • No competing metal ions studied
Samp: laboratory Hg(II) Dig: none Ox: none Red: electrochemical on GFE	Sep.: none Conc: direct Au amalgamation	DPASV (50 ng/L)	Pub: 1997 Ref.[88] • Anodic stripping speciation of Pb, Cu and Hg in chloride electrolyte • Thicker gold film increased stripping
Samp: plant material, Dig/Ox: 170 C HNO3 Red: Sn(II)	Sep: N2 purge Conc: AuPt gauze	DPASV (none given)	Pub: 1994 Ref.[89] • DPASV, in DOM free electrolyte, after volatilized Hg(0) is amalgamated on Au/Pt gauze
Samp: Hg(0) vapor Dig: none Ox: none Red: none	Sep.: none Conc: Au amalgamation	Reflectivity Change (6 ppb)	Pub: 1990 Ref.[90] • Vapor phase Hg(0) amalgamates a gold surface creating pores, decreasing the reflectivity,
Samp: sea water Dig/Ox: UV light, Red: electrochemically on Au RDE	Sep.: none Conc: direct Au amalgamation	DPASV (2 ng/L)	Pub: 1986 Ref.[91] • DL by standard addition curve • Gold surface regenerated by electrochemical oxidation and polishing
Samp: laboratory Hg(II), As(III), Dig: none Ox: none Red: electrochemical onto GFE	Sep.: none Conc: direct Au amalgamation	LSV (0.4 ng/L)	Pub: 1997 Ref.[92] • Simultaneous detection of As and Hg with out sample prepartation • Correlation with AAS tested natural waters within 15%

Table 1.5 cont.: Analytical Methods for Determining the Total Mercury			
Sample Preparation	**Mercury Separation**	**Detection (Limit)**	**Comments**
Samp: laboratory Hg(II), Me2Hg Dig: none Ox: none Red: electrochemically on GFE	Sep.: none Conc: direct Au amalgamation	SWACASV (500 ng/L)	Pub: 1998 Ref.[93] • Square Wave Altenating Current techinque used to improve sensitivity • Tap water had better detection limit than the DW samples
Samp: laboratory Hg(II) Dig: none Ox: none Red: electrochemical on GFE	Sep.: Chromosorb-W (HCl), HgCl2; Tenax-GC (poly 2, 6-diphenyl-p-phenylene oxide), MeHgCl; Carboseive, Me2Hg; Au beads Hg(0) Conc: Au beads after	AAS (none given)	Pub: 1998 Ref. [94] • Gold beads are reported to have 99-100% efficiency for all Hg species.[95][Ref192] • Hg compounds thermally desorbed from collectors to gold trap then pyrolysis for AAS.
Samp: plant material, Dig/Ox: 170 C HNO3 Red: Sn(II)	Sep.: Ar purge Conc: Au sand	CVAFS, unidirectional flow (4 pg/L water)	Pub: 1993 Ref.[96] Single stage Au trapping is as efficient and sensitive as 2 stage Au trapping, if the peak area is measured and not peak height.
Samp: laboratory Hg(II), As(III), Dig: none Ox: none Red: electrochemical onto GFE	Sep.: Au/Pt gauze Conc: direct amalgamation	CVAAS (30ng/m3)	Pub: 1995 Ref.[97] • Au/Pt has nearly constant adsorption coefficient from 20 200 C: Au decreased to 30% efficiency. • Thermal desorption has 1-2% retention with high Hg concentrations (> 3ng/L for this apparatus). • Hg(0) and Me2Hg adsorbed equally well on Au and Au/Pt

Table 1.5 cont.: Analytical Methods for Determining Total Mercury			
Sample Preparation	**Mercury Separation**	**Detection (Limit)**	**Comments**
Samp: laboratory Hg(II), Me2Hg Dig: none Ox: none Red: electrochemically on GFE	Sep.: Ar purge Conc: Au/Pt gauze	ICP-MS (0.2 ng/L)	Pub: 1996 Ref.[98] • Inductively Coupled Plasma-Mass Spectrometry doesn't have the spectral interferences that AA and AF techniques have. • Hg ionization efficiency is only about 32%, most other elements are around 90%.
Samp: water, sediments Dig: 90 °C aqua regia Ox: $KMNO_4$ / K_2CrO_7 Red: none	Sep.: Adsorption onto Modified Film Electrode of tri n-octylphosphine oxide over Au electrode Conc: none	MFE-ASV (20 ng/L)	Pub: 1989 Ref.[99] • Anodic peak at (+ 0.42 V vs. SCE) • TOPO film must be chemically regenerated with K_2CrO_7 after each Hg determination
Samp: water, sediments Dig: 90 °C aqua regia Ox: UV radiation with H_2O_2 Red: electrochemical	Sep.: none Conc: reduction onto electode surface	DPASV (20 ng/L)	Pub: 1987 Ref.[100] • DL of GC-RDE, GF-RDE and Au RDE (3200, 300, 20 ng/L respectively) • Interfering cations and their maximum concentrations determined for AuRDE: Cd(II), Pb(II), Zn(II), Co(II), Ni(II), Mn(II): 100 mg/L; Cu(II) 10 mg/L;
Samp: water, liquors, fruit juices Dig: none (water); HNO_3, UV with TiO_2 catalyst (juices) Ox: 0.15% H_2O_2 (water); 1% H_2O_2, UV (juices) Red: electrochemical onto GFE	Sep.: none Conc: reduction onto electode surface	LSV (100 ng/L)	Pub: 1996 Ref.[101] Without extensive oxidation, organic matter in the juices samples interfered with Hg stripping signal.

Table 1.5 cont.: Analytical Methods for Determining Total Mercury

Sample Preparation	Mercury Separation	Detection (Limit)	Comments
Samp: freash water Dig.: H_2SO_4/HNO_3 60 °C Ox.: $KMnO_4/K_2S_2O_8$ Red.: $NH_2OH \rightarrow$ Sn(II)	Sep.: N_2 purge Conc.: Au	ISE (60 microg/L)	Pub: 1995 Ref.[102] • $Ag_8HgS_2I_6$ superionic crystal interface has Hg/Ag transference ratio is 10^2 • No interfering ions were tested.
Samp: whole blood Dig/Ox: 90 °C $HNO_3/HClO_4$ (1:5) Red: Sn(II)	Sep.: Ar purge Conc: Au wire	CVAAS (60 pg/g)	Pub: 1995 Ref.[103] • Air purging caused passivation of gold wire trap. • N_2 purging decreased the Hg peak intensity by 35%.
Samp: coal Dig: grind to powder Radiation: 48h in neutron flux of 5.5×10^{13} n/cm^2/s Red: none	Sep.: pyrolysis at 550 °C, with N_2 purge Conc: Au mesh	RNNA (5 ng/g)	Pub: 1997 Ref.[104] • Radiochemical Neutron Activation Analysis has linearity from DL to 10 mg/kg. • Coal samples completely dried at 40 C, prior to irradiation, may be a source of volatilized Hg. • ^{203}Hg gamma ray at 279.2 keV used to detect Hg with correction for ^{75}Se gamma ray at 279.5 keV allows for simultaneous multielement detection.
Samp: fresh and waste water Dig: 200 °C HNO_3 4 hours, for all but fresh water Ox: none Red: electocemically onto GFE	Sep.: none Conc: direct Au amalgamation	CCSV (45 ng/L)	Pub: 1996 Ref.[105] • Many different biological samples tested. • The detection limit of CCSV vs. potentiometric stripping is about 50% better[106]

Table 1.5 cont.: Analytical Methods for Determining Total Mercury			
Sample Preparation	**Mercury Separation**	**Detection (Limit)**	**Comments**
Samp: fresh and sea water Dig/Ox: HNO_3 to pH 1, H_2O_2 with UV 6 hours Red: electrochemical onto GFE	Sep.: none Conc: direct Au amalgamation	CCSV (100 ng/L)	Pub: 1995 Ref.[107] • Simultaneous analysis of Se(IV), Hg(II), Cu(II) and Pb(II) is possible when Cl^- is the electrolytic anion. • Mercury stripping varies from + 650 to +260 mVvs. SCE when going from 1 mM KCl to sea water (0.55 M NaCl); where its stripping potential is the same as that of Cu in sea water. • Without Cl^- as part of the electrolyte, the Hg
Samp: fresh water, biological samples Dig/Ox: HNO_3/HCl (2:1), microwave heating 2 hours Red: none	Sep.: CCl_4 to digested sample, → dithiocarbamate to organic layer, → Au(III) to organic layer (releases Hg(II) from dithiocarbamate) with collection of aqueous phase. Conc: dithiocarbamate then by	DPASV (25 µg/kg, solid samples)	Pub: 1994 Ref. [108] • Dithiocarbamate has a high affinity for Hg(II) to the exclusion of 10 fold concentrations of Zn(II), Cd(II), Pb(II), Cu(II). • Greater than 95% recovery from spiked tap, lake and sea water samples.
Samp: laboratory, fresh and sea water Dig: photooxidation of sea water Ox: none Red: electrochemical onto Modified Film GFE	Sep.: none Conc: reduction onto GFE electrode modified with poly(4-vinylpyridine)	SWASV (100 ng/L)	Pub: 1995 Ref.[109] • PVP film over the GFE traps anionic complexes preventing DOM interference and, in the presence of chloride, traps $HgCl_x$ complexes as the electrode surface during stripping allowing for surface build-up of Hg analyte. • Electrode performance is directly related to film thickness. • Regeneration of electrode by oxidative

Mercury Speciation:

There are two general analytical roads for the detection of selective or all major mercury compound groups (Hg(0), Hg(II) RHg(I), R_2Hg). The selective techniques separate one of the mercury compound groups either before detection or as part of the detection process. Subtraction from a total mercury detection technique allows for partial speciation of the mercury in a sample. To speciate between all the major groups of mercury compounds, the mercury almost always is subjected to chemical derivatization and then separation and detection.

The determination of Hg(II) and RHg species combines two reactions carried out sequentially on one or more aliquots of a given sample.[110] The first reaction is a selective reduction, usually Sn(II), that reduces Hg(II) to Hg(0).[111] The sample is them purged with a gas to remove all the Hg(0) with subsequent strong oxidation to cleave the alkyl mercury bond of MeHg and Me_2Hg species, converting them to Hg(II). This Hg(II) is again reduced and detected. [79, 110, 111] In this particular scheme the initial mercury compounds are detected as such: Hg(0) either in the first purging or, as a substraction of Hg(II), RHgX, and R_2Hg from total Hg; Hg(II) is detection after the first Sn(II) reduction; RHgX and R_2Hg after the strong oxidation and subsequent reduction. A summary of the reactions is given in Equations 1.3 to 1.6. When determining Hg(II) the mercury must be free from any organic complexation. Chemical digestion with KOH/MeOH, frees Hg(II) from the biologic matrix without cleaving the RHg bond.[110a]

$$Hg(0)_{aq} \xrightarrow{N_2 \text{ purge}} Hg(0)_{vap} \quad (1.3)$$

$$Hg(II)_{aq} + Sn(II)_{aq} \longrightarrow Hg(0)_{aq} + Sn(IV)_{aq} \quad (1.4)$$

$$MeHgX_{aq} \text{ or } Me_2Hg_{aq} + Sn(II)_{aq} \longrightarrow \text{No Reaction} \quad (1.5)$$

$$MeHgX_{aq} \text{ or } Me_2Hg_{aq} \xrightarrow{K_2Cr_2O_7 / HNO_3} Hg(II) \quad (1.6)$$

There are disadvantages to this method of selective reduction, purging and determining the mercury left over. The first purging step can remove Me_2Hg along with the initial reduced Hg(0)[112] This technique also cannot distinguish between MeHgX and Me_2Hg, because these two are both oxidized to Hg(II) in the strong oxidation step and detected together as Hg(0) at the end. However the early assumptions is that in biological samples Me_2Hg did not exist and that the only organic species was RHgX.[110c]

To distinguish between all the various mercury compound groups it is necessary to derivatize them. The early work used $NaBEt_4$ as an ethylating agent that permitted the speciation of Hg(0), Hg(II), MeHgX, and Me_2Hg.[113] Sodium tetraethylborate was selected because nobody had ever detected any biologic ethylated mercury compounds. The general speciation scheme of aqueous phases ethylation is depicted in Equations 1.7 to 1.10.[49a, 53, 114]

$$Hg(0)_{aq} + NaBEt_4 \longrightarrow \text{No Reaction} \quad (1.7)$$

$$Hg(II)_{aq} + NaBEt_4 \longrightarrow Et_2Hg \quad (1.8)$$

$$MeHgX_{aq} + NaBEt_4 \longrightarrow MeHgEt \quad (1.9)$$

$$Me_2Hg_{aq} + NaBEt_4 \longrightarrow \text{No Reaction} \quad (1.10)$$

After derivatization, the reaction products are separated from the sample matrix. This is usually by some type of chromatograhy (GC, CC, HPLC)[56-58] or after gas purging they are collected on a trap (e.g. carbotrap or gold) and then detected (usually by an AA or AF technique).[49a, 53, 114] The elution order through GC columns is Hg(0), Me_2Hg, MeHgEt, and Et_2Hg. The early work used ethylation for the derivatizations; but, the discovey of naturally occurring ethylmercury[115] and greater GC resolution with other alkyl groups (e.g. isopropyl, butyl) has prompted other derivatization schemes.[116] All but Hg(0) needs to be thermally decomposed before detection by AA or AF techniques. Although elegant, the speciation schemes have there own problems as the method for determining the amount of mercury in an environmental setting. The reactions are never 100% yeild, there can be loss of volatile species, Hg(0) and Hg(II), during the reactions, there is cross derviatization during the reaction phase and sometimes during the collection and separation phase(especially on Carbotrap); and it is more difficult to preconcentrate the speciated compounds.116 A cross-section of these various techniques are found in Table 1.6.

Table 1.6: Analytical Methods for Mercury Speciation: Selective and Total

Sample Preparation	Mercury Separation	Detection (Limit)	Comments
Samp: fresh water Dig.: none Red.: Sn(II)/HCl Ox.: 0.16M $HNO_3/KmnO_4$	Sep.: air purge after Sn(II) reductions Conc.: none	CVAA (1 ng/L)	Pub: 1975 Ref. [117] • Selective reduction of Hg(II) and RHgX with Sn(II) with air purge to remove Hg(0), remaing sample to determing R_2Hg and RHgX. • Air purge can also remove R_2Hg and RHgH • Hg(II) and RHgX equal Hg_{tot} –
Samp: seawater, fresh water Dig.: none Red.: Sn(II)/ HCl	Sep.: N_2 purge Conc.: Au	CVAA (42 ng/L)	Pub: 1981 Ref. [118] • Selective reduction of Hg(II) and RHgX with Sn(II) with air purge, remaing sample to determing R_2Hg. • Air purge can also remove R_2Hg
Samp: fish Dig.: Hom→ KOH/MeOH 70°C → neutralize Red.: $NaBEt_4$	Sep.: N_2 purge Conc.: carbotrap	CVAF (0.5 ng/g, MeHg), 0.1 ng/g, Me_2Hg)	Pub: 1989 Ref. [80] • MeHg is detected at the MeHgEt derivative and Hg(II) as Et_2Hg. • Me_2Hg is not derivatized. • The order of desorption from the Cbt is Hg(0), Me_2Hg, MeHgEt, Et_2Hg
Samp: fish Dig.: Hom → 6N HCl Red.: none	Sep.: $CCl_4/Na_2S_2O_3$ extraction → HPLC → N_2 purge Conc.: none	Pyrolysis → CVAA (0.37 ng/g)	Pub: 1982 Ref. 56 • MeHgX is extracted with the aid of $Na_2S_2O_3$. • It is necessary to thermally decomose MeHgX and Me_2Hg before CVAA detection. • A Hg_{tot} analytical procedure is needed to determine Hg(II)

Table 1.6 cont.: Analytical Methods for Mercury Speciation: Selective and Total			
Sample Preparation	**Mercury Separation**	**Detection (Limit)**	**Comments**
Samp: water, laboratory Hg(II) Dig: none Ox: none Red: none	Spec: Hg(II) only Sep.: Adsorption onto thin film of 2-(5-amino-3, 4-dicyano-2H-pyrol-2-ylidene)-1,1,2-tricyanoethanide (Hg(II) specific complexing agent)	Colorimetry: $\Delta \lambda_{max}$ from 549 nm to 650 nm (10 μg/L, soln.), (100 μg/L, polymer matrix)	Pub: 1997 Ref.[119] • KCN added to regenerate electrode surface • Interfering anions are CN^-, Cl^-, CNS^- • Interfering cations are Au(III) > Pd(II) >> Cu(II) > Sn(II) > Fe(II) > Ru(III) > Ir(III); where Hg(II) reacts twice as
Samp: whole blood Dig: 45 °C 16M H_2SO_4 16 hours Ox: none Red: Sn(II)	Spec: Hg(II) only Sep.: Ar purge Conc: Au wire	CVAAS (5 ng/g, Hg(II) only)	Pub: 1995 Ref.[120] • H_2SO_4 frees Hg(II) from organic matrix and allows reduction by Sn(II). • Determination of MeHg is made by subtracting Hg(II) measured from total Hg. • Convesion of MeHg to Hg(II) during digestion was proportional to time and
Samp: laboratory Hg(II) Dig: none Ox: none Red: none	Spec: Hg(II) only Sep.: Hg (II) complexation with urease Conc: none	EI-SAW frequency shift attenuaton from urease inhibition (20 μg/L)	Pub: 1995 Ref. [121] • Detection based on standard calibration with urea and Hg(II) additions. SAW frequency dependant on soln. osmolarity which doesn't increase as much in the presence of Hg(II) • Ag(I) and Fe(III) interfere significantly.

Table 1.6 cont.: Analytical Methods for Mercury Speciation: Selective and Total			
Sample Preparation	**Mercury Separation**	**Detection (Limit)**	**Comments**
Samp: laboratory Hg(II) Dig: none Ox: none Red: none	Spec: Hg(II) only Se: Hg(II) complexation with invertase Conc: none	EI-bulk electrolysis (2 microg/L)	Pub: 1995 Ref.[122] Invertase converts sucrose to glucose which is oxidized in the presence of glucose oxidase to gluconic acid and H_2O_2. Glucose oxidase in a polymer matrix on a Pt electrode held at +0.65 V registers a current as H^2O^2 is oxidized at the surface.
Samp: laboratory Hg(II), MeHgCl Dig: none Ox: none Red: none	Spec: Hg(II), MeHg(I) Sep.: none Conc: none	EI-colorimitry (200 ng/L)	Pub: 2002 Ref.[123] • Hg(II) inhibits urease which is bound to one side of a cellulose acetate layer, facing a yellow pH indicator disc impregnated with urease. In water, Hg(II) inhibits the urease activity and the yellow spot does not fade away. • Concentration is based on time for spot to disappear. • MeHgCl reacts
Samp: laboratory Hg(II) Dig: none Ox: none Red: none	Spec: Hg(II) Sep.: Nafion membrane cation selection, safranin Hg(II) selectivity Conc: none	CI-Colorimetry (1 g/L)	Pub: 2001 Ref.[124] • Safranin, a red organic dye, in a pool with iodide behind the Nafion membrane reacts with iodide in the presence of Hg(II) to form a colorless compound. • Ag(I) interferes with the Hg(II)

Table 1.6 cont.: Analytical Methods for Mercury Speciation: Selective and Total

Sample Preparation	Mercury Separation	Detection (Limit)	Comments
Samp: water, biological solids Dig: water none, MeOH/KOH Prep: ethylation (NaBEt4)	Spec: Hg(II) MeHg(I), Me_2Hg Sep: N_2 purge Conc: Carbo trap Sep: GC, reverse flow	CVAFS, reverse flow Me_2Hg (50 pg/L, water) (1.4 ng/g, solids) MeHgCl (100 ng/g, solids)[Ref194]	Pub: 1994 Ref.[125] • Blanks for DL from repetitive sample purging • Carbotraps had highly variable efficiency • Similar detection limits were found for NaBH4 reductions[126][Ref194]
Samp: laboratory Hg(II) Dig: none Ox: none Red: none	Spec: Hg(II) only Sep.: Enzyme specificity for Hg(II) in genitically engineered E. Coli.	BS-luminescence intensity (20 ng/L)	Pub: 1994 Ref.[127] • Hg(II) activates detoxification genes from *Serratia marcescens and E. coli* bacteria that have been placed next to "Lux genes" in other *E. coli*. Lux genes code for aldehyde and luciferase which in living biological cells facilitates a light producing reaction. • Cd(II), Co(II), Ni(II), Zn(II) and
Samp: laboratory water with Hg(II), MeHgCl, and Me_2Hg Dig: none Dir: aqueous ethylation with $NaBEt_4$	Spec: Hg(II), MeHg(I), Me_2Hg Sep: He purge Conc: Carbotrap or Tenax-TA GC columns Sep: isothermal GC (15% OV-3 packing) → pyrolysis	CVAFS (12 pg/L, Me_2Hg and MeHgCl), (25 pg/L Hg(II)0	Pub: 1994 Ref.[128] • Organomercury species are known to decompose on Carbotrap column and non silanized glass tubing. • Elemental Hg(0) not determined.

Table 1.6 cont.: Analytical Methods for Mercury Speciation: Selective and Total

Sample Preparation	Mercury Separation	Detection (Limit)	Comments
Samp: laboratory Hg(II), Me_2Hg, Dig: none, Ox: none Red: electrochemically on GFE	Spec: Hg(II), Me_2Hg Sep.: none Conc: Au amalgamation	CCSV (500 ng/L)	Pub: 1993 Ref.[63c] • Differential stripping between Se and Hg • Interference from Pb, Cd, Ni, Cu, Fe, Bi, Sb, Mn, Co, Cr, V, Sn, Se, In, Tl, Ga, Ti, Mo, and Al determined not significant • Rh and Pd decrease Hg stripping peak intensity • Me_2Hg readily detected with CCSV • Au electrode regenerated by electrochemical oxidation only
Samp: laboratory Hg(II), MeHgCl, EtHgCl, PhHgCl Dig/Ox none Red: electrochemically on Modified Carbon Paste Electrode	Spec: Hg(II), MeHg(I) Sep.: chemical chelation by thiolic resin (Duolite GT-73, a thiolic resin) Conc: none	MFE-ASV (4 μg/L, Hg(II)) (2 μg/L, MeHg(I))	Pub: 1995 Ref.[129] • Hg(II) and alkyl-Hg(I) species are chelated by electrode resin and speciated by selective reduction in the order of Hg(II), MeHg(I), EtHg(I) from –0.3V to –1.35 V vs. sat. Ag/AgCl • Surface oxidation occurs at +0.15 V. • Regeneration of the electrode surface is done by abrasive polishing. • Me2Hg is not determined.

Prologue to the Thesis

Our study of the electrodeposition and stripping of mercury on gold foil electrodes came about as the impetus from Dr. Jeffrey C. Andle of the Biode Corporation. A local, Maine research and development company, that was working on sensor research and one aspect of that was a mercury sensor based on a surface acoustic wave (SAW) resonance frequency shift of a gold film.[68 b, c, 71] Biode was interested in developing the electrochemical characteristics of their films in the electrodeposition and subsequent stripping of mercury. This project was supported by a grant from the Department of Energy.* Biode's test gold sensor films were prepared by chemical vapor deposition (CVP) in the University of Maine's Laboratory for Surface Science and Technology. Our intention was to study the films electrochemically and see how they responded in comparison to the known literature and conduct some surface analysis of the films to see if there would be structural alterations that would impede the SAW measurements.

Based on the literature already characterizing the electrodeposition and stripping of mercury on gold electrodes, we had the expectation that the basic electrochemistry in determining redox potentials for the deposition and stripping of mercury on the gold surfaces would be a formality.[63, 87, 91, 107b, 130] It was widely suggested that mercury is easily deposited and easily oxidized away. There were some questions as to the surface states of the mercury as the anodic sweep of the cyclic voltammograms were complex;[87] but, the gold electrodes were considered to be free of mercury after the electrochemical

oxidative stripping and cleaning processes. It was also well known that mercury would amalgamate with the gold surfaces; yet, there was no report that this was not a reversible phenomenon. We initiated our experimentation with bulk polycrystalline gold foil electrodes that could be easily used for electrochemistry experiments and taken to the surface science laboratory for surface analysis.

The initial experiment was, as many are, a disaster; but, observations made at the time have played a role into our thinking about some of the phenomena that we saw later and for that, it is worth mentioning. So on March 8, 1996, we made our first attempt at the electrochemical deposition of mercury onto a 1 cm^2 gold electrode. The experimental set-up is well described in Chapter II. We were using 0.01 M $HgCl_2$ with 3 M KCl, with an intended deposition potential of – 0.5 V vs. our Ag/AgCl reference electrode. The laboratory note reads as follows:

> " error message on potentiostat, too much current. $HgCl_2$ solution started boiling, turned gray, then clear and back again several times until the experiment was stopped. The gold electrode has lost its sheen, and the $HgCl_2$ solution is clear."

The problem with the experiment was that the reference electrode was not connected and the potentiostat was wildly searching to apply the programmed deposition potential. X-ray photoelectron spectroscopy (XPS) analysis of that particular gold foil showed the presence of mercury. It was then subjected to electrochemical oxidation in mercury free electrolyte for 10 minutes and again reanalyzed by XPS. Again a mercury peak was seen

---

* DOE Grant DE-FG02-94ER80707

on the gold foil. Potential contamination in the XPS system was ruled out, by the analysis of a gold foil standard that was a permanent resident on the reverse side of the sample rod for the high vacuum surface analysis system. The electrochemical oxidation was repeated 5 more times and XPS analysis consistently showed the presence of mercury. The gold electrode was finally cleaned of mercury with argon plasma sputtering, to levels not detectable by XPS. The systematic investigation of the retention of mercury on gold foil electrodes is what comprises Chapter II.

The experimental parameters that we used were non classical from an electrochemical perspective. Our experimental set-up isolated the working gold electrode from the counter electrode to eliminate the risk of mercury contamination of subsequent gold films. Our choice of electrolyte is rather dilute being 2.5 mM KCl or KNO_3 acidified to pH 3 to 4 with the corresponding acid. This did increase the charging potential of our cyclic voltammograms (CV); but, our CVs were closely representative of CVs of Hg(II) on gold electrodes in more traditional electrochemical parameters.[87, 130f] Most experiments were run in the chloride electrolyte because, chloride is the most common anion in natural water systems. The concentration was chosen to be low to again to be a simple solution; but, with a total electrolyte concentration that may typically be found in a mildly polluted water system. The acidification was to eliminate the possibility of having CO_2 dissolve into the water and interfere with the coulombic count during mercury deposition. We continued this throughout our experimentation to be consistent; although, its necessity is dubious. A pH of 4 would be a severely acidified lake; but, known in North America and less acidic than many ponds and bogs.[131]

After having established that the complete removal of mercury from polycrystalline gold electrodes by electrochemical means was realistically impossible,♠ we felt that the possibility of accumulation needed to be investigated. Chapter II and all the existing literature suggested that the amount of mercury retained in any one electrochemical deposition and stripping step was quite small. It was also reported in the literature that repeated electrochemical deposition and stripping analysis of mercury with gold electrodes showed no significant change in signal.[132] Therefore we conducted experimentation to do repetitive cycling of electrodeposition followed by electrochemical stripping. Our stripping parameters were more exhaustive (in terms of time) than those reported in the literature and we conducted many more repetitions. We sought to establish whether there would be a change in the electrochemical stripping response and then later quantify the accumulation with thermal desorption spectroscopy (TDS). This block of work is featured in Chapter III.

The repetitive cycling electrodeposition / stripping experimentation employed a flow through system, which is important in considering certain real world environmental situations (flowing stream, ocean). Additionally, our work from Chapter II showed us that much of the mercury remains in solution even after its electrochemical activity ceases to be registered in bulk electrolysis deposition. A closed system for repetitive cycling doesn't allow for fresh analyte to be reintroduced to the electrode continually throughout the experiments. Since we were studying mercury that was retained on the

♠ It is conceivable, given enough time and with the right conditions, the mercury atoms in a mercury gold amalgam surface would all diffuse to the surface and be oxidized away.

gold after electrochemical stripping, we could not monitor that mercury with the cold vapor atomic absorption (CVAA) equipment available to us. However, the TDS experiments allowed greater flexibility in analyzing potential surface components of the retained mercury. The TDS experiments employed an experimental set-up that allowed temperature measurements to be made on a surface in the same orientation as the active surface of our gold electrodes. This is more reliable than simply measuring the heating plate temperature or measuring the temperature of the surface of the electrode that is not in the same configuration as the active electrode surface. This point was important during experimentation in that, the heating plate and underside surface of the gold electrode recorded temperatures up to 100 °C more than the exposed surface ever attained. During the TDS experiments, the active surface was oriented to the mass spectrometer through an inverted cone to eliminate the detection of spurious mercury.

As with most experimental work, we had a set back in terms of equipment failures. Our sample rod on the high vacuum surface analysis system was damaged and we had a lull in our study of mercury on gold electrodes. Fortuitously, our group was approached for a collaboration on the study of some metal-thiolate chalcogenides. Particularly, we were interested in correlating the electrochemistry of a number of compounds whose crystal structures had been determined by the Ruhlandt-Senge research group.[133] It is well known that mercury has an affinity for thiolate ions and that its toxicity is largely a result of mercury-thiolate interactions in biological organisms. Therefore, the study of metal-thiolate chalcogenides may very well be a reasonable study of a simple system that models complex proteins.[134] In proteins there are many cysteine

residues which contain free thiol groups and there are many metal ions solvated within the proteins. The crown ether moieties of our compounds can represent the metal ions bound in protein molecules and the thiolate compounds the cysteine residues. Our study of the electrochemical parameters of the metal-thiolate chalcogenides make up the contents of Chapter IV.

The experimental work for this thesis was conducted from March 1996 to July, 1999. The work in Chapter II is featured in two publications, which are found in Appendix E and F as they appear in print.[68b, 135] With the delay in obtaining our equipment the work for Chapter III was actually completed after that of Chapter IV. Part of the work of Chapter IV is featured in the publication found in Appendix G.[136] Chapters II – IV were all written in 1999; but, the author took a leave of absence to attend medical school. This thesis has been revised, completed and defended in 2003; but, no more experimental work has been done since July 1999.

References

[1] a) Goldwater L. J. Mercury, A History of Quicksilver. Baltimore, York Press, 1972. b) Takacs, L. Journal of Metal, 2000, 41, 12-13.

[2] Weeks, M. E. Journal of Chemical Education, 1968, 46-51.

[3] a) Butlet, A. R., Glidewell, C., Needhan, J.. Journal of Chemical Research, 1980, 47, 817-832. b) Kang-Yum, E, Oransky, S. H. Veterinary and Human Toxicology, 1992, 34, 235.

[4] Grauer, V. Other Voices, 2002, 2(2), 1-2.

[5] Sass, B. M. Salem, M. A., Smith, L. A., EPA Pub. No. PB94-165362AS, 1994, 1-4

[6] a) Mercury, P. Chevalier, in "Canadian Minerals Yearbook 1998, Chpt. 33, 1-4. B) Hylander, L. D., Meili, M. The Science of The Total Environment, 2003, 304, 13-27.

[7] Albert, M. R. Journal of the American Academy of Dermatology, 2000, 43(3), 519-26

[8] Goldman, L. R. Pediatrics, 2001, 108(1), 197-205

[9] Bittner, A. C. Jr., Echeverria D, Woods, J. S. et al. Neurotoxicology and Teratology, 20, 429-439, 1998.

[10] Troen P., Kaufman S. A., Katz, K. H. New England Journal of Medicine, 1951, 244, 459.

[11] a) Amin-Zaki, L., Majeed, M.A., Clarkson, T.W., et al. Brittish Medical Journal, 1978, 1, 610. b) Bakir, F., Damluji, S. F., Amin-Zaki, L., et al. Science 1973, 181, 230.

[12] a) Agocs, M. M., Etzel, R.A., Parrish, R. G., et al. New England Journal of Medicine, 1990, 323, 1096. b) Branches, F. J. P., Erickson, T. B., Aks, S. E., et al. Clinical Toxicology, 1993, 31, 295. c) Sasso, F. S., Ferraiuolo, R., Gursky, E., et al. Morbidity and Mortality World Report, 1996, 45, 422. e) Villanacci, J.F., Beauchamp, R., Perrotta, D.M., et al, Morbidity and Mortality World Report, 1996, 45, 400.

[13] The Encyclopedia of the Chemical Elements, Hampel, C. A. Ed., 1987, Reinhold Book Corporation, New York.

[14] Risher, J. F., Toxicology and Industrial Health, 1999, 15(5), 480-2

[15] Goyer, R.A., Casarett, A. Doull's Toxicology. The Basic Science of Poisons, 4th ed., Amdur, M.O., Doull, J., Klaasen, C.D. Eds., New York, Pergamon Press, 1991, pp 646–651.

[16] Shanker, G. Journal of Neuroscience Research, 2001, 66(5), 998-1002.

[17] a) Klaassen, C. D. "Heavy Metals and Heavy Metal Antagonists", in Goodman and Gilman's, The Pharmaceutical Basis of Therapeutics, 9th Ed. 1996, McGraw Hill, CD-ROM, section 66. b) Hadded, L. M., "Acute Poisoning" in Goldman, Cecil Textbook of Medicine, 21st ed., 2000, W. B. Saunders, 72-3. c) Chiang, W. K. "Mercury" in Ford, Clinical Toxicolocy, 1st Ed., 2001, W. B. Saunders, 737-42.

[18] Bredfeldt, J. E., Moeller, D. D. American Journal of Gastroenterology, 1978, 69, 478.

[19] Dzau, V.J., Szabo, S., Chang, Y.C. Journal of the American Medical Association, 1977, 238, 1531.

[20] Zillmer, E. A., Lucci, K.A., Barth, J.T., et al. Clinical Toxicology, 1986, 24, 91.

[21] Jung, R.C., Aaronson, J. Western Journal of Medicine, 1980, 132, 539.

[22] Celli, B., Khan, M.A. New England Journal of Medicine, 1976, 295, 883.

[23] Winek, C.L., Fochtman, F.W., Bricker, J.D., et al. Clinical Toxicology, 1981, 18, 261.

[24] a) Ross, W. D., Gechman, A. S., Sholiton, M. C., et al. Comprehensive Psychiatry 1977, 18, 595. b) Singer, R., Valciukas, J. A., Rosenman, K.D. Archives of Environmental Health, 1987, 42, 181.

[25] a) Aronow, R., Cubbage, C., Wierner, R., et al. Morbidity and Mortality World Report, 1990, 39, 125. b) Gotelli, G.W., Astolfi, E., Cox, C., Cernichiari, E., Clarkson, T. W. Science, 1985, 227, 638-40.

[26] a) Kales, S. N. Journal of Occupational and Environmental Medicine, 2002, 44(2), 143-54 b) Igata, A. Environmental Research, 1993, 63, 157.

[27] Clarkson, T.W., Magos, L., Cox, C., et al. Journal of Pharmacology And Experimental Therapeutics, 1981, 218, 74.

[28] a) Berlin, M, Rylander, R. Journal of Pharmacology And Experimental Therapeutics, 1964, 146, 236. b) Magos, L. Brittish Journal of Pharmacology 1976, 56, 479.

[29] a) Aaseth, J., Friedheim, E. A. H. Acta Pharmacology and Toxicology 1978, 42, 248. b) Bluhm, R.E., Bobbitt, R. G., Welch, L. W., et al. Human Experimental Toxicology 1992, 11, 201. vc) Campbell, J. R., Clarkson, T. W. Journal of the American Medical Association 1986, 256, 3127. d) Nielsen, J.B., Andersen, O. Human Experimental Toxicology, 1991, 10, 423.

[30] a) Al-Abbasi, A. H., Kostyniak, P. J., Clarkson, T.W. Clinical applications: Journal of Pharmacology And Experimental Therapeutics, 1979, 207, 249. b) Kostyniak, P. J., Greizerstein, H. B., Goldstein, J. et al. Human Toxicology, 1990, 9, 137.

[31] a) Fitzgerald, W. F., Mason, R. P., Vandal, G. M. Water Air Soil Poll, 1991, 56, 745-768. b) Mason, R. P., Fitzgerald, W. P., Morel, F. M. M. Geochimica et Cosmochimica Acta, 1994, 58, 3191-3198.

[32] Lindqvist, O., Johansson, M., Aastrup, A., Andersson, L., Iverfeldt, A., Meili, M., and Timm, B. Water Air and Soil Pollution, 1991, 55, 1-262.

[33] Hall, B. Water Air and Soil Pollution. 1995, 80, 301-315.

[34] Munthe, J., Xiao, Z. F., Lindquist, O. Water, Air and Soil Pollution, 1991, 56, 621-30. B) Lindberg, S. E., Brooks, S., Lin, C. J., Scott, K. J., Landis, M. S., Stevens, R. K., Goodsite, M., Richter, A. Environmental Science and Technology, 2002, 36, 1245-1256.

[35] Hudson, R. J. M., Gherini, S. A., Gitzgerald, W. F., Porcella, D. B. Water Air and Soil Pollution, 1995, 80, 265-72.

[36] a) Fitzgerald, W. F., Engstrom, D. R., Mason, R. P., Nater, E. A. Environmental Science and Technology, 1998, 32, 1-12. b) Guentzel, J.L., Landing, W. M., Gill, G. A., Pollman, C. D. Environmental Science and Technology, 2001, 35, 863-873.

[37] Amyot, M., Gill, G. A., Morel, F. M. M. Environmental Science and Technology, 1997, 31, 3606-11.

[38] Amyot, M., Lean, D. R. S., Mierle, G. Environmental and Toxicological Chemistry, 1997, 16, 2504-63.

[39] a) Coquery, M., Cossa, D., Martin, J. M. Water Air and Soil Pollution, 1989, 80, 653-64. b) Hurley, J. P., Watras, C. J., Bloom, N. S. Water Air and Soil Pollution, 1991, 56, 543-51.

[40] a) Luther, G. W., Tsamakis, E. Marine Chemistry, 1989, 127, 165-77. b) Paquett, D. E., Helz, G. R. Environmental Science and Technology, 1997, 31, 2148-53.

[41] Morel, F. M. M., Kraepiel, A. M. L., Amyot, M. Annual Review of Ecology Systems, 1998, 29, 543-66.

[42] Gutknecht, J., Tosteson, D. C. Science, 1973, 182, 1258-61.

[43] Gilmour, C. C., Henry, E. A. Environmental Pollution, 1991, 71, 131-69.

[44] Choi, S. C., Bartha, R. Applied Environmental Microbiology, 1994, 60, 4072-77.

[45] a) Mason, R. P., Reinfelder, J. R., Morel, F. M. M. Environmental Science and Technology, 1996, 30, 1835-45. b) Watras, C. J., Bloom, N. S. Limnology and Oceanography, 1992, 37, 1313-18.

[46] Clarckson, T. W. Critical Review of Clinical Laboratory Science, 1997, 34, 369-403.

[47] Boudou, A., Ribeyre, F. Metal Ions in Biological Systems, 1997, 34, 289-319.

[48] Blattmann, B., Saouter, E. Analytical Chemistry, 1994, 66, 13, 2031-7.

[49] A) Liang, L., Horvat, M., Bloom, N. S. Talanta, 1994, 41(3), 371-9. b) Fischer, R., Rapsomanikis, S., Andreae, M. O. Analytical Chemistry, 1993, 65, 763-7.

[50] Tsalev, D. L., Sperling, M., Wetz, B. Analyst, 1992, 117, 1729.

[51] Crecelius, E. A., Bloom, N. S. Marine Chemistry, 1983, 14(1), 49-59.

[52] Keeler, G. J., Landis, M. S. EPA Method 1631-821-R, 2001, 1-13.

[53] Rapsomanikis, S., Craig, P. J. Analytica Chimica Acta, 1991, 248, 563-7.

[54] a) Kandler, W., Hulanicki, A., Bulska, E. Spectrochimica Acta Part B, 1996, 51B(9-10), 1263-70. b) Denoyer, E. R., Debrah, E. Journal of Analytical Atomic Spectrometry, 1996, 11(2), 127-32.

[55] a) Rapsomanikis, S., Andreae, M. O. Interntional Journal of Environmental Analytical Chemistry, 1992, 49, 43-8. b) Jian, W., McLeod, C. W. Talanta, 1992, 37, 1537.

[56] Holak, W. Analyst, 1982, 107, 1457.

[57] Filippelli, M. Analytical Chemistry, 1987, 59, 116.

[58] Tsalev, D. L., Sperling, M., Wetz, B. Analyst, 1992, 117, 1729.

[59] McIntosh, S. Atomic Spectroscopy, 1993, 14(2), 47-9.

[60] Risova, J., Fisera, M., Hladky, Z. Journal of Analytical Atomic Spectrometry, 1990, 5(8), 691-2.

[61] Dubey, S. K., Gngoli, S., Holmes, D. S. Environmental Geochemistry and Health, 1994, 16(3/4), 229-33.

[62] Dumarey, R., Heindryckx, R., Dams, R., Hoste, J. Analytica Chimica Acta, 1979, 107, 159-67.

[63] A) Huang, H., Jagner, D., Renman, L. Analytica Chimica Acta, 1987, 201, 269-73. B) Huang, H., Jagner, D., Renman, L. Analytica Chimica Acta, 1987, 202, 117-22. C) Tian, B., Wang, J. Analytica Chimica Acta, 1993, 274(1), 1-6. D) Cladera, A., Estela, J. M., Cerda, V. Talanta, 1991, 38(12), 1475-9.

[64] a) Amine. A., Cremisini, C., Palleschi, G., Society of Photo-Optical Instrumentation Engineers, Pubication No. 2504, 1995, 209-20. b) Liu, D., Yin, A., Chen, K., Ge, K., Nie, L., Yao, S. Analytical Letters, 1995, 28(8), 1323-37.

[65] Porto da Silveira, C. L., Lima, R., Campos, R. C., Atomic Spectroscopy, 1997, 18(2), 55-59.

[66] Vlasov, Y. G., Ermolenko, Y. E., Kolodnikov, V. V., Ipatov, A. V., Al-Marok, S., Sensors and Actuators B, 1995, 24-5, 317-9.

[67] Panusa, A., Flamini, A., Sensors and Actuators B, 1997, B42(1), 39-46.

[68] a) Ho, M. H., Scheide, E. P., Guilbault, G. G., Analytica Chimica Acta, 1981, 130(1), 141-7. b) Andle, J., Schweyer, M., Munson, J., Roderick, R., McAllister, D., French, L., Vetelino, J., Watson, C., Foley, J., Bruce, A., Bruce, M. Proceedings of the IEEE International Frequency Control Symosium, 1997, 51, 90-95. c) French, L. A., Schweyer, M. G., Michael, G., Foley, J. B., Andle, J. C., Watson, C. M., Bruce, M. R. M., Bruce, A. E. Proceedings of SPIE-The International Society for Optical Engineering, 1998, 3539 (Chemical Microsensors and Applications), 161-9.

[69] Gifford, P. R., Bruckenstein, S. Analytical Chemistry, 1980, 52, 1024-28.

[70] Blanchard, L. J., Robertson, J. D., Analyst, 1997, 122(11), 1261-1264.

[71] a) Josse, F., Dahint, R., Schumacher, J., Grunze, M., Andle, J C., Vetelino, J. F. Sensors and Actuators, A, Physical, 1996, A53(1-3), 243-248. b) Schweyer, M. G., Andle, J. C., McAllister, D. J., Vetelino, J. F. Sensors and Actuators, B, Chemical, 1996, B35(1-3), 170-175.

[72] Buseck, P. R., Hanson, R. C., McNerney, J. J. Science, 1972, 178, 611-2, b) Murphy, P, J. Analytical Chemistry, 1979, 51(9), 1599-1600.

[73] Trittler, R., Schilcher, H. Fresenius' Journal of Analytical Chemistry, 1994, 349(8/9), 659-60.

[74] Ott, W. L., Hatch, R. Analytical Chemistry, 1968, 40, 2085.

[75] Savory, J., Toffaletti, J. Analytical Chemistry, 1975, 47, 2091.

[76] Bricker, J. L. Analytical Chemistry, 1980, 52, 492.

[77] Schubert-Jacobs, M., Wetz, B. Fresenius' Journal of Analytical Chemistry, 1988, 331, 324.

[78] Bloom, N. S. Canadian Journal of Fisheries and Aquatic Science, 1989, 46, 1131.

[79] Shuman, M. S., Robinson, K. G. International Journal of Environmental Analytical Atomic Spectrometry, 1989, 36, 111.

[80] Hawley, J. E., Ingle, J. D. Analytical Chemistry, 1979, 47, 719.

[81] Gill, G. A., W. F. Fitzgerald Marine Chemistry, 1987, 20, 227.

[82] Blattmann, B., Saouter, E. Analytical Chemistry, 1994, 66(13), 2031-37.

[83] Chan, C. C. Y., Sadana, R. S. Analytica Chimica Acta, 1993, 282, 109-15.

[84] McIntosh, S. Atomic Spectroscopy, 1993, 14(2), 47-9.

[85] Porto da Silveira, C. L., Lima, R., Campos, R. C. Atomic Spectroscopy, 1997, 18(2), 55-9.

[86] Risova, J., Fisera, M., Hladky, Z. Journal of Analytical Atomic Spectrometry, 1990, 5(8), 691-2.

[87] Andrews, R. W., Larochelle, J. H., Johnson, D. C. Analytical Chemistry, 1976, 48(1), 212-14.

[88] Svancara, I., Matousek, M., Sikora, E., Schachl, K., Kalcher, K., Vytras, K. Electroanalysis, 1997, 9(11), 827-833.

[89] Trittler, R., Schilcher, H. Fresenius' Journal of Analytical Chemistry, 1994, 349(8-9), 659-60.

[90] Butler, M. A., Ricco, A. J., Baughman, R. J., Journal of Applied Physics, 1990, 67(9), 4320-6.

[91] Gustavsson, I. Journal of Electroanalytical Chemistry and Interfacial Chemistry, 1986, 214(1-2), 31-6.

[92] Viltchinskaia, E. A., Seigman, L. L., Garcia, D. M., Santos, R. F. Electroanalysis, 1997, 9(8), 633-640.

[93] Kondrat'ev, V. V., D'yacnenko, Y. I. Journal of Analytical Chemistry, 1998, 53(4), 351-356.

[94] Herrero, E., Abruna, H. D. Journal of Physical Chemistry B, 1998, 102(2), 444-451.

[95] Liu, D., Yin, A., Chen, K., Ge, K., Nie, L., Yao, S. Analytical Letters, 1995, 28(8), 1323-37.

[96] Liang, L., Bloom, N. S. Journal of Analytical Atomic Spectrometry, 1993, 8(4), 591-4.

[97] a) Baxter, D. C., Dyvik, G., Dybdahl, B., Frech, W. Journal of Analytical Atomic Spectrometry, 1995, 10(10), 769-75. b) Leermakers, M., Baeyens, W. Journal of Analytical Atomic Spectrometry, 1989, 4(7), 635-40.

[98] Denoyer, E. R., Debrah, E. Journal of Analytical Atomic Spectrometry, 1996, 11(2), 127-32.

[99] Stulik, K., Lexa, J. Talanta, 1989, 36(8), 843-8.

[100] Hatle, M. Talanta, 1987, 37(12), 1001-7.

[101] Zakharova, E. A., Pichugina, V. M., Tolmacheva, T. P. Journal of Analytical Chemistry, 1996, 9(51), 918-923.

[102] Vlasov, Y. G., Ermolenko, Y. E., Kolodnikov, V. V., Ipatov, A. V., Al-Marok, S. Sensors and Actuators B 1995, 24-5, 317-9.

[103] Bergdahl, I. A., Schutz, A., Hansson, G.-A. Analyst, 1995, 120, 1205.

[104] Blanchard, L. J., Robertson, J. D., Analyst, 1997, 122, 1261-4.

[105] Beinrohr, E., Cakrt, M., Dzurov, J., Kottas, P., Kozakova, E. Fresenius' Journal of Analytical Chemistry, 1996, 256(3-4), 253-258.

[106] Jagner, D., Renman, L., Huang, H. Analytica Chimica Acta, 1987, 201, 1-9.

[107] A) Olsen, K., Zirino, A., Larson, D., Foster, N., Armalis, S., Lu, J., Rongrong, X., Wang, J. Analytical Chemistry, 1995, 67(8), 1481-5. B) Gil, E. P., Ostapczuk, P. Analytica Chimica Acta, 1994, 293, 55-65.

[108] Lee, J., Lo, J. Analytical Chemistry, 1999 1994, 66, 1242-48.

[109] Chung, M., Zen, J. Analytical Chemistry, 1995, 67, 3571-7.

[110] a) Magos, L., Analyst, 1971, 96, 847. b) Hawley, J. E., Ingle, J. D., Analytical Chemistry, 1979, 47, 719. c) Rezende, M. R., Compos, R. C., Curtius, J., Journal of Analytical Atomic Spectrometry, 1993, 8, 247.

[111] Oda, C. E., Ingle, J. D., Jr. Analytical Chemistry, 1981, 53(14), 2305-9.

[112] A) Amouroux, D., Tessier, E., Pecheyran, C., Donard, O. F. X. Analytica Chimica Acta 1998 H 377(2-3), 241-254. B) Reuther, Rudolf, Jaeger, Lars, Allard, Bert. Analytica Chimica Acta 1999, 394(2-3), 259-269. C) Wallschlaeger, D., Hintelmann, H., Evans, R. D. Wilken, R.-D. Water, Air, and Soil Pollution, 1995, 801-4, 1325-9.

[113] Bloom, N. S. Canadian Journal of Fisheries and Aquatic Science, 1989, 46, 1131.

[114] a) Bloom, Nicolas S. Canadian Journal of Fisheries and Aquatic Sciences. 1992, 49(5), 1010-17. b) Tseng, C. M., De Diego, A., Wasserman, J. C., Amouroux, D., Donard, O. F. X. Chemosphere, 1999, 39(7), 1119-1136.

[115] a) Falter, R., Schoeler, H. F. Fresenius' Journal of Analytical Chemistry, 1995, 353(1), 34-8. b) Emteborg, Haakan, Baxter, Douglas C., Frech, Wolfgang. Analyst, 1993, 118(8), 1007-13. c) Paudyn, A., Van Loon, J. C. , 1986, 325(4), 369-76.

[116] Emteborg, H., Snell, J., Qian, J., Frech, W. Chemosphere, 1999, 39(7), 1137-1152.

[117] Hawley, J. E., Ingle, J. D., Analytical Chemistry, 1979, 47, 719.

[118] Gill, G. A., Fitzgerald W. F. Marine Chemistry, 1987, 20, 227.

[119] Panusa, A., Flamini, A. Sensors Actuators B, 1997, B42(1), 39-46.

[120] Bergdahl, I. A., Schutz, A., Hansson, G.-A., Analyst, 1995, 120, 1205.

[121] Liu, D., Yin, A., Chen, K., Ge, K., Nie, L., Yao, S., Analytical Letters, 1995, 28(8), 1323-37.

[122] Amine. A., Cremisini, C., Palleschi, G. Society of Photo-Optical Instrumentation Engineers, Pubication # 2504, 1995, 209-20.

[123] Guo-Qing, S., Guibn, W. Journal of Analytical Sciences, 2002, 18(11), 1215-9.

[124] Kuswandi, B., Narayanaswamy, R. Sensors and Actuators B, Chemical, 2001, B74(1-3), 131-7.

[125] Blattmann, B., Saouter, E. Analytical Chemistry, 1994, 66(13), 2031-7.

[126] Rapsomanikis, S., Andreae, M. O. Interntional Journal of Environmental Analytical Chemistry, 1992, 49, 43-8.

[127] Dubey, S. K., Gngoli, S., Holmes, D. S. Environmental Geochemistry and Health, 1994, 16(3-4), 229-33.

[128] Liang, L., Horvat, M., Bloom, N. S. Talanta, 1994, 41(3), 371-9.

[129] Agraz, R., Hernandez, L., Sevilla, M. T. Journal of Electroanalytical Chemistry, 1995, 390, 47-57.

[130] a) Jayaratna, H. G. Current Separations, 1997, 16(3), 93-96. b) Ratana-ohpas, R., Kanatharana, P., Ratana-ohpas, W., Kongsawasdi, W. Analytica Chimica Acta 1996, 333(1-2), 115-118. a) Esteban, M., Arino, C., Ruisanchez, I., Larrechi, M. S., Rius, F. X. Analytica Chimica Acta, 1993, 284(2), 435-43. d) Wang J, Tian B. Analytical Chemistry, 1993, 65(11), 1529-32. e) Svoboda, G. J., Sottery, J. P., Anderson, C. W. Analytica Chimica Acta, 1984, 166 297-9. f) Schadewald, L. A., Lindstrom, T. R., Hussein, W. Evenson, E. E., Johnson, D. C. Journal of The Electrochemical Society, 1984, 131(7), 1583-7. g) Romeo, F. M., Tucceri, R. I., Posadas, D. Langmuir, 1990, 6(4), 839-42.

[131] a) Clair, T. A., Ehrman, J. M., Ouellet, A. J., Brun, G., Lockerbie, D., Ro, C.-U. Water, Air, and Soil Pollution, 2002, 135(1-4), 335-354. b) Dixit, A. S., Dixit, S. S., Smol, J. P. Canadian Journal of Fisheries and Aquatic Sciences, 1992, 49(Suppl. 1), 17-24. c) Dale, J. M., Freedman, B., Kerekes, J. Canadian Journal of Zoology, 1985, 63(1), 97-105.

[132] Tian, B., Lu, J., Wang, J., Luo, D.Wang, J. Electroanalysis, 1998, 10(6), 399-402.

[133] a) Chadwick, S., Englich, U., Noll, B., Ruhlandt-Senge, K. Inorganic Chemistry, 1998, 37(18), 4718-4725. b) Chadwick, S., Englich, U., Ruhlandt-Senge, K. Chemical Communications, 1998, (19), 2149-2150. c) Chadwick, S., Englich, U., Ruhlandt-Senge, K. Inorganic Chemistry, 1999, 38(26), 6289-6293.

[134] a) Gavina, F., Luis, S. V., Costero, A. M., Burguete, M. I., Rebek, J. Jr. Journal of the American Chemical Society, 1988, 110(21), 7140-3. b) Hamilton, A., Lehn, J., Marie, S., Jonathan L. Journal of the American Chemical Society, 1986, 108(17), 5158-67. C) Sato, H., Wakabayashi, M., Ito, T., Sugawara, M., Umezawa, Y. Analytical Sciences, 1997, 13(3), 437-446. D) Sillanaukee, P., Hurme, L., Tuominen, J., Ranta, E., Nikkari, S., Seppae, K. European Journal of Biochemistry, 1996), 240(1), 30-36. E) Zarkadas, C. G., Smillie, L. B., Madsen, N. B. Canadian Journal of Biochemistry, 1970, 48(7), 763-76.

[135] Watson, C. M., Dwyer, D. J., Andle, J. C., Bruce, A. E., Bruce, M. R. M. Analytical Chemistry, 1999, 71(15), 3181-3186.

[136] Chadwick, S., Englich, U., Ruhlandt-Senge, K., Watson, C., Bruce, A. E., Bruce, M. R. M. Dalton, 2000, 13, 2167-2173.

CHAPTER II

Stripping Analysis of Mercury Using Gold Foil Electrodes: Irreversible Adsorption of Mercury[1]

Introduction

The utilization of electroanalytical techniques for the detection of aqueous mercury, either alone or in conjunction with such emerging technologies as piezoelectric sensors, offers promise for the development of sensors capable of remote quantification of mercury in the environment.[2] The gold electrode, either alone or in a modified form, has been one of the electrodes of choice, for the detection of aqueous mercury, employing a variety of electrochemical stripping analysis techniques[†].[3] One reason for the use of gold is its high affinity for mercury, which enhances the pre-concentration effect.[4] A

[†] The electroanalytical techniques collectively termed stripping analysis include: anodic stripping voltammetry, controlled potential stripping analysis, Osteryoung square-wave anodic stripping voltammetry, differential pulse stripping voltammetry, and constant current stripping analysis.

distinct advantage of using electrochemistry, over conventional methods to detect mercury, is its suitability for use in the field where on-site measurements are highly desirable or a necessity (i.e. with radioactive samples, down-hole well monitoring, or during remediation).

Stripping techniques utilizing gold electrodes have demonstrated high sensitivity with detection limits below 1 ppb.[2d, 5] Repetitive use of any of these techniques necessitates a three-step cycle: pre-concentration (deposition), measurement (stripping), and regeneration (cleaning). Some reports in the literature suggest that a relatively short "cleaning" step results in complete removal of all deposited mercury prior to the next measurement.[6] Repetitive mercury measurement studies, typically employing up to twenty measurement cycles, result in standard deviations below 5%, supporting the idea that mercury is removed from the electrode after each cleaning step. However, there is also evidence in the literature that suggests the cleaning step may not result in a "fresh", analyte-free, gold surface. In the early 1980's, Johnson and coworkers reported that mercury accumulated on the electrode in cyclic voltammetry (CV) experiments and was not subsequently removed when the CV experiment was continued in fresh (mercury-free) electrolyte solution.[7]

In this investigation, we have set out to answer the question: is mercury retained on a gold electrode after a single controlled potential deposition, stripping, and cleaning cycle? The experimental conditions used in this study were chosen to mimic, in a controlled fashion, situations where a field device for mercury detection based on stripping analysis might be encountered: e.g. natural water with very little electrolyte

present. An investigation to answer a related question, whether mercury accumulates at a gold electrode after many deposition, stripping, and cleaning cycles is discussed in Chapter III. The justification for these investigations was based on the idea that if mercury were retained on a gold electrode, it would have a practical impact on the way stripping analysis is used to detect mercury. For example, would there be conditions when previously retained mercury is released during stripping? Would retained mercury alter the electrode composition enough to change the electrical properties of the electrode, such as the exchange current density,[8] which is orders of magnitude different for gold and mercury? Experimental and computational studies indicate that mercury has a metal-nonmetal transition in clusters at about 70 mercury atoms; thus, as a mercury cluster grows from 60 to 80 it goes from a non-metallic nature to a metallic one.[9] Would limited surface coverage of mercury on gold effect calibration of the electrode? Finally, in field applications, the number of desirable reproducible cycles will be many times greater than the limited number that have been typically employed in laboratory studies. Thus, these studies were initiated to determine whether the cleaning step leaves the electrode in a state that can be predicted from cycle-to-cycle; the answer to which is critical for the success of any long term repetitive electrochemical technique.

Experimental

Chemicals and Glassware:

Water for all electrolyte and soaking solutions and for glassware rinsing, was re-distilled from a *Barnstead NANOpure* water purification system to a final conductivity of less than 0.1 μS/cm. All chemicals, unless otherwise noted, were *Certified ACS Reagent* Grade. The supporting electrolyte solution (2.5 mM KCl / KNO_3, pH 3) was made daily by diluting a 1.0 M KCl, or KNO_3, stock solution with water that had been previously acidified to pH 3 with concentrated HCl or HNO_3. The pH of the electrolyte was stable in all electrochemical experiments. The electrolyte was acidified to minimize the effect of dissolved carbon dioxide. The concentration of the supporting electrolyte solution was chosen to limit interference from impurities and to mimic low electrolytic environmental conditions; where chloride ion concentrations normally range from a few to several hundred ppm.[10] Ostapczuk et al, have shown that chloride ion concentrations between 2 and 20 mM were adequate and stable for mercury potentiometric stripping analysis experiments.[5a] The electrolyte solution was sparged with nitrogen gas until just prior to transfer to the electrochemical cell. A 0.1M $HgCl_2$ stock solution was made by dissolving $HgCl_2$ (*Aldrich* 99.999%) in 2% HNO_3. Mercuric chloride solutions, of concentrations less than 1×10^{-4} M (20,000 ppm), were made fresh daily from this stock solution. Experiments employing solutions with no chloride ion were prepared in a similar manner except for: using $Hg(NO_3)_2$ (*Aldrich* 99.99%) to create the Hg^{2+} stock solutions; KNO_3 (*Fischer* 99 %) for the supporting electrolyte and HNO_3 (*EM analytical grade*) for

acidification purposes. Mercury (II) atomic absorption standard solutions, 1-5 ppb, were made by diluting acidified 1004 ppm Hg^{2+} (VWR *Certified Atomic Absorption Standard*) to a 1 ppm solution which was further diluted just prior to use with 2% HNO_3 (*ACS Analytical Grade*). A 10% $SnCl_2$ (*ACS Analytical Grade*) solution was diluted to 1.1% with 3% HCl (*ACS Analytical Grade*) to serve as the reducing agent in CVAA analysis.

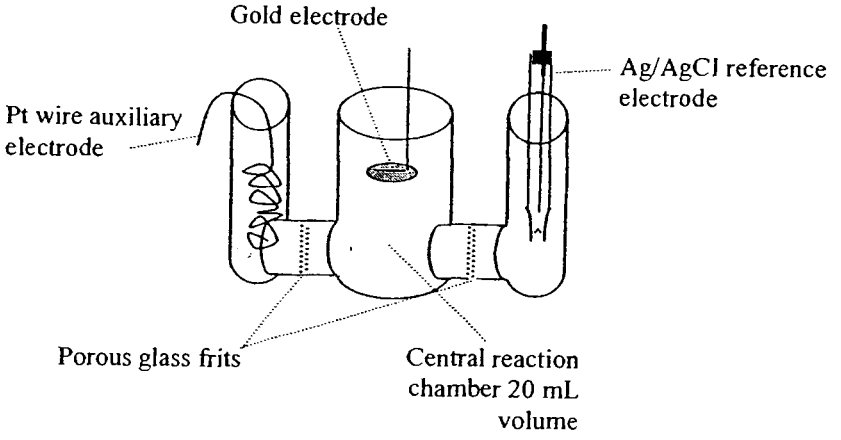

Figure 2.1: Experimental set-up for electrochemical experiments.

All glassware was rinsed several times with water and then soaked in 50% nitric acid for at least 24 hours until just prior to use; whereupon, it was well rinsed again with water. All solution storage bottles were treated in the same manner.

Electrochemistry:

The experimental set-up for the electrochemical experiments is shown in Figure 2.1. The electrochemical cell, fabricated by *Anderson Glass* of New Hampshire, was comprised of three chambers separated by porous glass frits. In all experiments, except as

noted, the outer compartments contained a platinum wire auxiliary electrode and a Ag/AgCl reference electrode (BAS MF-2074: $E^\circ = 0.194$ V vs. NHE), respectively. All potentials herein are in reference to this electrode unless otherwise noted. The center compartment contained a gold foil working electrode cut from 0.1 mm and 0.5 mm gold foil (*Aldrich* 99.99%). The working electrodes had 0.25 mm gold wire spot welded to one side providing a point for holding and for electrical contact. Coating the backside and most of the support wire with a clear insulating butyl acetate polymer (Revlon # 10) controlled the surface area of each electrode.

The three-compartment design was chosen to prevent contamination of the auxiliary and reference electrodes, preventing them from becoming sources of mercury in sequential experiments. The mercury was additionally restricted to the central chamber by always maintaining a superior fluid level in the side chambers containing the reference and auxiliary electrodes. The success of this mercury containment scheme was established by CVAA analysis of the contents of the outer chambers which confirmed that mercury concentrations were determined to be no higher than distilled water samples.

The applied potentials were controlled using an *EG&G* model 273 *Potentiostat/Galvanostat, EG&G*'s model 270 software, and a *Micron* 75 MHz Powerstation. The pH was monitored by using a *Beckman* Φ 11 pH meter with a *Corning* bulb-type ion selective electrode. The water conductivity measurements were made with a *YSI* model 3200 Conductivity meter using a *YSI* 3253 combination thermister conductivity cell.

Controlled Potential Deposition, Stripping and Cleaning

Before each constant potential (chronoamperometric) deposition, stripping and cleaning experiment, the electrodes underwent a blank deposition/stripping procedure in 18 mL of supporting electrolyte solution. The blank run was used to subtract the background current from the subsequent experiment with $HgCl_2$ solution. After the blank run, the electrolyte solution was replaced with 18 mL of fresh electrolyte solution and the electrode was used for a mercury deposition and stripping experiment according to the following procedure.

A cathodic current was established at a constant potential of -0.3 V in a stirred aqueous electrolyte solution. After 150 to 600 seconds, a 20 μL to 1 mL aliquot of a mercuric chloride solution was injected into the central chamber. The deposition was allowed to continue for a specified period of time; whereupon, the experiment was interrupted and the gold working electrode was removed from the solution, while still at the set deposition potential. The deposition solution in the central chamber was collected for CVAA analysis. The electrode and the central chamber were rinsed with water and the rinsings were combined with the deposition solution for CVAA analysis. The gold electrode was re-immersed in another 18 mL of fresh electrolyte in the central chamber and the experiment (at -0.3 V) was allowed to continue for a period of 50 to 200 seconds. At this point, the potential was switched from a cathodic deposition potential to an anodic potential which ranged from +0.7 V to +2.5 V. After an initial stripping event occurred

(usually within seconds), the electrode was held at that potential to clean it. The total duration of the chronoamperometric stripping and cleaning steps ranged from 500 to 4000 seconds. Just before the end of the prescribed stripping procedure, the experiment was stopped and the electrode was removed from the solution while still set at the oxidizing potential. The contents of the central chamber, along with solutions collected after rinsing several times, were then collected for CVAA analysis in the same manner as for the deposition solutions. After each experiment, the electrochemical cell was thoroughly rinsed with water and then nitric acid was allowed to flow through the frits from the outside chambers to the central chamber: completing the cleaning procedure for the cell.

The gold electrodes were cleaned after each contact with mercury. The electrodes that were used for XPS analysis were cleaned by argon plasma etching and the electrodes that did not undergo XPS analysis were cleaned in the following manner: rinsed with hot acetone, to remove the polymer coating; heated to redness for 30 seconds in an air/gas flame; polished with 1.0 μm water-soluble diamond suspension (*Buehler*) on a *Buehler Microcloth*; rinsed with water and boiled in nitric acid for at least 2 hours; rinsed with water again and heated at 400 °C in a ceramic crucible, with the polished surface exposed to air, for at least 12 hours. Thus cleaned, the clear polymer coating was applied to the electrodes followed by drying at 50 C for at least 24 hours. The electrodes were stored in a covered ceramic crucible.

Cyclic Voltammetry

The CV experiments, reported in this chapter, were all performed with the electrodes separated in the chambers of the three-compartment cell. We did CV experiments with all the electrodes together in the central chamber to measure the increased iR drop and as it was not significant (~ 50 mV) we made all of our CV measurements with the electrodes as shown in Figure 2.1. This arrangement was preferred so as give a more accurate indication as to what potentials to use in the subsequent controlled potential deposition and stripping experiments. Aliquots of the stock mercuric chloride solutions, 20 μL to 1 mL, were added to 18 mL of the supporting electrolyte solution in the central chamber once the starting potential was established. The solution was then stirred with a magnetic stirrer until 15 seconds before each CV run. The potential sweep rate was 100 mV/s for all CVs reported in this chapter.

Cold Vapor Atomic Absorption Spectroscopy:

The CVAA analysis was carried out on a *Perkin-Elmer Flow Injection Mercury Hydride Atomic Absorption Spectrometer* (FIMS) equipped with an electrodeless discharge lamp. The spectrometer employs an absorption wavelength of 253.7 nm passing through a 0.7 nm slit. The sample volume was 500 µL and the flow rate of the argon carrier gas (*grade 5.0*) was 100 mL/min. The mercury concentration was correlated to the absorption peak height with the *Perkin-Elmer's FIMS Software.* Immediately after collection, the deposition and stripping solutions were diluted with water and nitric acid to final concentrations of 1 to 5 ppb Hg^{2+} in 2% HNO_3. All samples were analyzed within 48 hours of collection.

Surface Analysis:

The experimental set-up for the x-ray photoelectron spectroscopy (XPS) experiments is shown in Figure 2.2 The XPS instrument was a prototype model with a differentially pumped x-ray source, fabricated by *Leybold-Heraeus* of Germany, that allows for XPS analysis of samples at relatively high pressures (1 mbar). All the spectra were recorded with magnesium K_α x-rays emanating from electron impact of a 20 mA emission current through an 11 kV voltage drop. The photoelectrons passed to the hemispherical energy analyzer, referenced to the Au $4f_{7/2}$ peak at 84.00 eV. The pass energy was usually set at 50 eV; but, this was increased to 100 eV when analyzing the electrode surfaces for residual mercury, chloride, oxygen etc. The angle between the analyzer and the incident X-ray beam is 75° with the analyzer normal to the sample surface.

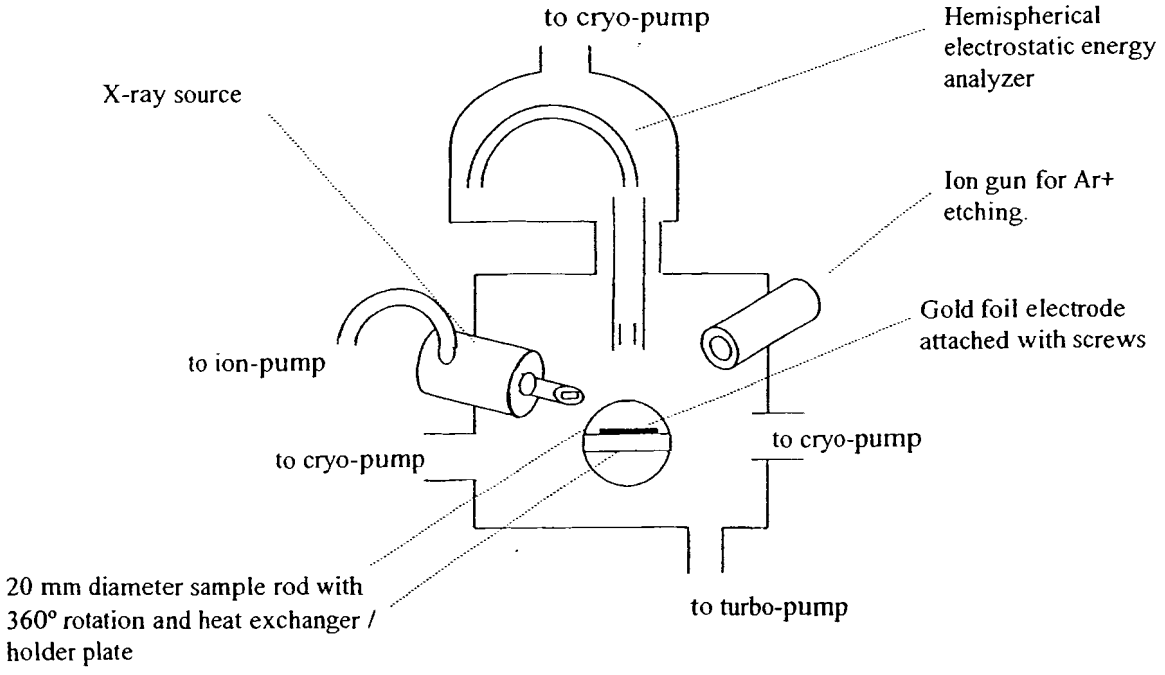

Figure 2.2: End on view of the experimental set-up for surface analysis experiments.

The argon (*grade 5.0*) plasma etching was conducted with a *Leybold-Heraeus* IQE-12/38 ion gun. The etching conditions were: 1×10^{-4} mbar argon, 10 A ionization current and 2250 V acceleration potential. The incident angle of the rastering plasma beam was 54.7° for the etching experiments; but, for electrode cleaning, the surface was rotated into the plasma beam giving incident angles between –30° and 60°.

X-ray Photoelectron Spectroscopy

Electrodes were transported to the XPS laboratory in closed (not airtight) containers. Before an electrode sample was introduced into the high vacuum system, a gold foil standard on the sample holder plate was analyzed for mercury contamination at a pass energy of 100 eV. If a mercury peak was observed in the XPS spectrum by scanning between binding energies from 95 to 110 eV, the gold foil was cleaned by argon plasma etching and then reanalyzed for mercury. At this point, the sample rod was removed from the XPS system and the gold electrode sample was placed on the holder plate on the side opposite of the gold foil standard. The sample rod was then reinserted into the XPS system and the gold electrode sample was pumped down, in an antechamber, to a pressure no greater than 1×10^{-7} mbar. This pump down time varied from 20 minutes to several hours (when left overnight). Once the pressure of 1×10^{-7} mbar was achieved, the sample was moved into the analysis chamber; where the XPS scans were recorded at base pressures less than 5×10^{-9} mbar. After all the desired spectra on the gold sample were recorded, the sample rod was rotated 180° and the gold foil standard was reanalyzed for the presence of mercury to see if contamination occurred during the time frame of the XPS experiment. No mercury peak was ever detected on the gold foil standard at this

point. The gold foil standard and the electrode were then etched clean with argon plasma etching, usually for 30 minutes for each foil. After etching, the electrode was again analyzed for the presence of mercury and then immediately removed from the system and stored for another electrochemical experiment.

Safety:

Any waste solutions of concentrations more than 20 ppb Hg were collected and stored for hazardous waste disposal pursuant EPA regulation 40CFR 261.24.[`]

[`] Code of Federal Regulations, Environmental Protection Agency, www.access.gpo.gov/nara/cfr/index.html.

Results and Discussion

The Latimer diagrams below indicate the formal oxidation potentials for mercury and gold as free cations in acidic media as well as for the corresponding chloride complexes (in parentheses)†.[11] The chloride complexes are at saturated concentrations. As illustrated in the diagrams and in Equation 2.1,[12] mercury oxidation, either from Hg^0 or Hg_2^{2+}, occurs at potentials below 0.8 V, whereas oxidation of gold generally requires higher potentials.

$$Au_2O_3 + 6\,H^+ + 6\,e^- \rightleftharpoons 2\,Au + 3\,H_2O \qquad E^0 \approx 1.0\ V\ (vs.\ Ag/AgCl) \qquad (2.1)$$

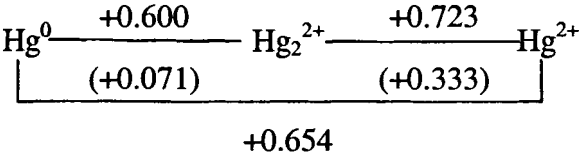

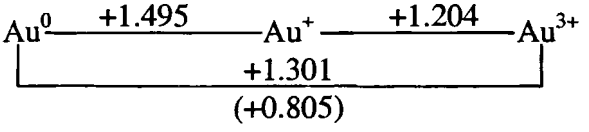

Johnson and coworkers reported cyclic voltammetry studies using a gold rotating disk electrode (ω = 3,600 rev min^{-1}, ϕ = 2.0 V/min) with 0.1 mM Hg^{2+} in aqueous 0.1 M $HClO_4$.[7] Cycling between 0 and +1.6 V (*vs.* SCE), they observed that mercury was readily reduced during each cathodic sweep, and that three oxidation processes occurred

---

† The Latimer diagram was constructed using Standard Reduction Potentials published in reference 11a and 11b, and converting the reference electrode, NHE, to a Ag/AgCl reference couple by subtracting 0.197 volts.

on each anodic sweep at +0.4, +0.8, and +1.2 V. The first oxidation wave at +0.4 V was assigned as one electron stripping of surface mercury, i.e. $Hg^0 \rightarrow Hg^{1+} + e^-$, while the second wave at +0.8 V was assigned as the stripping of mercury from the gold-mercury alloy. Interestingly, while the position and peak current of the first oxidation process remained fairly constant during 10 successive cyclic voltammetry scans, the oxidation signal at +0.8 V increased.

Cyclic Voltammetry:

The features of Johnson's CVs were reproduced in CV experiments we ran at 100 mV/s with 0.1 mM $HgCl_2$ and $Hg(NO_3)_2$ in 0.1 M $NaClO_4$ (Figure 2.3) however, the potential shifts are markedly different for each Hg^{2+} species. Figure 2.3a, the CV of $HgCl_2$, has the three oxidation processes at +0.3, +0.4 and +0.7V and corresponding potentials for of $Hg(NO_3)_2$ (Figure 2.3b) are at +0.5, +0.65 and +0.9V. These are related to the peaks in Johnson's CVs as: the one electron oxidation (+0.3 and +0.5V), the oxidation of mercury from the Hg-Au amalgam surface (+0.4 and +0.65), and a second mercury oxidation in the Hg-Au amalgam (+0.7 and +0.9V). In the $NaClO_4$ electrolyte, the surface of the gold electrodes started to oxidize at potentials more positive than +0.8 and +1.0 V in the presence of $HgCl_2$ and $Hg(NO_3)_2$ respectively. Figure 2.4 shows that, with our experimental set-up, the oxidation of the gold electrode starts at similar potentials in the chloride and nitrate-based electrolytes.

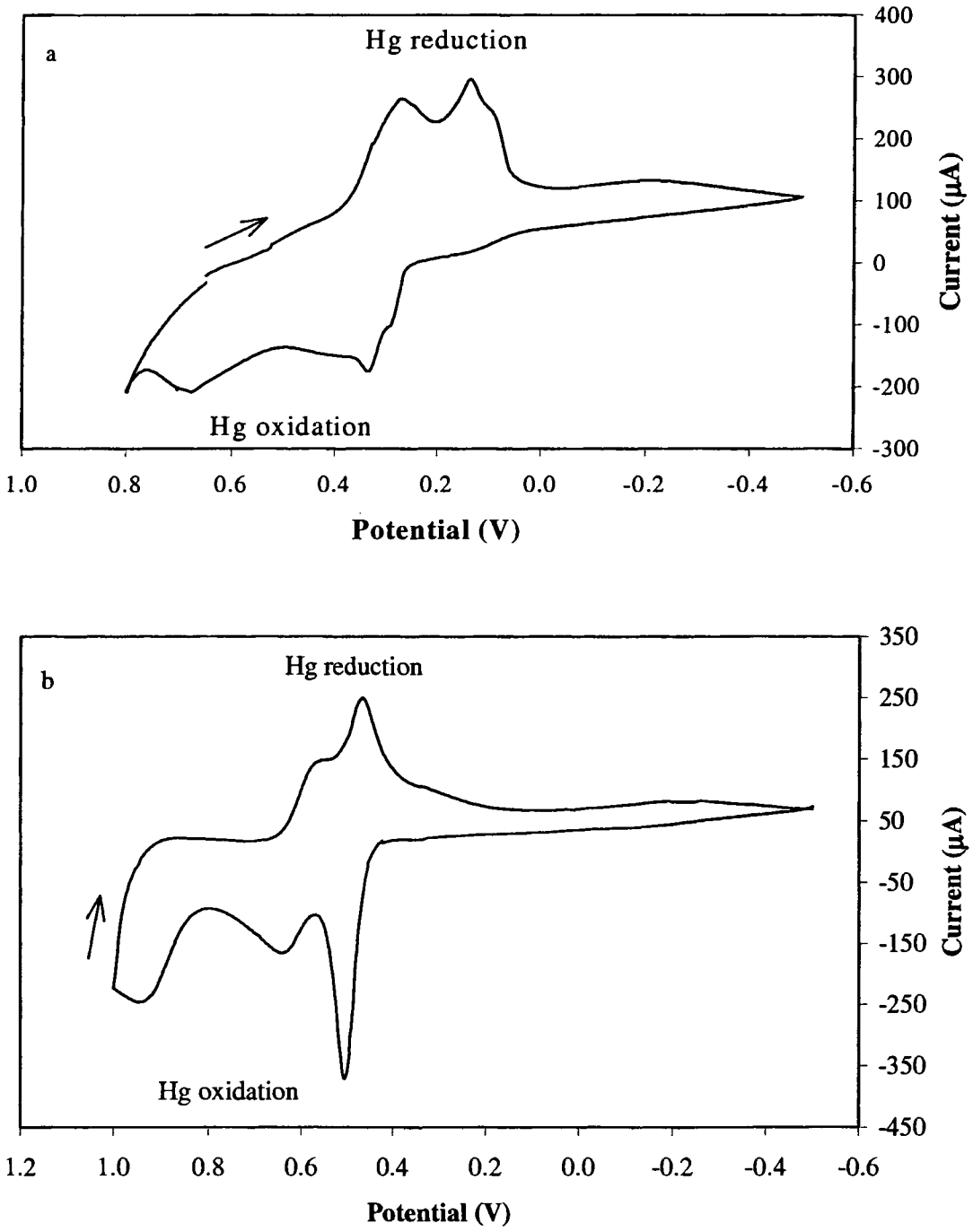

Figure 2.3: 100 mV/s Cyclic voltammograms of (a) 0.5 mM $HgCl_2$ and (b) 0.5 mM $Hg(NO_3)_2$ in 0.1 M $NaClO_4$ run on 0.5 cm^2 Au electrodes with a Ag/AgCl and a Pt wire as reference and auxiliary electrodes: separated by porous glass frits. The potential sweep profiles were: a) +0.65, –0.5, +0.8, +0.65 V and b) +1.0, –0.5, +1.0.

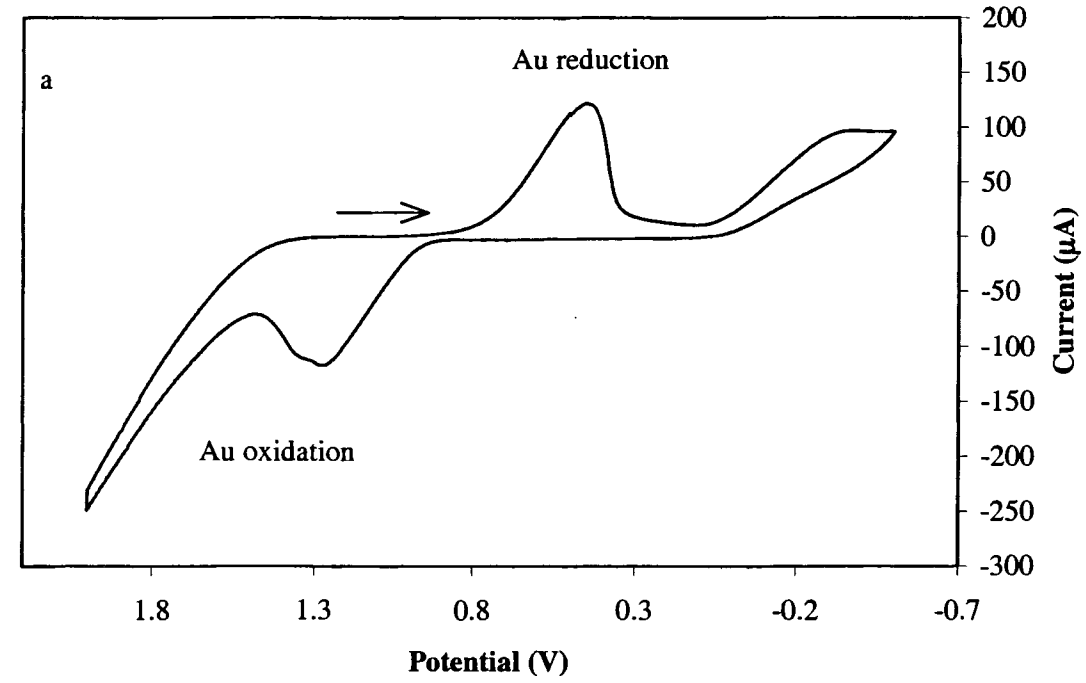

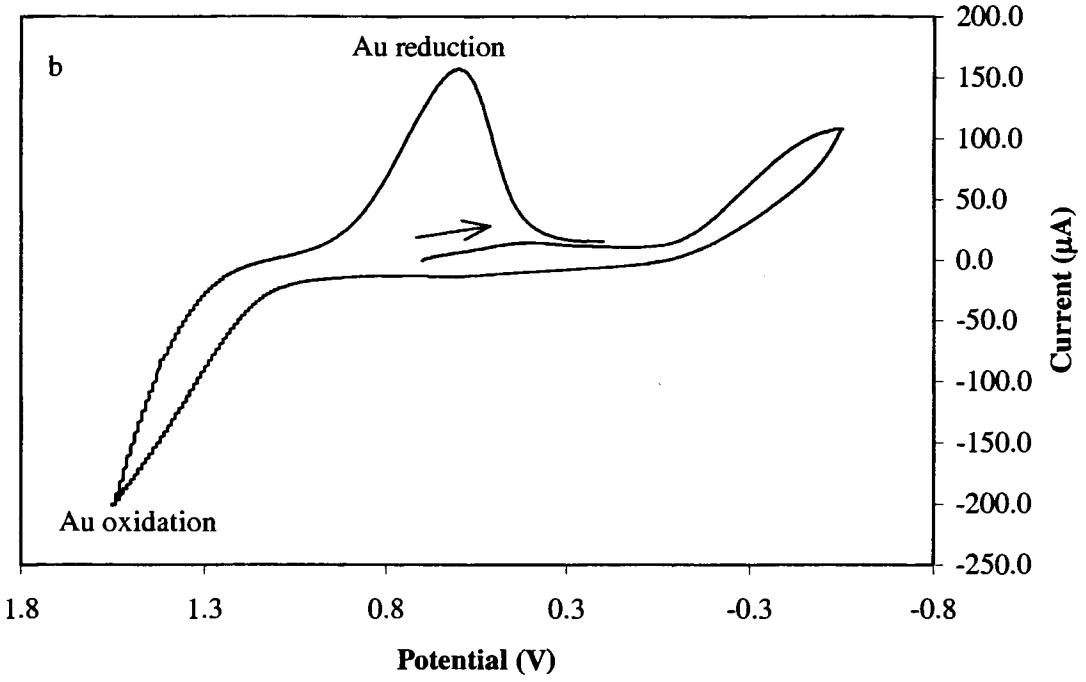

Figure 2.4: 100 mV/s Cyclic voltammograms of (a) 2.5 mM KCl and (b) 2.5 mM KNO_3, acidified to pH3 with HCl and HNO_3, run on 0.5 cm^2 Au electrodes with a Ag/AgCl and a Pt wire as reference and auxiliary electrodes: separated by porous glass frits. The potential sweep profiles were: a) +0.5, –1.0, +2.0, +0.5 V and b) +0.65, –0.5, +1.5, +0.65 V.

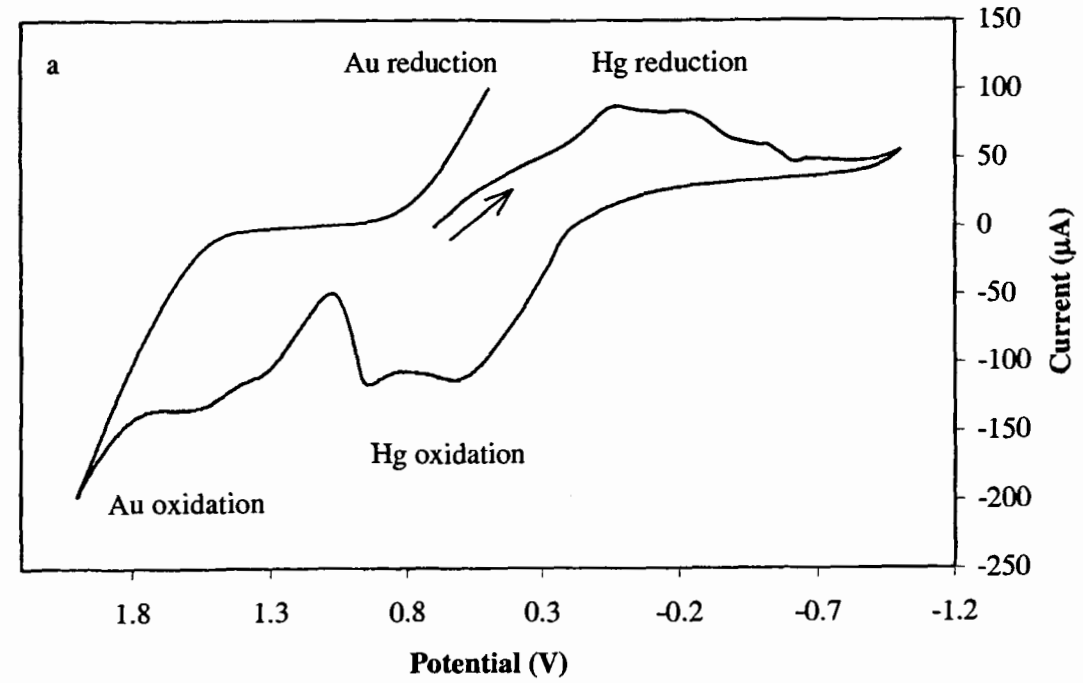

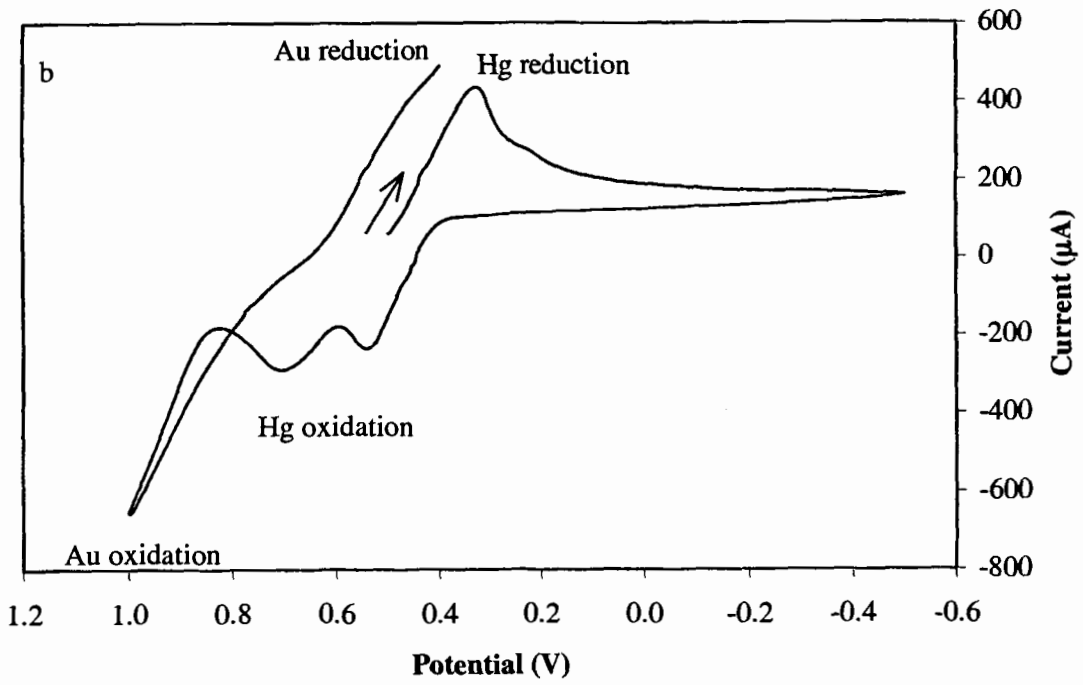

Figure 2.5: 100 mV/s Cyclic voltammograms of (a) 0.5 mM $HgCl_2$ in 2.5 mM KCl and (b) 0.5 mM $Hg(NO_3)_2$ in 2.5 mM KNO_3, acidified to pH3 with HCl and HNO_3, run on 0.5 cm^2 Au electrodes with a Ag/AgCl and a Pt wire as reference and auxiliary electrodes: separated by porous glass frits. The potential sweep profiles were: a) +0.5, –1.0, +2.0, +0.5 V and b) +0.65, –0.5, +1.5, +0.65 V.

Figure 2.3 shows that the reduction potentials of $Hg(NO_3)_2$, in 0.1 M $NaClO_4$, are shifted positively 400 mV from $HgCl_2$. The disparity in the redox potentials of these two Hg^{2+} species suggests that chloride is a better ligand than nitrate for mercury. This implies that there is a higher energy barrier to reduce Hg^{2+} (more negative potential) and a lower energy barrier for the oxidation of Hg^0 to Hg^{2+} (less positive potential) in the presence of Cl^- as opposed to NO_3^-. This suggests that stripping should be more efficient in media that contain chloride.

Cyclic voltammetry experiments on 0.5 mM $HgCl_2$ and $Hg(NO_3)_2$ in their respective supporting electrolytes (2.5 mM KCl / KNO_3 acidified to pH 3 with HCl / HNO_3) are shown in Figure 2.5. These aqueous solutions were investigated to establish the potentials of mercury and gold oxidation in the three compartment cell employed in this study. Cycling between –1.0 V and +2.0 V at 100 mV/s, the CVs have similar patterns to the CVs reported by Johnson and coworkers was observed with some minor variations. On each anodic sweep, a shoulder was observed at ca. +0.25 V (in comparison to the well-resolved peak observed at +0.2V by Johnson and coworkers[7]) followed by peaks at ~+0.55 , +1.0 , and +1.5 V. The additional oxidation wave observed at ~+1.5 V, due to the wider potential limit employed in our study, was assigned as oxidation of the gold electrode. Thus, the cyclic voltammetry investigation established that upon each anodic sweep, oxidation occurred at ~+0.25, +0.55, +1.0, and +1.5 V; the first two which appear to involve mercury and the latter two gold. All the features of the CV in 2.5 mM KCl were seen in CVs run in 1.0 M KCl, with the only differences being a tightening up of the voltammogram due to the decreased iR drop in the electrochemical cell. At higher

mercury concentrations, where the gold electrode becomes silvered in the course of the CV experiment, the deposition and stripping processes can be observed with the naked eye.

To complete the comparison of the electrochemical nature of chloride and nitrate-based mercuric salts in their respective electrolytes we see in Figure 2.5 the mercury reduction peak is shifted positively from about + 0.05 to +0.35 V. The bulk mercury oxidation process, which occurs at +0.55 V in chloride containing solutions, is shifted to +0.75 V in the nitrate solutions. With our experimental set-up, the oxidation of gold starts at about +0.9 V in nitrate solutions (Figure 2.5 b); a shift of 0.2 V to the negative compared to the chloride solutions (Figure 2.5a). Repeated CV cycling in 40 nM solutions of both Hg^{2+} species showed a more rapid increase in the area of the mercury oxidation peaks for the nitrate solutions. Additionally, in nitrate solutions, the areas of the mercury oxidation peaks did not diminish significantly when the CV cycling was continued in Hg-free electrolyte flowing at 40 mL/min for a period of 25 minutes. These results indicated that the mercury stripping efficiency is much better in chloride solutions than in nitrate solutions.

Having established the potentials at which various oxidation processes occur in the three compartment cell, the effects of mercury deposition, stripping, and cleaning of the gold foil electrode were studied using the $HgCl_2$ / KCl system. Deposition of mercury was accomplished by first introducing a cleaned 0.5 cm^2 gold working electrode into the central working electrode compartment. The potential of the electrode in a stirred, aqueous solution (2.5 mM KCl, pH 3) was then set to –0.3 V. After a current baseline was established, an aliquot of mercury chloride was injected into the central working

electrode chamber, resulting in an initial 0.1 mM Hg^{2+} concentration. Deposition of mercury onto the gold foil electrode readily occurs at -0.3V and was allowed to continue for 60 seconds. By switching to a positive potential between +0.7 and +2.5 V, the deposited mercury was oxidized and stripped from the electrode surface. The stripping step generally occurred within seconds after switching the potential and was characterized by a large current peak that quickly returned to baseline. The electrode was held at the positive potential for a total of 600 seconds, ten times longer than the deposition time, to ensure ample time for the electrode to be cleaned.

XPS Analysis:

XPS scans of the gold foil electrodes are shown in Figure 2.6. Each XPS spectrum (5a–e) represents a separate experiment in which deposited mercury was stripped and cleaned at potentials ranging from +0.7 to 2.5 V. Mercury is characterized by the doublet $4f_{7/2-5/2}$ photoelectron emissions occurring at 100 and 104 electron volts. Since the baseline noise is approximately the same intensity in each spectrum, the relative amounts of mercury can be qualitatively compared. The area of the mercury peaks in XPS scans of electrodes that had different amount of mercury adsorbed onto the surface before stripping (determined by the stripping peak area) were essentially the same. This indicates that there was no immediate passivation of the mercury-gold electrode surface that prevented further oxidation of the mercury. It was also noted that there was neither chloride, nor oxygen, detected by XPS on any electrode, after the electrochemical deposition of mercury, or after its stripping.

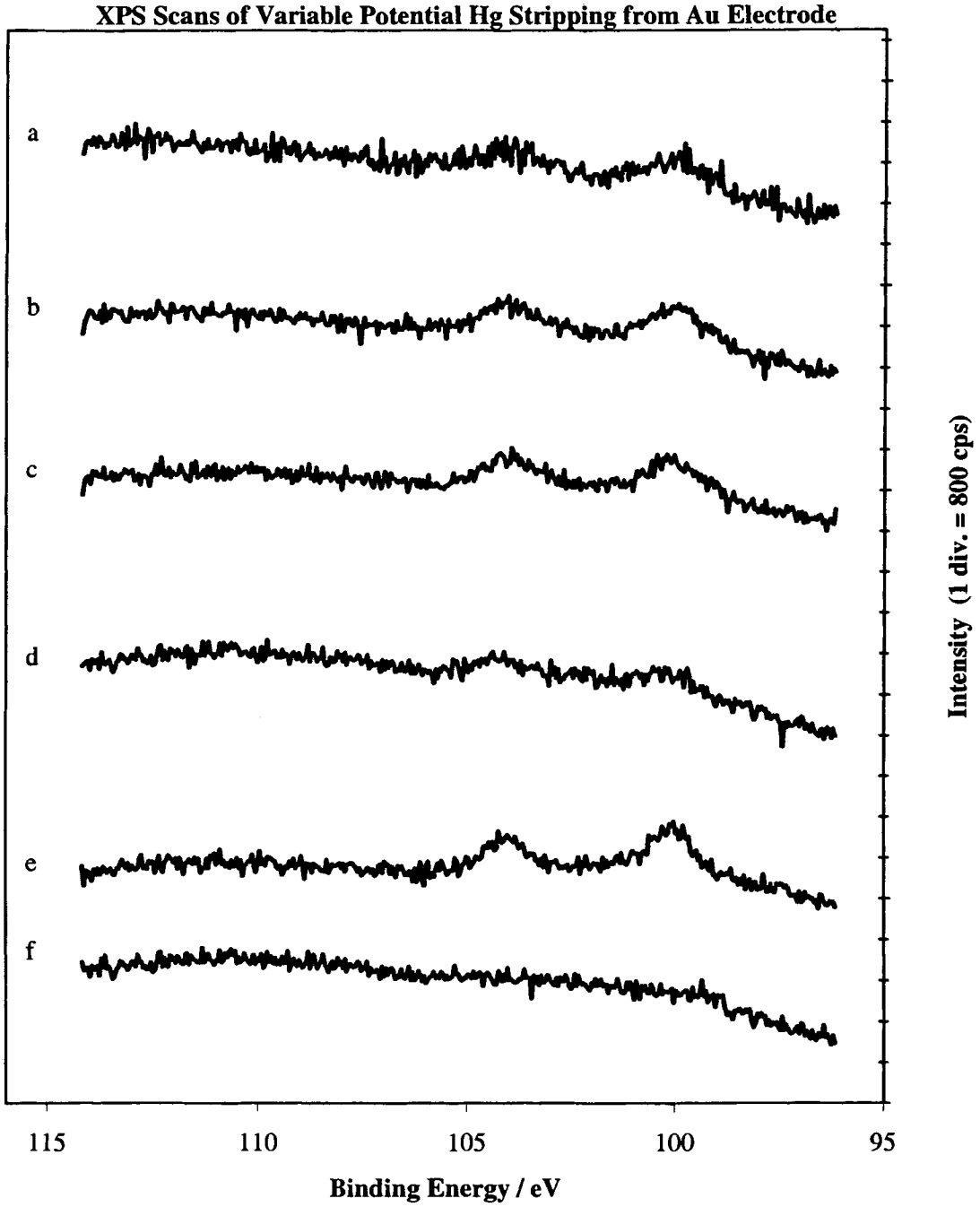

Figure 2.6: XPS scans of 1 cm^2 Au foils after 150 s electrochemical deposition at -0.3 V in 0.1 mM Hg(II) followed by stripping for 600 s at: a) 2.5; b) 1.9; c) 1.5; d) 1.1 and e) 0.7 V vs. Ag/AgCl. Spectra f) is the gold foil after argon plasma etching. Photoelectron emission was induced with Mg K_α X-rays from 20 mA emission current across a 11 kV potential with analysis at 50 eV pass energy. The base pressure was $< 1 \times 10^{-11}$ bar.

The most striking feature in Figure 2.6a–e is the presence of mercury on all of the gold foil surfaces. This is significant because it indicates a difficulty in electrochemically removing mercury from gold electrodes. Qualitatively, the amount of mercury remaining on the electrodes is lowest when the potential of +1.1 V is used to strip and clean it. Possible explanations for why the potential may effect removal of residual mercury are that at high over-potentials (> 1.1 V), oxidation of the gold surface to gold oxide may provide a barrier against further oxidation of mercury[7] and at +0.7 V, there may not be a significant driving force for oxidation and complete removal of mercury from the gold surface, due to underpotential deposition.[13] The experiment at +1.1 V may represent a potential which minimizes the formation of gold oxide; however, it is clear that at this potential, mercury remains even after stripping and cleaning the electrode for a period ten times longer than the deposition time.

Bulk Electrolysis:

A series of bulk electrolysis experiments were run to gain insight into the fate of mercury during deposition and stripping. In the first set of experiments, Hg^{2+} was reduced at a gold foil electrode by applying a potential of -0.3 V for thirty minutes using initial Hg^{2+} concentrations ranging from 35 nM to 110 μM Hg^{2+}. After deposition, the solution was removed for analysis by CVAA. Then, fresh electrolyte was introduced into the working compartment and the mercury was stripped off the electrode into solution by applying an oxidizing potential of +1.0 V for thirty minutes. The working compartment solution was then analyzed again by CVAA. A representative set of amperograms of these experiments is shown in Figure 2.7.

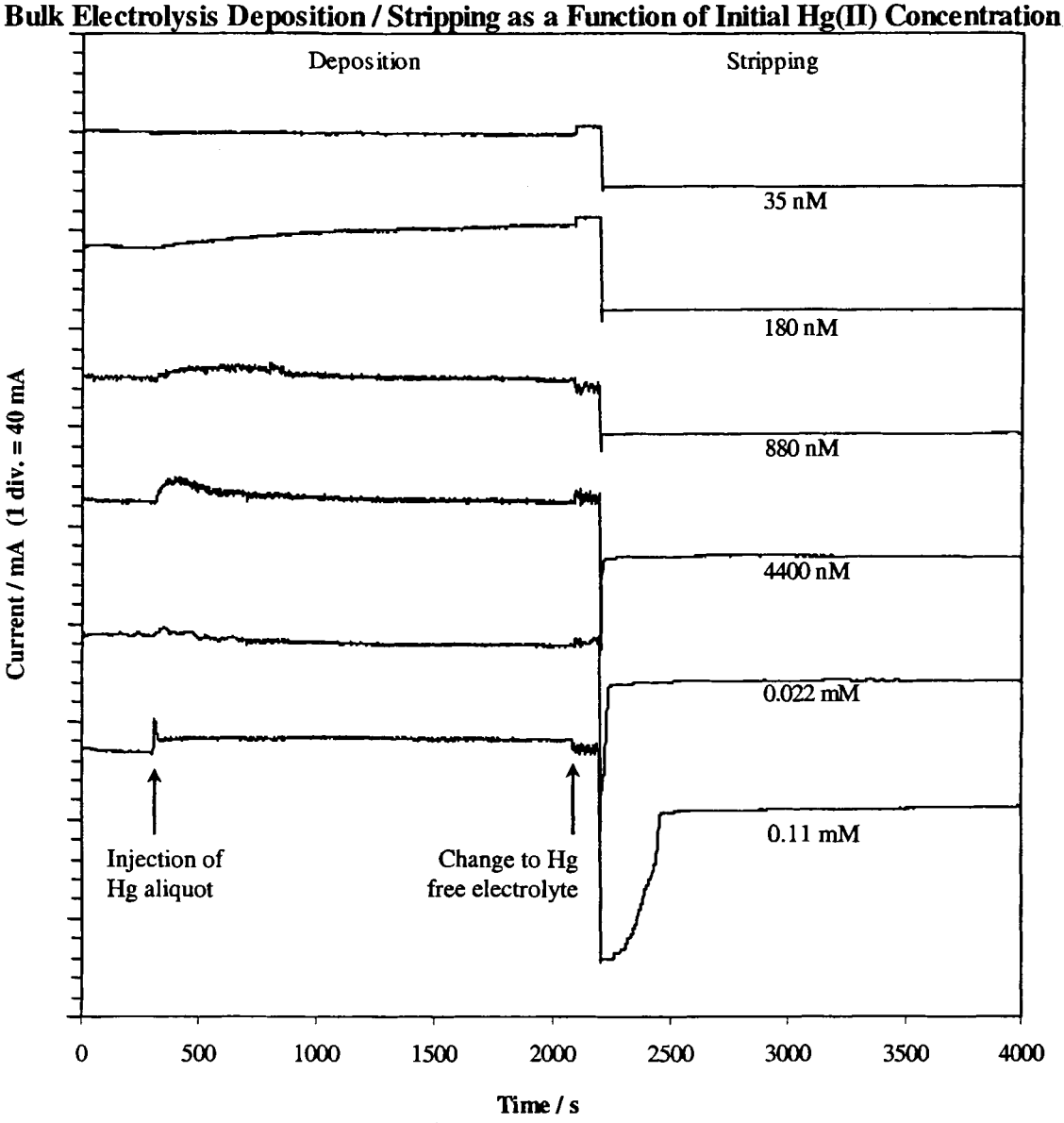

Figure 2.7: Amperograms of six deposition and stripping experiments run on 0.5 cm^2 Au electrodes in 18 mL 2.5 mM KCl (pH 3), with Pt wire auxiliary electrode and magnetic bar stirring at the following initial $HgCl_2$ concentrations (10^{-6} M): a) 0.035, b) 0.180, c) 0.880, d) 4.40, e) 22.0 and f) 110. The procedure was as follows: 300 s current stabilization at –0.3V (vs. Ag/AgCl), injection of a 0.2 mL aliquot of Hg(II), deposition continued at –0.3V for 1800s; interruption of the experiment to collect and replace the electrolyte with Hg-free electrolyte. The potential was again set at –0.3 V for 100 s and then switched to 1.0V for stripping and cleaning for 1800 s.

Table 2.1: μg Hg in Controlled Potential Deposition and Stripping with CVAA analysis of Solutions

Initial Injection[a] (CVAA)	In Solution After Deposition[b] (CVAA)	Stripping[c] (CVAA)	Deposition Peak Area[d] (current)	Stripping Peak Area[d] (current)	Theoretical % Recovered[e]
0.15	0.16	0.01	2.9	0.009	110
0.62	0.49	0.16	57	0.18	100
3.1	2.5	0.61	9.3	0.34	83
14	8.9	2.6	27	1.5	82
93	74	8.3	15	8.6	88
336	280	64	8.9	69	100

a) Initial Hg^{2+} injected into reaction chamber for a finial volume of 18 ± 0.5 mL. b) Mercury in solution after stripping for 30 minutes at 1.0V (assumed Hg^{2+}). c) Mercury of unknown oxidation state remaining in solution unabsorbed onto the gold electrode after 30 minutes of deposition at 0.3V. d) Values determined by subtracting the integrated background current from the integrated current of the stripping and deposition peaks and converting the charge to μg of mercury by assuming two electron processes. e) Percent of the available mercury recovered from the gold electrode as calculated by the sum of columns 2 and 3, divided by column 1, times 100.

As expected, we can see in Table 2.1 there was a 1:1 relationship, with a high linear correlation coefficient (0.9997), between the amount of mercury stripped, as calculated from integrated charge during stripping, assuming a two electron oxidation process, and the amount of mercury found in solution after stripping, determined by CVAA analysis.[14] This provides confirmation of the utility of the stripping procedure using Faraday's Law of electrolysis (equation 2.2). This law equates the charge (q) from

the integrated current (i), with respect to time (t), to the moles (m) of material involved in the electrochemical process by using the number of electrons per molecule (n) transferred and *Faraday*'s constant (F: 96 487 coulombs/mole).

$$q = \int_0^t i\,dt = mnF \tag{2.2}$$

There was no such correlation (0.0853) between mercury deposition, as calculated from integrated charge during deposition, and the amount of mercury in solution after stripping, determined by CVAA analysis (or calculated from integrated charge during stripping). This was an unexpected result, because the baseline background current (from non-Faradaic processes such as reduction of water or trace amounts of oxygen) was clearly well established before mercury was injected into the working compartment. Subtraction of the background current, which incorporates non-Faradaic processes, from the sample deposition current should have resulted in a relatively good correlation if there were no changes in the nature of the electrode.

In general, the integrated current during deposition (after subtracting out background current) predicted a much greater amount of mercury was deposited than subsequently was determined to be in solution after stripping. This led us to investigate whether a significant amount of mercury was diffusing into the electrode. Previous studies have suggested mercury atoms diffuse into gold when the coverage of mercury

exceeds a monolayer.[7,13a] To test this possibility, we performed argon plasma etching on two electrodes that had undergone one and ten deposition, stripping, and cleaning cycles, respectively (deposition in 0.02 mM Hg^{2+} at –0.3 V for 60 seconds followed by stripping and cleaning for 600 seconds at +1.0V). XPS monitoring was done concurrently with argon plasma etching. The etching rate for both electrodes was assumed to be the same because they were analyzed under the same conditions: 1×10^{-4} mbar argon, 10 A ionization current and 2250 V acceleration potential. After establishing the presence of mercury by XPS, the etching was started and within the time for an additional XPS scan (60 seconds), the mercury peaks had disappeared. Although the sputtering rate has not been calibrated on the UHV system that we used, the etching depth is estimated to be approximately 50 ± 25 Å, based on etching rates published by Matsunami et al.[15] This result demonstrates that mercury does not diffuse deeply into the gold at concentrations detectable by XPS. This is discussed further in Chapter III.

One way to explain the discrepancy between the deposition and stripping integrated current is to assume that a fundamental change to the electrode occurs during deposition. Figure 2.8 shows results from an experiment that was designed to explore this possibility. After a baseline was established at –0.3 V, a solution containing a total of 40 ng of Hg^{2+} was injected into the solution and deposition was allowed to occur for 50 seconds. Thereafter, the electrolyte solution was changed, i.e. all solution forms of mercury were removed. It is clear from Figure 2.8 that a new baseline was established. The overall effect of a similar change in baseline during a bulk electrolysis experiment

would be to over estimate the amount of current involved in the Faradaic process. This is, in general, exactly what was observed at low mercury concentrations. The baseline shift is consistent with a change in the nature of the electrode and suggests that a gold-mercury amalgam electrode forms, which has very different electrochemical properties than a pure gold electrode. It is interesting to note that the response of the electrode was not always the same and at higher concentrations, the baseline shift actually reversed itself (compared to what is seen in Figure 2.8) and is the reason that a near zero correlation coefficient is found.

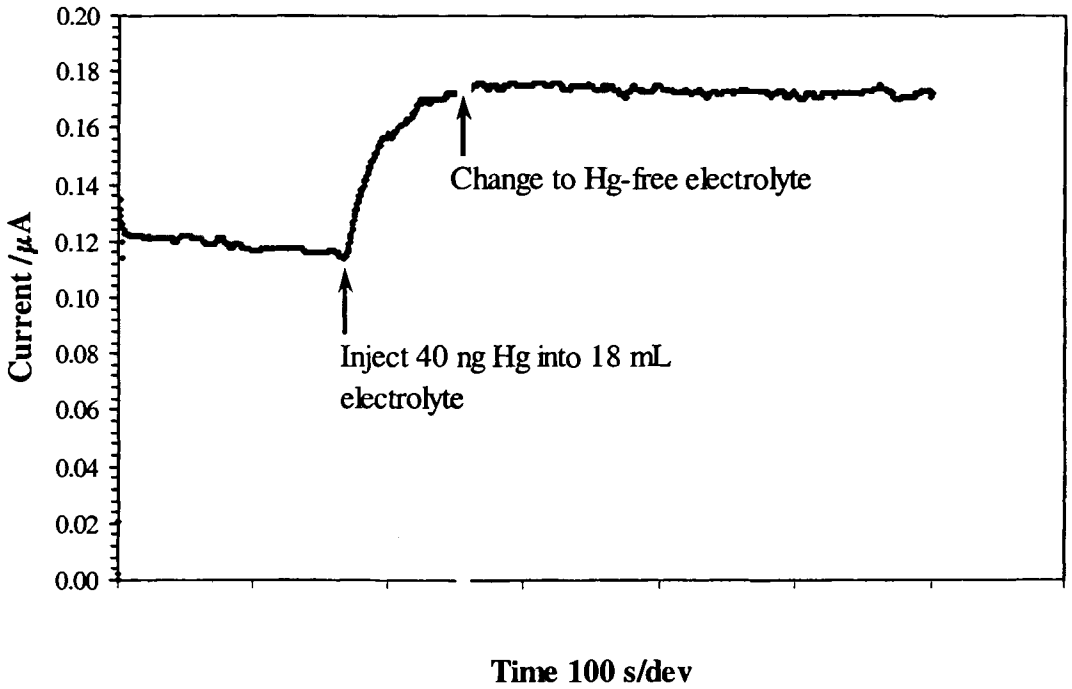

Figure 2.8: Amperogram, before and after, injection of 40 ng Hg^{2+} in 18 mL, 2.5 mM KCl, at pH 3 (1×10^{-8} M Hg^{2+}) after 200 s at –0.3 V vs. Ag/AgCl. The break in the figure indicates the point at which the electrolyte solution was changed. Electrolysis was continued at –0.3 V in Hg(II) free electrolyte.

Comparison of the amount of mercury left in solution after each 30 minute deposition (3rd column), to the amount initially added to the cell (1st column) shows that most of the mercury remains in solution and is not adsorbed onto the electrode. As discussed above, it is difficult to establish the amount of mercury reduced due in part to the fundamental changes occurring at the electrode as electrolysis proceeds. However, with the exception that a different baseline is established after deposition is started, the current-time response during a 30 minute bulk electrolysis experiment is typical for an electrochemical process that has gone nearly to completion (i.e. current levels out and thereafter remains unchanged). The fact that a significant amount of mercury remains in solution at the end of the deposition step suggests at least two possibilities. Either the electrode becomes passivated during the electrolysis experiments or Hg^0 has an adsorption probability less than 1 at the electrode and thus is washed off the electrode during the experiment. To test for passivation, a gold electrode was removed at the end of a 30 minute deposition experiment in 4 μM Hg^{2+} and then used to perform another bulk electrolysis (with fresh mercury solution). Figure 2.9 shows the amperograms for when this procedure was performed five times (Figure 2.9b–f) as compared to only once(Figure 2.9 a). In the five successive depositions without stripping, the total current measured during deposition appears to diminish significantly. However, when the electrode was stripped at the end of these five cumulative depositions, more than five times the stripping area (8.1 μC) was observed compared to when the procedure was performed only once (1.3 μC). This suggests that passivation of the electrode is not occurring, but rather that the fundamental characteristics of the electrode are changing as a result of mercury accumulating on the electrode surface. Migration of reduced mercury into solution remains a possibility and has been reported when dilute Hg^{2+} solutions were used to deposit mercury onto glassy carbon electrodes.[16]

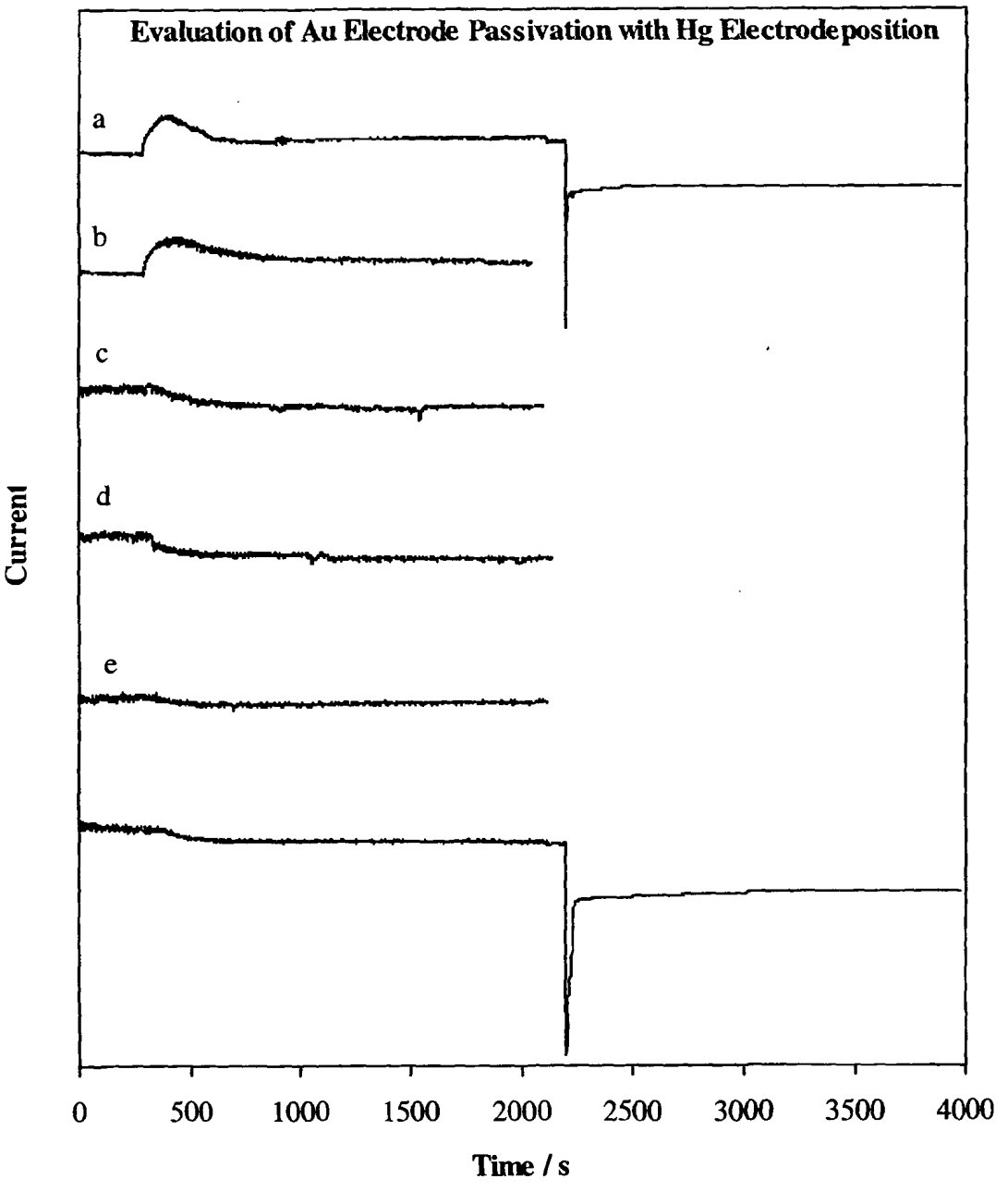

Figure 2.9: Amperograms of deposition and stripping experiments on 0.5 cm^2 Au electrode in 2.5 mM KCl at pH 3, containing 4 μM Hg(II), with Pt wire auxiliary electrode and magnetic bar stirring. The procedure was as follows: 300 s current stabilization at –0.3V vs. Ag/AgCl followed by injection of a 0.2 mL aliquot of 4×10^{-4} M Hg(II). Experiment (a): 1800s of deposition at – 0.3V, interruption of experiment to change to Hg free electrolyte, then stripping at 1.0V for 1800s. Experiments (b – e): 1800s of deposition at –0.3V, interruption of experiment to change to Hg free electrolyte, then starting over with new Hg(II) injection **without stripping**. Experiment (f) immediately followed (e) and was conducted the same as (a).

Conclusions

As outlined in the introduction, gold electrodes offer many attractive features for electrochemical stripping analysis of mercury. However, the present study, demonstrates that some of the mercury that is adsorbed during deposition is retained even after stripping and electrochemical cleaning. While the concentration range on mercury used in this study was relatively high, preliminary data using mercury levels near the safe drinking water limits suggest that irreversible adsorption of mercury also occurs under these conditions. This is developed further in Chapter III. These results indicate that in long term, repetitive, stripping analysis situations, the deposition, stripping and adsorption processes need to be better understood and taken into account before the goal of developing a sensor capable of remote quantification of mercury in the environment is realized.

One attractive strategy that may be employed is to add a complimentary technique, such as a piezoelectric sensor.[2,17] The added sensor would be able to monitor mass changes at the electrode during deposition, stripping, and cleaning cycles. A piezoelectric sensor could be used to recalibrate the electrode after each stripping analysis cycle, thus overcoming some of the problems that are resultant of the retention of mercury on the gold electrodes. Another attractive feature of combining piezoelectric and traditional electrochemical technology would be that it could offer additional ways to analyze the data. For example, mass to charge ratios could be used to identify analytes as they are removed from the electrode.

For Further Experimentation

The natural continuance of the work featured in this chapter is the investigation of the accumulation of mercury on gold electrodes: Chapter III. However, there are many unexplained phenomena observed in these experiments that could be continued in other thesis projects. Why does approximately 80% of the mercury at various concentrations remain in solution during bulk electrolysis deposition?" The first experiment, explained in the introduction, gave an interesting macroscopic look at what may be occurring microscopically and that is the formation of stable mercury clusters on the electrode surface that readily desorb form the gold electrode.

It has been concluded in careful underpotential deposition on ring disk electrodes that the reduction of Hg(II) occurs by two one electron processes,[18] and that on the surface of the electrode there exist at the same time charged mercury species along with neutral mercury.[18 a, b] Charged mercury clusters combine with uncharged mercury to rapidly form larger stable clusters.[19] The size stability of the mercury clusters increases with increasing cationic cluster charge. This has been studied to Hg_{100}^{3+}.[20]

The examination of the nature of the mercury that remains in solution after bulk electrolysis could simply first be analyzed for Hg(0) by CVAAS, with out the use of the Sn(II) reducing agent, or the $KMnO_4$ oxidizing agent. This experimentation could conceivably be done by an undergraduate student. The solution could also be analyzed by Raman spectroscopy for the presence of mercury mercury metal bonds.[21]

References

[1] Watson, C. M., Dwyer, D. J., Andle, J. C., Bruce, A. E., Bruce, M. R. M. Analytical Chemistry, 1999, 71(15), 3181-3186.

[2] a) Andle, J., Schweyer, M., Munson, J., Roderick, R., McAllister, D., French, L., Vetelino, J., Watson, C., Foley, J., Bruce, A., Bruce, M. Proceedings of the IEEE International Frequency Control Symosium, 1997, 51, 90-95. b) Evans, O. McKee, G.. Analyst, 1988, 113(2), 243-6. c) Ho, M., Guilbault, G., Scheide, E. Analytica Chimica Acta, 1981, 130(1), 141-7. d) Wu, Q., Apte, S., Batley, G., Karl, C. Analytica Chimica Acta, 1997, 350(1-2), 129-34. e) Svancara, I., Matousek, M., Sikora, E., Schachl, K.. Electroanalysis, 1997, 9(11), 827-833. f) Viltchinskaia, E., Zeigman, L., Garcia, D. Santos, P. Electroanalysis, 1997, 9(8), 633-40. g) Korolczuk, M. Fresenius' Journal of Analytical Chemistry, 1997, 357(4), 389-91. h) Uhlig, A., Schnakenberg, U., Hintshce, R. Electroanalysis, 1997, 9(2), 125-9.

[3] Dewald, H. D. In, Modern Techniques in Electroanalysis, Vanysek, P., Ed., Wiley: New York, 1996, pp 151-185.

[4] Zen, J.-M., Chung, M.-J. Analytical Chemistry, 1995, 67, 3571-3577.

[5] a) Gil, E. P., Ostapczuk, P. Analytica Chimica Acta, 1994, 293, 55-64. b) Ostapczuk, P. Analytica Chimica Acta, 1993, 271, 35-40.

[6] a) Rievaj, M., Mesáros, S., Bustin, D. Collection of Czechoslovak Chemical Communications, 1993, 58, 2918-2923. b) Wang, J., Larson, D., Foster, N., Armalis, S., Lu, J., Rongrong, X., Olsen, K., Zirino, A. Analytical Chemistry, 1995, 67, 1481-1485.

[7] Schadewald, L. A., Linstrom, T. R., Hussein, W., Evenson, E. E., Johnson, D. C. Journal of the Electrochemical Society, 1984, 131, 7.

[8] Greef, R., Peat, R., Peter, L., Pletcher, D., Robinson, Journal of Instrumental Methods in Electrochemistry, Ellis Horwood Ltd.: Chichester, 1985, 233.

[9] a) Rademann, K., Kaiser, B., Even, U., Hensel, F. Physical Review Letters, 1987, 59(20), 2319-21. b) Jortner, J. In, Physics and Chemistry of Finite Systems: From

Clusters to Crystals, Jena, P., Khanna, S. N., Rao, B. K., Eds., NATO ASI Series, Klumer Academic Publishers: Dorrecht, 1991, chap.1. c) Haberland, H., Kornmeier, H., Langosch, H., Oschwald, M., Tanner, G. Journal of the Chemical Society, Faraday Transactions, 1990, 86(13), 2473-81.

[10] The Nalco Water Handbook 2nd Ed., Kremmer, F. Ed., McGraw-Hill, New York, 1988, 231-4.

[11] a) Vanysek, P. In CRC Handbook of Chemistry and Physics, 71st Ed. D. R. Lide, D. R., Ed., CRC Press: Boca Raton, 1990-1991, Table 1, p. 8-16. b) Latimer, W. M. The Oxidation States of the Elements and their Potentials in Aqueous Solutions 2nd Ed., Prentice-Hall, Englewood Cliffs, 1952. c) Mohamed, A. A., Bruce, A. E., Bruce, M. R. M. In Organic Derivatives of Silver and Gold, Patai, S., Rappaport, Z., Eds., John Wiley & Sons: London.

[12] Burke, L. D. and Nugent, P.F., Gold Bulletin, 1997, 30, 143-53.

[13] a) Li, J., Abruña, H. Journal of Physical Chemistry: B, 1997, 101, 2907-2916. b) Sherwood, W., Bruckenstein, S. Journal of the Electrochemical Society. 1978, 125, 1098-1102.

[14] a) Osteryoung, J., Stojek, Z. Analytical Chemistry, 1988, 60, 131-141. b) Tokoro, R., Tavares, M. Analytical Letters., 1986, 19, 2079-2094.

[15] Matsunami, I. N., Yananura, Y., Itikawa, Y., Itoh, N., Kazumata, Y., Miyagawa, S., Morita, K., Shimizu R., Tawara, H. Atomic Data Nuclear Tables, 1984, 31, 1.

[16] Yoshida, A., Kihara, S. Journal of Electroanalytical Chemistry, 1979, 95, 159-68.

[17] Buttry, D. A., Ward, M. D. Chemical Reviews, 1992, 92, 1355-1379

[18] a) Salie, G., Bartels, K. Journal of Electroanalytical Chemistry and Interfacial Electrochemistry, 1988, 245(1-2), 21-38. b) Salie, G., Bartels, K. Electrochimica Acta, 1994, 39(8-9), 1057-65. c) Herrero, E., Abruna, H. D. Journal of Physical Chemistry B, 1998, 102(2), 444-451.

[19] Sukhov, N. L., Ershov, B. G. Izvestiya Akademii Nauk SSSR, Seriya Khimicheskaya 1992,(1), 9-12. (abstract only).

[20] a) Wang, Y., Flad, H.-J., Dolg, M. Physical Review B: Condensed Matter and Materials Physics, 2000, 61(3), 2362-2370. b) Blanc, J., Broyer, M., Dugourd, P. H., Labastie, P., Sence, M., Wolfe, J. P., Woste, L. Journal of Chemical Physics, 1995, 102(2), 680-9.

[21] a) Hermon, H., Roth, M., Schieber, M., Shamir, J. Vibrational Spectroscopy, 1991, 2(2-3), 155-9. b) Myund, L. A., Kozhevnikova, G. V., Chernykh, L. V., Burkov, K. A. Vestnik Leningradskogo Universiteta, Seriya 4: Fizika, Khimiya, 1978, (3), 67-71. (absract only). c) Keller, A., Atabek, O. Physical Review A: Atomic, Molecular, and Optical Physics, 1993, 48(5), 3741-56.

CHAPTER III

Accumulation of Mercury on Gold Electrodes in Repetitive Controlled Potential Stripping Analysis

Introduction

The utilization of gold for the detection and quantification of mercury in the environment is highly desired because of its high affinity for mercury. In both aquatic[1] and atmospheric environments, gold's attraction for mercury allows for lower detection limits, by enhancing the effectiveness of pre-concentration steps over other electrode materials.[2] We have shown, in Chapter II, by x-ray photoelectron spectroscopic (XPS) analysis of gold foil electrodes, that in aqueous environments, with relatively high concentrations of mercury(II) species (10-100 μM), these gold electrodes retain a portion of the mercury electrodeposited (pre-concentrated) on them in stripping analysis procedures.[3] In

noting that the safe drinking water limit for mercury is 10 nM (2 μg/L, 2 ppb)[4] we can see that these concentrations would be found in only highly contaminated environments. Our XPS analysis of gold electrodes in solutions less than 1 μM Hg(II) did not reveal any mercury retained after one electrochemical deposition and stripping process. However, there was still a latent mercury oxidation peak in linear sweep voltammetry (LSV) after the stripping step had been completed. What is not clear is whether the retained mercury accumulates on the gold electrode or if it simply remains at a relatively constant surface concentration, to be easily factored into a stripping analysis procedure with perhaps a differential or subtractive stripping analysis that allows for continual recalibration.[5]

The accumulation of mercury on the gold electrodes used in potentiometric stripping analysis (PSA) could have several effects. It could give rise to either residual or enhanced stripping peaks; which would, respectively, indicate the presence of mercury when there is none or, register higher mercury concentrations than actually exist in a particular sample. Accumulation of mercury could alter the adsorption characteristics of the electrode, leading to mismeasurement of the actual environmental concentrations. It could alter the stripping potential of the electrode, giving rise to the misidentification of the species being electrochemically stripped. Thus, for any detection of mercury based on solely on electrochemical stripping, it is imperative to evaluate whether or not the mercury retained after one electrochemical deposition, stripping and

cleaning procedure continues to accumulate on gold electrodes in repetitive cycling. Finally, in field applications, the number of desirable reproducible cycles will be many times greater than the limited number that have been typically employed in laboratory studies. There continue to be new and innovative devices developed for the detection of mercury in the environment, with improving sensitivity; but, a thorough reading of the reports indicates that the emphasis is upon sensitivity and not the longevity of reliable results.[6]

We have thus extended our study of the irreversible adsorption of mercury on gold electrodes in controlled potential stripping analysis to include repetitive cycling of electrochemical deposition, stripping and cleaning procedures. We feel one aspect of such a study that has possibly been overlooked by others studying the same phenomena is the necessity of making such an evaluation with a constant supply of mercury. In most situations where mercury would be monitored, outside of laboratories, (i.e. rivers, lakes, wells, refuse sites) there is a constant renewal of the water to be analyzed. Thus, it is important to incorporate a flow-through type of system for analyzing solutions with low mercury concentrations. In Chapter II we demonstrated that even with exhaustive bulk electrolysis, most of the available mercury was not adsorbed onto the gold electrodes and we showed that this is not the result of electrode passivation We feel that experiments that employ a single beaker of a mercury solution will not give results that can be realistically extrapolated to environmental monitoring situations.

In this Chapter, we report the accumulation of mercury on gold foil electrodes from dilute Hg(II) solutions (40 to 4000 nM) that have either chloride or nitrate anionic counter-ions. The accumulation is shown by cyclic voltammetry (CV), linear sweep voltammetry (LSV) and thermal desorption spectroscopy (TDS). The potential and time parameters of the deposition and stripping cycles are drawn from our previous work and what others have done. The duration for most potentiometric stripping analysis (PSA) procedures, we have seen in the literature, are from 2 to 5 minutes.[1a-d, 7] The bulk of this time is taken up by the deposition (pre-concentration) step which ranges from 10 s to a few minutes: depending on the mercury concentration being tested. After electrodeposition of mercury on the gold electrodes there is usually a 15 s period to allow the stirred solution to become quiescent, and then the potentiometric stripping scan is run: taking approximately 30s. In some procedures there is an additional electrochemical oxidative cleaning step that lasts no more 30 s. However, we have not seen any reports of exhaustive repetitive cycling employing a flow-through system that provides a constant and renewed supply of analyte solution.

Experimental

Chemicals and Glassware:

Water for all electrolyte and soaking solutions and for glassware rinsing, was from a *Barnstead NANOpure* water purification system where the conductivity measured from the storage bottles was less than 0.1 μS/cm. All chemicals, unless otherwise noted, were *Certified ACS Reagent* Grade. The supporting electrolyte solutions (2.5 mM KCl, or KNO_3, at pH 3) were made daily by diluting either a 1.0 M KCl, or $KN0_3$, stock solution with water previously acidified to pH 3 with concentrated HCl or $HN0_3$. The pH of the electrolyte was stable during all electrochemical experiments. These electrolyte parameters have been shown to be adequate for conducting electrochemical deposition and stripping experiments with mercury(II) on gold electrodes[86] and our justification is reported earlier.[3] A 0.1 M $HgCl_2$ stock solution was made by dissolving $HgC1_2$ *(Aldrich* 99.999%) in 2% $HN0_3$. Mercuric chloride solutions of concentrations less than 1 x 10^{-4} M (20,000 ppm) were made fresh daily from this stock solution. Experiments employing solutions with no chloride ion were prepared in a similar manner except for: using $Hg(N0_3)_2$ *(Aldrich* 99.99%) to create the Hg(II) stock solutions.

All glassware was rinsed several times with water and then soaked in 50% nitric acid for at least 24 hours until just prior to use; whereupon, it was well rinsed again with water. All solution storage bottles were treated in the same manner.

Electrochemistry Equipment:

We employed the same three-chamber electrochemical cell, fabricated by *Anderson Glass* of New Hampshire, in the same manner as described in Chapter II and for the same reasons. The CV, LSV and controlled potential deposition and stripping

experiments were conducted with an *EG&G* model 273 Potentiostat/Galvanostat, *EG&G's* model 270 software, and a *Micron 75* MHz Powerstation. The pH monitoring was done with *Beckman* Φ11 pH meter with a *Corning* bulb-type pH Ion-selective Electrode. The water conductivity measurements were made with a *YSI* model 3200 conductivity meter using a *YSI* 3253 combination thermistor/conductivity cell.

For all the electrochemical experiments the auxiliary electrode (a coiled Pt wire: 0.5 mm × 6 cm) and the Ag/AgCl reference electrode (BAS MF-2074: $E^0 = 0.194$ V vs. Normal Hydrogen Electrode) were each in one of the side chambers of the three chamber electrochemical cell. All potentials herein, unless otherwise noted, are in reference to this Ag/AgCl electrode. The central chamber housed the gold foil working electrodes, which were made from 0.1 mm and 0.5 mm gold foil *(Aldrich* 99.99%). The working electrodes for the CV and repetitive controlled potential deposition and stripping experiments, cut with a specially fabricated 0.5 cm^2 punch, had a 0.25 mm diameter gold wire spot welded to one side providing a means for holding and for electrical contact. The contact/support wire and the back side of these gold disc electrodes were coated with a clear insulating butyl acetate polymer *(Revlon* # 10) to control the active area of the electrode. The gold working electrodes that were used in the TDS experiments were machined from the 0.5 mm gold foil to rectangles (8.4 × 9.5 mm), with two 1.0 × 1.0 mm tabs at diagonal corners for handling and attachment, effectively giving the electrodes a 0.8 cm^2 surface. Only one face of these electrodes was exposed to the electrolyte solutions by suspending them such that they were just in contact with the liquid surface. This was accomplished by vacuum sealing these rectangular electrodes to a brass support with a colloidal graphite suspension in isopropanol *(AquaDag).*

Thermal Desorption Spectroscopy Equipment:

The TDS experiments were run in a ultra high vacuum (UHV) chamber: fabricated by *Leybold-Heraeus* of Germany. The base pressure for all TDS experiments was less than 2×10^{-7} mbar: achieved with a *Balzer's* TMP 150 turbomolecular pump and a *Leybold-Heraeus* two stage mechanical fore pump. The rectangle gold electrodes were introduced to this UHV system on a modified SRT-11 load-lock sample manipulation rod: fabricated by *IGT Instrumente* of Germany. The SRT-11 rod allows for heating and cooling of the samples through the heater/holder plate with a resistive *nichrome* heater element, or with a liquid nitrogen cooled heat exchanger. Our SRT–11 rod was modified, with the addition of two new thermocouple feed-throughs, to allow heating of the gold foils through the heater/holder plate with direct monitoring of the samples temperature with a type K (chromel/alumel) thermocouple. The desorbing mercury was detected with a *Balzer's* QME 311 mass spectrometer employing QMA 20 quadrupole mass analyzer. The mass spectrometer has a resolution of 100 and was used with an emission current of 0.40 mA for electron impact ionization. The temperature ramp was controlled with a *Leybold-Heraeus* IQ 383065 temperature controller. The TD spectra were collected with a data acquisition program, written by *Intelligent Instrumentation* of Tucson, Arizona, interfaced through a IBM 486 workstation, as the amplified analogue voltage outputs from the QME 311 electrometer/amplifier, for the mass ion current signal, and from a custom amplifier for the thermocouple potential.

Repetitive Controlled Potential Deposition, Stripping and Cleaning:

The experimental set-up for these experiments is shown in Figure 3.1. These experiments started with 500 mL of mercury free electrolyte flowed through from the

separatory funnel. The volume of electrolyte in the central chamber was kept at a relatively constant value of 10 mL by vacuum aspiration of the flowing electrolyte. After an initial volume of 50 or 75 mL was run through the system, the flow was stopped; whereupon, a CV scan was recorded. The CV, run at 100 mV/s, started at the stripping potential of either +0.8, +0.9 or +1.0V, went to +0.4 or +0.1 V (respectively, for the chloride and nitrate based electrolytes) and finished at the stripping potential. After this initial CV scan, the flow of mercury free electrolyte was started, at 5 to 7 mL/min, as was the deposition stripping cycling. The deposition stripping cycling was programmed as follows: 60 s stripping at the appropriate potential, switch to deposition potential of –0.5 or –0.6 V (respectively, for the two different electrolytes or, for experiments where the electrode was attached with *AquaDag)* for 30 seconds and then repeat. The switching between the potentials was at 1000 mV/s.

The automatic deposition and stripping cycling was periodically interrupted during the stripping phase to monitor the build up of mercury by CV. At about 40 seconds into the stripping phase of the cycle to be interrupted, the flow of analyte was stopped and approximately 15 seconds later the CV monitoring scan was initiated. The CVs were run as described above. At the end of the CV monitoring scans, the potential was at the oxidation potential. The potentiostat was again set to continue the deposition stripping cycling as described above and the flow of electrolyte was reestablished.

A CV scan was taken just as the mercury free electrolyte was finished and just after the addition of the electrolyte containing mercury. Each change in electrolyte composition was done with the electrode at the stripping potential and the flow rate was increased to 80 mL/min (maximum flow rate) to flush the cell and give a uniform

solution in the central chamber. During the entire process of controlled potential deposition, stripping and cleaning coupled with CV monitoring of the Hg accumulation, the cell is never at an open circuit. The cleaning step and the stripping step during repetitive cycling are one in the same, as explained in Chapter II. The square wave potentiometry experiments, indicated that, at these concentrations, the stripping current reaches a baseline value within seconds. The accumulation of mercury on the electrode surface was determined as the integrated area of the Hg stripping peaks. The integration of the area was done with the *EG&G* M270 software either directly from the CV scan or from a differential CV: made by subtracting the first CV run in the mercury containing media from each of the successive CVs.

The repetitive controlled potential deposition, stripping and cleaning cycling on the gold foil electrodes for the TDS experiments were not interrupted for CV monitoring during the 3 hours of cycling. A CV scan, from +0.9 $\rightarrow$ −1.0 $\rightarrow$ +1.5 $\rightarrow$ +0.9 V, at 100 mV/s, for these experiments was done at the start of each experiment when the mercury containing electrolyte solution was introduced and at the end of the experiment. After the final CV, the potential was held at the oxidative cleaning potential with the electrolyte flowing, at the maximum rate, for a period of 60 s, whereupon the electrode was removed from the solution and then the cell was switched to an open circuit. The electrode was rinsed with water and acetone and transported to the UHV system in a closed (not airtight) container.

Thermal Desorption Spectroscopy:

The experimental set-up is shown in Figure 3.2. The TDS phase of the experiments was completed within 30 minutes of the end of the repetitive electrochemical

deposition and stripping. The rectangular gold foil electrodes were attached to the SRT–11 heater/holder plate by use of the 1 mm^2 tabs. As the gold foils were introduced into the UHV chamber they passed through two differentially pumped stages, where their atmosphere was reduced to 2×10^{-3} mbar. Upon entering the UHV chamber, pumped by the turbomolecular pump, they were cooled to $-100\ ^0C$[†] as the atmosphere was reduced to the base pressure of 2×10^{-7} mbar. This typically took about 5 minutes. After the base pressure was reached the cooling was stopped and the programmed temperature ramp was started. When the gold foil temperature was just about to $-50\ ^0C$ the recording of the TD spectra was started. The TD spectra were made by monitoring the ion current of the 202 a.m.u. mass peak. The TD spectra was run until the gold foil temperature was $600\ ^0C$ (~190 s). After the each TD spectra was recorded the foil was left to anneal for 30 minutes in the UHV chamber at a temperature of $660\ ^0C$.

The gold electrodes were cleaned after each contact with mercury. The electrodes used for TDS experiments were polished after each TD spectra. The polishing consisted of bulk surface removal with 6 μm water-soluble diamond suspension, followed by polishing with 1 μm water-soluble diamond suspension, then with 0.3 μm alumina and finally on a clean *Buehler Microcloth* moistened with water. Each stage of the polishing was done with *Buehler* abrasives on separate *Buehler Microcloths.* The other electrodes, not used for TDS analysis, were cleaned according to the procedure in Chapter II with the addition of 0.3 μm alumina polishing.

[†] The temperature of the gold foil electrodes was made by use of a second smaller piece of gold foil (same thickness) affixed to the SRT–11 holder heater plate in the same manner as the electrode foil. This smaller piece of gold foil had the type K thermocouple spot welded to its exposed surface and remained in the UHV system throughout all the TPD experiments.

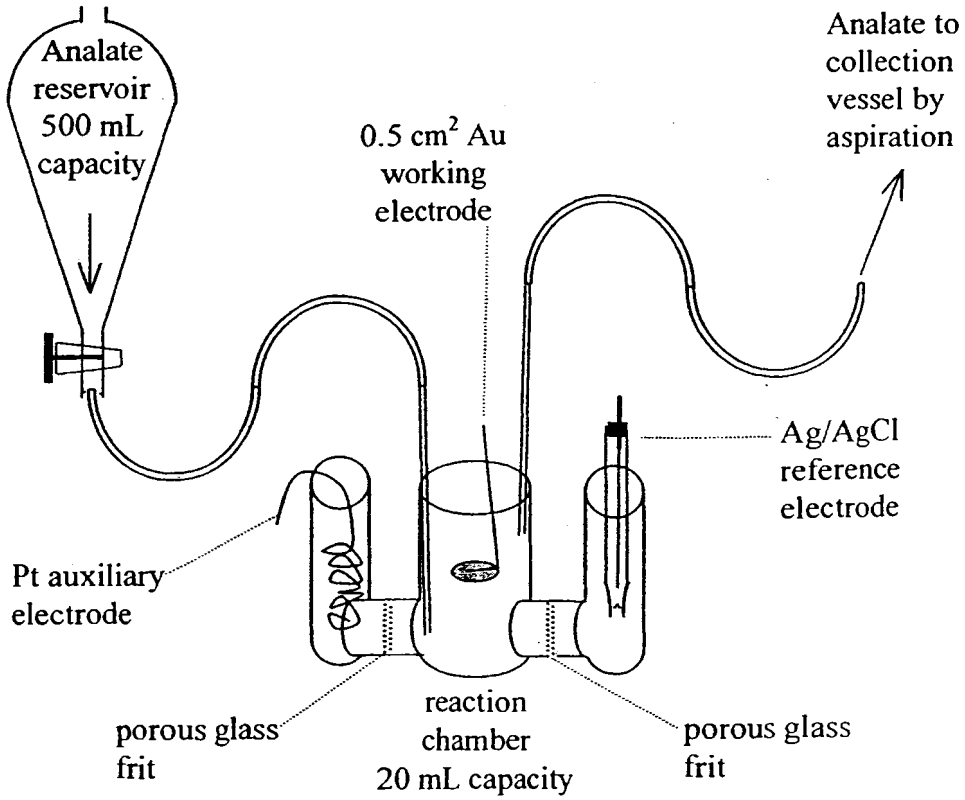

Figure 3.1: Experimental set-up for CV and repetitive deposition stripping and cleaning experiments

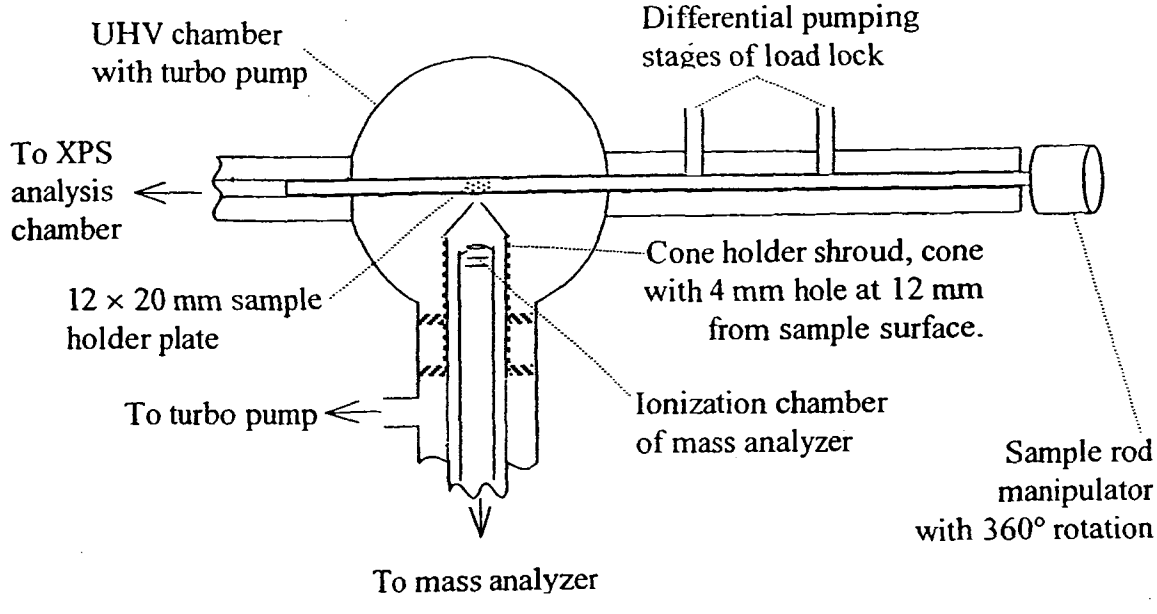

Figure 3.2: Experimental set-up for recording the TD spectra

Results and Discussion

Electrochemistry Experiments:

Two observations made in Chapter II - the fact that mercury is retained on gold foil electrodes after a single electrodeposition procedure followed by exhaustive electrochemical stripping and that the current response of the mercury stripping peak increased more rapidly, in repetitive CV cycling, for nitrate based electrolyte as opposed to the chloride based electrolyte — logically led to experimental probing. XPS analysis of gold foil electrodes established that mercury was retained on the gold electrodes when undergoing electrochemical deposition and stripping at relatively high concentrations (0.1 mM).

In order to study the accumulation of mercury during repeated controlled potential deposition and stripping experiments we integrated the mercury stripping peak area of CVs that were run periodically during repetitive electrochemical deposition and stripping processes. The CVs were used instead of LSV scans, because then we could start and end the survey at stripping potentials. If the potentiostat had to jump from stripping to +0.4 V to start a LSV stripping scan, there may be a momentary potential bounce to potentials negative enough to deposit a small amount of mercury onto the electrode surface. These experiments were run at considerably lower Hg(II) concentrations (40 to 4000 nM) in the same 2.5 mM (KCl or KNO_3) electrolyte. The repetitive deposition and stripping was done with the electrolyte flowing at approximately 7 mL/min; but, for the CV monitoring, of the accumulation of mercury, the flow was stopped. Figures 3.3 – 3.8 show the areas of the mercury stripping peak and representative CVs from each experiment.

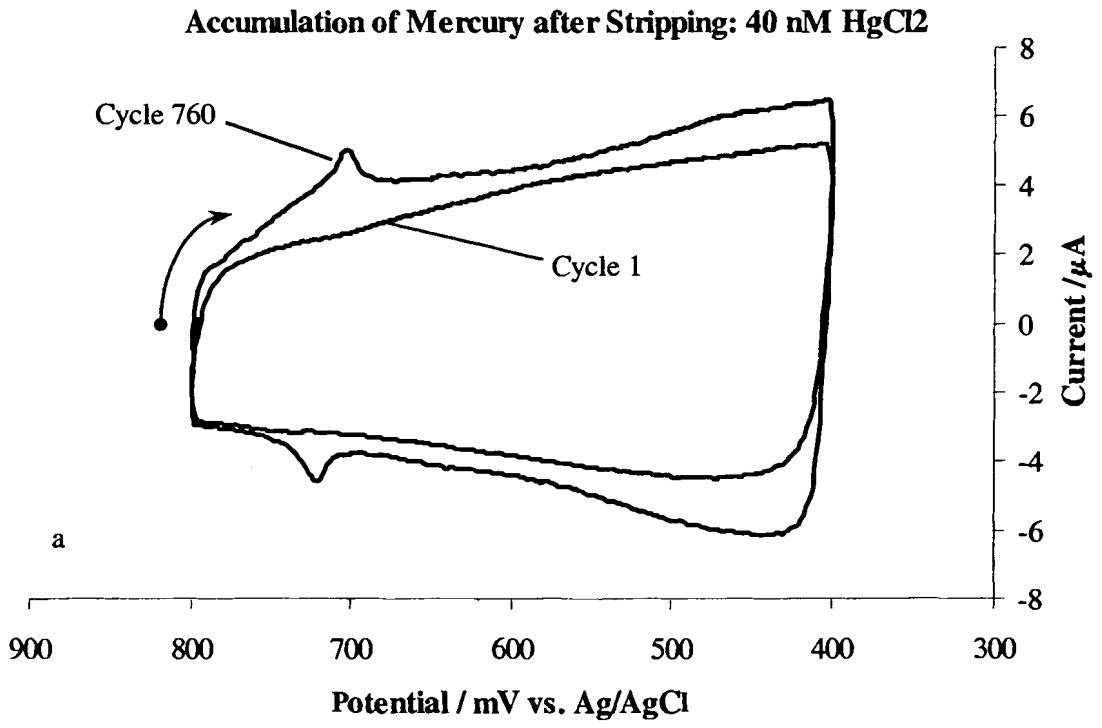

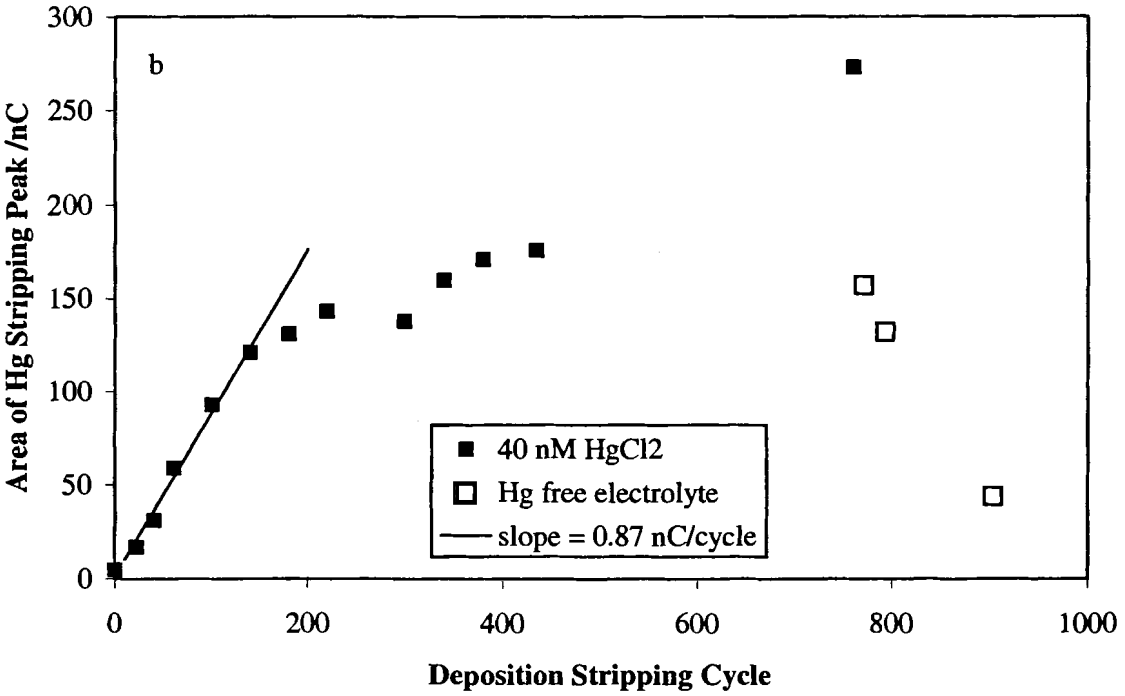

Figure 3.3: (a) CVs at 100 mV/s in stationary 40 nM $HgCl_2$, 2.5 mM KCl, pH 3, after cycles 1 and 760 on a *0.5* cm^2 Au working electrode, with a Pt wire auxiliary electrode and Ag/AgCl reference electrode. (b) Plot of the Hg stripping peak area vs. the number of deposition and stripping cycles transpired: Hg(II) in electrolyte (solid points); supporting electrolyte only (open points). The 30 s deposition and 60 s stripping phases were done at −0.5 and + 1.0 V respectively with the solution flowing at ~7 mL/min.

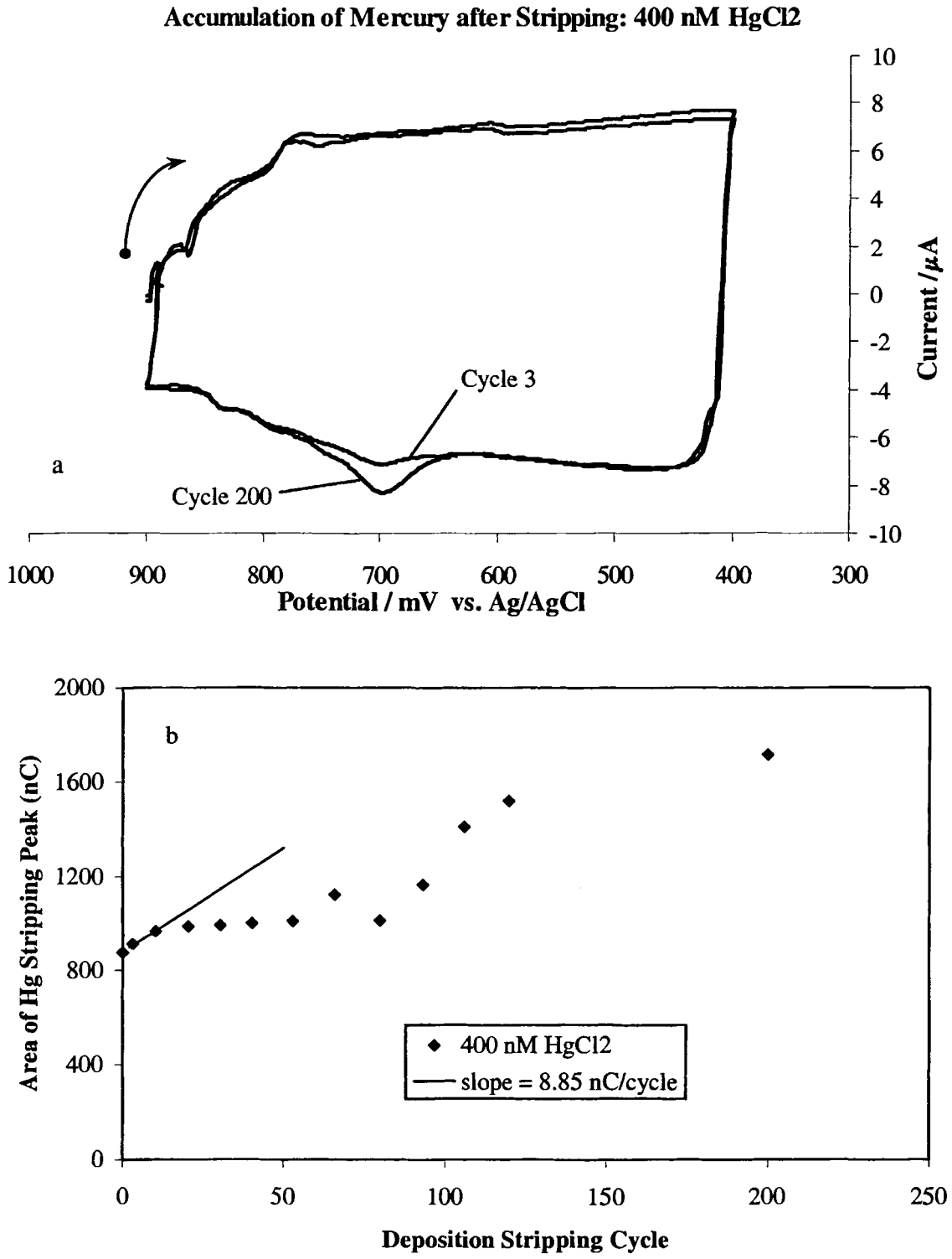

Figure 3.4: (a) CVs at 100 mV/s in stationary 400 nM $HgCl_2$, 2.5 mM KCl, pH 3, after cycles 3 and 202 on a 0.5 cm^2 Au working electrode, with a Pt wire auxiliary electrode and Ag/AgCl reference electrode. (b) Plot of the Hg stripping peak area vs. the number of deposition and stripping cycles transpired. The 30 s deposition and 60 s stripping phases were done at –0.5 and + 1.0 V respectively with the solution flowing at ~7 mL/min.

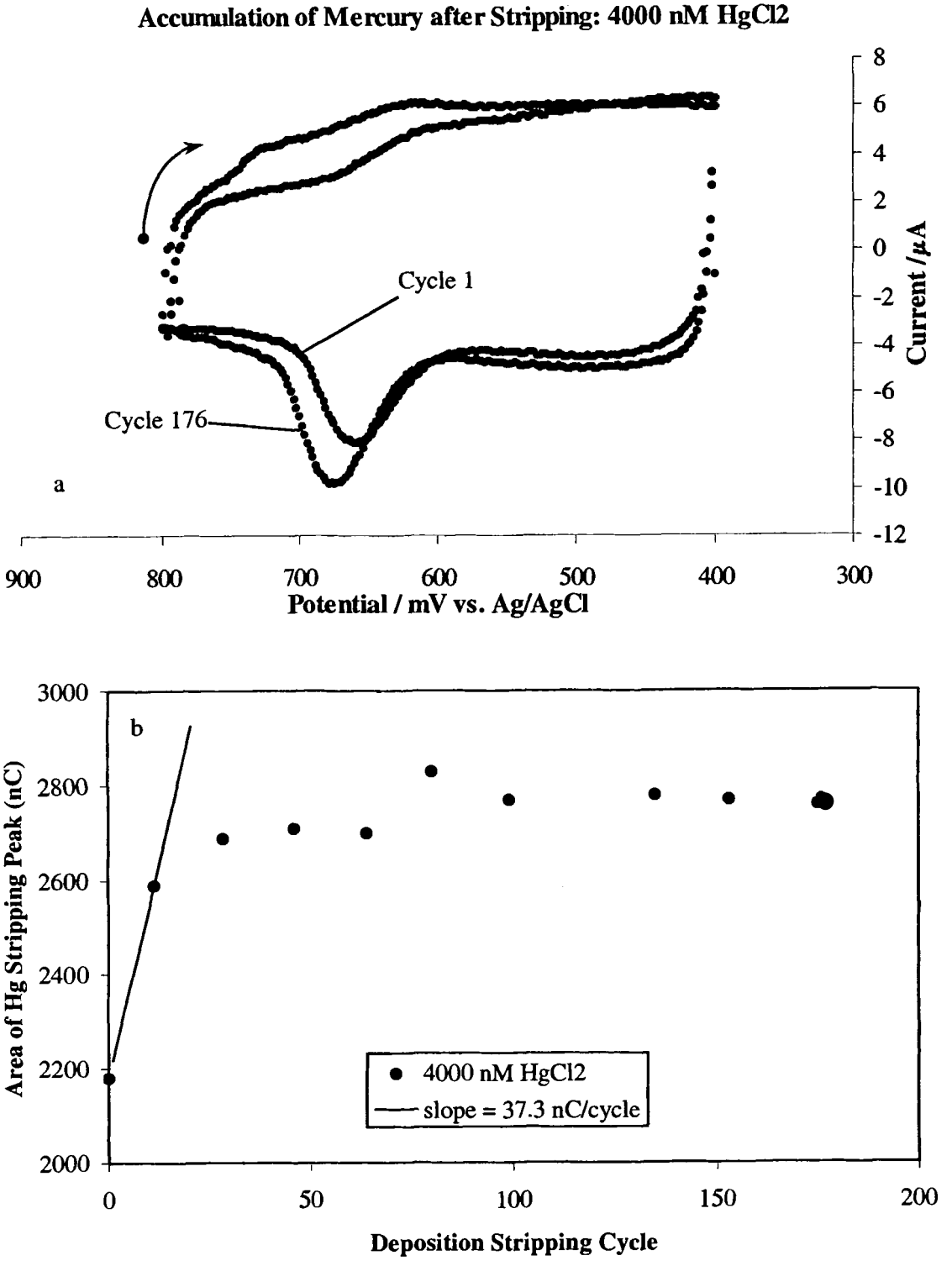

Figure 3.5: (a) CVs at 100 mV/s in stationary 4000 nM $HgCl_2$, 2.5 mM KCl, pH 3, after cycles 1 and 176 on a 0.5 cm^2 Au working electrode, with a Pt wire auxiliary electrode and Ag/AgCl reference electrode. (b) Plot of the Hg stripping peak area vs. the number of deposition and stripping cycles transpired. The 30 s deposition and 60 s stripping phases were done at –0.5 and +1.0 V respectively with the solution flowing at ~7 mL/min.

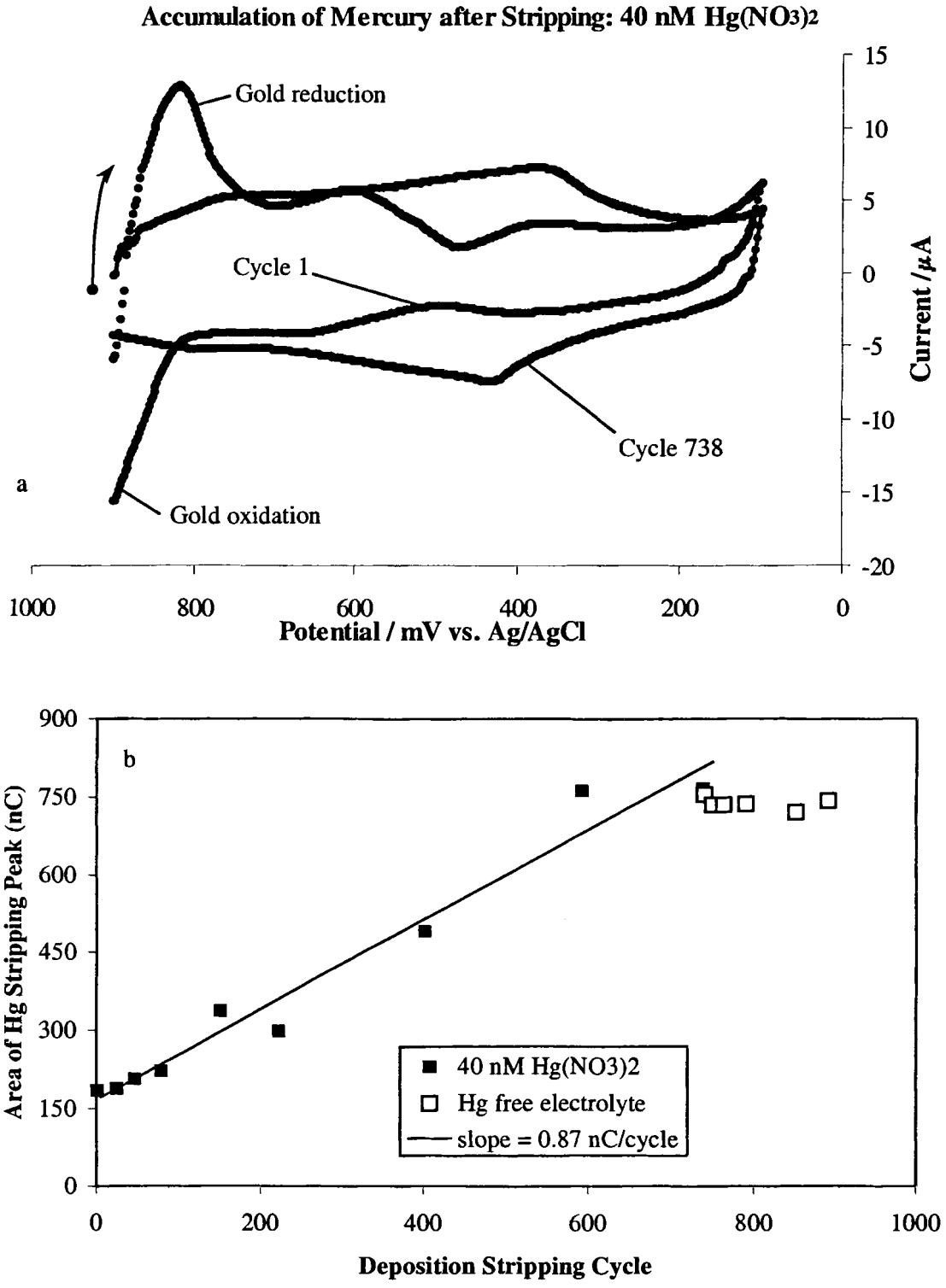

Figure 3.6: (a) CVs at 100 mV/s in still 40 nM $Hg(N0_3)_2$, 2.5 mM KNO_3, pH 3, after cycles 1 and 738 on a 0.5 cm^2 Au working electrode, with a Pt wire auxiliary electrode and Ag/AgCl reference electrode. (b) Plot of the Hg stripping peak area vs. the number of deposition and stripping cycles transpired: with Hg(II) in electrolyte (solid points); in supporting electrolyte only (open points). The 30 s deposition and 60 s stripping phases were done at −0.5 and +1.0 V respectively with the solution flowing at ~7 mL/min.

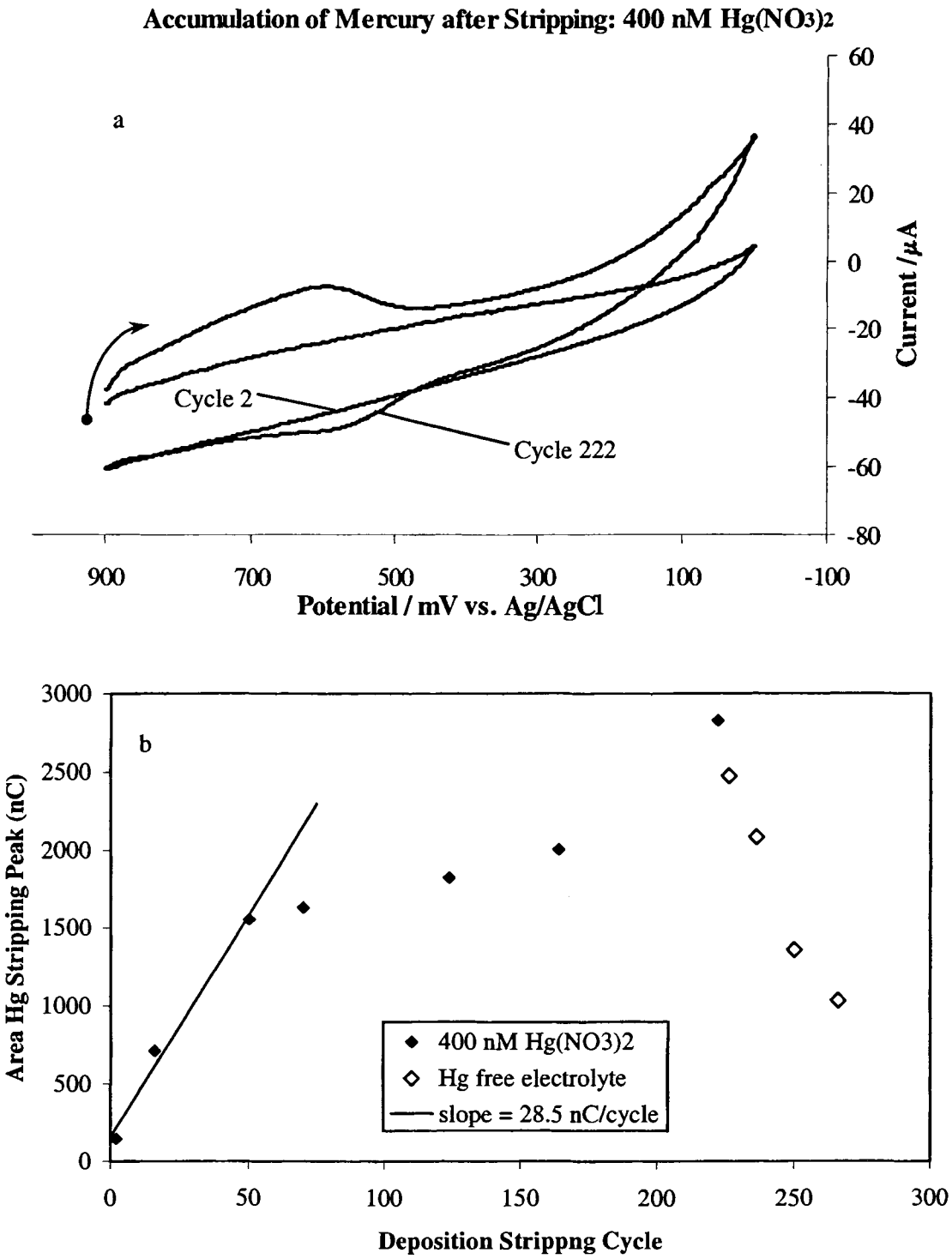

Figure 3.7: (a) CVs at 100 mV/s still 400 nM $Hg(N0_3)_2$, 2.5 mM KNO_3, pH 3, after cycles 2 and 222 on a 0.5 cm^2 Au working electrode, with a Pt wire auxiliary electrode and Ag/AgCl reference electrode. (b) Plot of the Hg stripping peak area vs. the number of deposition and stripping cycles transpired: with Hg(II) in electrolyte (solid points); in supporting electrolyte only (open points). The 30 s deposition and 60 s stripping phases were done at –0.5 and +1.0 V respectively with the solution flowing at ~7 mL/min.

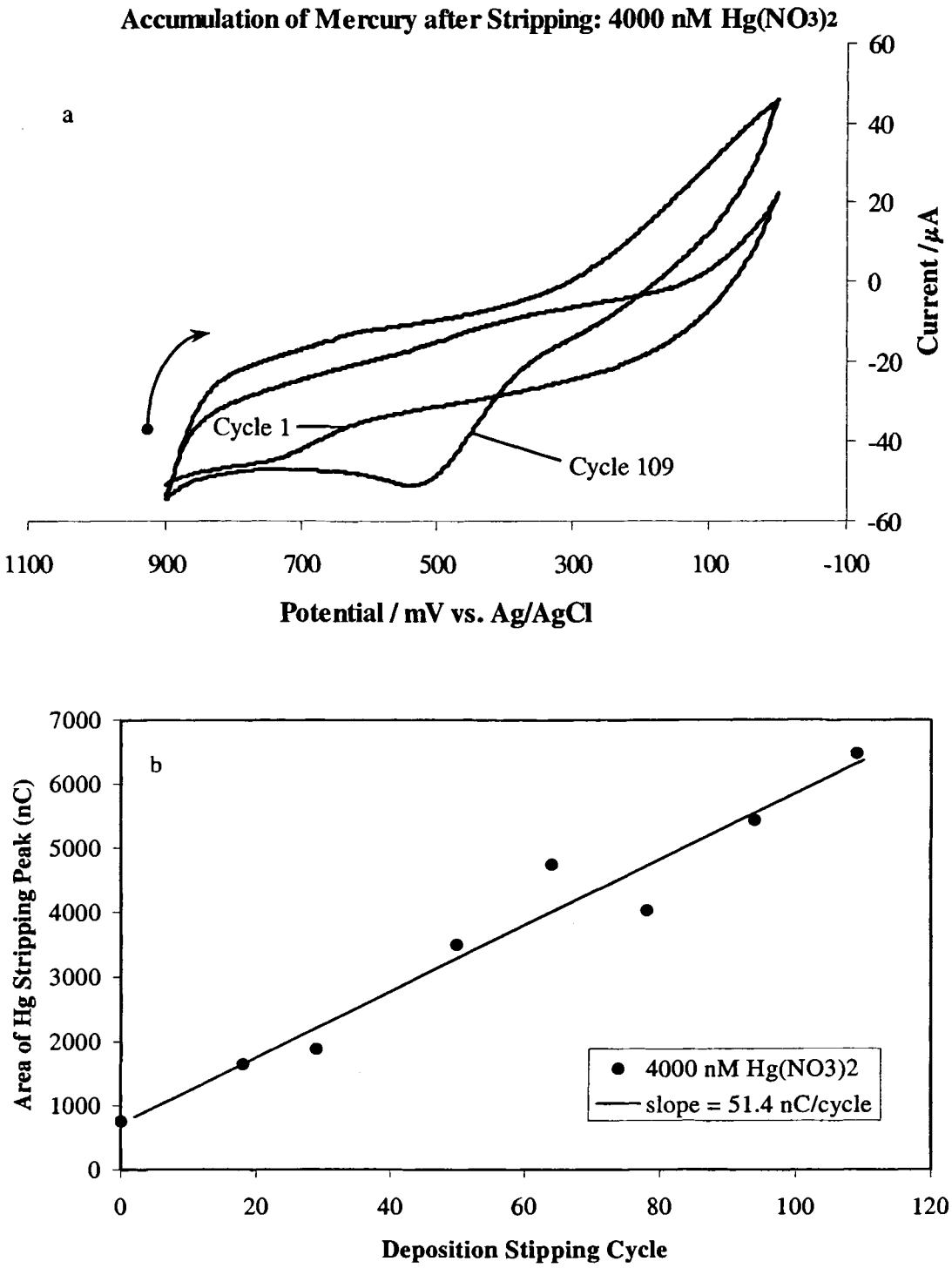

Figure 3.8: (a) CVs at 100 mV/s still 4000 nM $Hg(N0_3)_2$, 2.5 mM KNO_3, pH 3, after cycles 1 and 109 on a 0.5 cm^2 Au working electrode, with a Pt wire auxiliary electrode and Ag/AgCl reference electrode. (b) Plot of the Hg stripping peak area vs. the number of deposition and stripping cycles transpired. The 30 s deposition and 60 s stripping phases were done at –0.5 and +1.0 V respectively with the solution flowing at ~7 mL/min.

What is most evident in Figures 3.3 through 3.8 is that the area of the mercury stripping peak increases as a gold foil electrode is subjected to repeated electrochemical deposition and stripping processes. It is important to recall three things: 1) at these low concentrations (less than 4000 nM) the square-wave deposition and stripping experiments, discussed in Chapter II, showed that the stripping current returned to a baseline value within 10 seconds; 2) our experiment employs a continual supply of Hg(II) at the prescribed concentration and 3) these CVs are recorded at the end of a 60 s stripping and cleaning step at +1.0 V. Comparison of Figures 3.3-5 shows that at each concentration there is an initial period of uptake of mercury on the electrode and that after a period of time the surface layer may reach saturation. This point seems to have been reached by the 4000 nM $HgCl_2$ solution (Figure 3.5); but, not necessarily for the 40 and 400 nM $HgCl_2$ solutions. Conversely, the area of the stripping peak does not achieve an obvious plateau, when the experiments were repeated in chloride free electrolyte (Figures 3.6–8).

In several of the experiments we continued to run the deposition and stripping cycling in mercury-free electrolyte, after there had been an accumulation. During this phase of the experiments, the flow rate was increased to 15 to 20 mL/min. This ensured that in anyone stripping period, the electrolyte in the reaction chamber would be completely renewed at least once. For the chloride electrolyte, the mercury stripping peak did diminish; but, not immediately. With the 40 nM $HgCl_2$ experiment (Figure 3.3), there was still a significant mercury stripping peak after 200 deposition and stripping cycles in Hg free electrolyte. The nitrate-based electrolyte was even less efficient for removing the mercury accumulated on the surface of the gold electrodes. In Figure 3.6, when the

electrolyte was switched to Hg free 2.5 mM KNO_3, the stripping peak area remained relatively constant for an additional 160 deposition / stripping cycles.

In any direct comparison between the chloride and nitrate electrolytes, we notice that the latter always produces a larger stripping peak. A comparison Figures 3.3-5 and 3.6-8 shows that the initial rate of mercury accumulation tracks very well with the Hg(II) concentration. Additionally, the rate of mercury accumulation is about 1.4 times greater with nitrate, as the anionic counter-ion in the electrolyte solution, as compared to chloride.

Wang *et al* report that repetitive PSA analysis of Hg(II) did not show the type of increases in the stripping peak area that we have seen.[5c] Their measurements of 150 successive deposition, stripping and cleaning cycles with a gold microfiber electrode in artificial seawater, spiked with Hg(II) to 100 nM, showed a relatively stable response with stripping peak areas smoothly ranging from 80 to 100 ms.[†] Wang's cycle consisted of a 120 s deposition at +0.2 V (vs. Ag/AgCl), stripping at +0.5 μA from +0.2 to +0.8V and finally 30 seconds of cleaning at +0.8 V. The cycling experiments were done in a 400 mL *Erlenmeyer* flask without stirring. The stripping peak that Wang monitors is close to + 500 mV and this appears to be the stripping of mercury from a mercury-gold amalgam.[3, 9] We took note of two phenomena from his report. First, as the PSA cycles progressed there was a slightly positive slope leading to more and more mercury being recorded in the stripping signal. Second, the fact that the solution was neither replenished with fresh mercury nor stirred during the procedure. They reported that in experiments where stirring was incorporated the stripping signal had a 3-fold increase.

[†] Wang's PSA employs constant current stripping; therefore milliseconds are related to coulombs.

The reproducibility that Wang observed is certainly not surprising. In our experiments, that measured the latent mercury stripping peak after the 60 s stripping and cleaning step, we found that with 20 successive deposition and stripping cycles the variation in the stripping peak deviated less than 10% of the average for 40, 400 and 4000 nM $HgCI_2$ solutions. This indicates that, in the long term, the amount of mercury remaining at the electrode surface, available for oxidation, increases; whereas, in the short term, the stripping analysis looks reproducibly stable. It must be restated that our solutions were flowing and that there was a continual supply of analyte solution. It also must be noted that our latent stripping peak measurements were made after the square wave deposition and stripping and that the stripping peaks represent retained mercury and mercury underpotentially deposited during the cathodic sweep of the CV scans.

The amount of mercury retained on the gold foil electrodes appears to increase with repetitive electrochemical deposition and stripping. Figures 3.9-15 contain 100 mV/s LSV scans of mercury stripping from gold electrodes after 30s deposition at –0.5 V in 40, 400 and 4000 nM $HgC1_2$ and $Hg(N0_3)_2$ solutions. In each of the different solutions we notice that there are two principle stripping events one at +0.45 V and the other at +0.7 V. In Figures 3.3-5 we see that the mercury stripping peak at +0.7 V appears to migrate from +0.74 (40 nM) to +0.66 V (4000 nM). However, this migration is believed to be the oxidation Hg(0) to Hg(II) from two different surface environments. In Figure 3.9a we see in the LSV stripping scan after the first deposition (cycle 1) a large stripping peak at +0.4 V and then a smaller one at +0.74 V. The peak at +0.4V grows as the number of deposition and stripping cycles increases as does the peak at +0.7V. However, it is clear in the LSV trace of cycle 515, (Figure 3.9a) that the +0.7 V stripping peak involves mercury oxidation from two different surface sites.

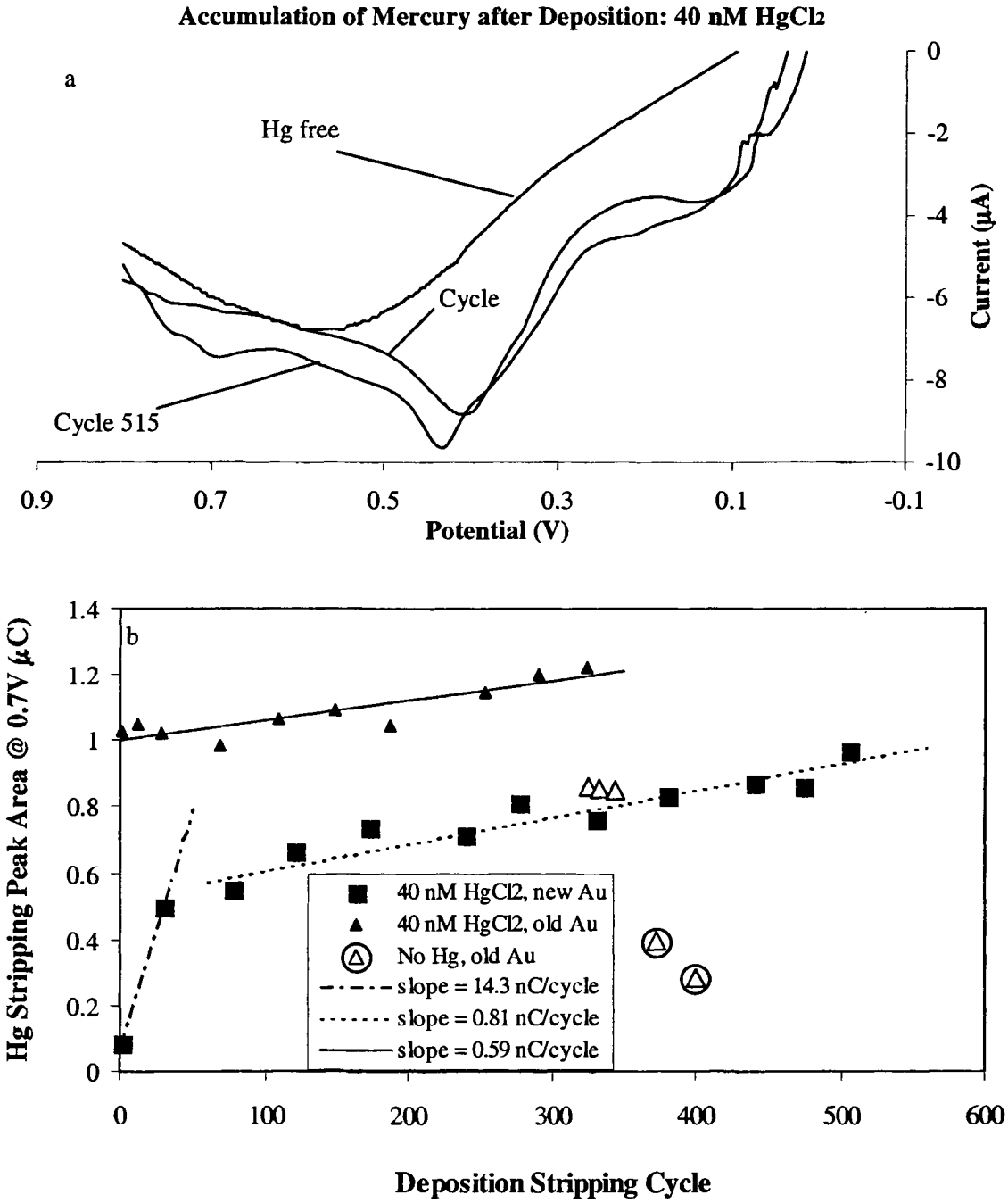

Figure 3.9: (a) 100 mV/s LSVs run on 0.5 cm^2 Au after deposition in repetitive cycles of 30 s depositions at –0.5 V, followed by 60 s stripping and cleaning at 1.0 V (vs. Ag/AgCl) with at Pt auxiliary electrode in 40 nM $HgCl_2$, 2.5 mM KCl, pH 3, flowing at ~8 mL/min. Cycle 1 is before any stripping and cleaning step. Included is a LSV scan after cycling in Hg-free electrolyte. (b) Plot of the Hg stripping peak area at +0.7 V vs. the number of deposition and stripping cycles transpired: with Hg(II) in electrolyte (solid points), in supporting electrolyte only (open points). *Square* points represent a gold electrode used fresh from polishing and flame annealing. *Triangular* points represent a gold electrode cleaned by electrochemical oxidation only after use in 4000 nM $HgCl_2$ experiments. *Circled triangles* represent points where there was continual stripping at 1.0 V with no intermittent deposition steps except for one just before the LSV scan.

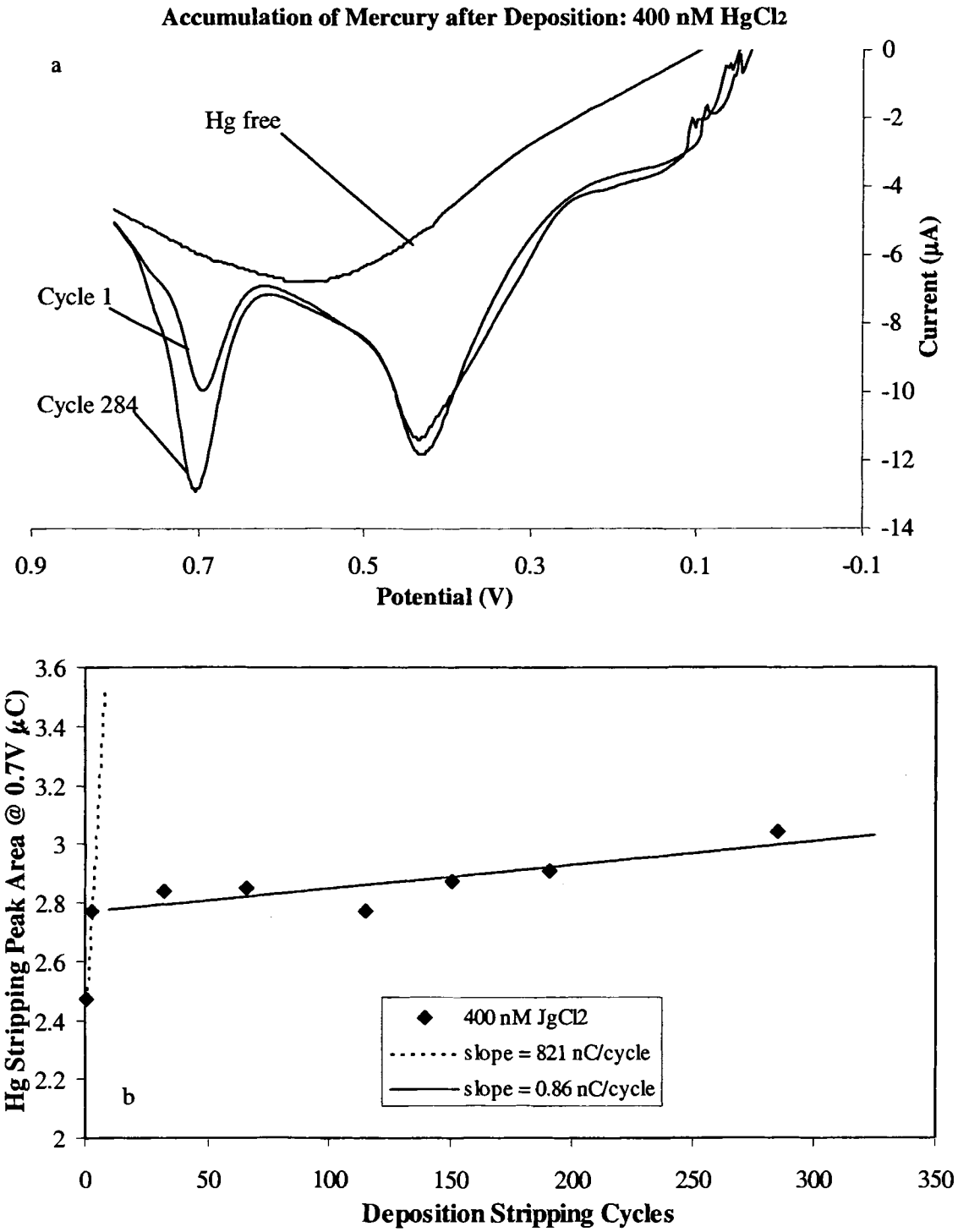

Figure 3.10: (a) 100 mV/s LSVs run on 0.5 cm^2 Au after deposition in repetitive cycles of 30 s depositions at –0.5 V, followed by 60 s stripping and cleaning at 1.0 V (vs. Ag/AgCl) with at Pt auxiliary electrode in 400 nM $HgCl_2$, 2.5 mM KCl, pH 3, flowing at ~8 mL/min. Cycle 1 is before any stripping and cleaning step. Included is a LSV scan after cycling in Hg-free electrolyte. (b) Plot of the Hg stripping peak area at +0.7 V vs. the number of deposition and stripping cycles transpired.

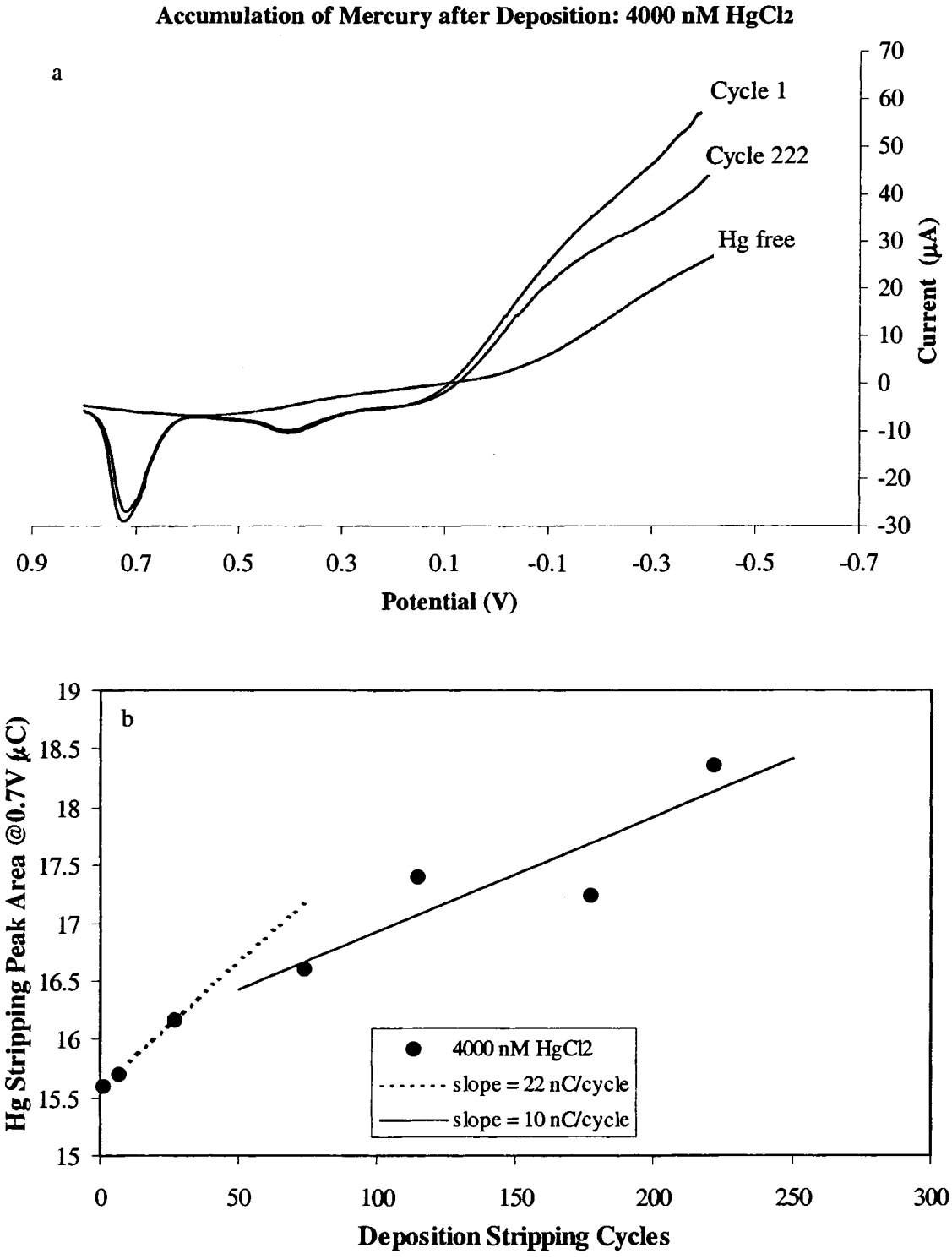

Figure 3.11: (a) 100 mV/s LSVs run on 0.5 cm^2 Au after deposition in repetitive cycles of 30 s depositions at –0.5 V, followed by 60 s stripping and cleaning at 1.0 V (vs. Ag/AgCl) with at Pt auxiliary electrode in 4000 nM $HgCl_2$, 2.5 mM KCl, pH 3, flowing at ~8 mL/min. Cycle 1 is before any stripping and cleaning step. Included is a LSV scan after cycling in Hg-free electrolyte. (b) Plot of the Hg stripping peak area at +0.7 V vs. the number of deposition and stripping cycles transpired.

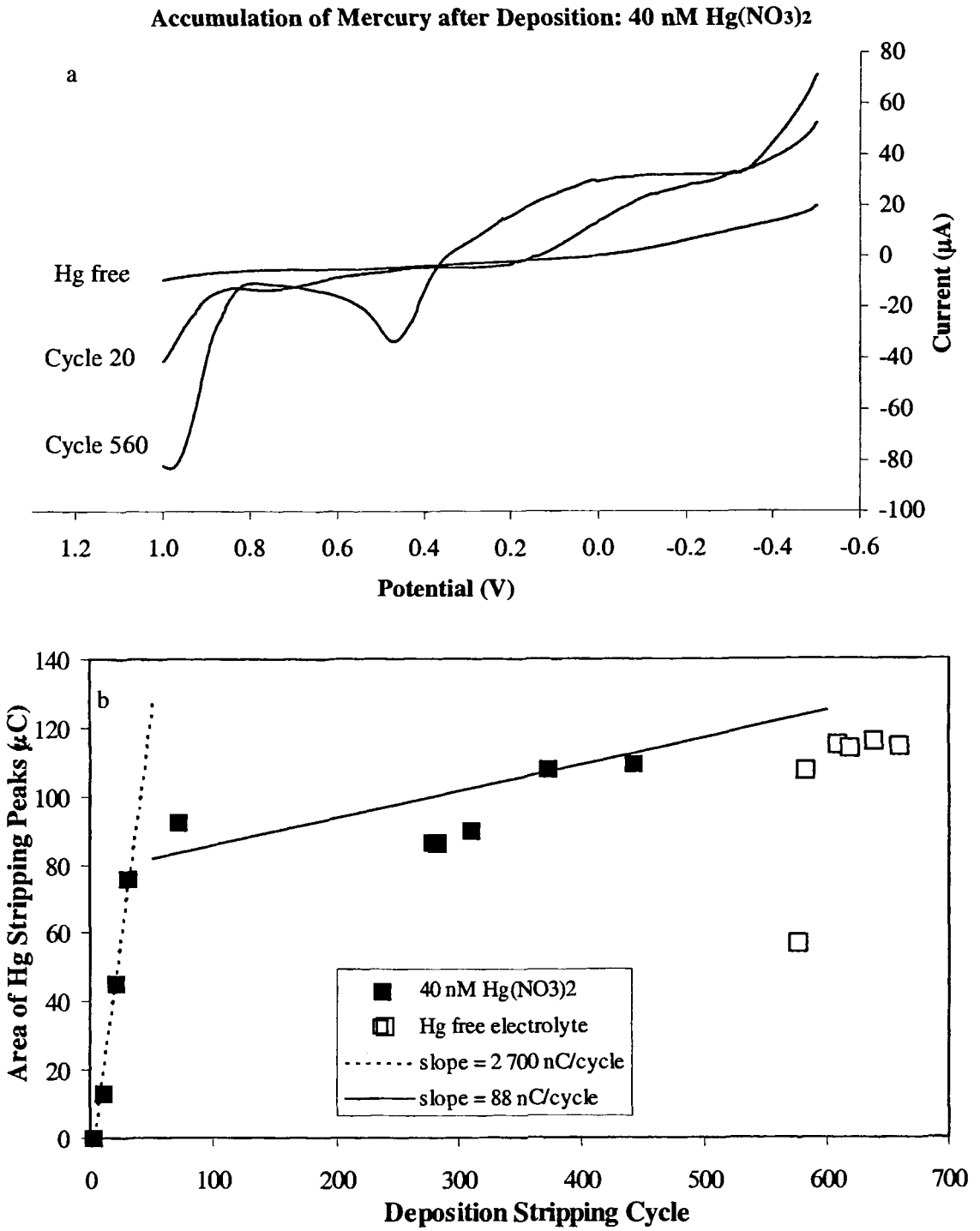

Figure 3.12: (a) 100 mV/s LSVs run on 0.5 cm^2 Au after deposition in repetitive cycles of 30 s depositions at –0.5 V, followed by 60 s stripping and cleaning at 1.0 V (vs. Ag/AgCl) with at Pt auxiliary electrode in 40 nM $Hg(NO_3)_2$, 2.5 mM KCl, pH 3, flowing at ~8 mL/min. Cycle 1 is before any stripping and cleaning step. Included is a LSV scan after cycling in Hg-free electrolyte. (b) Plot of the Hg stripping peak area at +0.7 V vs. the number of deposition and stripping cycles transpired: with Hg(II) in electrolyte (solid points), in supporting electrolyte only (open points).

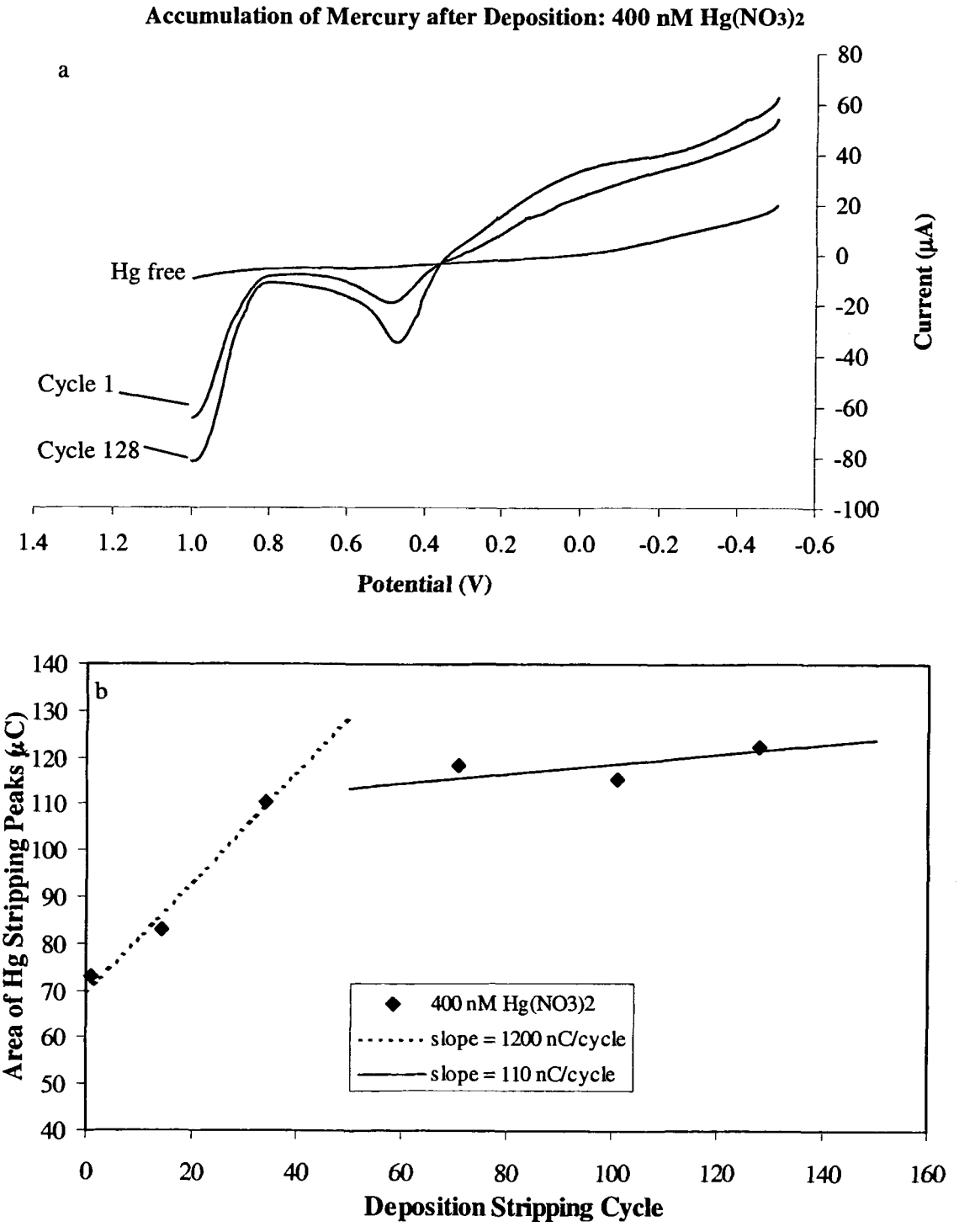

Figure 3.13: (a) 100 mV/s LSVs run on 0.5 cm^2 Au after deposition in repetitive cycles of 30 s depositions at –0.5 V, followed by 60 s stripping and cleaning at 1.0 V (vs. Ag/AgCl) with at Pt auxiliary electrode in 400 nM $Hg(NO_3)_2$, 2.5 mM KCl, pH 3, flowing at ~8 mL/min. Cycle 1 is before any stripping and cleaning step. Included is a LSV scan after cycling in Hg-free electrolyte. (b) Plot of the Hg stripping peak area at +0.7 V vs. the number of deposition and stripping cycles transpired: with Hg(II) in electrolyte (solid points).

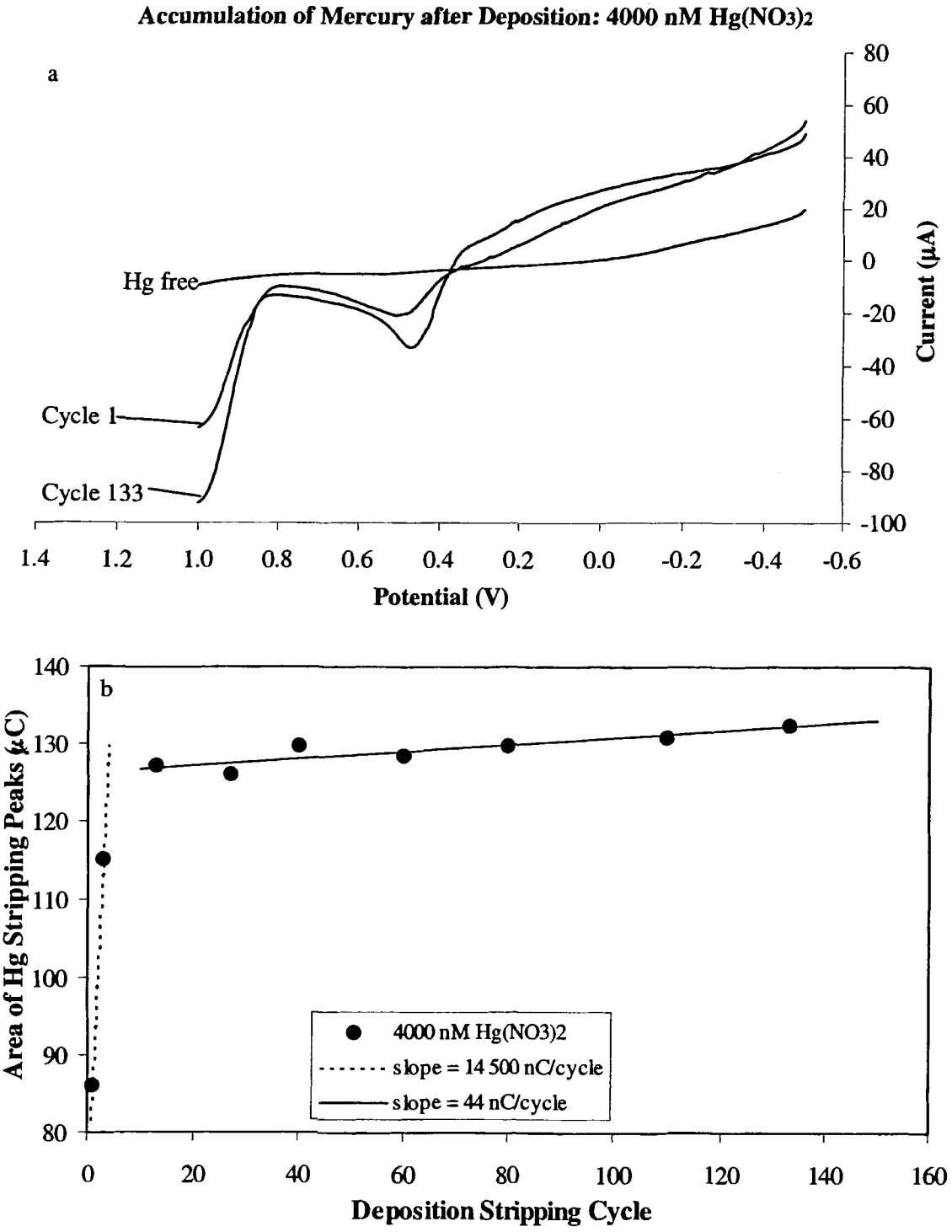

Figure 3.14: (a) 100 mV/s LSVs run on 0.5 cm^2 Au after deposition in repetitive cycles of 30 s depositions at –0.5 V, followed by 60 s stripping and cleaning at 1.0 V (vs. Ag/AgCl) with at Pt auxiliary electrode in 4000 nM $Hg(NO_3)_2$, 2.5 mM KCl, pH 3, flowing at ~8 mL/min. Cycle 1 is before any stripping and cleaning step. Included is a LSV scan after cycling in Hg-free electrolyte. (b) Plot of the Hg stripping peak area at +0.7 V vs. the number of deposition and stripping cycles transpired.

The amount of mercury stripped from the electrodes in certainly not constant over long periods of deposition and stripping. Figures 3.9b – 14b clearly show that there are two different rates for the uptake of mercury on the gold electrodes. The initial rate is at least an order of magnitude greater than that after the deposition and stripping cycles have been going for a while. This is presumably due to the creation of a mercury-gold amalgam electrode after a period of time. However, there is still an increase in the stripping peak areas as the deposition and stripping cycling continues in flowing solutions of constant Hg(II) concentrations. The comparison of the chloride-based solutions (Figures 3.9–11) with the nitrate based solutions (Figures 3.12–14).reveals that in the absence of chloride, there is a greater amount of mercury adsorbed onto the electrode surface. The area of the mercury stripping peaks in nitrate solutions are at least an order of magnitude greater than the area of the mercury stripping peaks in chloride solutions. The disparity, in the stripping peak areas, between the nitrate and chloride solutions is about five times greater when the LSV stripping is run after deposition instead of after the cleaning step (comparison of Figures 3.3–5 and 3.6–8). Again this indicates that chloride ion retards the adsorption of mercury on the gold electrodes in relation to nitrate.

Another remarkable feature of Figures 3.9b and 3.12b is that after there has been an accumulation of mercury on the electrode, there continues to be a significant residual mercury stripping peak when the cycling process is continued in mercury free electrolyte. Initially the area of the stripping peak remains relatively constant. When the electrode is simple held at a stripping potential for a long period of time, the area of the stripping peak does decrease significantly; however, the peak does not immediately fall back to the

same value seen at the beginning of the cycling procedure (Figure 3.9b: circled open triangles). Even an electrode, that had had an accumulation of mercury by deposition and stripping cycling in 400 nM $Hg(N0_3)_2$, and subsequently underwent electrochemical oxidation at +1.0V for 3 hours in flowing 2.5 mM KCl, still showed evidence of a mercury stripping peak.

These phenomena suggest a model for the surface evolution of the gold electrodes in repetitive electrochemical deposition and stripping of mercury. There appears to be a period, at very low Hg(II) concentrations (i.e. 40 nM), where mercury accumulates on the gold electrodes and slowly transforms the surface from gold to a gold electrode with patches (starting at grain boundaries and surface defects)[2b,9] of mercury-gold amalgam and finally to an electrode with a mercury-gold amalgam surface. The rate of this transformation depends on the amount of mercury adsorbed onto the surface, which depends on parameters such as: deposition time, Hg(II) concentration, deposition potential, electrolyte, and deposition conditions. It is reported that on single crystal Au(111) electrodes, amalgamation commences when the first monolayer of mercury has been deposited[10] and that on polycrystalline Au surfaces, amalgamation starts at grain boundaries and defects during underpotential deposition.[†] [7a] After the surface of the gold electrode has been transformed to a gold-mercury alloy, diffusion of mercury continues into the gold as does accumulation of mercury on the surface of the electrode.

[†] Underpotential deposition is the phenomena of adsorption of a species at potentials positive of its Nernstian potential, where the bulk species is oxidized. The exploitable characteristic of UPD is that the adsorption will not continue past the formation of a monolayer.

The stripping peaks from this model can be assigned as the oxidation of Hg(0) to Hg(II) as mercury on the mercury gold amalgam surface (+0.45 V oxidation peak) and as Hg(0) to Hg(II) from the mercury-gold amalgam itself (+0.7 V oxidation peak). Chen et al, indicate that the rate of surface amalgamation is almost instantaneous:[8] presumably when the mercury nucleation clusters reach the 60 atom size or so.[11] The diffusion of mercury into gold is reported to be on the order of 10^{-25} cm^2/s [12] and for gold into mercury 7×10^{-6} cm^2/s.[13] The direction of the amalgamation is debatable and may depend upon the surface coverage, as Yang *et al* noticed that the amalgamation process proceeded by dissolution of gold clusters near to an mercury-gold amalgam site.[14] Thus, it seems that the gold surface is rapidly transformed to an mercury-gold amalgam surface and that deep diffusion of mercury into the bulk of the gold substrate (electrode) proceeds at a slower rate. When a gold electrode has had its surface transformed to a mercury-gold amalgam, then continued PSA cycles in mercury-free electrolyte will continue to manifest mercury stripping peaks.

When there is more than a monolayer's worth of mercury (330 ng/ cm^2) on the surface of a gold electrode then the chemical potential of the surface Hg(0) is higher than that of the Hg(0) in the gold-mercury amalgam and diffusion will be into the gold electrode.[15] As far as we can determine, during stripping, the bulk Hg(0) surface on the mercury-gold amalgam is for the most part removed. With this, the direction of diffusion ceases to be unidirectional and mercury in the amalgam surface may separate out of the amalgam as metallic mercury clusters and thus, be available for stripping at the +0.4 V potential. Therefore, even when there is no more mercury being deposited on the surface,

because the electrolyte is Hg-free, the mercury stripping peaks will continue to be manifested. Figures 3.9b and 3.12b show exactly this phenomena. The data indicates that repetitive PSA measurements in a flowing, low concentration, Hg(II) environment would tend to indicate falsely inflated mercury concentration levels and the presence of mercury when there is none.

Based on the results of these experiments, it appears that mercury would certainly accumulate on gold electrodes in repetitive PSA experiments. Our experimentation was designed to mimic, in terms of time scale, what others researching the electrodeposition and stripping of mercury from gold electrodes have reported. It could be argued that all that is necessary to eliminate the accumulation or retention of mercury on gold electrodes is for the stripping duration to be extended. The question is how long? We have already shown by XPS analysis, in Chapter II that even stripping for up to an hour in mercury free electrolyte, not all the mercury is removed from the gold electrodes. A more sensitive analysis of the electrodes would most likely reveal retention and accumulation at lower Hg(II) concentrations *(vide infra).* Our experimental process of repeated deposition for 30 seconds followed immediately by a 60 second stripping and cleaning step allows mercury deposition for the same duration and then stripping and cleaning for a longer period than what has been done by others researchers.[1a-d, 5] With PSA there is continued deposition of mercury during the initial ramping of the potential from the pre-concentration step to the stripping potential and there is the possibility of underpotential deposition after the stripping peak has attenuated to baseline. Our experiments go directly from deposition to stripping at overpotentials where no underpotential deposition

occurs[16] and where we saw qualitatively the most efficient stripping of mercury from the gold electrodes.[3] With this in mind it seems clear that high frequency measurements (20 to 30 per hour) of mercury concentrations by PSA will result in the build-up of mercury on the surface of the electrodes and lead to false readings as to the real mercury concentration.

The fact that the accumulation of mercury on the surface of the electrode is more pronounced in nitrate-based electrolyte as opposed to chloride-based electrolyte can be related to the reduction and oxidation potentials observed in the CVs on these species in Chapter II. There we reported that when going from the chloride to the nitrate-based electrolyte the deposition potential shifted positively from 0 V to +300 mV and that the highest potential mercury stripping peak was also shifted positively from +550 to +750 mV. These potential shifts indicate that Hg(II) is reduced more easily when the anionic counter-ion is nitrate and that its subsequent oxidation is facilitated more by chloride than by nitrate. With the chloride-free electrolyte, the combination of the two results is, more mercury adsorbed onto the electrode surface during the deposition phase and less removed during electrochemical oxidation.

The LSV accumulation plots of Figures 3.9b-14b indicate that the surface of the electrode was completely amalgamated, even after an hour of deposition and stripping cycling in 40 nM $HgCl_2$. However, at that concentration, the total amount of mercury present in the cell, at any one time, is about a third of a monolayer's worth. The cumulative effect of deposition and stripping cycling is to completely amalgamate the surface, and have Hg(0) diffusing into the bulk of the gold, even at low Hg(II)

concentrations; although, the deposition of more than a monolayer's worth of mercury, in one deposition cycle, does not likely occur until somewhere between 400 and 4000 nM in our experiments. When there is more than a monolayer being deposited at one time then the diffusion of mercury into the gold is into enhanced by the chemical potential of the metallic Hg(0) adlayers.

The difference in the amount of mercury accumulation in the chloride and nitrate ion systems suggests that solutions containing anionic counter-ions with relatively strong mercury ligand bonds will have different desorption and stripping characteristics than solutions with anions that form less stable complexes with mercury. This inference is in line with electrodeposition results from metal plating experiments;[17] where, coordinating ligands are used to retard electrodeposition giving a "brighter" and more structurally sound surface. The disparity between mercury stripping and accumulation characteristics in the chloride and nitrate-based electrolytes means that the PSA of mercury with gold electrodes cannot be compared from one solution to another. Thus the calibration of these PSA techniques must be adjusted due to the accumulation, it must also be adjusted for electrolyte composition. This type of matrix effect parameterization is done for complex solutions with many varied ionic and non-ionic species (i.e. blood, urine, natural waters).[18]

Thermal Desorption Spectroscopy Experiments:

The increased current responses in the CVs of Figures 3.3-8 and the LSVs of Figures 3.9-14 indicate that, as the experiments progress, the amount of mercury retained and accumulated on the gold electrode surface increases even though the Hg(II)

concentration remains constant. Some highly sensitive analytical techniques for the detection and quantification of mercury involve the thermal desorption of mercury from gold.[2a-e, 19] These techniques demonstrate that nearly 100% of the mercury is desorbed from the gold surfaces at temperatures greater than 250^0C. We know from our cold vapor atomic absorption experiments that most of the mercury, adsorbed during an electrochemical deposition, is removed from the gold electrodes by electrochemical stripping and that the integrated stripping current correlates extremely well with the amount of mercury stripped.[3]

With these assumptions we were able to establish a curve correlating the area of a TD spectrum of mercury desorbed from gold with the amount of mercury adsorbed onto the electrode during one electrochemical deposition procedure. A series of 60 second depositions of varying $Hg(N0_3)_2$ solutions on a 0.8 cm^2 gold foil electrode were done to make the curve. The first deposition was stripped and the stripping peak of the current vs. time plot was integrated. The mercury from the second deposition was desorbed from the gold electrode in a TDS experiment performed within 30 minutes of the electrochemical deposition. Table 3.1 relates the microcoulombs (μC) mercury adsorbed on the gold electrode with the integrated flux of mercury detected by the mass spectrometer in the TD spectra†. The relationship between the Hg(II) concentration and the integration of the TDS desorption peak is linear (correlation 0.997) as is the relationship between the integrated area of the stripping peaks from the 0.18, 0.88 and 4.4 μM Hg(II) solutions with their corresponding thermal desorption peaks (correlation 0.999). The data from the

35 nM experiment are not figures into the calculation, because the stripping peak area from that low concentration of mercury is highly variable due to the background charging current (see Figure 2.7).

Table 3.1: Relationship between electro-deposited and thermally desorbed mercury

Solution Concentration μM Hg(II)	μC Hg Stripped	TDS Peak Area
0.035	22	5 400
0.18	270	8 700
0.88	320	14 000
4.4	980	60 000

The linear relationship between electrodeposited and thermally desorbed mercury gives us a means of quantifying the amount of mercury accumulated on a gold electrode that has been subjected to repetitive electrochemical deposition and stripping cycles. The linear regression of the values from Table 3.1, for the experiments at the 0.18, 0.88 and 4.4 μM Hg(II) solutions, gives us a line corresponding the thermal desorption peak area with the amount of mercury adsorbed onto the gold electrode: Equation 3.3.

$$\mu C\ Hg = 0.014 \times (\text{Area of TDS 202 a.m.u. peak}) + 140\ \mu C \qquad (3.3)$$

The slope of the line is 0.01414 μC per unit area of the TD spectra and the intercept is 140 (μC). The equation neglects the amount of mercury retained in any one individual deposition and stripping procedure. This approximation is made based on our CVAA experiments reported in Chapter II and the widely held belief that mercury is readily oxidized and stripped from gold electrode surfaces.[3] However, the non-zero intercept

† The integrated peaks are from the Hg flux vs. time plot instead of the Hg flux vs. temperature plots featured in figures 3.15–17.

corresponds to mercury retained in the gold electrode that is unmeasured in electrochemical stripping but desorbed and detected by TDS. Equation 3.3 allows us to measure, with TDS, the amount of mercury accumulated on gold electrodes in repetitive electrochemical deposition and stripping processes.

To measure the accumulation of mercury on a gold foil electrode we used 0.8 cm^2 gold electrodes. The annealed and polished electrodes were conditioned by repeated 30 s depositions at −0.6 V and 60 s stripping steps at +1.0 V in Hg-free electrolyte flowing at 20 mL/min. After 500 mL of the Hg-free electrolyte had passed through the system, we changed to an electrolyte containing either 40, 400 or 4000 nM $HgCl_2$ or $Hg(NO_3)_2$ in the appropriate electrolyte. An initial CV, at 100 mV/s from +0.9 → −1.0 → +1.5 → +0.9 V, was run upon introduction of the Hg(II) laden electrolyte. Then the deposition and stripping cycling continued as in the mercury-free electrolyte for a period of 180 minutes without interruption except the flow rate was reduced to ~7 mL/min. After the 180 minutes of deposition and stripping cycling another CV scan was run and then the electrode was stripped for 60 s at +1.0 V in the Hg(II) containing electrolyte flowing at ~20 mL/min. Thus during each experiment, the gold electrode is subjected to 120 deposition and stripping cycles and to approximately 50, 500 and 5000 nmols of Hg(II) for the three different experimental Hg(II) concentrations. The amount of mercury exposure during the 30 s deposition phases is one third of these values and corresponds to 3.3, 33 and 330 μg Hg(II): enough for 12.5, 125 and 1250 monolayers.

Figures 3.15-17 are the TD spectra from each Hg(II) species pair ($HgCl_2$ and $Hg(N0_3)_3$) at 40, 400, and 4000 nM, respectively, in their counter-ion appropriate 2.5 mM supporting electrolytes. The spectra are all shown at the same Hg-flux intensity. It is

immediately apparent that more mercury accumulates on the electrode when the electrolyte does not contain any chloride ion. The relative area of the TDS peaks from the $Hg(N0_3)_2$ solutions is about 50% greater than that of the $HgC1_2$ TD spectra. Considering all the uncertainties, this corresponds very well with the value determined in the electrochemical deposition and stripping experiments discussed in Chapter II.

Another interesting feature Figures 3.15 – 3.17 is that in the 40 nM Hg(II) experiments there are clearly two different mercury desorption peaks at ~225 and ~400 °C. The 400 °C peak clearly appears in the 400 nM $HgCl_2$ TD spectra and as a shoulder in the 4000 nM TD spectra. There are several possibilities for the nature of these peaks. The most likely may be that there are two different surface sites for the mercury adsorbed onto the gold electrode. There is presumably no bulk mercury on the electrodes, because these TD spectra were recorded after an oxidative stripping procedure. However, the large peaks may represent mercury on the surface of the gold electrode as a mixed amalgam layer. Once this surface mercury desorbs and the surface amalgam is depleted of mercury atoms, others mercury atoms from deeper amalgam layers migrate to the surface and desorb. It is also possible that the two peaks represent two types of deposition sites as opposed to two different layers. In this case much of the mercury is on the gold surface covering the ordered surface areas. The other type of sites are the surface defects, step edges, groves and pits. Mercury atoms populating these spaces have more mercury-gold interactions and are thus held more tightly to the electrode surface. A third possible explanation is that the high temperature peak represents a different mercury species (i.e. mercury oxide, or mercurous chloride). These molecules breakdown as the gold is heated and mercury can desorb from the surface.

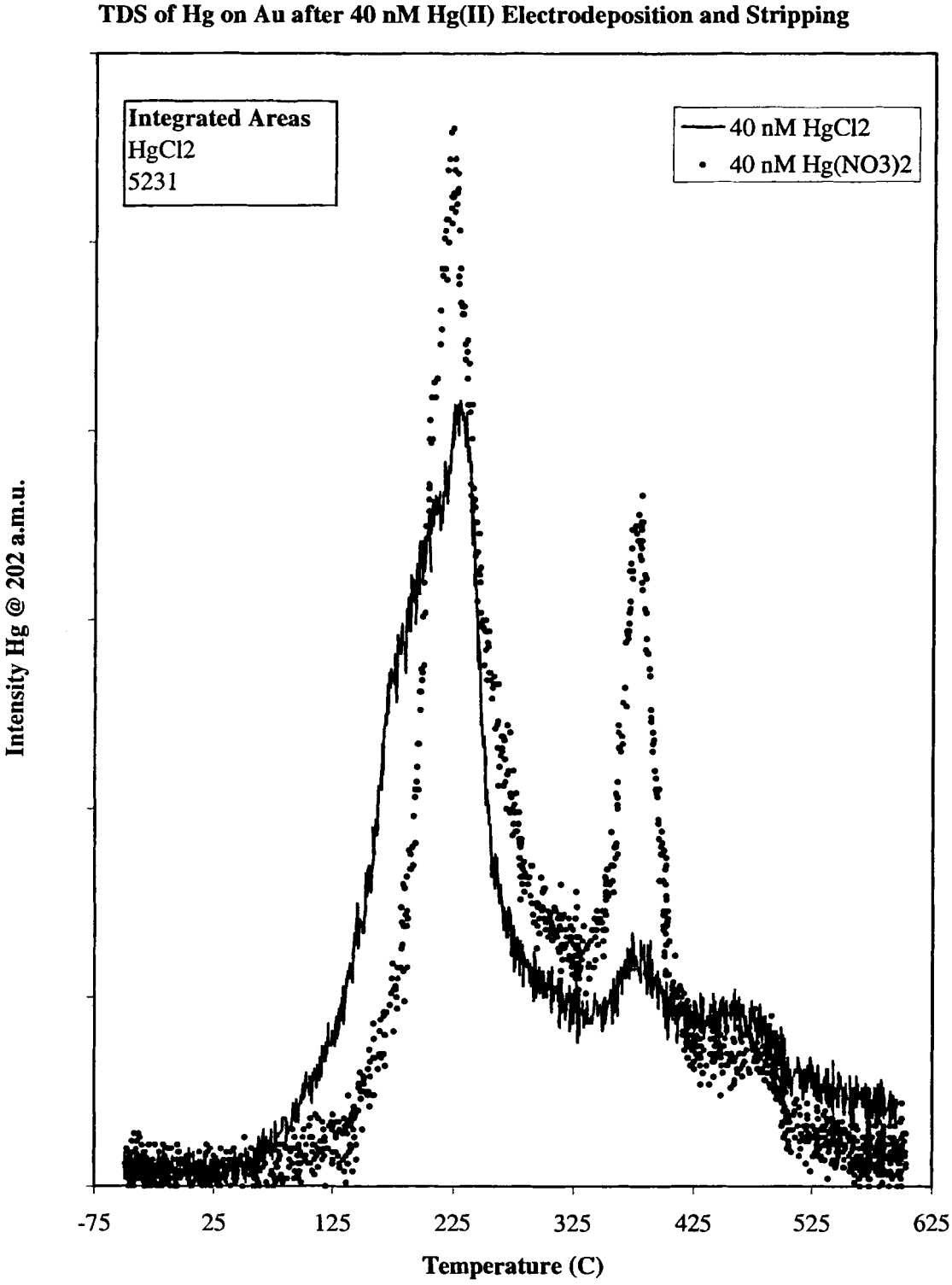

Figure 3.15: 4°C/s TD spectra made by monitoring the thermal desorption, of ^{202}Hg from a 0.8 cm^2 Au foil that had been subjected to 180 minutes of repeated cycles of electrochemical deposition (30 s, at −0.5 V), and stripping (60 s, at +1.0 V) in 40 nM $HgCl_2$ and $Hg(NO_3)_2$ in 2.5 mM KCl or KNO_3 at pH 3, flowing at ~7 mL/min.

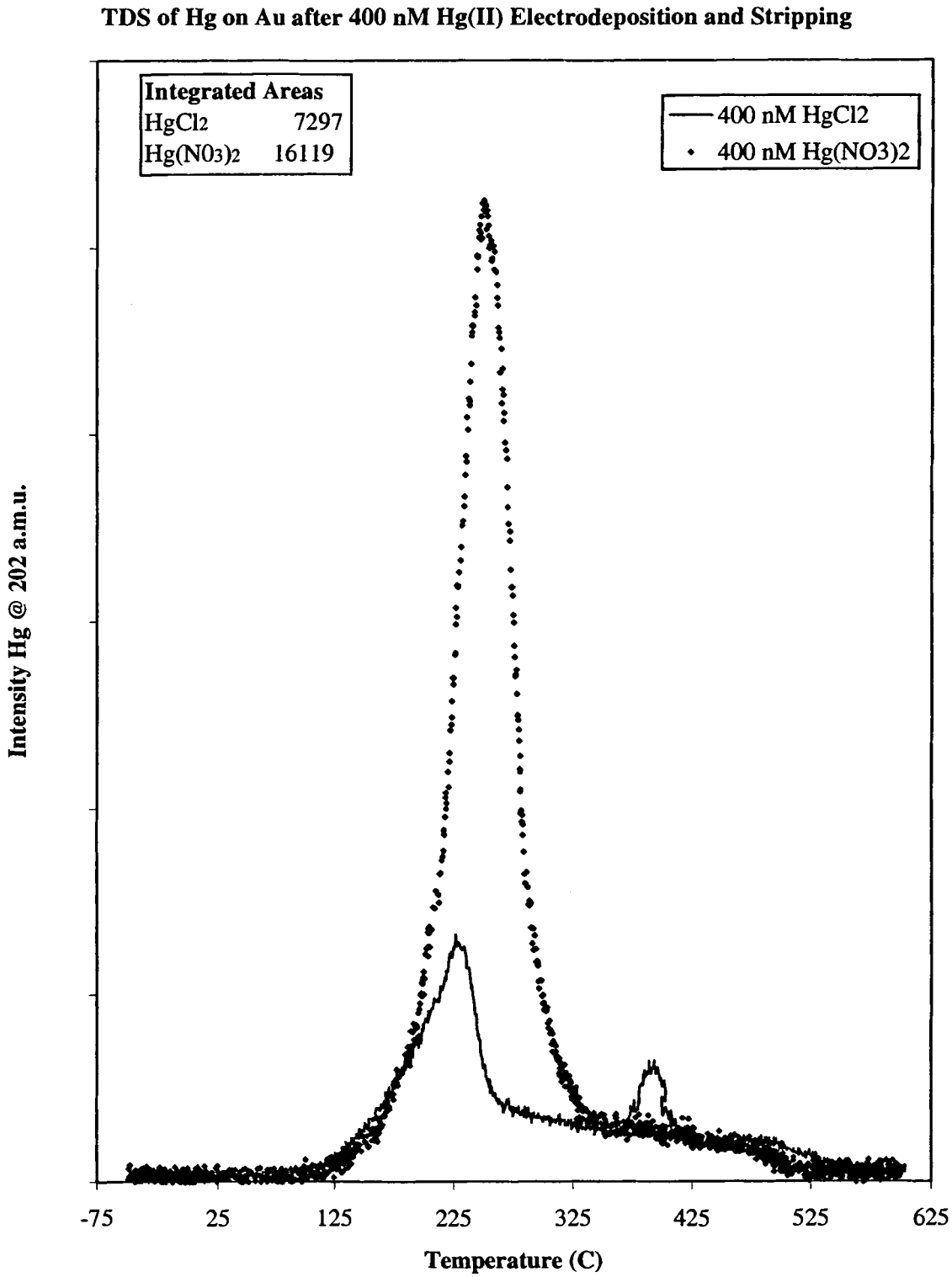

Figure 3.16: 4°C/s TD spectra made by monitoring the thermal desorption, of ^{202}Hg from a 0.8 cm^2 Au foil that had been subjected to 180 minutes of repeated cycles of electrochemical deposition (30 s, at –0.5 V), and stripping (60 s, at +1.0 V) in 400 nM $HgCl_2$ and $Hg(N0_3)_2$ in 2.5 mM KC1 or KNO_3 at pH 3, flowing at ~7 mL/min.

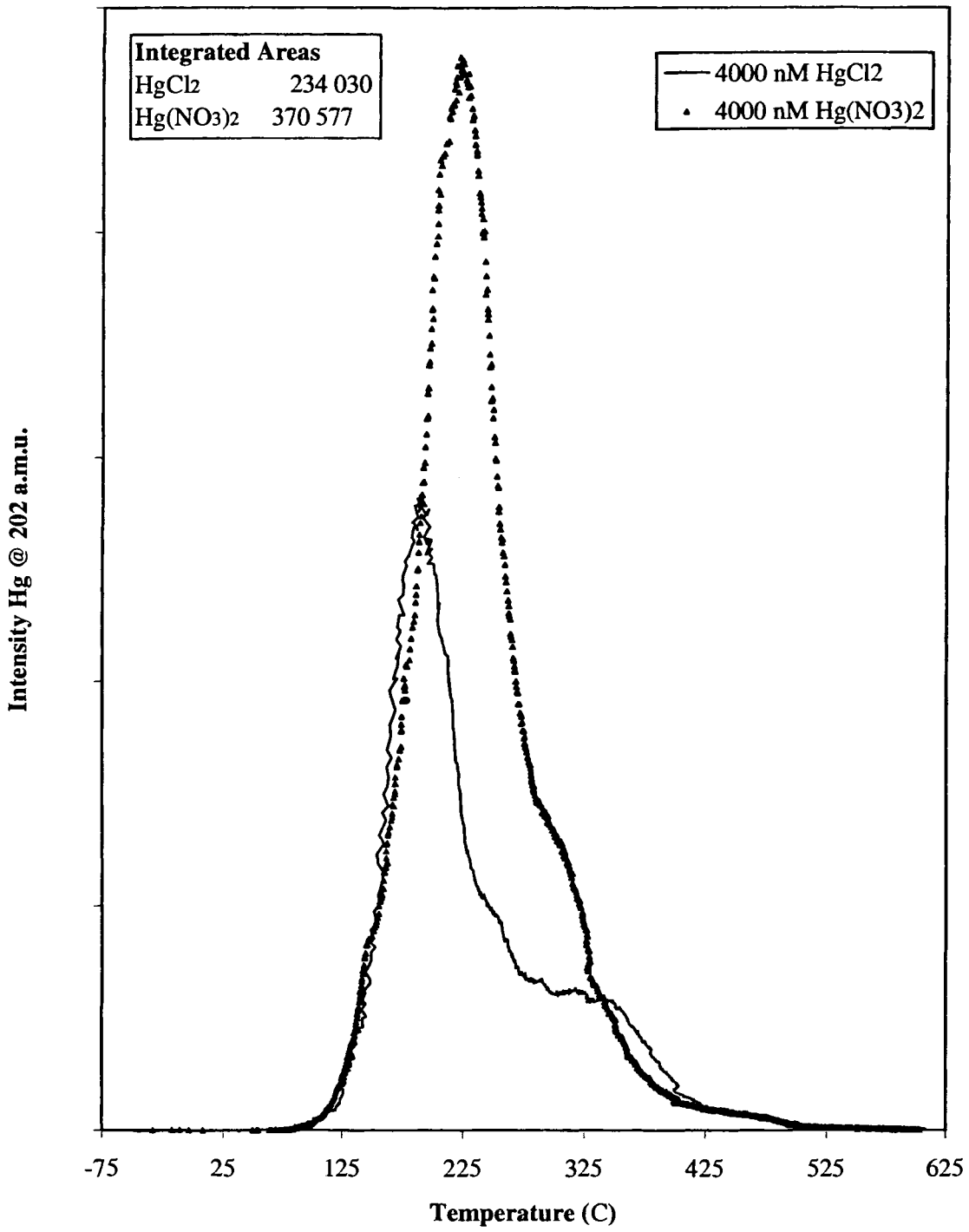

Figure 3.17: 4°C/s TD spectra made by monitoring the thermal desorption, of ^{202}Hg from a 0.8 cm^2 Au foil that had been subjected to 180 minutes of repeated cycles of electrochemical deposition (30 s, at –0.5 V), and stripping (60 s, at +1.0 V) in 4000 nM $HgCl_2$ and $Hg(N0_3)_2$ in 2.5 mM KC1 or KNO_3 at pH 3, flowing at ~7 mL/min.

In the experimentation for Chapter II, it had been suggested by a reviewer of our publication that the retained mercury was from calomel. However, we had looked for evidence of this with XPS and there was never a hint of a chloride peak, even when we didn't rinse the electrode when removing it from the electrochemical cell and transporting it to the surface analysis laboratory. Another possibility could be that it is mercury oxide. Our solutions are exposed to air, and although sparged before use, this does not continue during the repetitive deposition / stripping cycling. As with chloride ion, we never did see an oxygen peak with XPS. Further, we did a TDS experiment where we monitored ^{16}O at 16 a.m.u. of the gold electrodes after deposition / stripping cycling with Hg(II). There was never any 16 a.m.u. oxygen peak detected, yet, it was easily monitored when we let a small amount of an HgO slurry dry onto the surface of a gold electrode (see supplemental figures in Appendix D). It seems likely that the mercury is desorbed from two different surface sites. The question remains whether they are more horizontally oriented or vertically oriented.

Table 3.2 employs equation 3.3 to relate the amount of mercury accumulated on gold electrodes during the repetitive electrochemical deposition and stripping processes. There are two remarkable observations to be made about the data in Table 3.2. First, there is a significant increase in the amount of mercury accumulated on the electrode in the

Table 3.2: TDS Determination of Hg Accumulation on Gold Electrodes

	TDS Peak Area	ng Hg	% of Total Hg
40 nM $HgCl_2$	5 200	260	7.79
40 nM $Hg(NO_3)_2$	7 200	290	8.66
400 nM $HgCl_2$	7 300	290	0.87
400 nM $Hg(NO_3)_2$	16 000	420	1.26
4000 nM $HgCl_2$	230 000	3600	1.09
4000 nM $Hg(NO_3)_2$	370 000	5600	1.69

deposition / stripping experiments conducted in 4000 nM Hg(II). The accumulated amount of mercury from the from the 4000 nM cycling is more than 20 times that of the 400 nM runs for both Hg(II) species; whereas, the difference between TDS peak areas, from the 40 and the 400 nM solutions, are at most doubled. Second, the percentage of the total mercury retained is much higher in the 40 nM experiments than in either of the other experimental concentrations. If we recall that in one 60 second deposition, the adsorption of at least one monolayer's worth of mercury was achieved when the Hg(II) concentration was about 180 nM. The explanation of this phenomenon is likely related to the manner in which the mercury is deposited.

When the Hg(II) concentration is high (e.g. 4000 nM) the mercury is deposited as clusters and the clusters grow to metallic size sufficiently fast to allow significant amalgamation and adlayer formation during the 30 second deposition period. In the more dilute Hg(II) solutions (e.g. 40 and 400 nM), there are fewer deposition clusters that are sufficiently large to possess metallic characteristics allowing for rapid amalgamation. We note in Table 3.2 that the amount of accumulated mercury is almost the same for the 40 and 400 nM solutions. This indicates that although the relative number of metallic mercury deposition clusters is the same in the 40 and 400 nM solutions. The dramatic difference between the 400 and 4000 nM experiments is likely due to the surface being completely covered in Hg(0) during the 30 second deposition phases. When this is the case surface amalgamation will proceed at a maximal rate. We would expect there to be an inflection point in a plot of Hg(II) concentration and mercury accumulation. That inflection point would represent the Hg(II) concentration above which there could be no increase in the rate of amalgamation. Presumably, this is when the surface is entirely covered with Hg(0) and further deposition is the simple adsorption of Hg(0) adlayers.

Conclusions

The extremely small amount of mercury retained on gold electrodes after a single electrochemical deposition, stripping and cleaning process develops into a non negligible quantity, when such a process is repeated several hundred times. The accumulation of mercury on gold electrodes occurs whether the electrodeposition is from very dilute (40 nM) or, very concentrated (0.01 mM) Hg(II) solutions. It occurs whether or not any one deposition cycle results in the adsorption of a monolayer's worth of mercury on the gold electrode. The propensity for mercury to amalgamate with gold seems to defeat a simple PSA procedure for mercury using gold electrodes. It is likely that mercury's tendency to amalgamate with most metals may lead to the same problems with other electrode materials (e.g. platinum, iridium) as well; although, as a slower rate than with gold. The accumulated mercury gives a latent stripping signal in electrolyte solutions that no longer contain mercury.

The electrodeposition and stripping characteristics of mercury on gold electrodes is dependent on the nature of the electrolyte. Electrolytes containing modest amounts of strongly complexing counter-ions (e.g. 2.5 mM chloride ion) facilitate the electrochemical stripping of mercury from the gold electrodes: shifting the stripping potential negatively with respect to weakly complexing counter-ions (e.g. nitrate). The chloride based electrolytes adsorb less mercury onto the gold electrode surface at any one concentration, or deposition potential when compared to nitrate based electrolytes.

For Further Study

Although we have answered the questions we intended to when starting the work on the accumulation of mercury on gold foil electrodes in protracted electrochemical deposition and stripping cycles, we do not know exactly where the retained mercury is on the electrode. We also did not fully explain the variations in the amount of mercury that was retained on the gold electrodes as a function of solution Hg(II) concentration, seen in Table 3.2. These are two areas that warrant further investigation.

In discussing the latter first, it should be mentioned that there was a fifth data point in Table 3.1 that was well outside the region in which we needed to cover for our TPD calibration. However, the data point was for a deposition at 110 μM after which 1860 μC of mercury was stripped and the TD spectra integration gave count of 101 000. This amount of mercury thermally desorbed at that concentration fit well with the initial solution concentration; but, the stripping peak area was lower than would be expected. If we remember that the TDS experiments are theoretically desorbing all of the mercury and we know that electrochemical stripping does not remove all the mercury then, the data from Table 3.1 and 3.2 can be explained. There will be a point, in the electrochemical deposition of mercury, that the rate, or the amount, of the mercury deposition will be sufficient enough to create adlayers of bulk mercury to the surface of the electrode. At that amount, or rate of deposition, of mercury, the rate of amalgamation will be maximal at a given temperature. Careful electrodeposition / stripping and TDS experimentation of several additional concentrations should allow one to measure the maximum rate of amalgamation of the surface layer.

The question of where is the accumulated mercury on the gold foil electrodes, requires a surface depth profile for the mercury concentration. There have been depth profiles of mercury on gold surfaces before;[20] but, we have not seen a study done on a gold surface that has undergone electrochemical deposition and stripping. Gold surfaces that have had mercury vapor or liquid applied to them would be expected to have regular concentration gradient as the amalgamation process proceeds into the gold lattice. However, the electrochemical deposition and stripping amalgam surface has two interesting aspects. First, is there a mercury depleted surface layer over another amalgam layer and second, does the process of electrodeposition create a different type of amalgam surface for the same amount of mercury coverage as would vapor exposure. The argon plasma etching experiments mentioned in Chapter II indicate that the mercury is fairly near the surface. We conducted some preliminary experiments to determine where lay the accumulated mercury on the gold foil electrode.

To answer the first question, we conducted a preliminary surface analysis by laser desorption Fourier Transformation Ion Cyclotron Resonance Mass Spectroscopy (LD-FT-ICR-MS). The experiment confirmed that the retained mercury was within approximately the first 100 Å of the electrode surface. The pulsed experiment showed a 49:1 Au:Hg ratio on the first pulse and no mercury after that. The depth profile was not calibrated; but, what was clear was that the mercury was still just at the surface, otherwise, the second pulsing of the laser would have measured some mercury.

We also did some preliminary Angle Resolved X-ray Photoelectron Spectroscopy (ARXPS). This technique measures the relative abundance of the analyte and the substrate at different "take off angles".[21] The mean free path of the

photoelectrons does not depend on the orientation of the material; thus, surface thickness of the layer they are escaping from becomes a trigonometry problem. The inelastic mean free path for the Au 4f electrons is about 2 nm.[22] As the surface is tilted a thinner and thinner surface layer is analyzed. This is depicted in Figure 3.18. We conducted some preliminary ARXPS studies on some gold foil electrodes that had under gone the same deposition / stripping cycling with 4000 nM $HgCl_2$ in its supporting electrolyte. Some representative XPS scans are shown in Figure 3.19 and a graph of the relative abundance of mercury and gold at different take off angles comprised Figure 3.20.

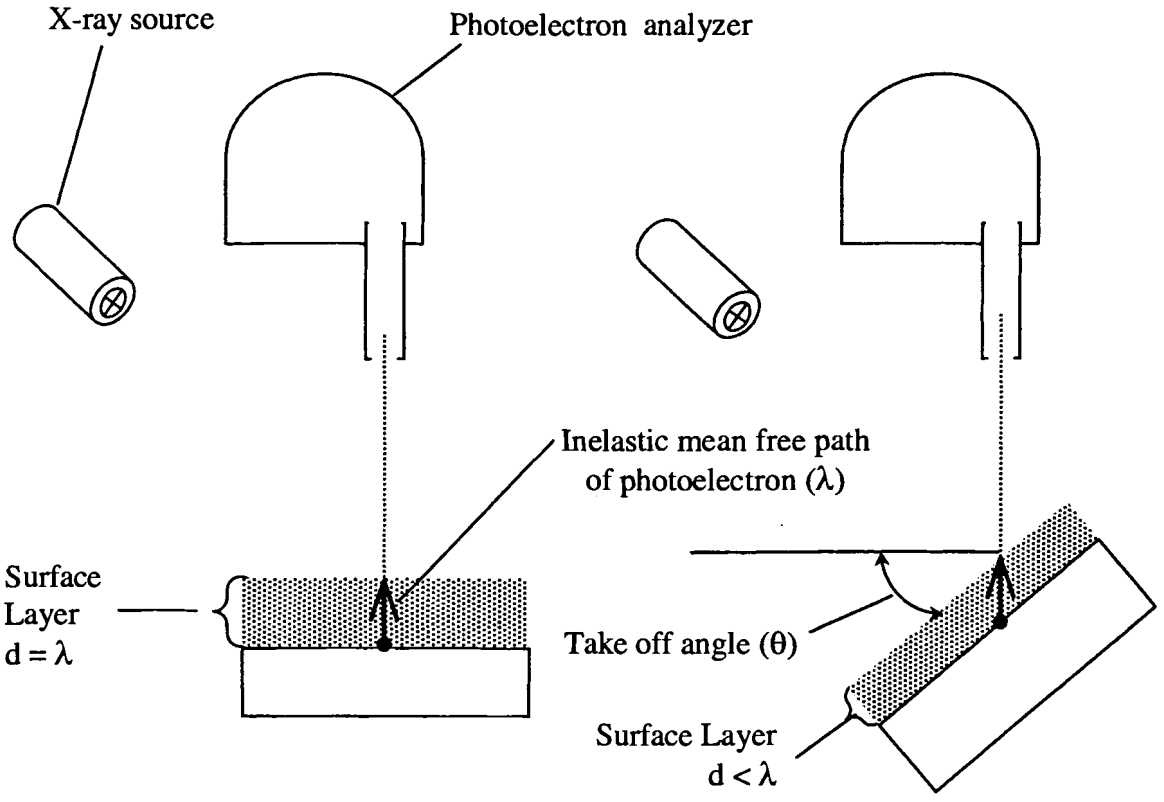

Figure 3.18: Experimental set up for ARXPS studies

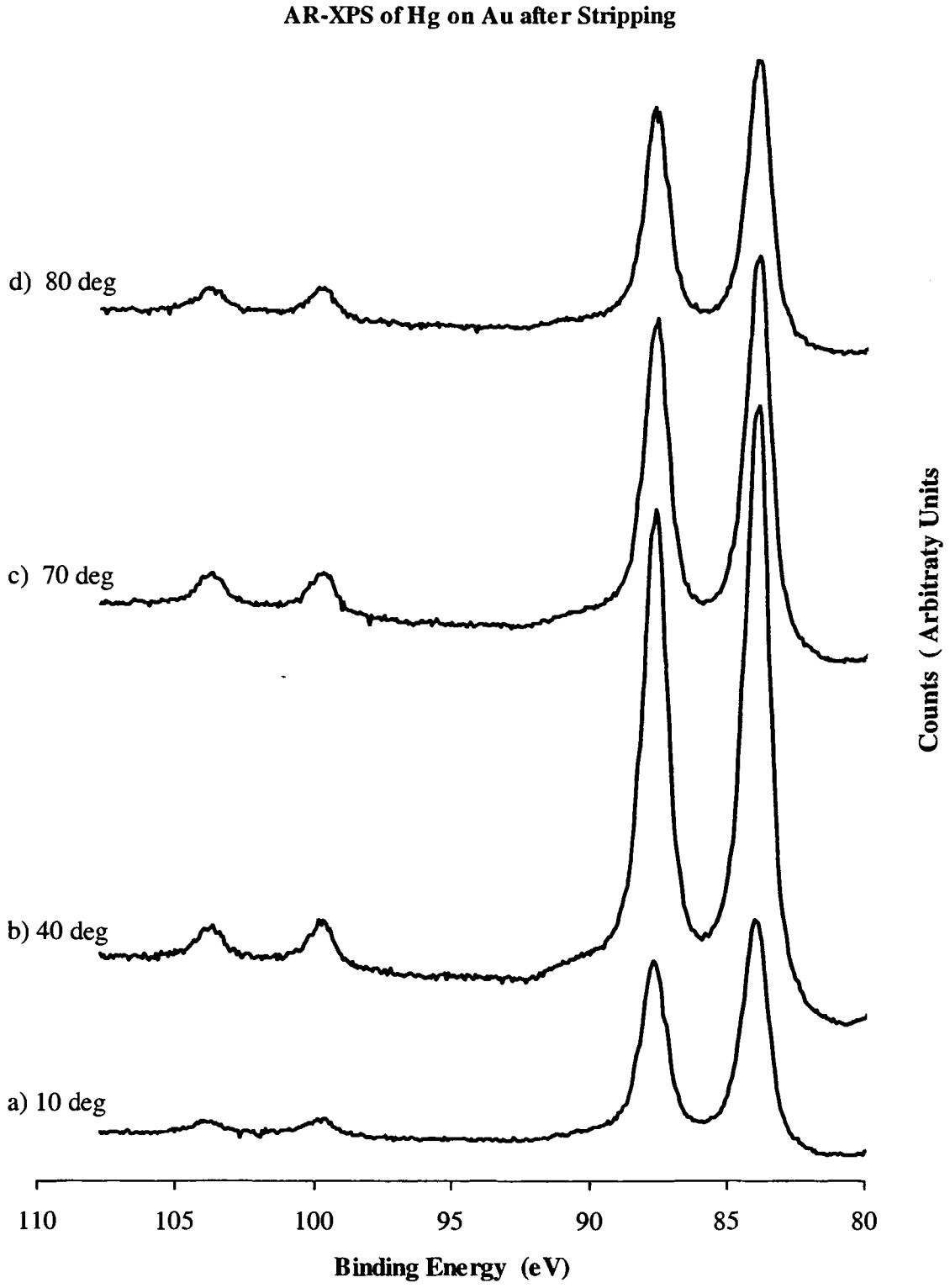

Figure 3.19: AR-XPS of a 0.8 cm^2 Au foil, subjected to 180 minutes of repeated deposition / stripping cycles of (30 s, at –0.5 V) and (60 s, at +1.0 V) in 4000 nM $HgCl_2$. The take off angles shown are: a) 10°, b) 40°. c) 70°, d) 80°.

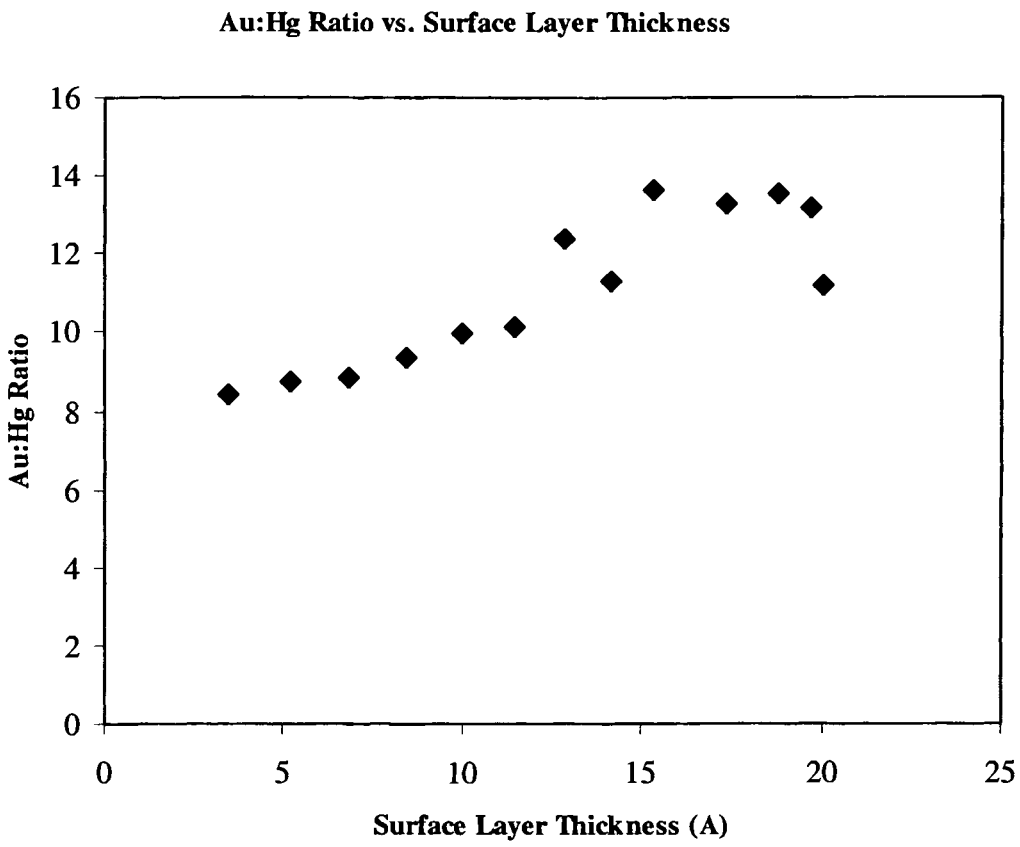

Figure 3.20: Au:Hg ratio as a function of surface thickness from AR-XPS.

Figure 3.19 and 3.20 show that there is some variation of the mercury concentration with respect to the depth of the surface analyzed. Although the data points of Figure 3.20 look like a fairly linear relationship at high take off angles (low surface thickness), we need to remember that as thicker layers of the surface are analyzed we are seeing a summation through that surface. The Au:Hg abundance ratios were calculated using Equation 3.4 with a summation of the Au and Hg 4f

photoelectron peak areas (after background subtraction) and using Hartree-Slater subshell photoionization cross-sections to generate the relative abundances from the AR-XPS data.[23♦]

$$Au : Hg = \frac{(Au_{5/2} / 7.68 + Au_{7/2} / 9.79)}{(Hg_{5/2} / 8.43 + Hg_{7/2} / 10.75)} \qquad (3.4)$$

To complete the depth profile analysis of where the accumulated mercury resides on the gold film electrodes, these AR-XPS data need to be fitted to models calculating the theoretical abundances of Hg and Au. The models need to consider: the mean free path of the photoelectrons and whether it is fixed or attenuated and various functions to represent the changes in the ratios of mercury and gold atoms as a function of depth.[24] Other means of examining the mercury concentration on the gold foil electrodes as a function of depth means of would be by calibrated argon plasma etching with either XPS detection of mass spectroscopy. The LD-FT-ICR-MS experiments that we attempted could be conducted at softer desorption energies.

The most useful may be the modeling. Not necessarily for this particular system that is a difficult one to study and fairly inert in terms of its usefulness. However, the adequate characterization of the residual mercury gold amalgam from electrodeposition and stripping experiments would help understand the modeling capabilities of other complex layered surfaces.

♦ The Hartree-Slater photoionization cross sections for Au and Hg, 5/2 and 7/2 spin orbit coupling are: 7.68, 9.79,8.43,10.75 respectively for a Mg Kα x-ray source at 1254 eV.

References

[1] a) Gustavsson, I. Journal of Electroanalytical Chemistry, 1986, 214, 31-6. b) Huang, H., Jagner, D., Renman, L. Analytica Chimica Acta., 1987, 202, 117-22. c) Huang, H., Jagner, D., Renman, L. Analytica Chimica Acta., 1987, 201, 1-9. d) Wang, J., Tian, B. Analytica Chimica Acta., 1993, 274, 1-6. e) Andrews, R. W., Larochelle, J. H., Johnson, D. C. Analytical Chemistry., 1976, 48(1), 212-4. f) Svoboda, G. J., Sottery, J. P., Anderson, C. W. Analytica Chimica Acta., 1984, 166, 297-99. g) Zakharova, E. A., Pichugina, V. M., Tolmacheva, T. P. Journal of Analytical Chemistry., 1996, 51(9), 918-23. h) Vincente-Beckett, V. A. Australian Journal of Chemistry, 1989, 42, 2107-18. i) Beinrohr, E., Cakrt, M., Dzurov, J., Kottas, P., Kozáková, E. Fresenius' Journal of Analytical Chemistry., 1996, 356, 253-8. j) Zen, J.-M., Chung, M.-Journal of Analytical Chemistry. 1995, 67, 3571-7.

[2] a) Gil, G. A., Fitzgerald, W. F. Marine Chemistry., 1987, 20, 227-43. b) Levlin, M., Niemi, H. E.-M., Hautojärvi, P., Ikävalko, E., Laitnen, T. Fresenius' Journal of Analytical Chemistry. 1996, 355, 2-9. c) Campos, R. C., Porto de Silverira, C. L., Lima, R. Atomic Spectroscopy, 1997, 18(2), 55-9. d) Schroeder, W. H., Jackson, R. A. International Journal of Environmental Analytical Chemistry, 1988, 22, 1-18. e) Hldky, Z., Risova, J., Fisera, M. Journal of Analytical and Atomic Spectroscopy, 1990, 5, 691-2. f) Liang, L., Bloom, N. S. Journal of Analytical and Atomic Spectroscopy 1993, 8, 591-4. g) Ebenezer, D., Denoyer, E. C., Tyson, J. F. Journal of Analytical and Atomic Spectroscopy, 1996, 11, 127-32. h) Butler, M. A., Ricco, A. J., Baughman, R. J. Journal of Applied Physics, 1990, 67(9), 4320-6.

[3] Watson, Charles M., Dwyer, Daniel J., Andle, Jeffrey C., Bruce, Alice E., Bruce, Mitchell R. M. Stripping Analyses of Mercury Using Gold Electrodes: Irreversible Adsorption of Mercury. Analytical Chemistry, 1999, 71(15), 3181-3186.

[4] The NALCO Water Handbook 2nd Ed., Kremmer, Frank N. Ed., McGraw-Hill, New York, 1988.

[5] a) Bonfil, Y., Brand, M., Kirowa-Eisner, E. Reviews in Analytical Chemistry, 2000, 19(3-4), 201-216. b) Bonfil, Y., Brand, M., Kirowa-Eisner, E. Analytica Chimica Acta, 2000, 424(1), 65-76.

[6] a) Khustenko, L. A., Larina, L. N., Nazarov, B. F. Journal of Analytical Chemistry, (Translation of Zhurnal Analiticheskoi Khimii) 2003, 58(3), 262-267. b) Ugo, P., Zampieri, S., Moretto, L. M., Paolucci, D. Analytica Chimica Acta, 2001, 434(2), 291-300. c) Richter, Pablo, Toral, M. Ines, Abbott, Bernardo. Electroanalysis, 2002, 14(18), 1288-1293. d) Sancho, D., Deban, L., Barbosa, F., Pardo, R., Vega, M. Food Chemistry, 2001, 74(4), 527-531. e) Berchmans, S., Arivukkodi, S., Yegnaraman, V. Electrochemistry Communications, 2000, 2(4), 226-229. f) Daniele, S., Bragato, C., Baldo, M. A., Wang, J., Lu, J. Analyst, 2000, 125(4), 731-735. g) Wang, J., Grundler, P., Flechsig, G.-U., Jasinski, M., Lu, J., Wang, J., Zhao, Z., Tian, B. Analytica Chimica Acta, 1999, 396(1), 33-37.

[7] a) Rievaj, M., Mesáros, S., Bustin, D. Collection of Czechoslovak chemical communications, 1993, 58, 2918-2923. b) Wang, J., Larson, D., Foster, N., Armalis, S., Lu, J., Rongrong, X., Olsen, K., Zirino, A. Analytical Chemistry, 1995, 67, 1481-1485. c) Wang, J., Tian, B., Lu, J., Wang, J., Luo, D. Electroanalysis, 1998, 10(6), 399-402. d) Svancara, I., Matousek, M., Sikora, E., Schachl, K., Kalcher, K., Vytras, K. Electroanalysis, 1997, 9(11), 827-33

[8] a) Gil, E. P., Ostapczuk, P. Analytica Chimica Acta 1994, 293, 55-64. b) Ostapczuk, P. Analytica Chimica Acta, 1993, 271, 35-40. c) Wu, Q., Apte, S. C., Batley, G. E., Bowles, K. C. Analytica Chimica Acta, 1997, 350, 129-134.

[9] a) Nowakowski, R., Kobiela, T., Wolfram, Z., Dus, R. Applied Surface Science, 1997, 115, 217-231. b) George, M. A., Glaunsinger, W. S. Thin Solid Films, 1990, 189, 59-72. c) George, M. A., Glaunsinger, W. S. Thin Solid Films, 1994, 245, 215-25. d) Yang, X.-M., Tonami, K., Nagahara, L. A., Hashimoto, K., Wei, Y., Fujishima, A. Surface Science, 1995, 324, L362-L366.

[10] a) Schadewald, L. A., Linstrom, T. R., Hussein, W., Evenson, E. E., Johnson, D. C., Journal of The Electrochemical Society, 1984, 131(7), 1583-7. b) Chen, C., Gerwirth, A. A. Physical Review Letters, 1992, 68(10), 1571-4.

[11] Physics and Chemistry of Finite Systems: From Clusters to Crystals, Jortner, J., Jena, P., Khanna, S. N., Rao, B. K. Eds. Nato ASI Series, Klumer Academic Publishers, Dorrecht, 1991. Chpt. 1.

[12] Salié, G., Bartels, K. Journal of Electroanalytical Chemistry., 1988, 245, 21-38.

[13] The Encyclopedia of the Chemical Elements, Hampel, C. A. Ed., 1987, Reinhold Book Corporation, New York.

[14] Yang, X.-M., Tonami, K., Nagahara, L. A., Hashimoto, K., Wei, Y., Fujishima, A. Surface Science, 1994, 319, Ll7-L22.

[15] Diffusion in Solids, Shewmon, P. G. 1983, J. Williams Book Co., Jenks, OK, Chpt 1 and 3.

[16] a) Herrero, E., Li, J., Abruña, H. D. Proceedings of The Electochemical Society, 1997, 17, 277-91. b) Inukai, J., Sugita, S., Itaya, K. Journal of Electroanalytical Chemistry. 1996, 403, 159-68. c) Herrero, E., Abrufla, H. D. J Phys. Chem. B, 1988, 102(2), 444-51.

[17] a) Brewer, G. E. F. Electrodeposition of Coatings: Advances in Chemistry Series 119, 1973, American Chemical Society, Washington. b) Mayer, A. Journal of The Electrochemical Society, 1990, 137(9), 2806.

[18] a) Ostapczuk, P. Analytica Chimica Acta, 1993, 273, 35-40. b) Oliveira, C. M. R. R., Rebelo, M. J. F., Camoes, M. F. G. F. C. Analyst, 1996, 121(12), 1907-10. c) Covington, A. K,, Katay, R. Journal of The Chemical Society: Faraday Transactions, 1993, 89(2), 369-76. d) Ciszewski, A., Lukaszewski, Z. Talanta, 1988, 35(3), 191-7. d) Hatle, M. Talanta, 1987, 34(12), 1001-7. e) D'yachenko, Y. I., Kondratev, V. V. Journal of Analytical Chemistry., 1998, 53(4), 351-6. f) Zakharova, E. A., Pichugina, V. M., Tolmacheva, T. P. Journal of Analytical Chemistry., 1996, 51(9), 918-23.

[19] a) Sallsten, G., Nolkrantz, K., Analyst, 1998, 123, 665-8. b) Blanchard, L. J., Robertson, J. D. Analyst, 1997, 122, 1261-4. c) Horvat, M., Lupsina, V., Pihlar, B. Analytica Chimica Acta, 1991, 243, 71-9. d) Ho, M. H., Guilbault, G. C. Analytica Chimica Acta, 1981, 130, 141-7.

[20] a) Battistoni, C., Bemporad, E., Galdikas, A., Kaciulis, S., Mattogno, G., Mickevicius, S., Olevano, V. Applied Surface Science, 1996, 103(2), 107-111. b) Mroz, S. Progress in Surface Science, 1998, 59(1-4), 323-330. c) Tougaard, S., Hansen, H. S., Neumann, M. Surface Science, 1991, 244(1-2), 125-34.

[21] a) Siuda, R. Vacuum, 1997, 48(3/4), 391-394. b) Palacio, C., Ocon, P., Herrasti, P., Diaz, D., Arranz, A. Journal of Electroanalytical Chemistry, 2003, 545 53-58. c) Cherkashinin, G. Yu. Journal of Electron Spectroscopy and Related Phenomena, 1995, 74(1), 67-75. d) Gries, Werner H. Applied Surface Science, 1996, 100/101(Proceedings of the 13th International Vacuum Congress and the 9th International Conference on Solid Surfaces, 1995), 41-46.

[22] Somorjai, G. A. Introduction to Surface Chemistry and Catalysis, Wiley-Interscience, 1994, New York, 383.

[23] Scofeild, J. H. Journal of Electron Spectroscopy and Related Phenomena, 1976, 8, 129-37.

[24] a) Paynter, R., Angle-resolved X-ray Photoelectron Spectroscopy, http://goliath.inrs-ener.uquebec.ca/surfsci/xpslinks.html, 2000. b) Siuda, R. Vacuum, 1997, 48(3/4), 391-394.

CHAPTER IV

Investigation of the Formation of Free Thiolate Ions from Metal-Thiolate Chalcogenides

Introduction

The study of molecules that give rise to free thiolate ions is an important area of chemistry primarily because of the role that sulfur atoms have in biochemistry. The tertiary and quaternary structure of proteins is determined significantly by the interactions of the cysteine residues and their formation of disulfide bonds (figure 4.1)[1]. The chemistry of cysteine residues in proteins is of great interest since this thiol amino acid plays such an important role in protein function, and in the interaction of proteins with metals either as beneficial cofactors or as toxins[2]. The cysteine residues are targets of medicinal chemists as binding sites for metal-based drugs. The chemistry of cysteine in proteins can be generally characterized as the equilibrium between thiolate, thiol and disulfide[1].

a)

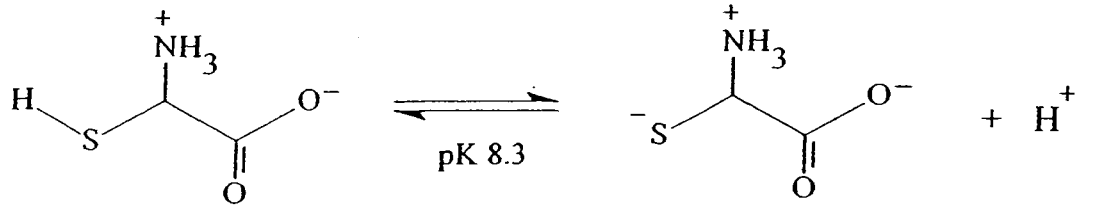

b)

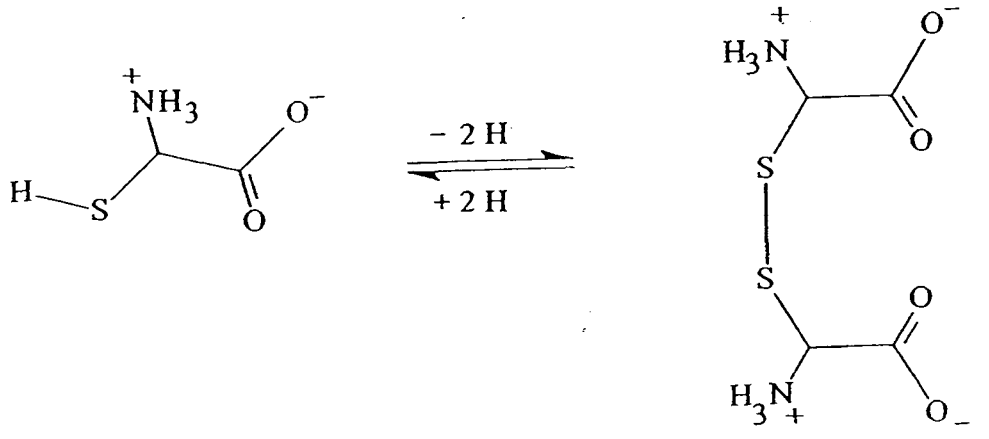

Figure 4.1: a) The equilibrium between the thiol and thiolate forms of cysteine. b) A representation of the enzyme mediated equilibrium between the thiol and disulfide forms of cysteine.

An important part of this equilibrium is the existence of free thiolate ionic sites. There are several groups investigating the role of the free thiolate sites in protein functions.[2, 3] Another reasons for studying molecules that produce free thiolate ions is that such molecules could serve as reagents to produce the nucleophillic anion.

Currently, the routes to obtaining a free thiolate nucleophile are from alkali metal salts, which have solubility difficulties in most organic solvents, or from the reduction of disulfide molecules[4]. Thus, molecules that produce free thiolate may be useful as model compounds for studying the fundamental chemistry of cysteine residues of proteins or as reagent molecules for synthetic chemistry. Metal-thiolate chalcogenides, comprised of a crown-ether stabilized metal ions and thiolate ligands, may be the type of molecules for the studies mentioned above. Figure 4.2 depicts the molecular components of the compounds used in this study and Table 4.1 indicates the molecular formula of each compound investigated. Several of these molecules have solid-state structures with varying degrees of interaction between the alkali metal atom and the thiolate ligand[5]. These interactions range from contact ion pairs to separated ion pairs. The distinction between them is based on the Van der Waals radii at the requisite hapticity of the ligand and the metal ion. Contact ion pairs have sulfur/metal bonds near the sum of the radii of the metal atom center and the sulfur anion and the separated ion pairs have sulfur/metal bond lengths considerably longer than the sum of these radii.

We initiated a study of the electrochemical behavior of these molecules, by means of cyclic voltammetry and conductivity, to see if there was any correlation between the solid-state structures, as determined by X-ray crystallography, and their properties in solution. Proton Nuclear Magnetic Resonance Spectroscopy (^{1}H-NMR) was used in follow-up experiments to confirm the dissociation of free thiolate as a function of compound concentration.

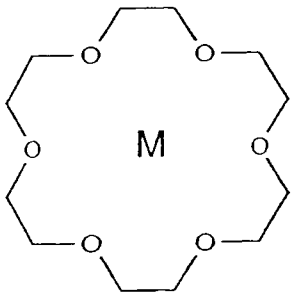

18 Crown 6 (18crn6)
M = Na, K, Sr, Ca, Mg

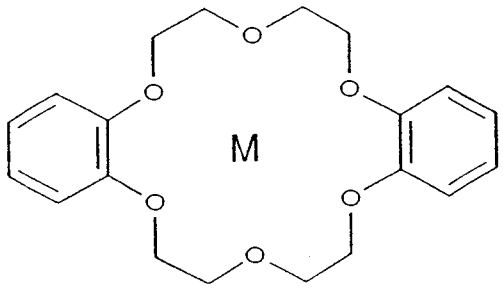

Dibenzo-18 Crown 6 (DB18crn6)
M = Na, K

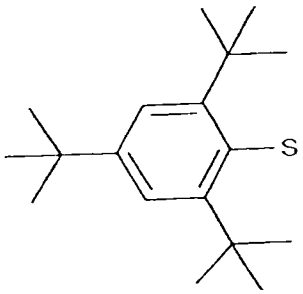

2,4,6-tritertiarybutylphenyl thiolate
(SMes*)

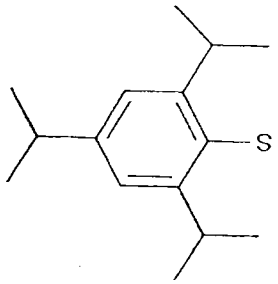

2,4,6-triisopropylphenyl thiolate
(SMes^{x})

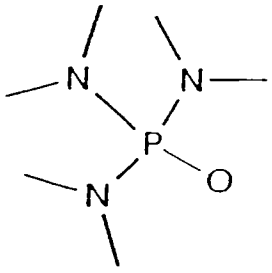

hexamethylphosphoramide
(hmpa)

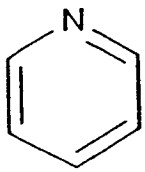

pyridine
(py)

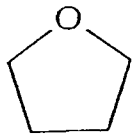

tetrahydrofuran
(thf)

Figure 4.2: Molecular components of the alkali-metal thiolate chalcogenides used in this study.

Experimental

Complex Preparation:

The preparation of the various alkali-metal thiolate chalcogenides was performed by Karin Ruhlandt-Senge et al, at Syracuse University, Syracuse, New York and is described in the literature.[5] In general the thiolate chalcogenides are prepared by dissolving equimolar amounts of the alkali metal hydride, the appropriate crown-ether and the thiol ligand in tetrahydrofuran (THF). The crown-ether and metal hydride are dissolved and the thiol in solution is added. Hydrogen gas evolves as the thiol is reduced to the thiolate. After reducing the solvent, hexane is added and crystals precipitate out after a period of time. The thiolate ligand precursor thiols were made according to procedures outlined by Blower et al.[6]

Table 4.1: Molecular composition of alkali-metal thiolate chalcogenides.

Complex	Structure	Complex	Structure
1	[K(DB18crn6)][SMes*]	**6**	$[Sr(18crn6)_2(hmpa)_2][SMes^*]_2$
2	$[K(18crn6)(thf)_2][SMes^*]$	**7**	$[Ca(18crn6)][SMes^*]_2$
3	$[K(DB18crn6)][SMes^x]$	**8**	$[(Mg(15\text{-}crn\text{-}5)(thf)_2][SMes^*]_2$
4	[Na(DB18crn6)][SMes*]	**9**	$(py)_3Mg(\mu_2\text{-}SPh)_3Mg(\mu_2\text{-}SPh)_3Mg(py)_3$
5	$[Na(18crn6)(thf)_2][SMes^*]$		

Cyclic Voltammetry:

In a VAC *model HE-493* dry-box, tested for oxygen with diethyl zinc (Aldrich 1.0 M in hexane), ~0.1 to 10 ± 2 mg of the crown-ether metal thiolate compounds was added

to 6 mL of 0.25 M tetrabutylammonium hexafluorophosphate (TBA-HFP) (Aldrich 98%), in dry THF (*EM analytical grade*). The THF had been distilled with sodium metal (in paraffin) and benzophenone, added as indicator, in a purging dry nitrogen atmosphere. Cyclic Voltammetry (CV) experiments were conducted on these solutions using an EG&G model 273 potentiostat/galvanostat interfaced with a *Micron* 75 MHz *Powerstation* employing EG&G's m270 software. The working electrode was a 3.25 mm^2 Pt disc, polished with 1.0 μm water-soluble diamond suspension (*Buehler*) on a *Buehler microcloth*, with a 0.5 mm Pt wire auxiliary electrode, coiled parallel to the working electrode at a distance of 4 mm, and a Ag/AgCl reference electrode (BAS # MF 2063; 0.194 mV vs. NHE).[♦] Unless otherwise noted, the working electrode was polished between each CV, and the other electrodes and the cell were well rinsed with dry THF. CVs of ferrocene and the electrolyte solution were recorded in the same conditions.

Conductivity:

In the VAC *model HE-493* dry-box, ~1 to 40 ± 1 mg of the crown-ether metal thiolate compounds was dissolved in 4 to 10 mL of dry THF and then 4 mL of this initial solution was transferred to a graduated cylinder in which a YSI 3253 conductivity cell was immersed. This conductivity cell is equipped with a temperature sensor and the conductivities were read on the YSI model 3200 conductivity meter when the solution was at 25 ± 0.1 °C. After each measurement 1 mL of the solution was diluted with an additional 3 mL of dry THF. The graduated cylinders used for the conductivity

[♦] All potentials cited herein are in reference to this electrode, unless otherwise stated.

measurements and the dilution were rinsed one into the other to assure uniform solution in each and that the walls were not contaminated with higher concentration residues. Between each conductivity measurement the conductivity cell was rinsed in a separate vessel with dry THF, which was renewed for each new measurement. This process was repeated until the variation in conductivity ceased to be greater than 10%. The conductivities of the dry THF and the electrolyte (TBA-HFP) were measured as well.

Nuclear Magnetic Resonance Analysis:

In the VAC *model HE-493* dry-box, 5 ± 1 mg and a trace of **4** was dissolved in two 0.85 mL ampoules of THF-*d*6 (Aldrich 99.99% dry, sealed under nitrogen) to form two solutions of 7 and 0.07 μM. The second concentration was calculated from the integrated ratios of the crown ether protons and the internal standard added to each tube. These solutions were transferred to 5 mm NMR tubes (*Norel* borosilicate) and sealed with rubber septa. In air, 10 μL trimethylphosphate (Aldrich 99%) was diluted in 0.85 mL THF-*d*8 to which 10 μL tetramethylsilane (Aldrich 99%) had been added. This resulted in a solution where 10 μL contained 1 μmol trimethylphosphate (TMP). Upon removal of each tube from the dry-box 60 and 10, μL of the TMP reagent solution was injected through the septa and the recording of ^{1}H-NMR on a Varian 300 MHz spectrometer at room temperature was started immediately.

Results and Discussion

Conductivity:

The conductivity measurements on complexes **1 – 4**, **6**, and TBA-HFP indicates that all these thiolate chalcogenides are weak electrolytes with conductivities 20% or less than the conductivity of the electrolyte (figure 4.3). Table 4.2 has the molar conductivities of these compounds at infinite dilution (Λ_o). These values are for comparative purposes only as the purity and extent of decomposition of the compounds could not be completely assured and these extraneous materials may have a significant effect on the conductivity measurements. Nevertheless, the data in Table 4.2 suggests a correlation between conductivity and the nature of the ion pairing in the crystal structures. Presumably, this implies that the strength of the metal-thiolate interaction seen in the solid-state structure has a parallel in solution.

Cyclic Voltammetry:

Preliminary CV experiments revealed that concentration has a dramatic effect on the oxidation processes observed by cyclic voltammetry. This is illustrated in Figures 4.4a and 4.4b, CVs of compound **4**; where, CV trace 4.4a is ten times more concentrated than that of CV trace 4.4b (approximately 3 and 0.3 mM respectively). At the lower concentration (trace 4.4b), only a single irreversible oxidation process, labeled "II", is observed (~ +0.2 V *vs.* Ag/AgCl), while at the higher concentration, two additional processes, labeled "I" and "III" appear (ca. –0.15 V and +0.5 V, respectively). This pair of CVs is representative of the other thiolate chalcogenides with the dibenzo-crown-ether.

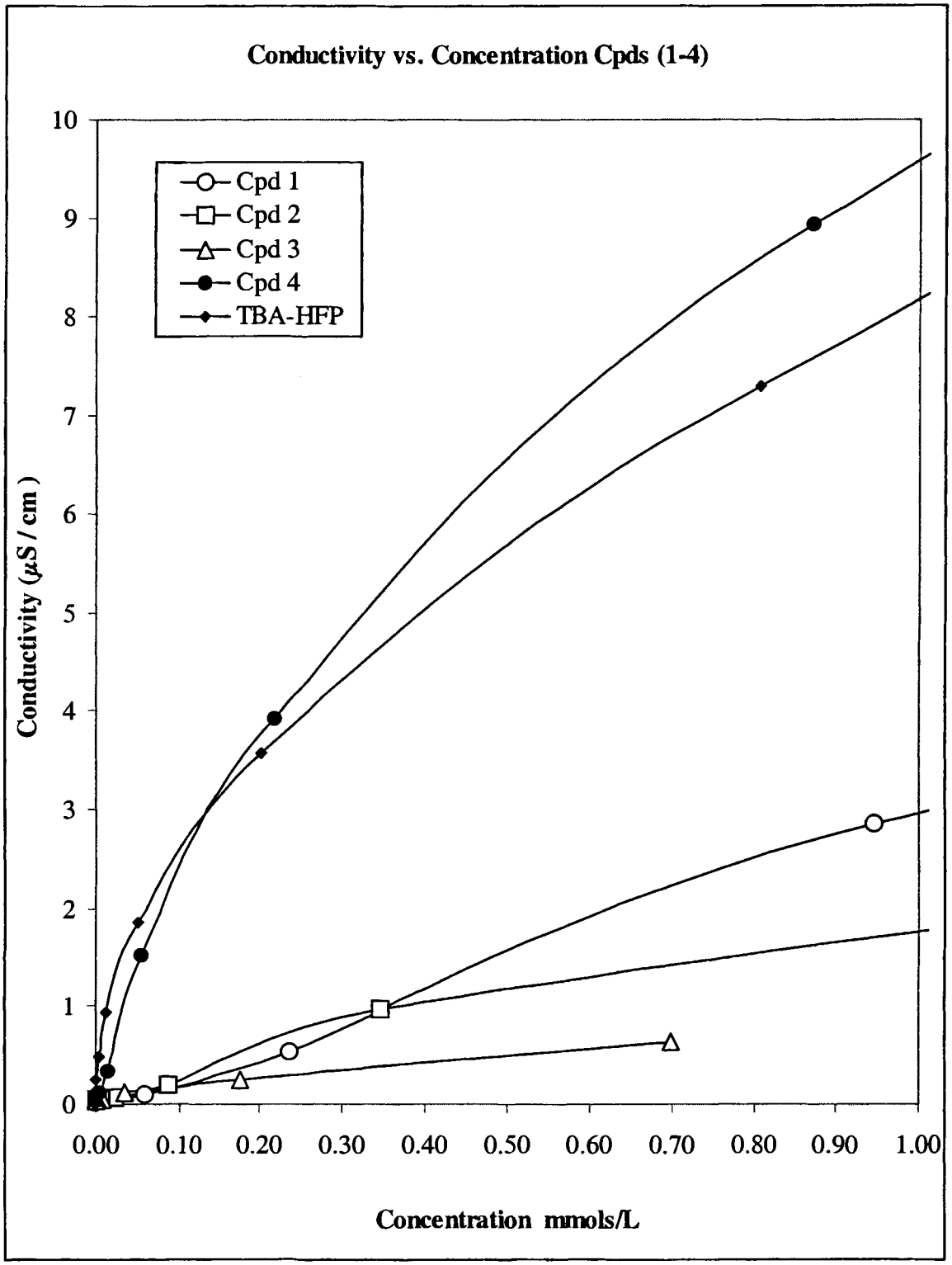

Figure 4.3: Conductivity of complexes **1** – **4**, **6** and TBA-HFP in dry, nitrogen sparged, THF at 25 °C in a nitrogen atmosphere.

Process "I" is an irreversible oxidation while "III" appears to be reversible, or at least quasi-reversible. The appearance of the oxidation "I" is observed when both starting from a concentrated solution and diluting it with electrolyte solution and when adding more thiolate chalcogenide complex to a dilute electrolyte solution. Figure 4.5 shows the electroactive portions of CVs of **1** at a series of concentrations, from 17 mM to 0.35 mM. There is a smooth transition from a CV like 4.4a to one similar to of 4.4b. All the thiolate chalcogenides studied (complexes **1–8**) show concentration dependent appearance of oxidation "I"; however, only the dibenzo-crown-ether complexes develop the reversible redox couple "III". The current intensity of this reversible couple does not increase when the CV experiment is allowed to continue for at least 50 cycles with stirring of the solution every fifth scan.

The reversible redox process "III" does not appear with the thiolate chalcogenide complexes that are not prepared with the dibenzo-crown-ether. Figure 4.6, a CV of **2**, is typical of these complexes. These simple crown-ether thiolate chalcogenides (complexes: **2**, **5** and **6–8**) have either separated or mixed ion pairs in their solid state structures. These designations along with the electrochemical parameters of the thiolate chalcogenides are found in Table 4.2.

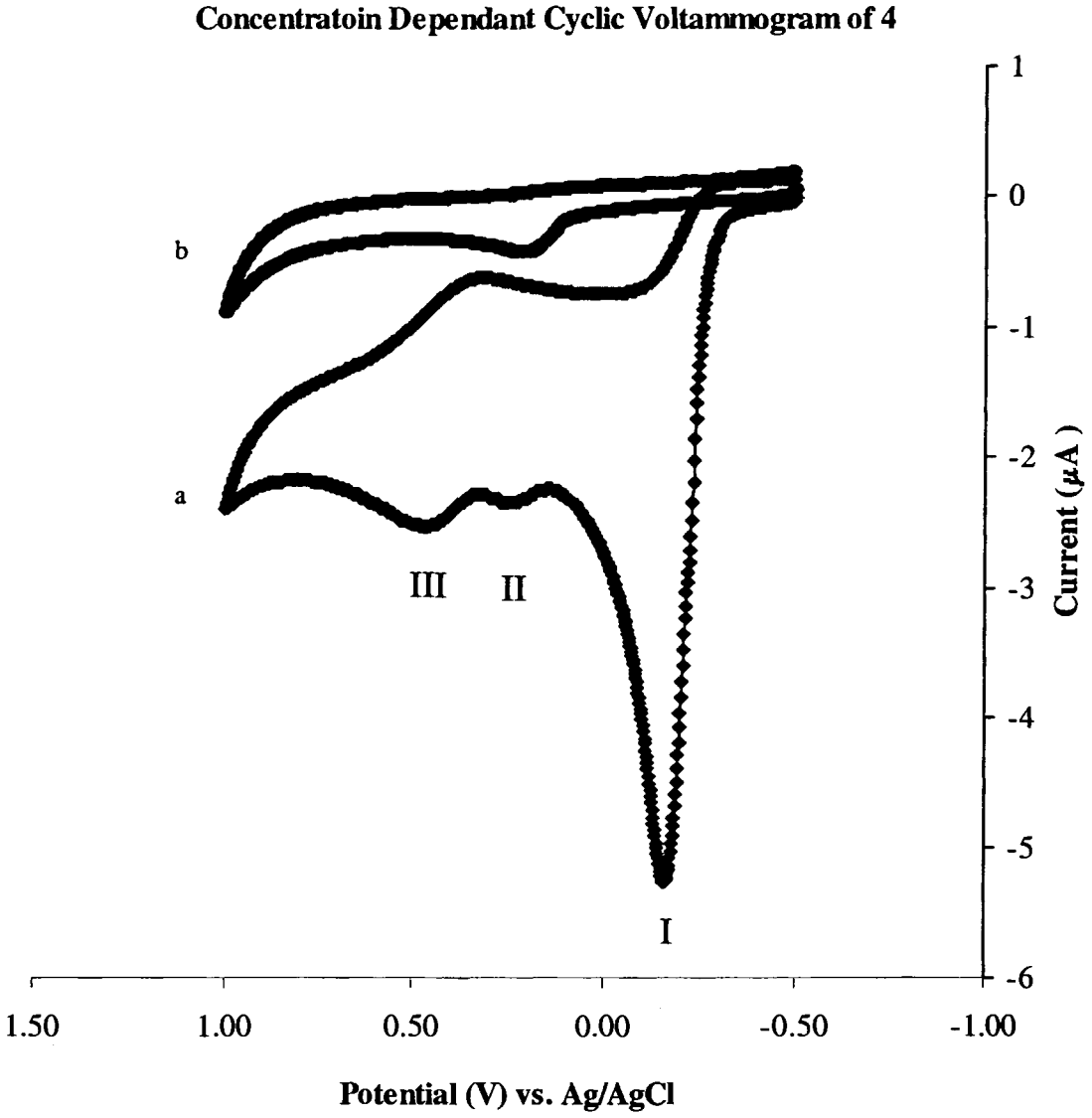

Figure 4.4: Cyclic voltammograms of **4** at: a) 3 ± 0.5 mM and, b) 0.3 ± 0.05 mM, in 0.25 M TBA-HFP (dry THF), using 3.25 mm^2 Pt working electrode, Pt wire auxiliary electrode and a Ag/AgCl reference electrode with a scan rate of 0.1 Vs^{-1}.

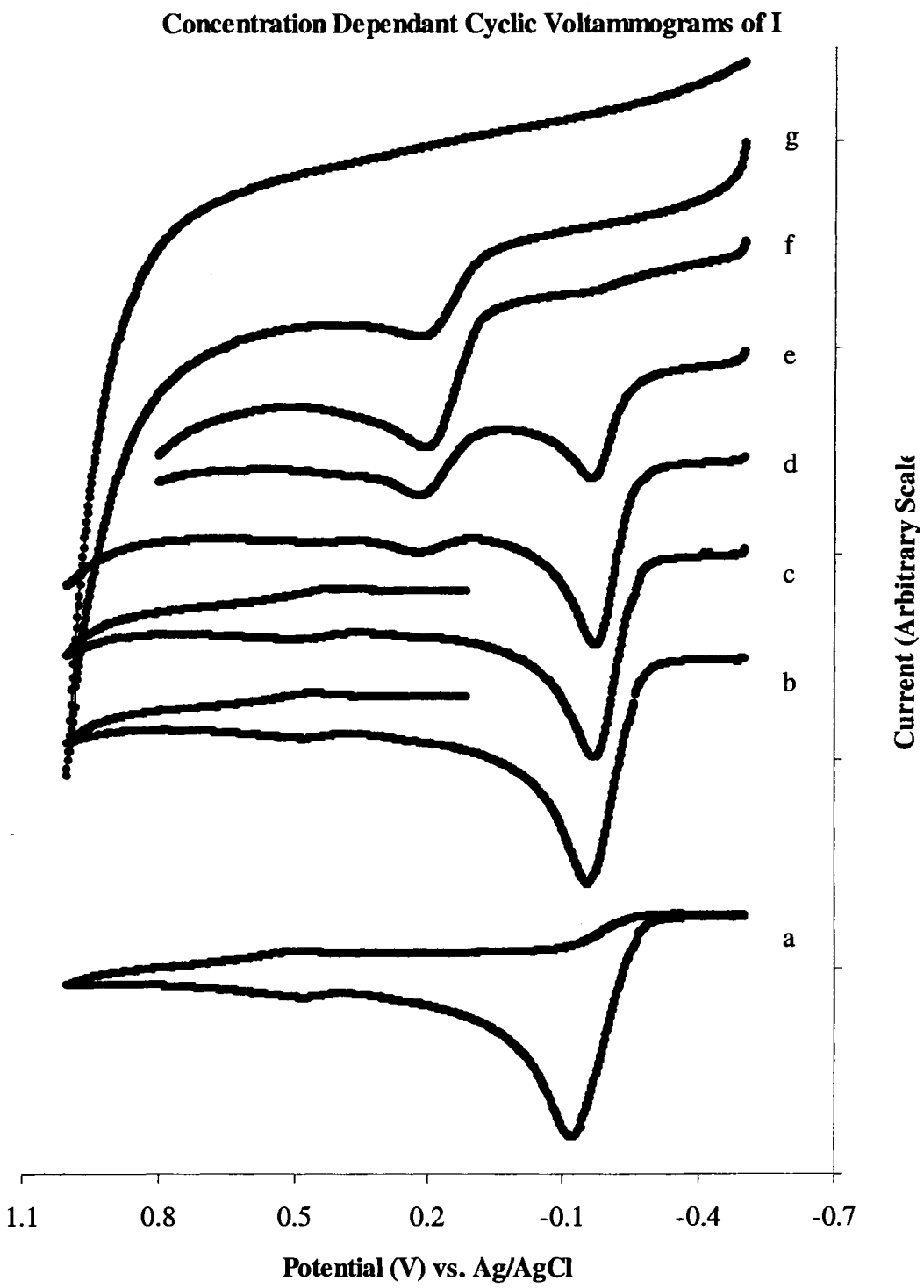

Figure 4.5: Cyclic voltammograms of **1** in 0.25 M TBA-HFP (dry THF), using 3.25 mm^2 Pt working electrode, Pt wire auxiliary electrode and a Ag/AgCl reference electrode with a scan rate of 0.1 Vs^{-1} at: a) 17.5 ± 2 mM; b) 8.0 ± 1 mM, 2× current; c) 3.6 ± 0.5 mM, 5× current; d) 1.6 ± 0.25 mM, 10× current; e) 0.75 ± 0.15 mM, 25× current; f) 0.36 ± 0.1 mM, 40× current; and g) 0.15 ± 0.05 mM, 75× current.

Table 4.2 Electrochemical parameters of metal-thiolate chalcogenides.

Compound	X-Ray ion pairing[b]	Redox Process (mV)[a]			Conductivity Λ_0 ($S \cdot cm \cdot mol^{-1}$)
		I *irreversible oxidation*	II *irreversible oxidation*	III *quasi-reversible*	
TBA-HFP	c				9.9×10^6
(**1**)[K(DB18crn6)][SMes*]	contact	–136	254	473[d]	4.0×10^6
(**2**)[K(18crn6)$(thf)_2$][SMes*]	separate	–126	320	none	5.8×10^6
(**3**)[K(DB18crn6)][$SMes^x$]	contact	–66	350	458[f]	3.4×10^6
(**4**)[Na(DB18crn6)][SMes*]	contact	–166	246	392	3.4×10^6
(**5**)[Na(18crn6)$(thf)_2$][SMes*]	separate	g	238	g	c
(**6**)[Sr(18crn6)$_2$(hmpa)$_2$][SMes*]$_2$	both	–202	258	none	4.3×10^6
(**7**)[Ca(18crn6)][SMes*]$_2$	both	–164	472	none	c
(**8**)[(Mg(15-crn-5)$(thf)_2$][SMes*]$_2$	separate	–172	500	none	c
(**9**)$(Mg(py)_3)_2Mg(\mu_2\text{-}SPh)_6$	c	none	975	none	c

a) Potential vs. Ag/AgCl reference electrode (BAS M1520: 194 mV vs. NHE). b) As determined by Ruhlandt-Senge et al.[5] c) No measurement or determination was made. d) $\Delta E_{iPa\ iPc} \approx 66$ mV. e) $\Delta E_{iPa\ iPc} \approx 144$ mV. f) irreversible oxidation. g) Value not determinable due to insufficient compound.

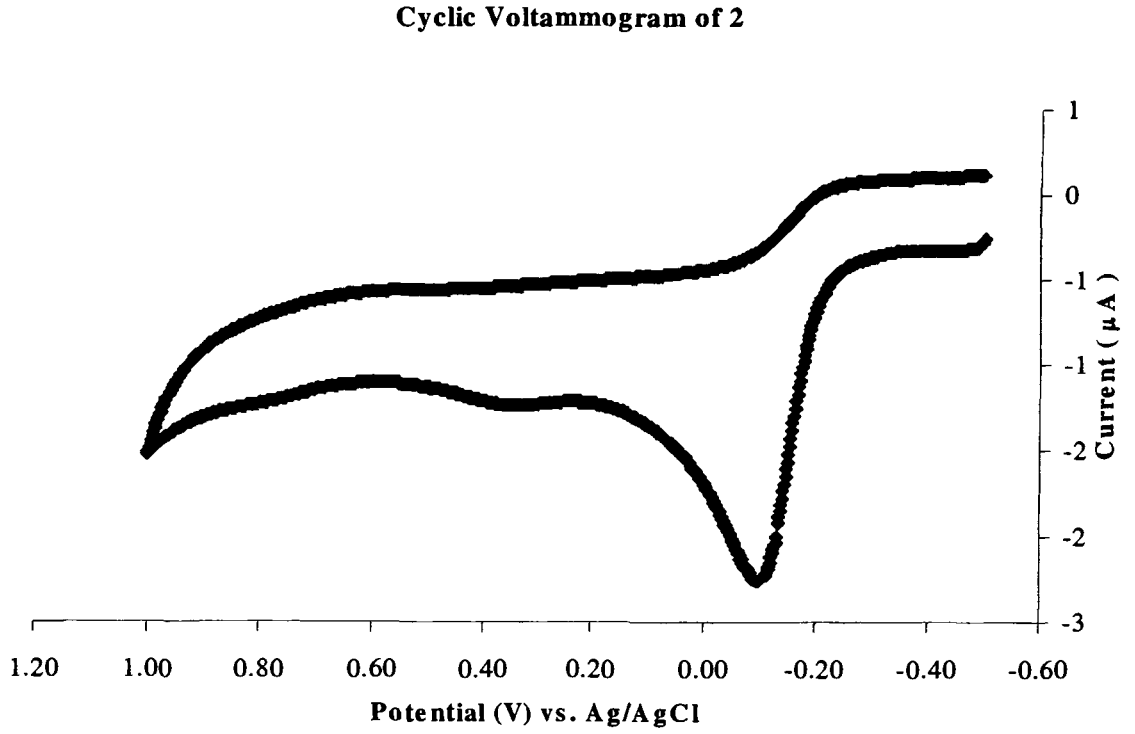

Figure 4.6: Cyclic voltammogram of **2**, 10 ± 1 mM in 0.25 M TBA-HFP (dry THF), using 3.25 mm^2 Pt working electrode, Pt wire auxiliary electrode and a Ag/AgCl reference electrode with a scan rate of 0.1 Vs^{-1}.

Initially, the cyclic voltammetry experiments were conducted to determine if a correlation existed between the oxidation potential of thiolate chalcogenide complexes such as **1** – **3** and the distance and type of sulfur-metal interaction revealed by X-ray analysis. Free thiolates, such as phenyl thiolate (PhS^-), have been shown to undergo oxidation near 0 V (vs. SCE)[♦] followed by a very fast dimerization step with rate constants in the range of 2×10^8 to 2×10^{10} $M^{-1} \cdot s^{-1}$, as indicated in equation 4.1.[7]

$$RS^- \rightleftharpoons 2\ RS^{\bullet} + 2e^- \longrightarrow RSSR \qquad \textbf{(4.1)}$$

However, thiolate groups attached to metals are "protected" from oxidation; thus, shifting the oxidation potentials positively. For example, in phosphine gold thiolate complexes, an irreversible sulfur-based oxidation process is observed at potentials above +0.5 V (vs. SCE)[8] and our measurements on **8**, the magnesium complex with bridging thiolates, only has an irreversible oxidation at +0.975 mV (vs. Ag/AgCl).

The results depicted in figures 4.3–6 and in Table 4.2 reveal that there are some strikingly different complexes in solution at various concentrations than simply the heteroanions and heterocations revealed by x-ray crystallography. To consider what type of oxidation process is involved in wave "II" (the irreversible oxidation occurring at low concentrations: *ca.* ≤ 0.3 mM) it is useful to recognize that **4** is composed of three parts: 1) DB18crn6, 2) Na^+, and 3) SMes*. The oxidations of free DB18crn6 and, DB18crn6 in the presence of alkali metal ions, have been investigated by cyclic voltammetry.[9] No oxidation process is observed if the potential is kept negative of +1.5 V (vs. SCE). In comparison to $Ph_3PAuSC_6H_4CH_3$, which oxidizes at +0.56 V (vs. SCE), "II" occurs around +0.2 (vs. Ag/AgCl). This is reasonable, since the more covalently-bound gold-thiolates are expected to be better protected from oxidation. Thus, "II" is believed to be the oxidation of the SMes* moiety of the thiolate chalcogenide complex: where the thiolate is closely associated with the alkali metal atom.

At higher concentrations (> 0.3 mM), we see, in figure 4.5, the appearance of the new redox processes "I" and "II" in the cyclic voltammograms. Table 4.2 shows that the irreversible oxidation "I" occurs at –0.17 ± 0.03 V (vs. Ag/AgCl) for all the SMes* complexes. Savéant and coworkers have determined that the potential for the oxidation of 0.08 mM of the thiolate $[p\text{-}SC_6H_4CH_3]^-$ to the thiyl radical $[p\text{-}SC_6H_4CH_3]^\bullet$ in

---

[†] The SCE reference electrode is within 50 mV of the Ag/AgCl reference electrode used in this study. Thus these reference scales are very similar.

acetonitrile is +0.04 V (vs. SCE). Their study of the effect that the *para* substituent has on the thiolate oxidation potential showed there is a linear relationship with the Hammett σ coefficient of the substituent group and the fundamental oxidation potential of the free thiolate. In figure 4.7, we extrapolate Savéant's work to the thiolate ligands in our study.

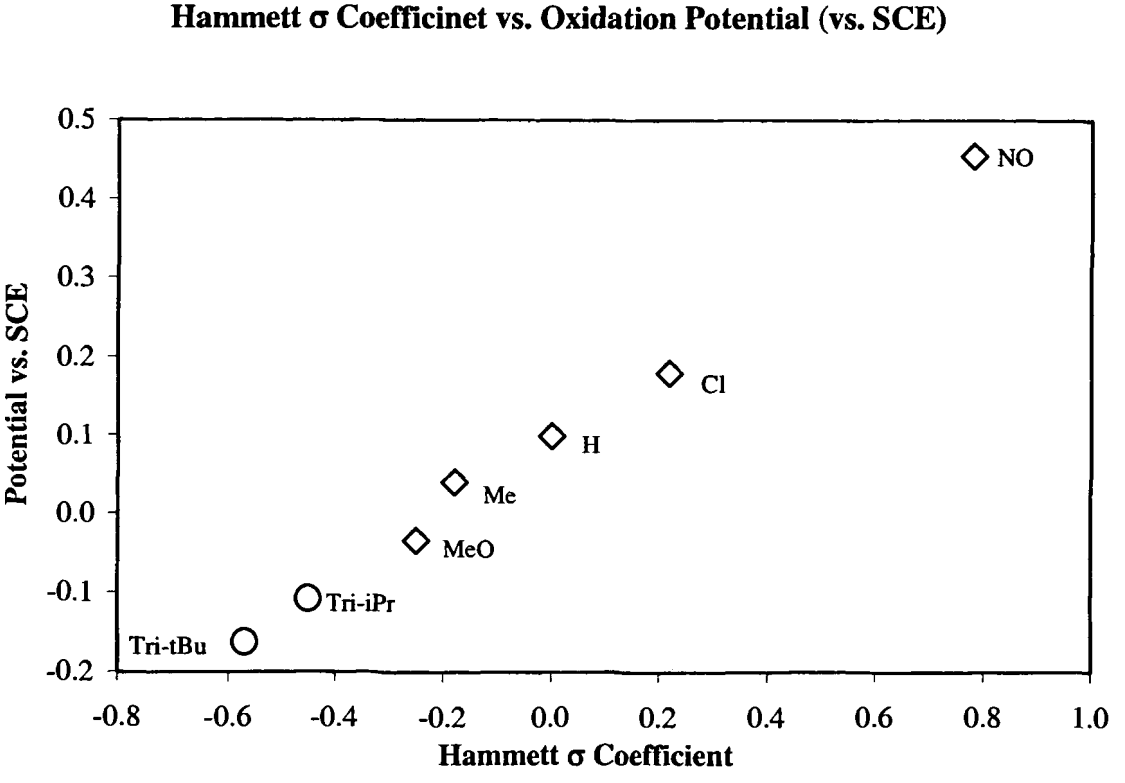

Figure 4.7: *Para*-substituted phenylthiolate oxidation potentials (□) measured by Savéant vs. their Hammett σ coefficients and the extrapolation to *2,4,6*-substituted phenylthiolate complexes (○) vs. their Hammett σ coefficients calculated from the *para*-substituent values reported by Jaffé.

Assuming additivity and using the Hammett σ parameters, reported by Jaffé,[10] we determined that the SMes* and SMes^x ligands would oxidize around –160 and –110 mV, respectively, in the conditions employed by Savéant. Since the resonance and electronic

effects of tertiarybutyl groups in the 2,4,6 positions, neglecting steric effects, are expected to be more electron-donating than a single methyl group in the para position, free thiolate (SMes*) would be expected to oxidize at a potential more negative than $[p\text{-}SC_6H_4CH_3]^-$. On this basis, we assign "I" as the oxidation of free thiolate ($SMes^{*-}$) to the thiyl radical ($SMes^{*\bullet}$). This analysis is somewhat vindicated by the analysis of **3**. The thiolate ligand of this complex has three isopropyl groups as opposed to three tertiarybutyl groups (σ coefficients of –0.153 and –0.197 respectively).[10a] Oxidation "I" occurs at –0.07 V (vs. Ag/AgCl), some 80 mV more positive than it does for **1**.

Redox process "III" in figure 4.4a, occurs at +0.4 V (vs. Ag/AgCl) and, in contrast to "I" and "II", it is reversible (or quasi-reversible). As mentioned above, Cauliez and Simonet investigated the oxidation of the dibenzo-crown-ethers used in our experiments and peak "III" resembles those observed in the oxidation of free DB18crn6 and DB18crn6 associated with alkali metal ions.[9] The oxidation is reported to promote polymerization of the dibenzo-crown-ether. Because the redox potentials for polymerized DB18crn6, in the absence and presence of alkali metal ions, are 500 and 1000 mV (respectively) higher than that observed in the cyclic shown in figure 4.4a, the incorporation of thiolate with the crown-ether metal complex, or polymer, could explain this shift. This suggestion is intriguing, since free thiolate oxidation is expected to produce thiyl radicals ($SMes^{*\bullet}$) at the electrode surface which presumably could instantly react with adsorbed DB18crn6 or alkali metal-DB18crn6 complex, initiating a free radical polymerization process. It is worth renoting that when substituting 18crn6 for DB18crn6, i.e. **2** for **1**, the reversible redox couple "III" does not appear. This, and the

previous work on these crown-ethers, suggests that "III" is the redox couple of a dibenzo-crown-ether alkali-metal thiolate complex. The negative shift in redox potential indicates that there is significant electron density donated by thiolate ligand. It is possible that the peak is an oligomer of the crown-ether polymerization; however, because of the lack of increased current response in continued CV cycling, there was no indication of a polymer product on the electrode surface.

Nuclear Magnetic Resonance Analysis:

Although the dissociation of free thiolate from "concentrated" solutions of these thiolate chalcogenides is well supported by the electrochemical evidence there remains the question of whether or not oxidation peak "I" is really from free thiolate. To test whether or not free thiolate is formed we used trimethylphosphate, a thiolate trapping compound, that reacts with free thiolate creating a methylsulfide and $[(CH_3O)_2PO_2]^-$ as shown in equation 4.2: R is the tertiarybutyl ligand (SMes*).

$$RS^- + (CH_3O)_3PO \longrightarrow CH_3SR + [(CH_3O)_2PO_2]^- \qquad \textbf{(4.2)}$$

Our ^{1}H-NMR spectrum of **1,** in THF-*d*8, corresponded well with the spectrum reported by Ruhlandt-Senge et al).[5d] The proton peaks with their respective integrations were as follows (our data are in parentheses): singlet, 2H, δ 7.02, (δ 7.24); doublet m, 8H, δ 6.95/6.84 (δ 6.9/6.8); broad doublet, 8H, δ 4.13 (δ 4.13); broad doublet, 8H, δ 4.02 (δ 3.97); singlet, 18H, δ 1.76 (δ)1.71; and singlet, 9H δ 1.22 (δ 1.0). Based on the chemical shifts and the integrations, it is fairly easy to attribute these resonances to the protons of **1**. What we noticed is that the region of 2 to 3 ppm is free of peaks and it is in

precisely this region where we would expect the resonance of the methyl protons of the aromatic methyl sulfide we would form in the reaction (4.2).[11] Additionally, the trimethylphosphate reagent does not react with thiolates bound to transition metals.[12] This allows not only the ability to confirm the presence of free thiolate; but, also the possibility to distinguish whether or not the thiolate chalcogenides, at low solution concentrations, produce free thiolate in the same way as the concentrated solutions.

Based on this information, we reacted **4**, at ~7 and ~0.07 mM, in THF-*d*8 (6 and 0.06 μmol respectively) with approximately 6 and 1 μmol of $(CH_3O)_3PO$, respectively. These concentrations of **4** corresponded to CVs that indicated free thiolate at 3 mM and no free thiolate at 0.3 mM. We monitored the 11 Hz doublet at δ 3.70, of $(CH_3O)_3PO$, and the singlet at δ 2.1, from the methyl protons from the methyl tertiarybutylmesityl sulfide, in successive ^{1}H-NMR experiments.

The reaction of **4**, at 7 mM with, $(CH_3O)_3PO$ is very fast where, within 4 minutes, most of the $(CH_3O)_3PO$ reagent is consumed. Comparison of figures 4.8 and 4.9 shows the sharp singlet at 2.1 ppm in the NMR spectra. After 20 minutes the doublet from $(CH_3O)_3PO$ is almost imperceptible. The addition of $(CH_3O)_3PO$ to the 0.07 mM solution of **4** gives no indication of any reaction. Figure 4.10 is the ^{1}H-NMR spectra 5 hours after $(CH_3O)_3PO$ was added to 0.07 mM **4** and there is no noticeable change from the initial spectrum. There is absolutely no evidence of a peak in the region of 2.1 ppm. This indicates that for these thiolate chalcogenides at concentrations ≤ 0.3 mM the thiolate ligand is closely associated with the alkali-metal ion otherwise we would expect to see a reaction with $(CH_3O)_3PO$.

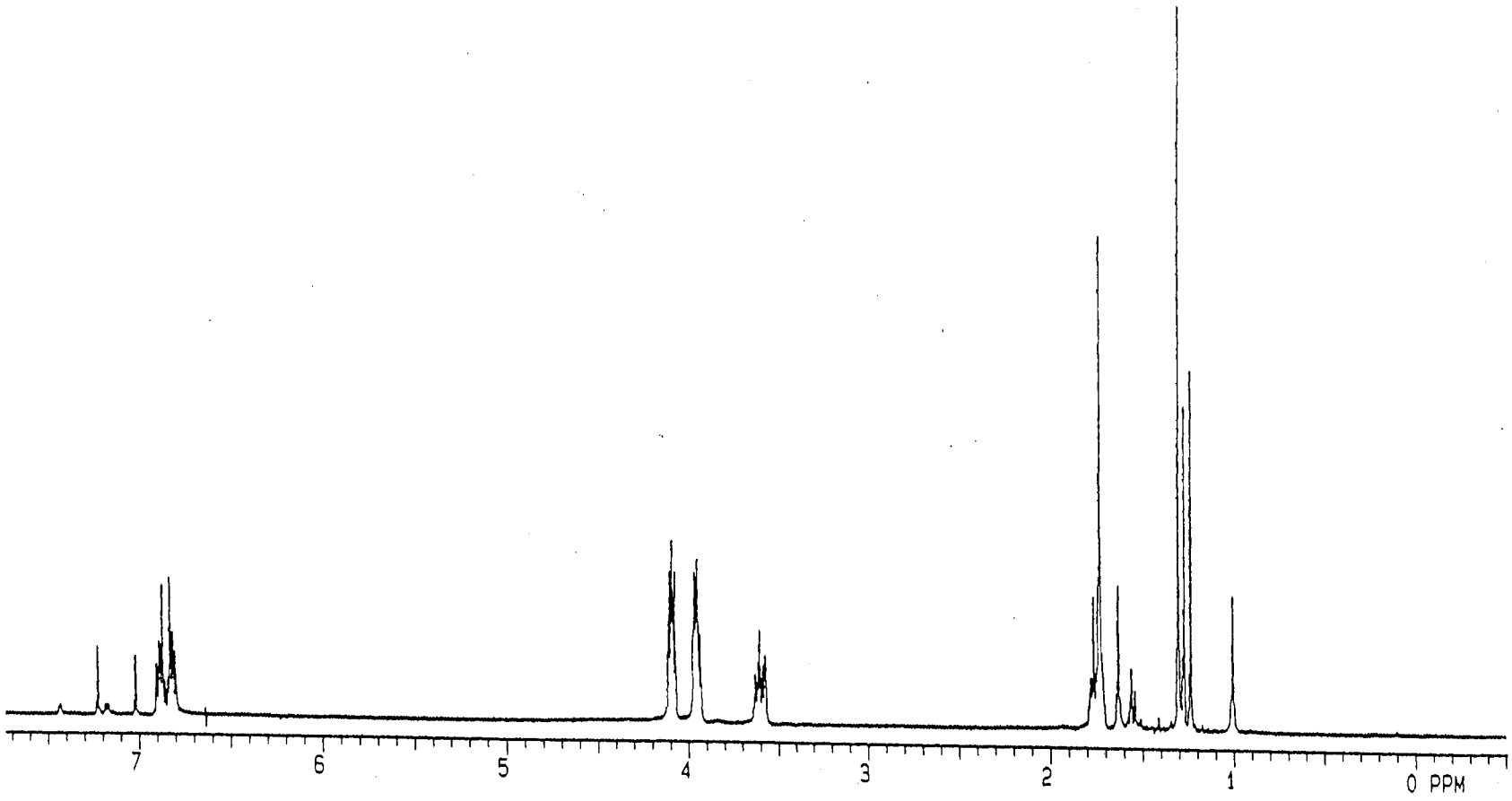

Figure 4.8: ^{1}H-NMR of 7 mM [Na(DB18crn6)][SMes*], in THF-*d*8

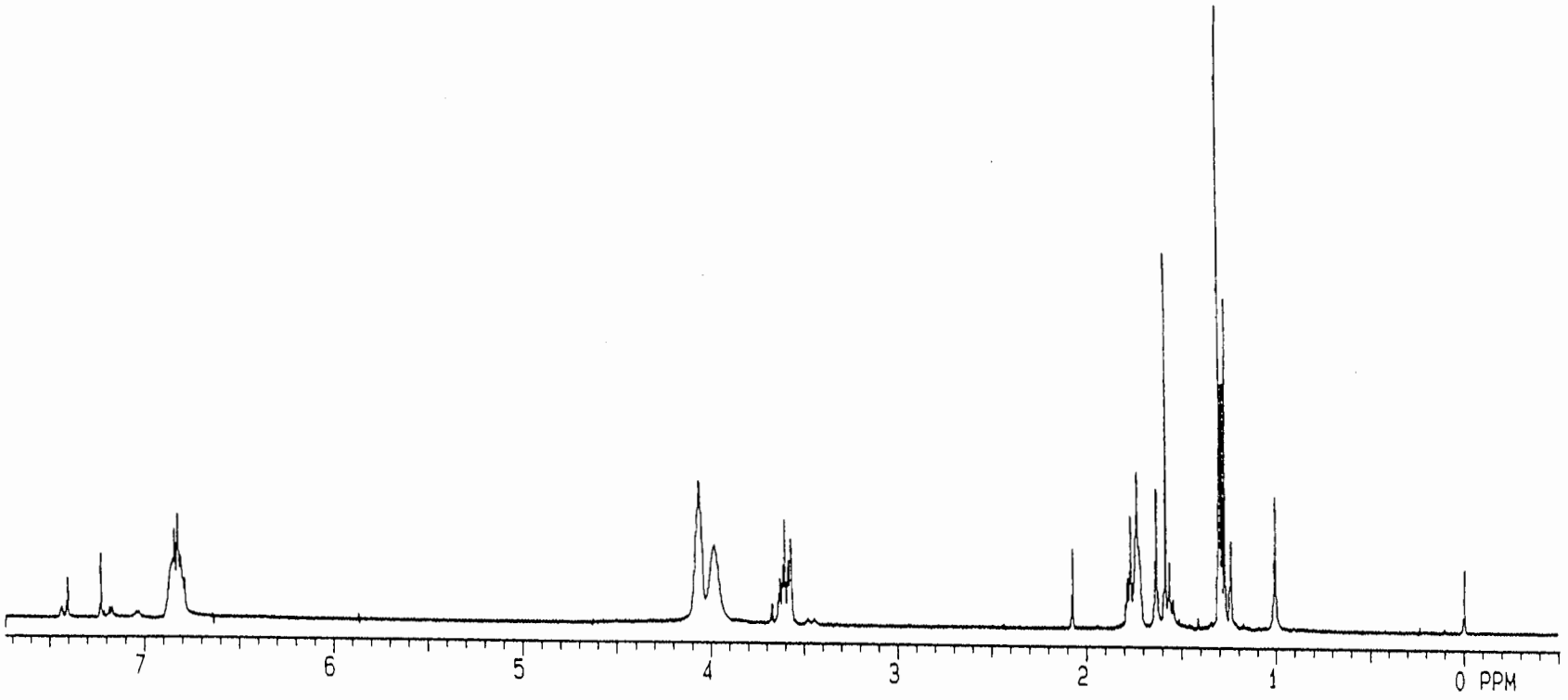

Figure 4.9: ^{1}H-NMR of 7 mM [Na(DB18crn6)][SMes*], in THF-*d*8, 4 min after adding 5×10^{-6} mols trimethylphosphate.

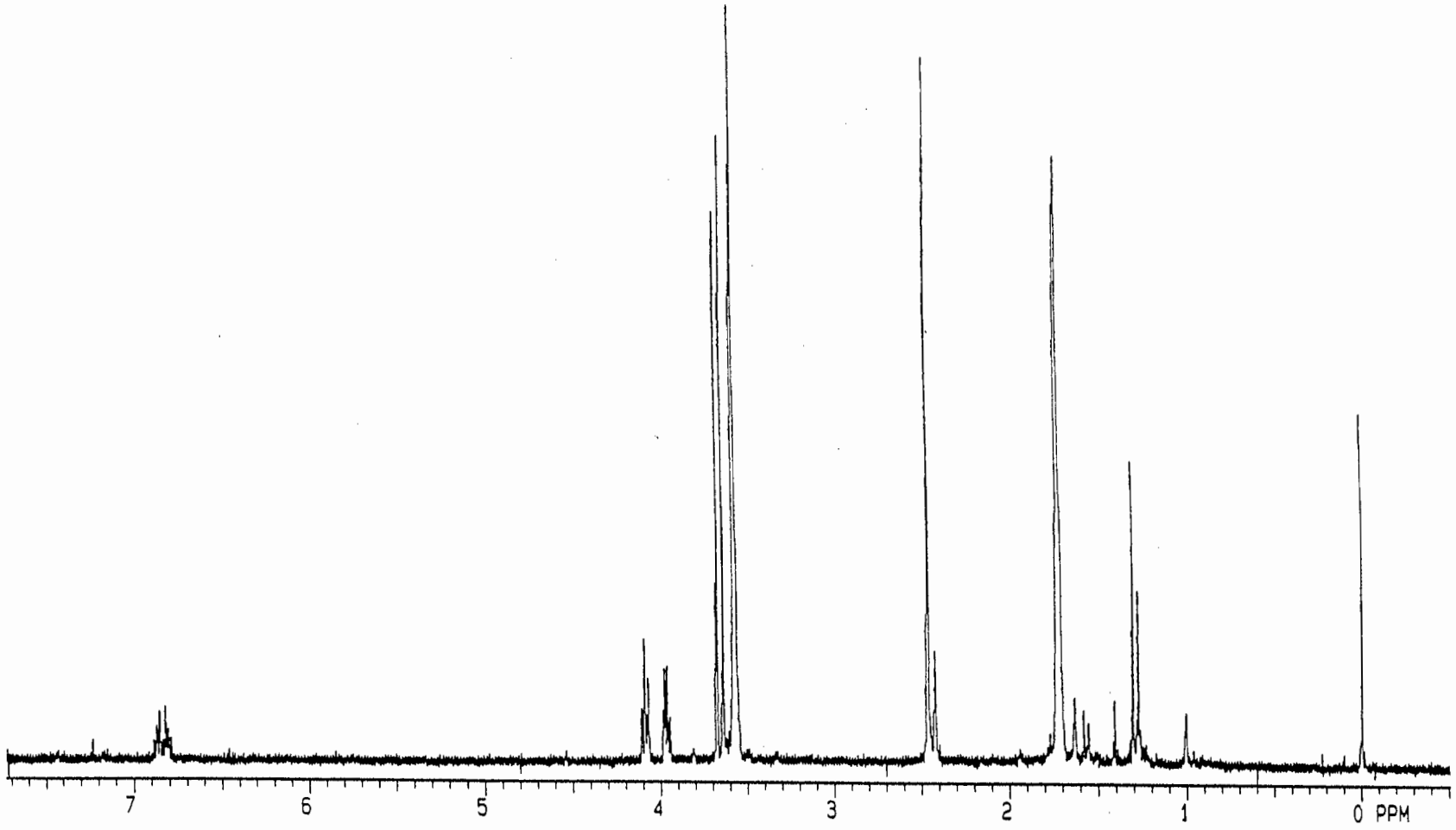

Figure 4.10: ^{1}H-NMR of 0.07 mM [Na(DB18crn6)][SMes*], in THF-*d*8, 5 hours after adding 5×10^{-7} mols trimethylphosphate.

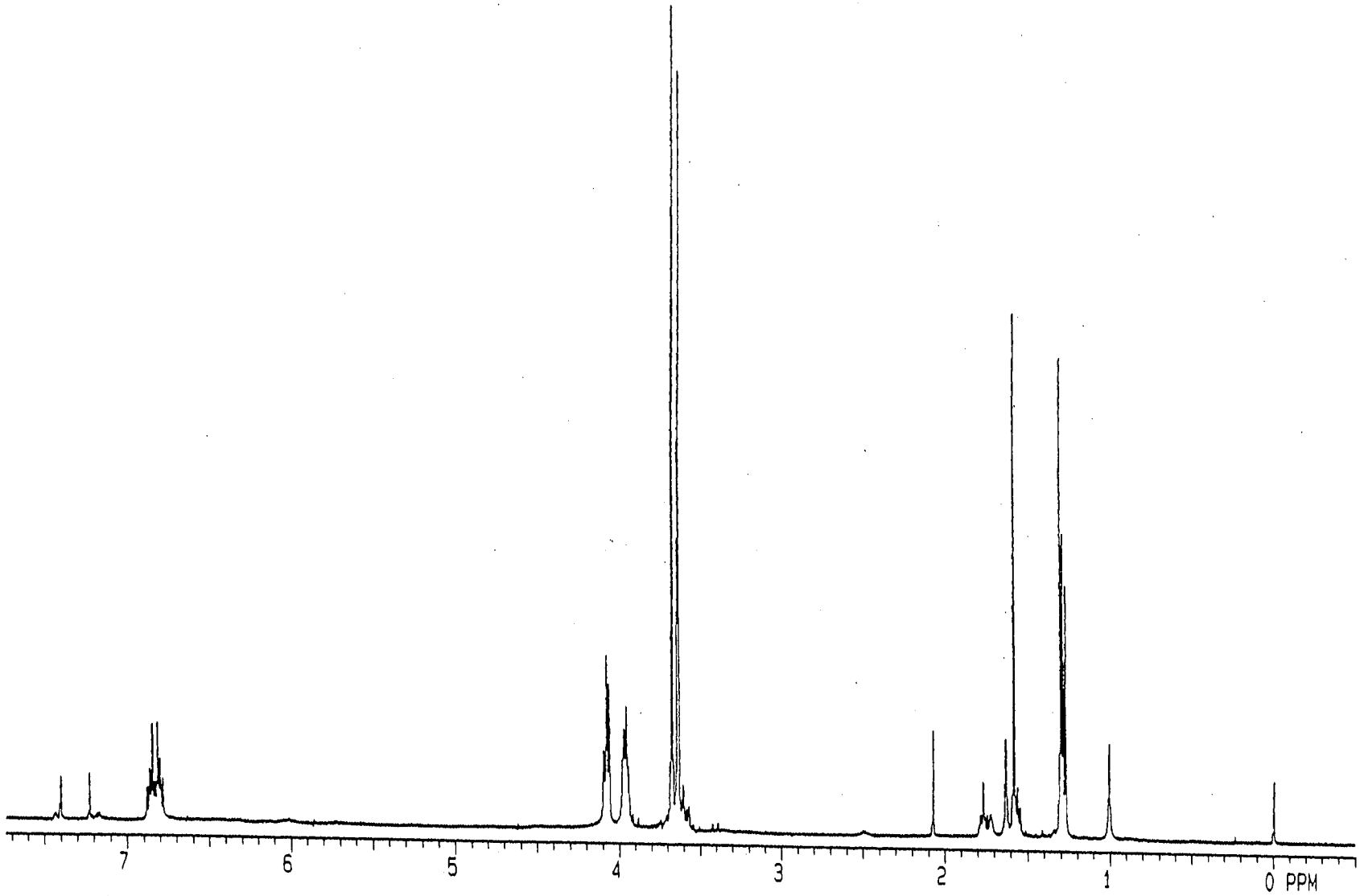

Figure 4.11: ^{1}H-NMR of 7 mM [Na(DB18crn6)][SMes*], in THF-*d*8, 5 min after adding excess trimethylphosphate.

Our dilute ^{1}H-NMR of **4** corresponds very well with the spectrum of the Ruhlandt-Senge group, for this compound;[5d] however, there are some remarkable aspects in the spectra of our NMR experiments on the different concentrations of **4**. A comparison of figures 4.8 and 4.10 reveal that with 7 mM **4**, in THF-*d*8, there are several extra peaks at δ: 7.03 (singlet), 3.61 (triplet and multiplet), 3.57 (singlet), 1.75 (singlet) and 1.23 (singlet). Also, upon addition of less than 1 molar equivalent of $(CH_3O)_3PO$ to the 7 mM sample, the peaks of the crown-ether protons (δ 4.10 and 3.95) go from peaks with well defined fine structure to broad peaks each resembling a coalesced doublet. Likewise, the doublet of the crown-ether's aromatic protons merge into a single multiplet (figure 4.9). The chemical shifts of several peaks change: the singlet at δ7.03 to δ 7.41, the singlet at δ 1.75 to δ 1.58 and the singlet at δ1.23 to δ1.28. Figure 4.11 shows some subtle changes after excess $(CH_3O)_3PO$ is added to the 7 mM sample. The crown-ether peaks redevelop their initial splitting patterns; but, the singlets at δ 1.58 and δ1.28 remain shifted and the intensity of the peaks at δ3.6 and 1.7 diminish by a factor of 4. A yellow powder starts to form in solution and further crystallization occurs with time.

It is most likely that the new peaks, at δ 7.03, 1.75 and 1.23, in the 7 mM spectra, are from free thiolate which then shift upon formation of the methyl sulfide when $(CH_3O)_3PO$ is added. The peaks at δ~3.6 ppm are thought to be the crown-ether protons from the aggregation of alkali-metal crown-ether thiolates alluded to by the electrochemistry. Hückel theory would predict that when the free thiolate is converted to the methyl sulfide, the perturbation of the molecular orbitals causes a significant increase

in electron density at C_1 C_3 and C_5. There would be a decease in electron density at C_2 and C_6 and a smaller increase in electron density in the tertiarybutyl group attached to C_4. These perturbations explain the chemical shifts of these protons. The downfield shifting of the δ7.03 singlet is the increase in electron density at C_3 and C_5. The upfield shifting of the δ1.75 peak due to the *ortho* tertiarybutyl protons going from free thiolate to the methyl tertiarybutylmesityl sulfide.

When the amount if $(CH_3O)_3PO$, that has been added to the concentrated thiolate chalcogenide solutions, is insufficient to react with all the free thiolate, the peak broadening and then resharpening of the crown-ether protons indicates that there is an exchange processes going on. What is possible, is that the exchange is between $[(CH_3O)_2PO_2]^-$, formed in the reaction and thiolates that are still dissociating from the Na^+-crown-ether moiety of the complex. When there is an excess of $(CH_3O)_3PO$ all the thiolates that dissociate react to from methyl sulfides and $[(CH_3O)_2PO_2]^-$ and there is no further possibility for ligand exchange. The thioethers were not observed to coordinate with a Zn(II) center when $[(CH_3)_4N]_2[Zn(SC_6H_5)_4]$ was reacted with $(CH_3O)_3PO$.[12a]

Conclusions

From something so simple as varying the concentration of a compound we have a decidedly rich and complex chemistry taking place with these metal thiolate chalcogenides. There are a few hard conclusions that we can draw from the results of these experiments. Rather bulky thiolate ligands dissociate from the metal-crown-ether moiety of these thiolate chalcogenides, when their concentrations are sufficient to permit or promote rearrangement. The dissociation is a reversible equilibrium: where at concentrations inferior to 0.3 mM, the thiolates are closely associated with metal ion centers and at concentrations superior to ~0.3 mM there is a molecular rearrangement with some thiolate ligands dissociating and others remaining with the metal-crown-ether constructs. Thus, due to molecular rearrangement, these weak electrolytes behave anti-classically: i.e., ionic dissociation is promoted with increasing the concentration of the ion pair. Finally, it is clear that the concentration dependant molecular rearrangement drives the dissociation of the thiolate ligand. If it were the ligand that forced the rearrangement we would have seen the low concentration thiolate chalcogenide react with the trimethylphosphate.

For Further Study

There are several aspects of this investigation that warrant further study. Two focuses should be what is the role of the thiolate ligand's steric bulk in the dissociation and what is the reasonably stable rearranged product formed upon the molecular rearrangement of the concentrated thiolate chalcogenides. We can say these complexes are stable by the fact that they exhibit near reversible redox behavior in CV experiments.

To study the role of the ligand spatial requirements a series of thiol ligand precursors could be purchased or synthesized to investigate the dissociation as a function of the steric bulk of the ligands. The evaluation could be in much the same way as cone angles are used with phosphine ligands. Since the synthesis of the thiolate chalcogenides is relatively simple is should not be difficult to use a series such as: triphenylmethyl thiolate; 2,4,6 tritertiarybutylphenyl thiolate; 2,4,6 -triisopropylphenyl thiolate; 2,4,6 trimethylphenyl thiolate; phenyl thiolate; tertiarybutyl thiolate; isopropyl thiolate and n-propyl thiolate. Simple molecular mechanics calculations would allow one to develop the steric parameters with which to gauge the steric effect.

The investigation of the reorganized alkali-metal crown-ether thiolate complex should start with its isolation. The crystals that have formed upon reaction with TMP are certainly different from the complex that gave the reversible CV wave "III". It may be of interest to analyze these crystals as well; but, the first compound should also be studied. Isolation would mean removal of dissociated free thiolate. This might be accomplished by electrochemical or chemical oxidation of the thiolate to form the disulfide as shown in equation 4.1. Electrochemical oxidation poses the problem of supporting electrolyte and

its incorporation in further analyses. Chemical oxidation also requires some cleaning of the product to allow analysis of the remaining rearranged thiolate chalcogenide.

There are two chemical oxidation procedures that may prove useful. A concentrated mixture of the original thiolate chalcogenide might be reacted with ferrocenium ion[13] or with nitrosyl tetrafluorborate[14] to oxidize the thiolate to the radical which would then form a disulfide. The disulfide would be soluble in a very non-polar solvent. These would either leave behind non-coordinating ferrocene or tetrafluorborate. Certainly the complex could be analyzed by electrochemical methods, NMR and possible x-ray crystallography.

References

[1] Zubay, G. L., Biochemistry, Collier Macmillian, New York, 1988.

[2] a) Montie, T. C., Montie, D. B. Biochemistry 1973, 12(24), 4958. b) Garry, R. F., Koch, G. AIDS 1992, 6(12), 1541. c) Chen, S.-F., Hartmann, H. A., Kirsch, G. E. Journal of Membrane Biology,. 1997, 155(1), 11. d) Liu, J., Liu, Y., Habeebu, S. S. M., Klaassen, C. D. Toxicology and Applied Pharmacology, 1998, 149(1), 24. e) Giritch, A., Ganal, M., Stephan, U. W., Baumlein, H. Plant and Molecular Biology, 1998, 37(4), 701.

[3] a) Zanetti, G., Massey, V., Curti, B. European Journal of Biochemistry, 1983, 132(1), 201. b) Macheroux, P., Plattner, H. J., Romaguera, A., Diekmann, H. European Journal of Biochemistry, 1993, 213(3), 995. c) Jung, Y.-S., Vassiliev, I. R., Qiao, F., Yang, F., Bryant, D. A., Golbeck, J. H. Journal of Biological Chemistry, 1996, 271(49), 31135

[4] a) Imakura, Y., Konishi, T., Uchida, K., Sakurai, H., Kobayashi, S., Haruno, A., Tajima, K., Yamashita, S. Chemical and Pharmaceutical Bulletin, 1994, 42(3), 500. b) Stack, T. D. P., Holm, R. H. Journal of the American Chemical Society, 1988, 110(8), 2484-94. c) Strijtveen, B., Kellogg, R. M. Journal of Organic Chemistry, 1986, 51(19), 3664-71.

[5] a) Ruhlandt-Senge, K., Chadwick, S., Englich, U., Inorg. Chem. 1998, 37, 283. b) Ruhlandt-Senge, K., Englich, U., Chadwick, S. Organometallics 1997, 16, 5792. c) Chadwick, S., Englich, U., Senge, M. O., Noll, B. C., Ruhlandt-Senge, K. Organometallics, 1998, 17(14), 3077-86. d) Chadwick, S., Englich, U., Ruhlandt-Senge, K., Watson, C., Bruce, A. E., Bruce, M. R. M. Dalton, 2000, 13, 2167-2173.

[6] Blower, P. J., Dilworth, J. R., Hutchinson, J.P., Zubieta, J. A. Journal of T Chemical Society: Dalton Transactions, 1985, 1533.

[7] Savéant, J.-M., Pinson, J., Hapiot, P., Andrieux, C. P., Journal of the American Chemical Society, 1993, 115, 7783.

[8] Jian, T., Wei, G., Turmel, C., Bruce, A. E., Bruce, M. R. M. Metal Based Drugs, 1994, 1, 419-31.

[9] a) Le Berre, V., Angely, L., Simonet-Gueguen, N., Simonet, J. Nouveau Journeau de la Chimie, 1985, 9, 419-26. b) Le Berre, V., Angely, L., Simonet-Gueguen, N., Simonet, J. Journal of Electroanalytical Chemistry, 1986, 206, 115-31. c) Belloncle, C., Cauliez, P., Simonet, J. Journal of Electroanalytical Chemistry, 1998, 444, 101-12.

[10] a) Jaffé, H. H. Chemical Review, 1953, 191-261. b) Hansch, C., Leo, A., Substituent Constants for Correlation Analysis in Chemistry and Biology, Wiley: New York, 1979, pp 1-8. c) Tribble, M. T., Traynham, J. G. Journal of the American Chemical Society, 1969, 91, 379-88. d) Charton, M. J. Journal of Organic Chemistry, 1971, 36, 266-72. e) Charton, M. J. Journal of the American Chemical Society, 1969, 91, 6649-54.

[11] a) Silverstein, R. M., Bassler, C. G., Morill, T. C. Spectrometric Identification of Organic Compounds 5th Ed., 1991, John Wiley, New York. b) Wilker, J. J. Wetterhahn, K. E., Lippard, S. J., Inorganic Chemistry, 1997, 36(10), 2079-83.

[12] a) Wilker, J. J., Lippard, S. J. Journal of the American Chemical Society, 1995, 117(33), 8682-3. b) DiLorenzo, M., Ganesh, S., Tadayon, L., Chen, J., Bruce, M.., Bruce, A. Metal-Based Drugs, in press.

[13] Connelly, N. G., Geiger, W. E. Chemical Review, 1996, 96, 877.

[14] Mabbs, F. E., Collison, D., Ziegler, T., Hinman, A. S., Boorman, P. M., Kraatz, H.-B., Journal of The Chemical Society: Dalton Transactions, 1993, 1665.

EPILOGUE TO THE THESIS

One of the advantages of having completed the experimental work of this thesis almost fours years ago now is that we are able to see if there is any impact, or at least notice of our efforts thus far. At its inception this thesis was geared toward studying the feasibility of combining a SAW mercury detector with electrochemistry to the application and removal of the mercury. We have affronted the sensor world by paying attention to what is a seemingly insignificant issue. The mere fact that mercury is retained on gold electrodes and accumulates when those electrodes are used repeatedly, does not mean that anodic stripping voltammetry of mercury using gold electrodes is dead. Both problems can be over come and the more recent literature is beginning to reflect that.

To date our paper in analytical chemistry has been cited by 5 different research groups[1] and our Dalton paper was included in a review of alkali metal chemistry.[2] Four of those references refer directly to the fact that mercury is retained on gold foil electrodes and one of the four feels that our work was a comprehensive analysis of the surface interactions between mercury and gold in electrodeposition and stripping. Although, it appears that our first, initial simple point was appreciated by a few, it is also important to see if there are any changes. We have focused much of our experimental model upon the work of Dr. Joseph Wang of New Mexico State University. It was in a Wang paper that

[1] a) Sanna, G. et al, Electroanalysis, 2002, 14(21), 1512-1520. B) Xu, X. et al, Analytical Chemistry, 2002, 74(15), 3611-3615. C) Vasjari, M. et al, Fresenius' Journal of Analytical Chemistry, 2000, 368(7), 727-729. D) Brainina, K. et al, Fresenius' Journal of Analytical Chemistry, 2000, 368(4), 307-325. E) Bond, A. et al, Langmuir, 2000, 16(14), 6004-6012.

[2] Gorrell, I. Annual Reports on the Progress of Chemistry, Section A: Inorganic Chemistry, 2001, 97 5-23.

the "analyte free" gold electrode was declared.[3] And at the time there were very few limitations pronounced in the literature about the abilities of the gold microfiber electrodes. Four years after our paper came out and the same researcher is commenting on how complex subtraction schemes may have to be run to have continued reliable results.[4] Other researchers are taking retained mercury into consideration with the routine use of a subtractive anodic stripping analysis where each run has a background recorded before each analytical run.[5] However, as stated in Chapter III, the recent papers on anodic stripping voltammetry for the detection of mercury have not directly addressed the issue of mercury retention. It may be even more surprising to see the literature results when the results from Chapter III are published.

It is the fact that mercury accumulates during electrochemical deposition and stripping, that renders the retention problem so difficult and significant. It is possible that subtraction schemes may satisfy the problem of retained mercury. But, for a real world device it would theoretically be measuring mercury in some polluted water. If a background scan is run and subtracted from the measuring scan it will subtract out the mercury peak as well. It is clear that exhaustive testing should be used instead of a few measurements showing local reproducibility. This is not the trend in the literature. The new devices are heated electrodes that reduce background.[6] There is no question as to whether or not the heated electrodes are more responsive; but, heating to 60 °C during

[3] Wang, J. et al, Analytical Chemistry, 1995, 67, 1481-1485.
[4] Daniele, S. Analyst, 2000, 125(4), 731-735.
[5] Bonfil, Y Analytica Chimica Acta, 2000, 424(1), 65-76.
[6] Wang, J. Analytica Chimica Acta (1999), 396(1), 33-37.

sampling is not likely to desorb mercury from the gold. Our TPD showed that the temperature for the earliest desorption of Hg from a polycrystalline surface is 110 °C. With the heated electrode "6 successive scans" were shown to have 2 to 3% variability. Our work in Chapter III indicated that this is not nearly enough scans.

In the last four years not a lot has changed in the mercury detection field. There are devices still being developed for remote detection of mercury and they all work with similar detection limits 1-50 ng/L. Our published work has been noticed and appreciated; however, the section of this thesis with the most potential impact needs to be out in the world for consideration. A winning gold device for detecting mercury in the environment will be one that can be constantly recalibrated or, a device that removes the mercury by electrothermal heating. We are curious if the SAW device can continually recalibrate its resonance wave. If this is true, it may be possible to adsorb mercury onto the surface either by simple exposure or by electrochemical reduction. With mercury on the surface, a measurement is made and then the mercury is stripped from the surface electrochemically. A new resonance frequency is determined and it would account for the changes in surface morphology and retained mercury resulting from the previous electrochemical deposition and stripping cycle. We may be spiraling. We are not exactly at the starting point; but, the view is the same.

BIBLIOGRAPHY

Aaseth, J., Friedheim, E. A. H. Acta Pharmacology and Toxicology 1978, 42, 248.

Agocs, M. M., Etzel, R.A., Parrish, R. G., et al. New England Journal of Medicine, 1990, 323, 1096.

Agraz, R., Hernandez, L., Sevilla, M. T. Journal of Electroanalytical Chemistry, 1995, 390, 47-57.

Al-Abbasi, A. H., Kostyniak, P. J., Clarkson, T.W. Clinical applications: Journal of Pharmacology And Experimental Therapeutics, 1979, 207, 249.

Albert, M. R. Journal of the American Academy of Dermatology, 2000, 43(3), 519-26

Amine. A., Cremisini, C., Palleschi, G., Society of Photo-Optical Instrumentation Engineers, Pubication No. 2504, 1995, 209-20.

Amin-Zaki, L., Majeed, M.A., Clarkson, T.W., et al. Brittish Medical Journal, 1978, 1, 610.

Amouroux, D., Tessier, E., Pecheyran, C., Donard, O. F. X. Analytica Chimica Acta 1998 H 377(2-3), 241-254.

Amyot, M., Gill, G. A., Morel, F. M. M. Environmental Science and Technology, 1997, 31, 3606-11.

Amyot, M., Lean, D. R. S., Mierle, G. Environmental and Toxicological Chemistry, 1997, 16, 2504-63.

Andle, J., Schweyer, M., Munson, J., Roderick, R., McAllister, D., French, L., Vetelino, J., Watson, C., Foley, J., Bruce, A., Bruce, M. Proceedings of the IEEE International Frequency Control Symosium, 1997, 51, 90-95.

Andle, J., Schweyer, M., Munson, J., Roderick, R., McAllister, D., French, L., Vetelino, J., Watson, C., Foley, J., Bruce, A., Bruce, M. Proceedings of the IEEE International Frequency Control Symosium, 1997, 51, 90-95.

Andrews, R. W., Larochelle, J. H., Johnson, D. C. Analytical Chemistry, 1976, 48(1), 212-14.

Armalis, S., Lu, J., Rongrong, X., Wang, J. Analytical Chemistry, 1995, 67(8), 1481-5.

Aronow, R., Cubbage, C., Wierner, R., et al. Morbidity and Mortality World Report, 1990, 39, 125.

Assessed Au-Hg Phase Diagram, Okamoto, K., in Binary Alloy Phase Diagrams, Massalski, T. B., Chief Editor. American Society for Metals, 1990, Metals Park, 265-7.

Bakir, F., Damluji, S. F., Amin-Zaki, L., et al. Science 1973, 181, 230.

Battistoni, C., Bemporad, E., Galdikas, A., Kaciulis, S., Mattogno, G., Mickevicius, S., Olevano, V. Applied Surface Science, 1996, 103(2), 107-111.

Baxter, D. C., Dyvik, G., Dybdahl, B., Frech, W. Journal of Analytical Atomic Spectrometry, 1995, 10(10), 769-75.

Beinrohr, E., Cakrt, M., Dzurov, J., Kottas, P., Kozáková, E. Fresenius' Journal of Analytical Chemistry., 1996, 356, 253-8.

Belloncle, C., Cauliez, P., Simonet, J. Journal of Electroanalytical Chemistry, 1998, 444, 101-12.

Berchmans, S., Arivukkodi, S., Yegnaraman, V. Electrochemistry Communications, 2000, 2(4), 226-229.

Bergdahl, I. A., Schutz, A., Hansson, G.-A., Analyst, 1995, 120, 1205.

Berlin, M, Rylander, R. Journal of Pharmacology And Experimental Therapeutics, 1964, 146, 236.

EBittner, A. C. Jr., Echeverria D, Woods, J. S. et al. Neurotoxicology and Teratology, 20, 429-439, 1998.

Blanc, J., Broyer, M., Dugourd, P. H., Labastie, P., Sence, M., Wolfe, J. P., Woste, L. Journal of Chemical Physics, 1995, 102(2), 680-9.

Blanchard, L. J., Robertson, J. D. Analyst, 1997, 122, 1261-4.

Blattmann, B., Saouter, E. Analytical Chemistry, 1994, 66, 13, 2031-7.

Bloom, N. S. Canadian Journal of Fisheries and Aquatic Sciences. 1992, 49(5), 1010-17.

Bloom, N. S. Canadian Journal of Fisheries and Aquatic Science, 1989, 46, 1131.

Blower, P. J., Dilworth, J. R., Hutchinson, J.P., Zubieta, J. A. Journal of T Chemical Society: Dalton Transactions, 1985, 1533.

Bluhm, R.E., Bobbitt, R. G., Welch, L. W., et al. Human Experimental Toxicology 1992, 11, 201. v

Bond, Alan M., Miao, Wujian, Raston, Colin L. Mercury(II) Immobilized on Carbon Nanotubes: Synthesis, Characterization, and Redox Properties. Langmuir, 2000, 16(14), 6004-6012.

Bonfil, Y.; Brand, M.; Kirowa-Eisner, E. Trace determination of mercury by anodic stripping voltammetry at the rotating gold electrode, Analytica Chimica Acta, 2000, 424(1), 65-76.

Bonfil, Y., Brand, M., Kirowa-Eisner, E. Reviews in Analytical Chemistry, 2000, 19(3-4), 201-216.

Boudou, A., Ribeyre, F. Metal Ions in Biological Systems, 1997, 34, 289-319.

Brainina, Kh. Z., Malakhova, N. A., Stojko, N. Yu. Stripping voltammetry in environmental and food analysis. Fresenius' Journal of Analytical Chemistry, 2000, 368(4), 307-325.

Branches, F. J. P., Erickson, T. B., Aks, S. E., et al. Clinical Toxicology, 1993, 31, 295.

Bredfeldt, J. E., Moeller, D. D. American Journal of Gastroenterology, 1978, 69, 478.

Brewer, G. E. F. Electrodeposition of Coatings: Advances in Chemistry Series 119, 1973, American Chemical Society, Washington.

Bricker, J. L. Analytical Chemistry, 1980, 52, 492.

Burke, L. D. and Nugent, P.F., Gold Bulletin, 1997, 30, 143-53.

Buseck, P. R., Hanson, R. C., McNerney, J. J. Science, 1972, 178, 611-2,

Butler, M. A., Ricco, A. J., Baughman, R. J., Journal of Applied Physics, 1990, 67(9), 4320-6.

Butlet, A. R., Glidewell, C., Needhan, J.. Journal of Chemical Research, 1980, 47, 817-832.

Buttry, D. A., Ward, M. D. Chemical Reviews, 1992, 92, 1355-1379

Campbell, J. R., Clarkson, T. W. Journal of the American Medical Association 1986, 256, 3127.

Campos, R. C., Porto de Silverira, C. L., Lima, R. Atomic Spectroscopy, 1997, 18(2), 55-9.

Celli, B., Khan, M.A. New England Journal of Medicine, 1976, 295, 883.

Chadwick, S., Englich, U., Ruhlandt-Senge, K., Watson, C., Bruce, A. E., Bruce, M. R. M. Dalton, 2000, 13, 2167-2173.

Chadwick, S., Englich, U., Noll, B., Ruhlandt-Senge, K. Inorganic Chemistry, 1998, 37(18), 4718-4725.

Chadwick, S., Englich, U., Ruhlandt-Senge, K. Chemical Communications, 1998, (19), 2149-2150.

Chadwick, S., Englich, U., Ruhlandt-Senge, K. Inorganic Chemistry, 1999, 38(26), 6289-6293.

Chadwick, S., Englich, U., Senge, M. O., Noll, B. C., Ruhlandt-Senge, K. Organometallics, 1998, 17(14), 3077-86.

Chan, C. C. Y., Sadana, R. S. Analytica Chimica Acta, 1993, 282, 109-15.

Charton, M. J. Journal of Organic Chemistry, 1971, 36, 266-72.

Charton, M. J. Journal of the American Chemical Society, 1969, 91, 6649-54.

Chen, C., Gerwirth, A. A. Physical Review Letters, 1992, 68(10), 1571-4.

Chen, S.-F., Hartmann, H. A. and Kirsch, G. E. Journal of Membrane Biology,. 1997, 155(1), 11.

Cherkashinin, G. Yu. Journal of Electron Spectroscopy and Related Phenomena, 1995, 74(1), 67-75.

Chiang, W. K. "Mercury" in Ford, Clinical Toxicolocy, 1st Ed., 2001, W. B. Saunders, 737-42.

Choi, S. C., Bartha, R. Applied Environmental Microbiology, 1994, 60, 4072-77.

Chung, M., Zen, J. Analytical Chemistry, 1995, 67, 3571-7.

Ciszewski, A., Lukaszewski, Z. Talanta, 1988, 35(3), 191-7.

Cladera, A., Estela, J. M., Cerda, V. Talanta, 1991, 38(12), 1475-9.

Clair, T. A., Ehrman, J. M., Ouellet, A. J., Brun, G., Lockerbie, D., Ro, C.-U. Water, Air, and Soil Pollution, 2002, 135(1-4), 335-354.

Clarckson, T. W. Critical Review of Clinical Laboratory Science, 1997, 34, 369-403.

Clarkson, T.W., Magos, L., Cox, C., et al. Journal of Pharmacology And Experimental Therapeutics, 1981, 218, 74.

Code of Federal Regulations, Environmental Protection Agency, www.access.gpo.gov/nara/cfr/index.html.

Connelly, N. G., Geiger, W. E. Chemical Review, 1996, 96, 877.

Coquery, M., Cossa, D., Martin, J. M. Water Air and Soil Pollution, 1989, 80, 653-64.

Covington, A. K,, Katay, R. Journal of The Chemical Society: Faraday Transactions, 1993, 89(2), 369-76.

Crecelius, E. A., Bloom, N. S. Marine Chemistry, 1983, 14(1), 49-59.

D'yachenko, Y. I., Kondratev, V. V. Journal of Analytical Chemistry., 1998, 53(4), 351-6.

Dale, J. M., Freedman, B., Kerekes, J. Canadian Journal of Zoology, 1985, 63(1), 97-105.

Daniele, Salvatore; Bragato, Carlo; Baldo, M. Antonietta; Wang, Joseph; Lu, Jianmin. The use of a remote stripping sensor for the determination of copper and mercury in the Lagoon of Venice. Analyst (Cambridge, United Kingdom) (2000), 125(4), 731-735.

Denoyer, E. R., Debrah, E. Journal of Analytical Atomic Spectrometry, 1996, 11(2), 127-32.

Dewald, H. D. In, Modern Techniques in Electroanalysis, Vanysek, P., Ed., Wiley: New York, 1996, pp 151-185.

Diffusion in Solids, Shewmon, P. G. 1983, J. Williams Book Co., Jenks, OK, Chpt 1 and 3.

DiLorenzo, M., Ganesh, S., Tadayon, L., Chen, J., Bruce, M.., Bruce, A. Metal-Based Drugs, in press.

Dixit, A. S., Dixit, S. S., Smol, J. P. Canadian Journal of Fisheries and Aquatic Sciences, 1992, 49(Suppl. 1), 17-24.

Dubey, S. K., Gngoli, S., Holmes, D. S. Environmental Geochemistry and Health, 1994, 16(3/4), 229-33.

Dumarey, R., Heindryckx, R., Dams, R., Hoste, J. Analytica Chimica Acta, 1979, 107, 159-67.

Dzau, V.J., Szabo, S., Chang, Y.C. Journal of the American Medical Association, 1977, 238, 1531.

Ebenezer, D., Denoyer, E. C., Tyson, J. F. Journal of Analytical and Atomic Spectroscopy, 1996, 11, 127-32.

Emteborg, H., Snell, J., Qian, J., Frech, W. Chemosphere, 1999, 39(7), 1137-1152.

Emteborg, Haakan, Baxter, Douglas C., Frech, Wolfgang. Analyst, 1993, 118(8), 1007-13.

Esteban, M., Arino, C., Ruisanchez, I., Larrechi, M. S., Rius, F. X. Analytica Chimica Acta, 1993, 284(2), 435-43.

Evans, O. McKee, G.. Analyst, 1988, 113(2), 243-6.

Falter, R., Schoeler, H. F. Fresenius' Journal of Analytical Chemistry, 1995, 353(1), 34-8.

Filippelli, M. Analytical Chemistry, 1987, 59, 116.

Fischer, R., Rapsomanikis, S., Andreae, M. O. Analytical Chemistry, 1993, 65, 763-7.

Fitzgerald, W. F., Engstrom, D. R., Mason, R. P., Nater, E. A. Environmental Science and Technology, 1998, 32, 1-12.

Fitzgerald, W. F., Mason, R. P., Vandal, G. M. Water Air Soil Poll, 1991, 56, 745-768.

French, L. A., Schweyer, M. G., Michael, G., Foley, J. B., Andle, J. C., Watson, C. M., Bruce, M. R. M., Bruce, A. E. Proceedings of SPIE-The International Society for Optical Engineering, 1998, 3539 (Chemical Microsensors and Applications), 161-9.

Garry, R. F.and Koch, G. AIDS 1992, 6(12), 1541.

Gavina, F., Luis, S. V., Costero, A. M., Burguete, M. I., Rebek, J. Jr. Journal of the American Chemical Society, 1988, 110(21), 7140-3.

George, M. A., Glaunsinger, W. S. Thin Solid Films, 1990, 189, 59-72.

George, M. A., Glaunsinger, W. S. Thin Solid Films, 1994, 245, 215-25.

Gifford, P. R., Bruckenstein, S. Analytical Chemistry, 1980, 52, 1024-28.

Gil, E. P., Ostapczuk, P. Analytica Chimica Acta, 1994, 293, 55-64.

Gil, G. A., Fitzgerald, W. F. Marine Chemistry., 1987, 20, 227-43.

Gilmour, C. C., Henry, E. A. Environmental Pollution, 1991, 71, 131-69.

Giritch, A., Ganal, M., Stephan, U. W. and Baumlein, H. Plant and Molecular Biology, 1998, 37(4), 701.

Goldman, L. R. Pediatrics, 2001, 108(1), 197-205

Goldwater L. J. Mercury, A History of Quicksilver. Baltimore, York Press, 1972.

Gorrell, I. B. Alkali and alkaline-earth metals. Annual Reports on the Progress of Chemistry, Section A: Inorganic Chemistry (2001), 97 5-23.

Gotelli, G.W., Astolfi, E., Cox, C., Cernichiari, E., Clarkson, T. W. Science, 1985, 227, 638-40.

Goyer, R.A., Casarett, A. Doull's Toxicology. The Basic Science of Poisons, 4th ed., Amdur, M.O., Doull, J., Klaasen, C.D. Eds., New York, Pergamon Press, 1991, pp 646–651.

Grauer, V. Other Voices, 2002, 2(2), 1-2.

Greef, R., Peat, R., Peter, L., Pletcher, D., Robinson, Journal of Instrumental Methods in Electrochemistry, Ellis Horwood Ltd.: Chichester, 1985, 233.

Gries, Werner H. Applied Surface Science, 1996, 100/101(Proceedings of the 13th International Vacuum Congress and the 9th International Conference on Solid Surfaces, 1995), 41-46.

Guentzel, J.L., Landing, W. M., Gill, G. A., Pollman, C. D. Environmental Science and Technology, 2001, 35, 863-873.

Guo-Qing, S., Guibn, W. Journal of Analytical Sciences, 2002, 18(11), 1215-9.

Gustavsson, I. Journal of Electroanalytical Chemistry and Interfacial Chemistry, 1986, 214(1-2), 31-6.

Gustavsson, I. Journal of Electroanalytical Chemistry, 1986, 214, 31-6.

Gutknecht, J., Tosteson, D. C. Science, 1973, 182, 1258-61.

Haberland, H., Kornmeier, H., Langosch, H., Oschwald, M., Tanner, G. Journal of the Chemical Society, Faraday Transactions, 1990, 86(13), 2473-81.

Hadded, L. M., "Acute Poisoning" in Goldman, Cecil Textbook of Medicine, 21st ed., 2000, W. B. Saunders, 72-3.

Hall, B. Water Air and Soil Pollution. 1995, 80, 301-315.

Hamilton, A., Lehn, J., Marie, S., Jonathan L. Journal of the American Chemical Society, 1986, 108(17), 5158-67.

Hansch, C., Leo, A., Substituent Constants for Correlation Analysis in Chemistry and Biology, Wiley: New York, 1979, pp 1-8.

Hatle, M. Talanta, 1987, 34(12), 1001-7.

Hawley, J. E., Ingle, J. D., Analytical Chemistry, 1979, 47, 719.

Hermon, H., Roth, M., Schieber, M., Shamir, J. Vibrational Spectroscopy, 1991, 2(2-3), 155-9.

Herrero, E., Abruna, H. D. Journal of Physical Chemistry B, 1998, 102(2), 444-451.

Herrero, E., Li, J., Abruña, H. D. Proceedings of The Electochemical Society, 1997, 17, 277-91.

Hldky, Z., Risova, J., Fisera, M. Journal of Analytical and Atomic Spectroscopy, 1990, 5, 691-2.

Ho, M. H., Scheide, E. P., Guilbault, G. G., Analytica Chimica Acta, 1981, 130(1), 141-7.

Holak, W. Analyst, 1982, 107, 1457.

Horvat, M., Lupsina, V., Pihlar, B. Analytica Chimica Acta, 1991, 243, 71-9.

Huang, H., Jagner, D., Renman, L. Analytica Chimica Acta, 1987, 201, 269-73.

Huang, H., Jagner, D., Renman, L. Analytica Chimica Acta, 1987, 202, 117-22.

Huang, H., Jagner, D., Renman, L. Analytica Chimica Acta., 1987, 201, 1-9.

Hudson, R. J. M., Gherini, S. A., Gitzgerald, W. F., Porcella, D. B. Water Air and Soil Pollution, 1995, 80, 265-72.

Hurley, J. P., Watras, C. J., Bloom, N. S. Water Air and Soil Pollution, 1991, 56, 543-51.

Hylander, L. D., Meili, M. The Science of The Total Environment, 2003, 304, 13-27.

Igata, A. Environmental Research, 1993, 63, 157.

Imakura, Y., Konishi, T., Uchida, K., Sakurai, H., Kobayashi, S., Haruno, A., Tajima, K. and Yamashita, S. Chemical and Pharmaceutical Bulletin, 1994, 42(3), 500.

Inukai, J., Sugita, S., Itaya, K. Journal of Electroanalytical Chemistry. 1996, 403, 159-68.

Jaffé, H. H. Chemical Review, 1953, 191-261.

Jagner, D., Renman, L., Huang, H. Analytica Chimica Acta, 1987, 201, 1-9.

Jayaratna, H. G. Current Separations, 1997, 16(3), 93-96.

Jian, T., Wei, G., Turmel, C., Bruce, A. E., Bruce, M. R. M. Metal Based Drugs, 1994, 1, 419-31.

Jian, W., McLeod, C. W. Talanta, 1992, 37, 1537.

Jortner, J. In, Physics and Chemistry of Finite Systems: From Clusters to Crystals, Jena, P., Khanna, S. N., Rao, B. K., Eds., NATO ASI Series, Klumer Academic Publishers: Dorrecht, 1991, chap.1.

Josse, F., Dahint, R., Schumacher, J., Grunze, M., Andle, J C., Vetelino, J. F. Sensors and Actuators, A, Physical, 1996, A53(1-3), 243-248.

Jung, R.C., Aaronson, J. Western Journal of Medicine, 1980, 132, 539.

Jung, Y.-S., Vassiliev, I. R., Qiao, F., Yang, F., Bryant, D. A. and Golbeck, J. H. Journal of Biological Chemistry, 1996, 271(49), 31135

Kales, S. N. Journal of Occupational and Environmental Medicine, 2002, 44(2), 143-54

Kandler, W., Hulanicki, A., Bulska, E. Spectrochimica Acta Part B, 1996, 51B(9-10), 1263-70.

Kang-Yum, E, Oransky, S. H. Veterinary and Human Toxicology, 1992, 34, 235.

Keeler, G. J., Landis, M. S. EPA Method 1631-821-R, 2001, 1-13.

Keller, A., Atabek, O. Physical Review A: Atomic, Molecular, and Optical Physics

Khustenko, L. A., Larina, L. N., Nazarov, B. F. Journal of Analytical Chemistry, (Translation of Zhurnal Analiticheskoi Khimii) 2003, 58(3), 262-267.

Klaassen, C. D. "Heavy Metals and Heavy Metal Antagonists", in Goodman and Gilman's, The Pharmaceutical Basis of Therapeutics, 9th Ed. 1996, McGraw Hill, CD-ROM, section 66.

Kondrat'ev, V. V., D'yacnenko, Y. I. Journal of Analytical Chemistry, 1998, 53(4), 351-356.

Korolczuk, M. Fresenius' Journal of Analytical Chemistry, 1997, 357(4), 389-91.

Kostyniak, P. J., Greizerstein, H. B., Goldstein, J. et al. Human Toxicology, 1990, 9, 137.

Kuswandi, B., Narayanaswamy, R. Sensors and Actuators B, Chemical, 2001, B74(1-3), 131-7.

Latimer, W. M. The Oxidation States of the Elements and their Potentials in Aqueous Solutions 2nd Ed., Prentice-Hall, Englewood Cliffs, 1952.

Le Berre, V., Angely, L., Simonet-Gueguen, N., Simonet, J. Nouveau Journeau de la Chimie, 1985, 9, 419-26.

Le Berre, V., Angely, L., Simonet-Gueguen, N., Simonet, J. Journal of Electroanalytical Chemistry, 1986, 206, 115-31.

Lee, J., Lo, J. Analytical Chemistry, 1999 1994, 66, 1242-48.

Leermakers, M., Baeyens, W. Journal of Analytical Atomic Spectrometry, 1989, 4(7), 635-40.

Levlin, M., Niemi, H. E.-M., Hautojärvi, P., Ikävalko, E., Laitnen, T. Fresenius' Journal of Analytical Chemistry. 1996, 355, 2-9.

Li, J., Abruña, H. Journal of Physical Chemistry: B, 1997, 101, 2907-2916.

Liang, L., Bloom, N. S. Journal of Analytical and Atomic Spectroscopy 1993, 8, 591-4.

Liang, L., Horvat, M., Bloom, N. S. Talanta, 1994, 41(3), 371-9.

Lindberg, S. E., Brooks, S., Lin, C. J., Scott, K. J., Landis, M. S., Stevens, R. K., Goodsite, M., Richter, A. Environmental Science and Technology, 2002, 36, 1245-1256.

Lindqvist, O., Johansson, M., Aastrup, A., Andersson, L., Iverfeldt, A., Meili, M., and Timm, B. Water Air and Soil Pollution, 1991, 55, 1-262.

Liu, D., Yin, A., Chen, K., Ge, K., Nie, L., Yao, S., Analytical Letters, 1995, 28(8), 1323-37.

Liu, J., Liu, Y., Habeebu, S. S. M. and Klaassen, C. D. Toxicology and Applied Pharmacology, 1998, 149(1), 24.

Luther, G. W., Tsamakis, E. Marine Chemistry, 1989, 127, 165-77.

Mabbs, F. E., Collison, D., Ziegler, T., Hinman, A. S., Boorman, P. M. and Kraatz, H.-B., Journal of The Chemical Society: Dalton Transactions, 1993, 1665.

Macheroux, P., Plattner, H. J., Romaguera, A. and Diekmann, H. European Journal of Biochemistry, 1993, 213(3), 995.

Magos, L. Brittish Journal of Pharmacology 1976, 56, 479.

Magos, L., Analyst, 1971, 96, 847.

Mason, R. P., Fitzgerald, W. P., Morel, F. M. M. Geochimica et Cosmochimica Acta, 1994, 58, 3191-3198.

Mason, R. P., Reinfelder, J. R., Morel, F. M. M. Environmental Science and Technology, 1996, 30, 1835-45.

Matsunami, I. N., Yananura, Y., Itikawa, Y., Itoh, N., Kazumata, Y., Miyagawa, S., Morita, K., Shimizu R., Tawara, H. Atomic Data Nuclear Tables, 1984, 31, 1.

Mayer, A. Journal of The Electrochemical Society, 1990, 137(9), 2806.

McIntosh, S. Atomic Spectroscopy, 1993, 14(2), 47-9.

Mercury, P. Chevalier, in "Canadian Minerals Yearbook 1998, Chpt. 33, 1-4.

Mohamed, A. A., Bruce, A. E., Bruce, M. R. M. In Organic Derivatives of Silver and Gold, Patai, S., Rappaport, Z., Eds., John Wiley & Sons: London.

Montie, T. C. and Montie, D. B. Biochemistry 1973, 12(24), 4958.

Morel, F. M. M., Kraepiel, A. M. L., Amyot, M. Annual Review of Ecology Systems, 1998, 29, 543-66.

Mroz, S. Progress in Surface Science, 1998, 59(1-4), 323-330.

Munthe, J., Xiao, Z. F., Lindquist, O. Water, Air and Soil Pollution, 1991, 56, 621-30.

Murphy, P, J. Analytical Chemistry, 1979, 51(9), 1599-1600.

Myund, L. A., Kozhevnikova, G. V., Chernykh, L. V., Burkov, K. A. Vestnik Leningradskogo Universiteta, Seriya 4: Fizika, Khimiya, 1978, (3), 67-71. (absract only).

Nielsen, J.B., Andersen, O. Human Experimental Toxicology, 1991, 10, 423.

Nowakowski, R., Kobiela, T., Wolfram, Z., Dus, R. Applied Surface Science, 1997, 115, 217-231.

Oda, C. E., Ingle, J. D., Jr. Analytical Chemistry, 1981, 53(14), 2305-9.

Oliveira, C. M. R. R., Rebelo, M. J. F., Camoes, M. F. G. F. C. Analyst, 1996, 121(12), 1907-10.

Olsen, K., Zirino, A., Larson, D., Foster, N.,

Ostapczuk, P. Analytica Chimica Acta, 1993, 273, 35-40.

Osteryoung, J., Stojek, Z. Analytical Chemistry, 1988, 60, 131-141.

Ott, W. L., Hatch, R. Analytical Chemistry, 1968, 40, 2085.

Palacio, C., Ocon, P., Herrasti, P., Diaz, D., Arranz, A. Journal of Electroanalytical Chemistry, 2003, 545 53-58.

Panusa, A., Flamini, A., Sensors and Actuators B, 1997, B42(1), 39-46.

Paquett, D. E., Helz, G. R. Environmental Science and Technology, 1997, 31, 2148-53.

Paudyn, A., Van Loon, J. C. , 1986, 325(4), 369-76.

Paynter, R., Angle-resolved X-ray Photoelectron Spectroscopy, http://goliath.inrs-ener.uquebec.ca/surfsci/xpslinks.html, 2000.

Physics and Chemistry of Finite Systems: From Clusters to Crystals, Jortner, J., Jena, P., Khanna, S. N., Rao, B. K. Eds. Nato ASI Series, Klumer Academic Publishers, Dorrecht, 1991. Chpt. 1.

Porto da Silveira, C. L., Lima, R., Campos, R. C. Atomic Spectroscopy, 1997, 18(2), 55-9.

Public Health Statement: Mercury, www.atsdr.cdc.gov/toxprofiles/phs46.html

Rademann, K., Kaiser, B., Even, U., Hensel, F. Physical Review Letters, 1987, 59(20), 2319-21.

Rapsomanikis, S., Andreae, M. O. Interntional Journal of Environmental Analytical Chemistry, 1992, 49, 43-8.

Rapsomanikis, S., Craig, P. J. Analytica Chimica Acta, 1991, 248, 563-7.

Ratana-ohpas, R., Kanatharana, P., Ratana-ohpas, W., Kongsawasdi, W. Analytica Chimica Acta 1996, 333(1-2), 115-118.

Reuther, Rudolf, Jaeger, Lars, Allard, Bert. Analytica Chimica Acta 1999, 394(2-3), 259-269.

Rezende, M. R., Compos, R. C., Curtius, J., Journal of Analytical Atomic Spectrometry, 1993, 8, 247.

Richter, Pablo, Toral, M. Ines, Abbott, Bernardo. Electroanalysis, 2002, 14(18), 1288-1293.

Rievaj, M., Mesáros, S., Bustin, D. Collection of Czechoslovak Chemical Communications, 1993, 58, 2918-2923.

Risher, J. F., Toxicology and Industrial Health, 1999, 15(5), 480-2

Risova, J., Fisera, M., Hladky, Z. Journal of Analytical Atomic Spectrometry, 1990, 5(8), 691-2.

Romeo, F. M., Tucceri, R. I., Posadas, D. Langmuir, 1990, 6(4), 839-42.

Ross, W. D., Gechman, A. S., Sholiton, M. C., et al. Comprehensive Psychiatry 1977, 18, 595.

Ruhlandt-Senge, K., Chadwick, S. and Englich, U., Inorg. Chem. 1998, 37, 283.

Ruhlandt-Senge, K., Englich, U. and Chadwick, S. Organometallics 1997, 16, 5792.

Salie, G., Bartels, K. Electrochimica Acta, 1994, 39(8-9), 1057-65.

Salie, G., Bartels, K. Journal of Electroanalytical Chemistry and Interfacial Electrochemistry, 1988, 245(1-2), 21-38.

Sallsten, G., Nolkrantz, K., Analyst, 1998, 123, 665-8.

Sancho, D., Deban, L., Barbosa, F., Pardo, R., Vega, M. Food Chemistry, 2001, 74(4), 527-531.

Sanna, G., Pilo, M. I., Piu, P. C., Spano, N., Tapparo, A., Seeber, R. Microelectrodes for the determination of heavy metal traces in physiological conditions: Hg, Cu and Zn ions in synthetic saliva. Electroanalysis, 2002, 14(21), 1512-1520.

Sass, B. M. Salem, M. A., Smith, L. A., EPA Pub. No. PB94-165362AS, 1994, 1-4

Sasso, F. S., Ferraiuolo, R., Gursky, E., et al. Morbidity and Mortality World Report, 1996, 45, 422.

Sato, H., Wakabayashi, M., Ito, T., Sugawara, M., Umezawa, Y. Analytical Sciences, 1997, 13(3), 437-446.

Savéant, J.-M., Pinson, J., Hapiot, P. and Andrieux, C. P., Journal of the American Chemical Society, 1993, 115, 7783.

Savory, J., Toffaletti, J. Analytical Chemistry, 1975, 47, 2091.

Schadewald, L. A., Linstrom, T. R., Hussein, W., Evenson, E. E., Johnson, D. C., Journal of The Electrochemical Society, 1984, 131(7), 1583-7.

Schroeder, W. H., Jackson, R. A. International Journal of Environmental Analytical Chemistry, 1988, 22, 1-18.

Schubert-Jacobs, M., Wetz, B. Fresenius' Journal of Analytical Chemistry, 1988, 331, 324.

Schweyer, M. G., Andle, J. C., McAllister, D. J., Vetelino, J. F. Sensors and Actuators, B, Chemical, 1996, B35(1-3), 170-175.

Scofeild, J. H. Journal of Electron Spectroscopy and Related Phenomena, 1976, 8, 129-37.

Shanker, G. Journal of Neuroscience Research, 2001, 66(5), 998-1002.

Sherwood, W., Bruckenstein, S. Journal of the Electrochemical Society. 1978, 125, 1098-1102.

Shuman, M. S., Robinson, K. G. International Journal of Environmental Analytical Atomic Spectrometry, 1989, 36, 111.

Sillanaukee, P., Hurme, L., Tuominen, J., Ranta, E., Nikkari, S., Seppae, K. European Journal of Biochemistry, 1996), 240(1), 30-36.

Silverstein, R. M., Bassler, C. G., Morill, T. C. Spectrometric Identification of Organic Compounds 5th Ed., 1991, John Wiley, New York.

Singer, R., Valciukas, J. A., Rosenman, K.D. Archives of Environmental Health, 1987, 42, 181.

Siuda, R. Vacuum, 1997, 48(3/4), 391-394.

Somorjai, G. A. Introduction to Surface Chemistry and Catalysis, Wiley-Interscience, 1994, New York, 383.

Stack, T. D. P., Holm, R. H. Journal of the American Chemical Society, 1988, 110(8), 2484-94.

Strijtveen, B. and Kellogg, R. M. Journal of Organic Chemistry, 1986, 51(19), 3664-71.

Stulik, K., Lexa, J. Talanta, 1989, 36(8), 843-8.

Sukhov, N. L., Ershov, B. G. Izvestiya Akademii Nauk SSSR, Seriya Khimicheskaya 1992,(1), 9-12. (abstract only).

Svancara, I., Matousek, M., Sikora, E., Schachl, K., Kalcher, K., Vytras, K. Electroanalysis, 1997, 9(11), 827-833.

Svancara, I., Matousek, M., Sikora, E., Schachl, K.. Electroanalysis, 1997, 9(11), 827-833.

Svoboda, G. J., Sottery, J. P., Anderson, C. W. Analytica Chimica Acta., 1984, 166, 297-99.

Takacs, L. Journal of Metal, 2000, 41, 12-13.

The Encyclopedia of the Chemical Elements, Hampel, C. A. Ed., 1987, Reinhold Book Corporation, New York.

The Nalco Water Handbook 2nd Ed., Kremmer, F. Ed., McGraw-Hill, New York, 1988, 231-4.

Tian, B., Lu, J., Wang, J., Luo, D.Wang, J. Electroanalysis, 1998, 10(6), 399-402.

Tian, B., Wang, J. Analytica Chimica Acta, 1993, 274(1), 1-6.

Tokoro, R., Tavares, M. Analytical Letters., 1986, 19, 2079-2094.

Tougaard, S., Hansen, H. S., Neumann, M. Surface Science, 1991, 244(1-2), 125-34.

Tribble, M. T., Traynham, J. G. Journal of the American Chemical Society, 1969, 91, 379-88.

Trittler, R., Schilcher, H. Fresenius' Journal of Analytical Chemistry, 1994, 349(8-9), 659-60.

Troen P., Kaufman S. A., Katz, K. H. New England Journal of Medicine, 1951, 244, 459.

Tsalev, D. L., Sperling, M., Wetz, B. Analyst, 1992, 117, 1729.

Tseng, C. M., De Diego, A., Wasserman, J. C., Amouroux, D., Donard, O. F. X. Chemosphere, 1999, 39(7), 1119-1136.

Ugo, P., Zampieri, S., Moretto, L. M., Paolucci, D. Analytica Chimica Acta, 2001, 434(2), 291-300.

Uhlig, A., Schnakenberg, U., Hintshce, R. Electroanalysis, 1997, 9(2), 125-9.

Vanysek, P. In CRC Handbook of Chemistry and Physics, 71st Ed. D. R. Lide, D. R., Ed., CRC Press: Boca Raton, 1990-1991, Table 1, p. 8-16.

Vasjari, M., Mirsky, V. M. Calibrated nanoinjections of mercury vapor. Fresenius' Journal of Analytical Chemistry, 2000, 368(7), 727-729.

Villanacci, J.F., Beauchamp, R., Perrotta, D.M., et al, Morbidity and Mortality World Report, 1996, 45, 400.

Viltchinskaia, E. A., Seigman, L. L., Garcia, D. M., Santos, R. F. Electroanalysis, 1997, 9(8), 633-640.

Vincente-Beckett, V. A. Australian Journal of Chemistry, 1989, 42, 2107-18.

Vlasov, Y. G., Ermolenko, Y. E., Kolodnikov, V. V., Ipatov, A. V., Al-Marok, S., Sensors and Actuators B, 1995, 24-5, 317-9.

Wallschlaeger, D., Hintelmann, H., Evans, R. D. Wilken, R.-D. Water, Air, and Soil Pollution, 1995, 801-4, 1325-9.

Wang J, Tian B. Analytical Chemistry, 1993, 65(11), 1529-32.

Wang, J., Grundler, P., Flechsig, G.-U., Jasinski, M., Lu, J., Wang, J., Zhao, Z., Tian, B. Hot-wire stripping potentiometric measurements of trace mercury. Analytica Chimica Acta (1999), 396(1), 33-37.

Wang, J., Larson, D., Foster, N., Armalis, S., Lu, J., Rongrong, X., Olsen, K., Zirino, A. Analytical Chemistry, 1995, 67, 1481-1485.

Wang, J., Tian, B. Analytica Chimica Acta., 1993, 274, 1-6.

Wang, J., Tian, B., Lu, J., Wang, J., Luo, D. Electroanalysis, 1998, 10(6), 399-402.

Wang, Y., Flad, H.-J., Dolg, M. Physical Review B: Condensed Matter and Materials Physics, 2000, 61(3), 2362-2370.

Watras, C. J., Bloom, N. S. Limnology and Oceanography, 1992, 37, 1313-18.

Watson, Charles M., Dwyer, Daniel J., Andle, Jeffrey C., Bruce, Alice E., Bruce, Mitchell R. M. Stripping Analyses of Mercury Using Gold Electrodes: Irreversible Adsorption of Mercury. Analytical Chemistry, 1999, 71(15), 3181-3186.

Weeks, M. E. Journal of Chemical Education, 1968, 46-51.

Wilker, J. J. Wetterhahn, K. E., Lippard, S. J., Inorganic Chemistry, 1997, 36(10), 2079-83.

Wilker, J. J., Lippard, S. J. Journal of the American Chemical Society, 1995, 117(33), 8682-3.

Winek, C.L., Fochtman, F.W., Bricker, J.D., et al. Clinical Toxicology, 1981, 18, 261.

Wu, Q., Apte, S., Batley, G., Karl, C. Analytica Chimica Acta, 1997, 350(1-2), 129-34.

Xu, X., Thundat, T. G., Brown, G. M., Ji, H.-F. Detection of Hg2+ using microcantilever sensors. Analytical Chemistry. 2002, 74(15), 3611-3615.

Yang, X.-M., Tonami, K., Nagahara, L. A., Hashimoto, K., Wei, Y., Fujishima, A. Surface Science, 1995, 324, L362-L366.

Yoshida, A., Kihara, S. Journal of Electroanalytical Chemistry, 1979, 95, 159-68.

Zakharova, E. A., Pichugina, V. M., Tolmacheva, T. P. Journal of Analytical Chemistry., 1996, 51(9), 918-23.

Zanetti, G., Massey, V.and Curti, B. European Journal of Biochemistry, 1983, 132(1), 201.

Zarkadas, C. G., Smillie, L. B., Madsen, N. B. Canadian Journal of Biochemistry, 1970, 48(7), 763-76.

Zen, J.-M., Chung, M.-Journal of Analytical Chemistry. 1995, 67, 3571-7.

Zillmer, E. A., Lucci, K.A., Barth, J.T., et al. Clinical Toxicology, 1986, 24, 91.

Zubay, G. L., Biochemistry, Collier Macmillian, New York, 1988.

APPENDECES

APPENDIX A: MERCURY FACTS

Mol Weight .	200.59 g/mol
Atomic Mass	3.331×10^{-22} g/atom
Safe Drinking Water	2 μg/L = 1×10^{-8} M
Solubiblity in Water	.....56.16 μg/L = 0.28 μM
Vapor Pressure	1.9 mTorr

Isotope	a.m.u.	% abundance
Hg_{196}	195.9658	0.15
Hg_{198}	197.9667	10.02
Hg_{199}	198.9682	16.84
Hg_{200}	199.9683	23.13
Hg_{201}	200.9703	13.22
Hg_{202}	201.9706	29.80
Hg_{204}	203.9735	6.85

Mercury Conversions

4.985×10^{-12} M Hg → 1 ng/L Hg

1 ML Hg → 320 μC ($Hg^{2+} \rightarrow Hg^0$)

1 ML/cm^2 → 1×10^{15} atoms Hg → 333 ng

1 mol electrons → 96487 Coulombs

1 μC → 3.1×10^{12} atoms Hg ($Hg^{2+} \rightarrow Hg^0$)

1 ng Hg → 3×10^{12} atoms Hg

1 ng Hg → 4.985×10^{-12} moles

1 μC → 1.0325 ng Hg

1 μM → 200.59 ng/mL

Cyclic Voltammetry

Reversible Reactions

$$O + ne^- \Leftrightarrow R$$

$$I_p = -0.4463nF(nF/RT)^{1/2}c_O^{\infty}D^{1/2}v^{1/2}$$

$$I_p = -(2.99 \times 10^5)n^{3/2}c_O^{\infty}D_O^{1/2}v^{1/2}$$

T = 298 K

Diagnostics for Reversibility @ 298 K

1. $\Delta E_p = E_p^A - E_p^C = 59/n$ mV
2. $|E_p - E_{p/2}| = 59$ mV (56.5 mV)
3. $|I_p^A/I_p^C| = 1$
4. $I_p \propto v^{1/2}$
5. E_p is independent of v
6. at potentials beyond E_p, $I^2 \propto t$

Irreversible Systems

$$I_p = -(2.99 \times 10^5)n(\alpha_C n_\alpha)^{1/2}c_O^{\infty}D_O^{1/2}v^{1/2}$$

n = # of electrons in reaction

α_C = cathodic transfer coefficient

n_α = # of electrons before RDS

C_O^{∞} = concentration of oxidant in bulk

D_O = diffusivity of oxidized species

v = scan rate of potential sweep (V/s)

Diagnostics for total Irreversibility

1. No reverse peak.
2. $I_p^C \propto v^{1/2}$
3. E_p^C shifts $-30/\alpha_C n_\alpha$ mV for each decade increase in v.
4. $|E_p - E_{p/2}| = 48/\alpha_C n_\alpha$ mV

CV Diagnostic Tests for Quasi-reversible Systems

1. $|I_p|$ increases with $v^{1/2}$ but is not proportional to it.
2. $|I_p^A/I_p^C| = 1$, provided $\alpha_C = \alpha_A = 0.5$.
3. ΔE_p is greater than $59/n$ mV; increases with increasing v.
4. E_p^C shifts negatively with increasing v

APPENDIX B: SUPPLEMENTAL FIGURES FOR CHAPTER II

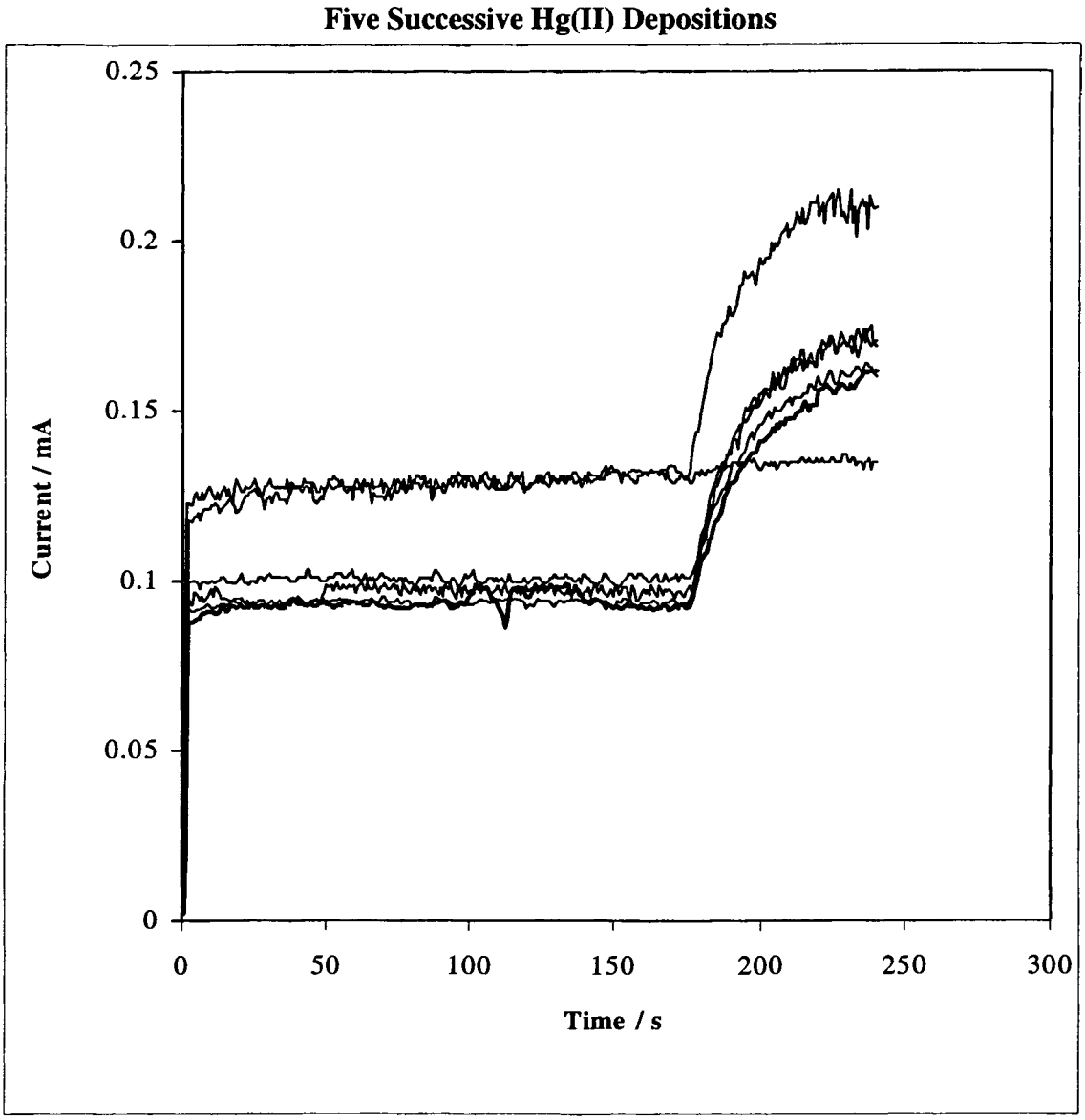

Figure B1: A gold electrode has five 60 s depositions in 0.01 mM Hg(II). Each deposition is followed by stripping at 1.0 V for 600 s.

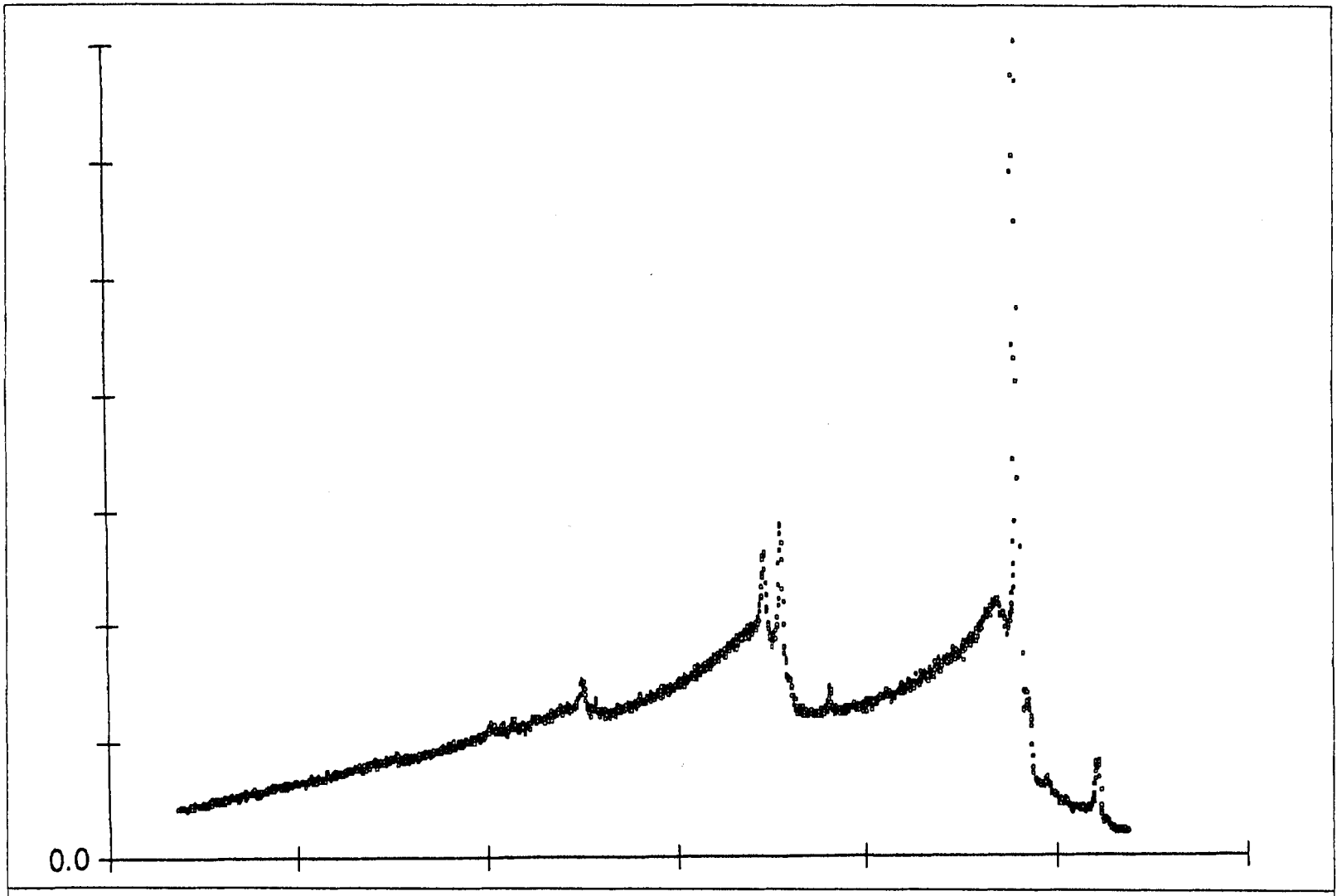

Figure B2: XPS Survery scan of Au with Mg Kα X-rays. Pass energy 50 eV.

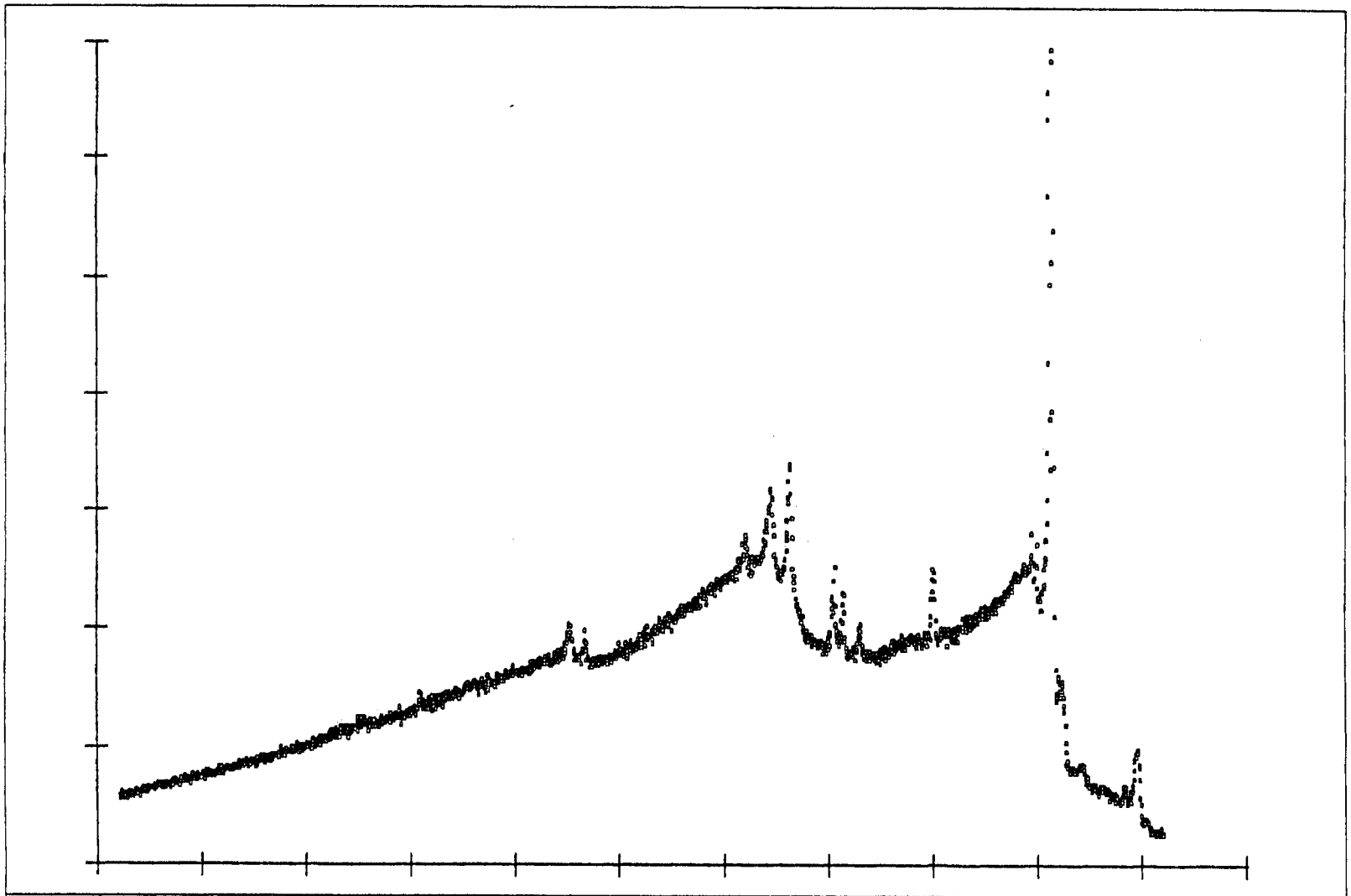

Figure B3: XPS Survey scan of Au with 30 s 0.1 mM Hg(II) deposition at −0.5 V vs. Ag/AgCl. Mg Kα X-rays. Pass energy 50 eV.

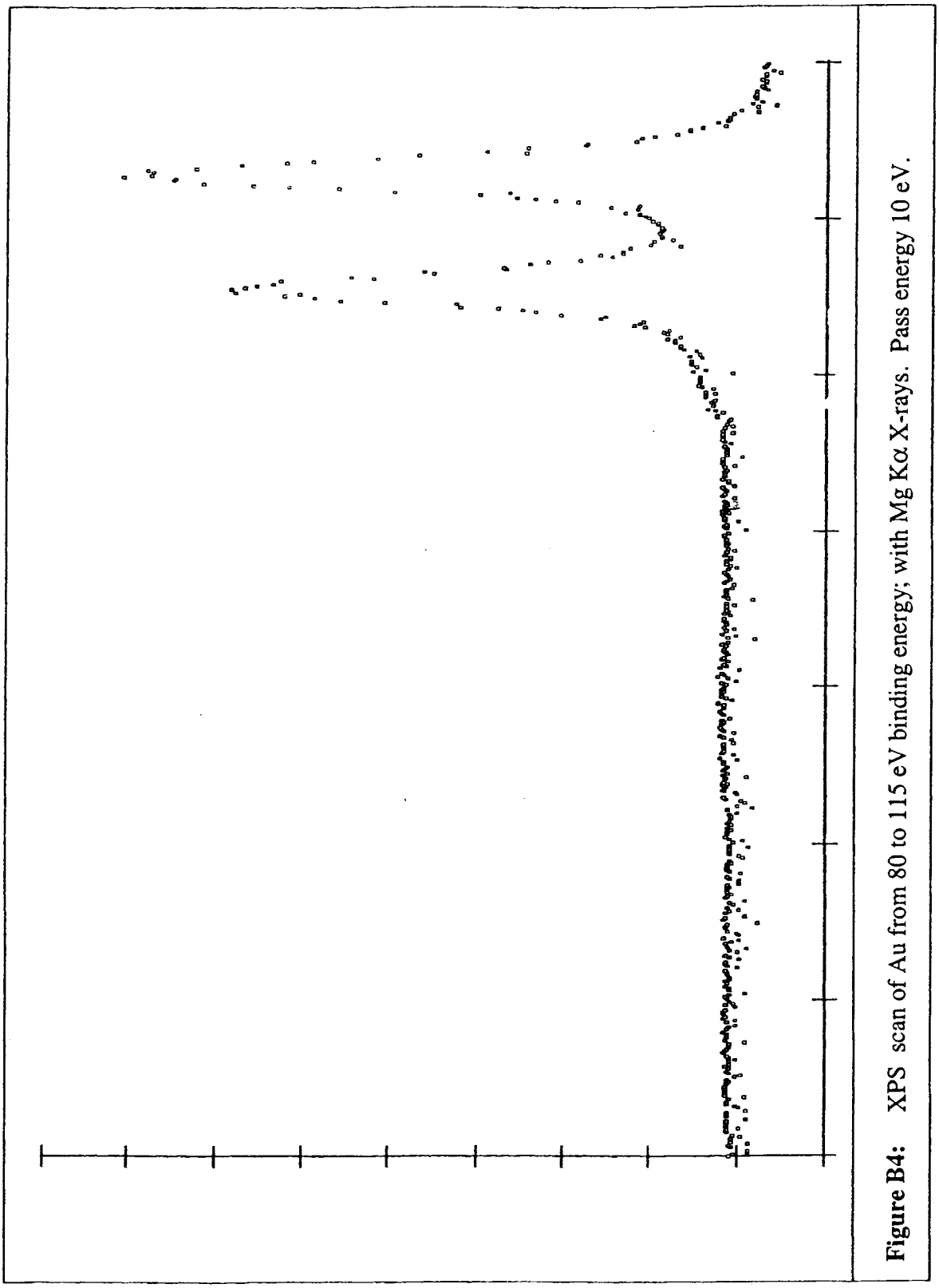

Figure B4: XPS scan of Au from 80 to 115 eV binding energy; with Mg Kα X-rays. Pass energy 10 eV.

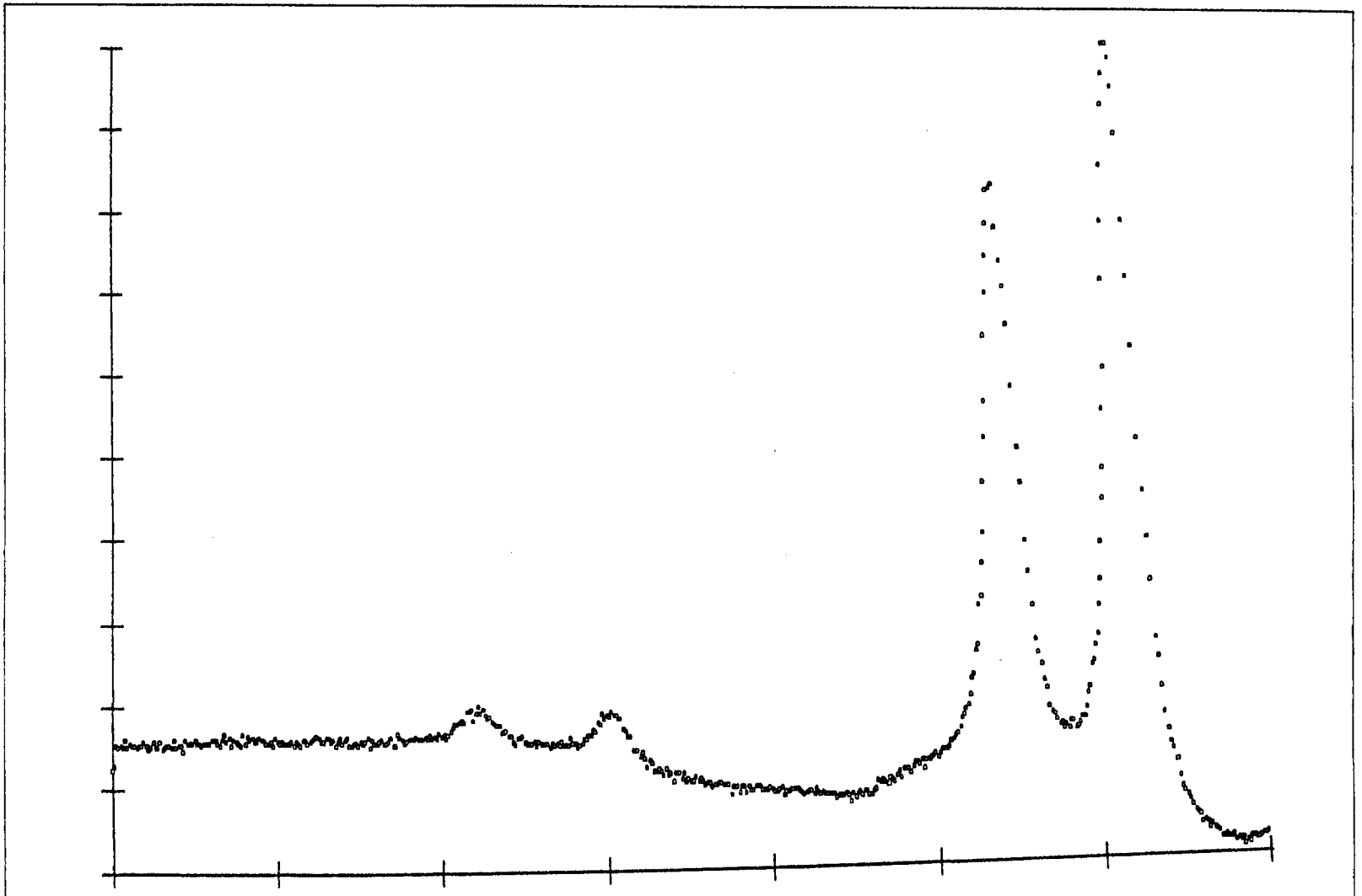

Figure B5: XPS scan from 80 to 115 eV binding energy of Au with 30 s 0.1 mM Hg(II) deposition at −0.5 V vs. Ag/AgCl. Mg Kα X-rays. Pass energy 10 eV.

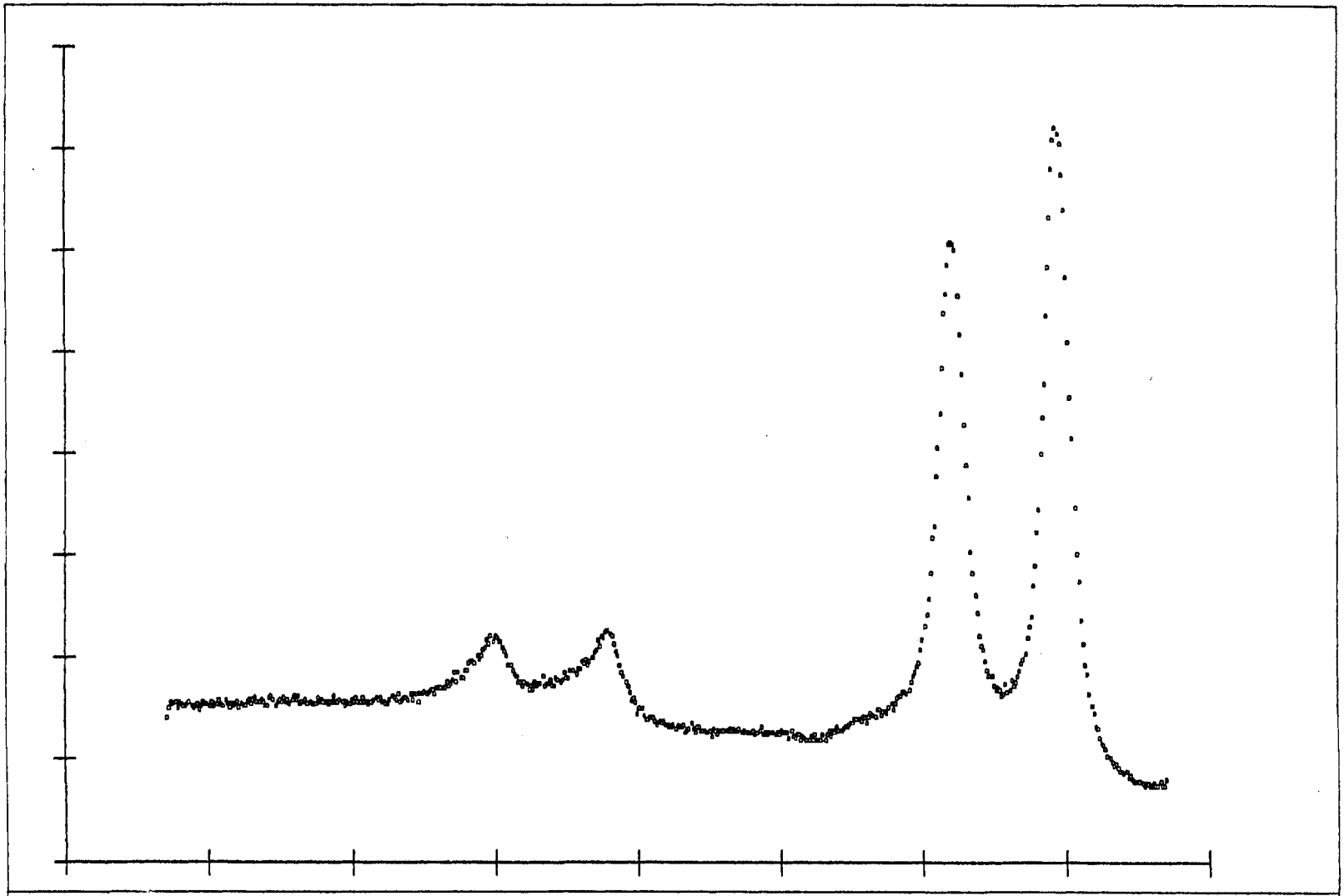

Figure B6: XPS scan from 80 to 115 eV binding energy of Au soaked in 0.01M $HgCl_2$ for 12 hours,. Then rinsed with water. No voltage potential applied to gold foil. Mg Kα X-rays. Pass energy 10 eV.

APPENDIX C: SUPPLEMENTAL FIGURES FOR CHAPTER III

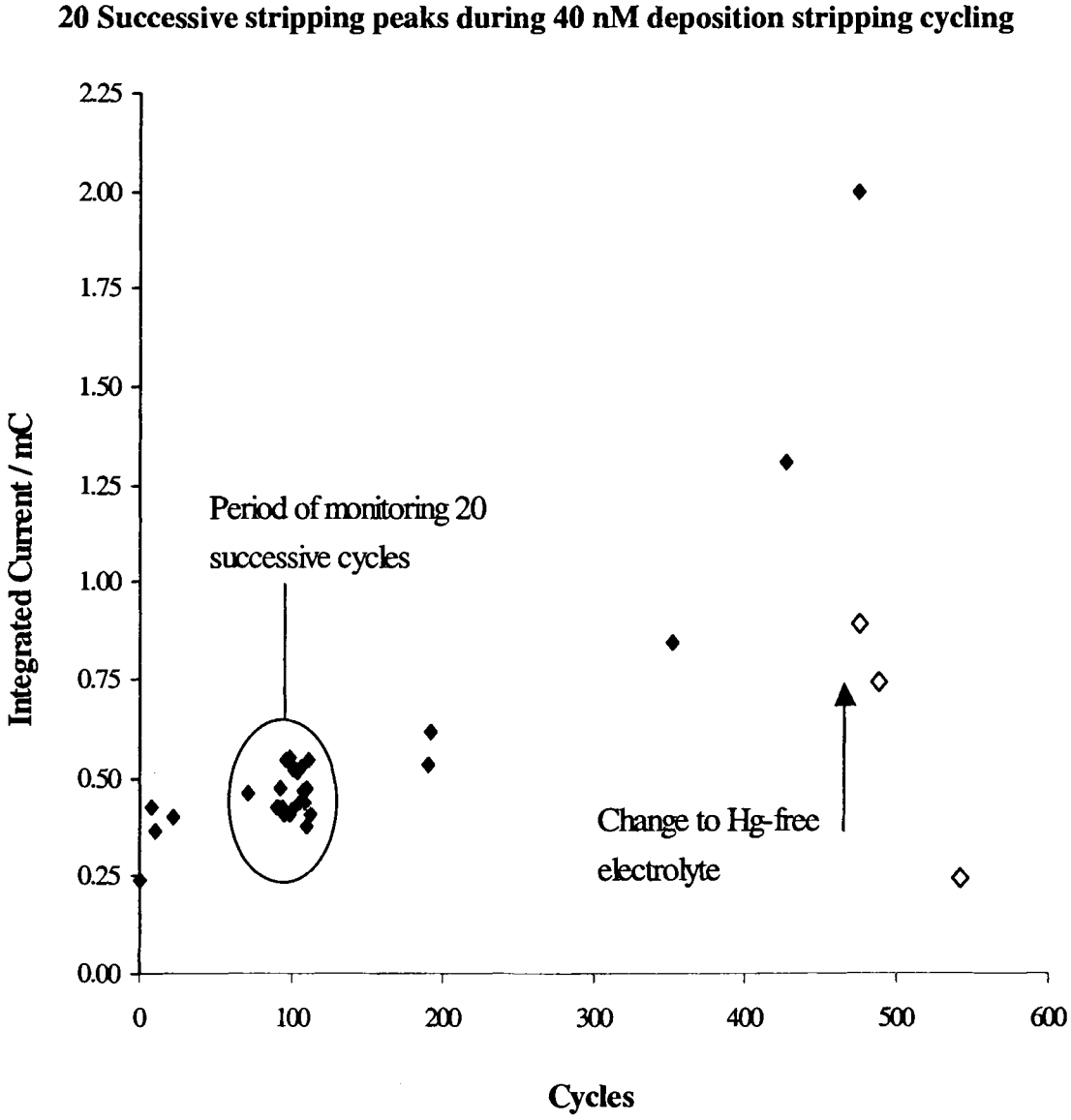

Figure C1: CV monitoring of 40 nM Hg(II) accumulation on gold electrode. 30 s deposition at – 0.3 V vs. Ag/AgCl follow by 60 s stripping at 1.0 V preceding CV scan from +0.8 V to +0.4V at 20 mV/s. Between deposition / stripping cycles 70 and 112 there were 20 successive CV monitoring scans (encircled) made every other depositon / stripping cycle.

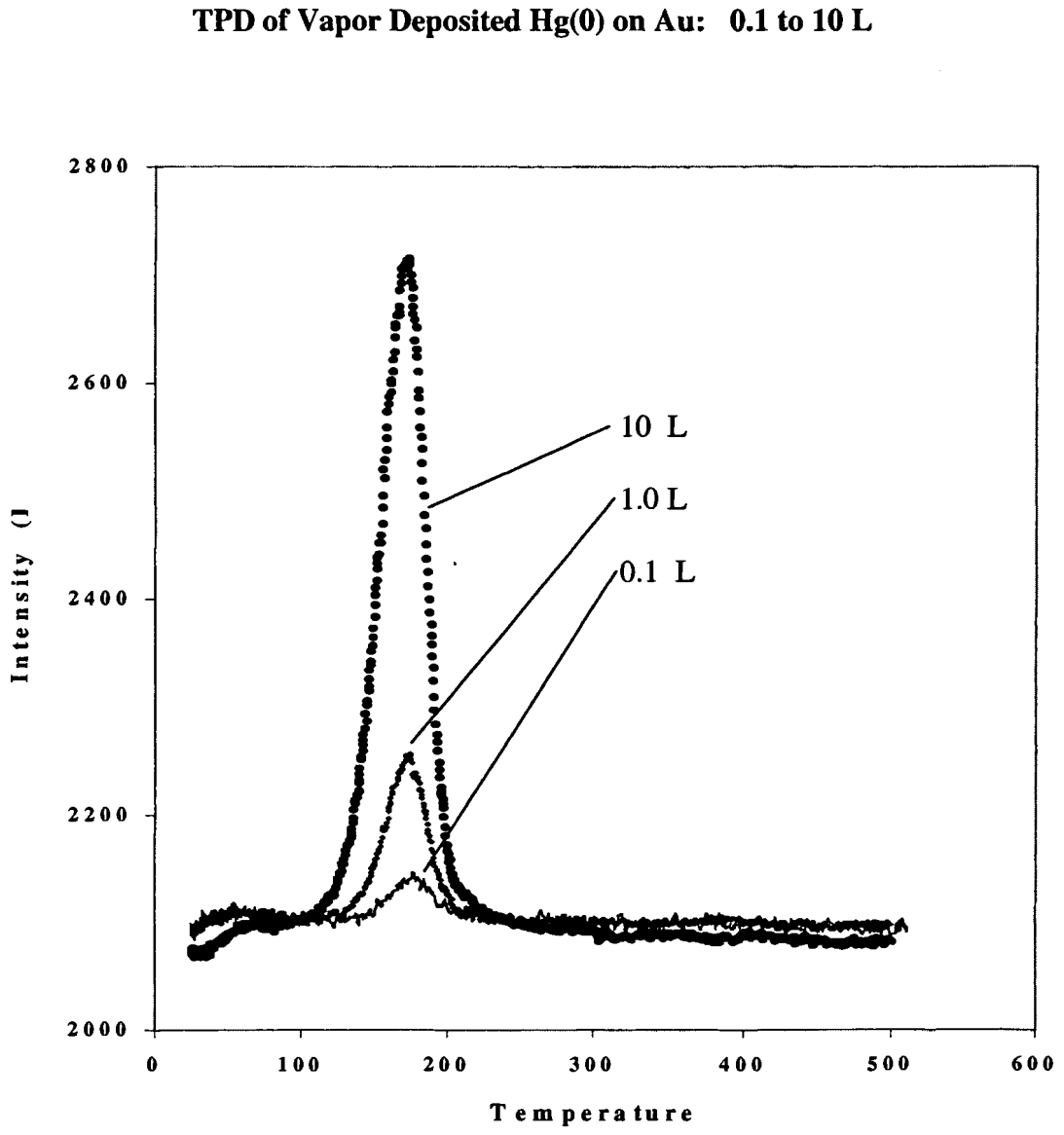

Figure C2: TPD of vapor deposited Hg on Au at 0.1, 1.0 and 10L. Heating rate 4.4 K/s

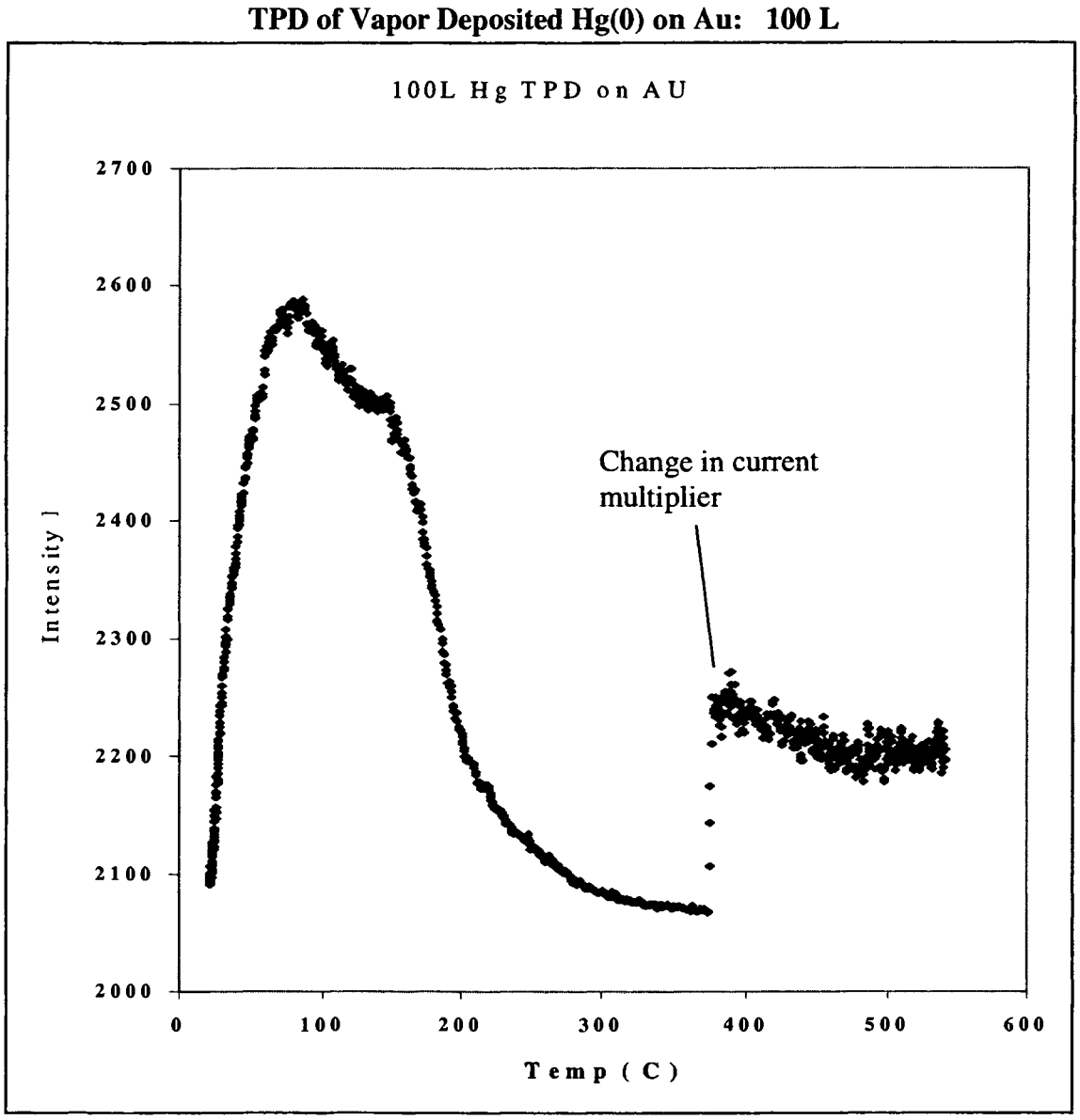

Figure C3: TPD of vapor deposited Hg on Au at 100 L. Heating rate 4.5 K/s

Isotherm TPD for distinction of high and low temperature Hg desorption peaks

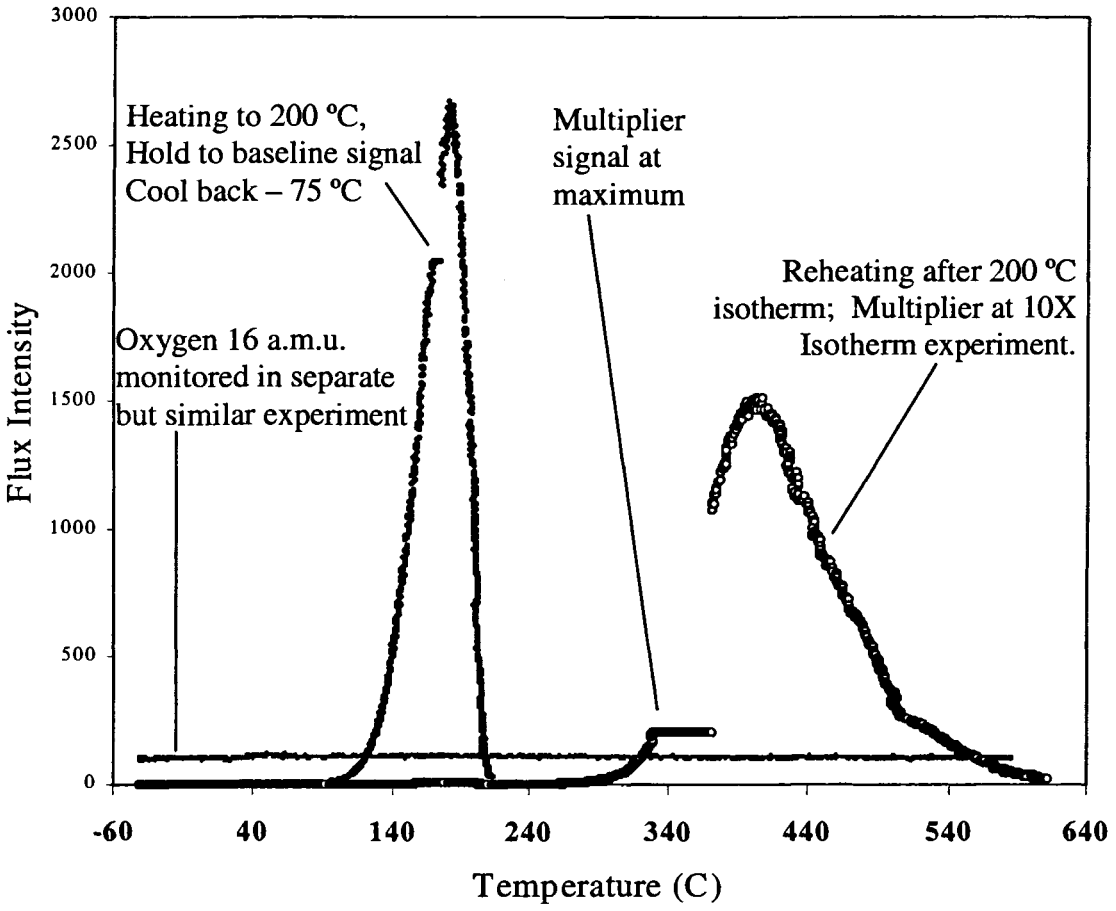

Figure C4: TPD of Hg on Au after 180 minutes of 30 s deposition / 60 s stripping cycling at – 0.4 and 1.0 V vs. Ag/AgCl respectively, in 40 nM $HgCl_2$. Au analyzed after final stripping at 1.0 V. Au heated at 5 K/s to 200 °C and held until signal attenuated. Au then reheated at 5 K/s to 600 °C. A separate Au foil, undergoing the same Hg(II) deposition and stripping process was monitored for oxygen at 16 a.m.u. with a 5 K/s TPD from – 75 °C to 600 °C.

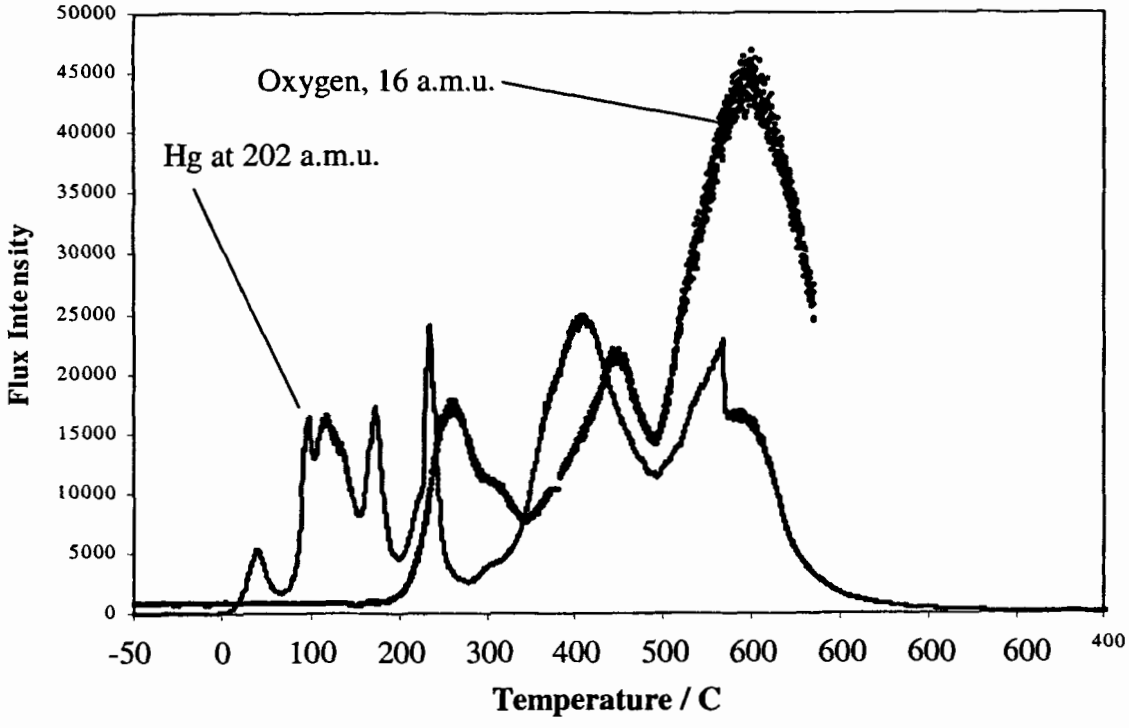

Figure C5: TPD of HgO from aqueous soln dried onto Au. TPD from – 50 °C to 600 °C at 4.5 K/s. Two separate foils were prepared in the same manner. ^{202}Hg was monitored for one foil and ^{16}O for the other Au foil.

APPENDIX D: MERCURY GOLD BINARY PHASE DIAGRAM[1]

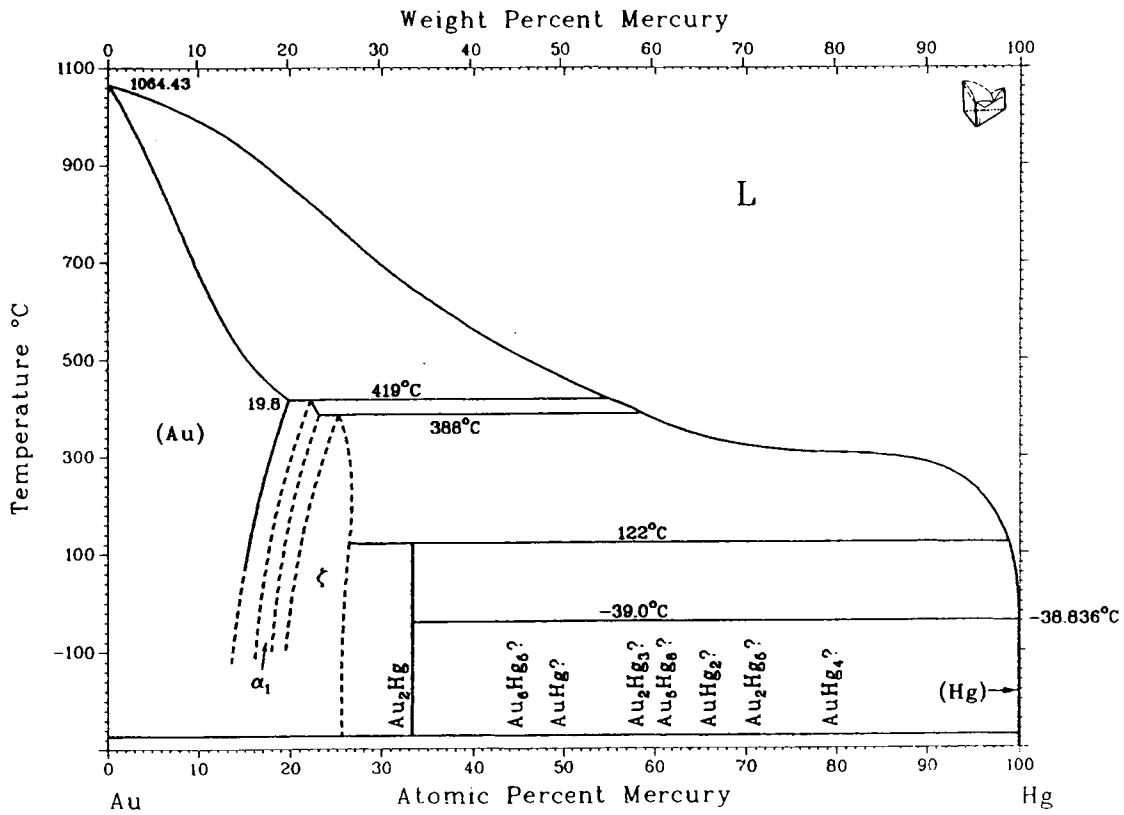

[1] Assessed Au-Hg Phase Diagram, Okamoto, K., in Binary Alloy Phase Diagrams, Massalski, T. B., Chief Editor. American Society for Metals, 1990, Metals Park, 265-7.

APPENDIX E: PUBLISHED PAPER, ANALYTICAL CHEMISTRY

Anal. Chem. 1999, *71*, 3181−3186

Stripping Analyses of Mercury Using Gold Electrodes: Irreversible Adsorption of Mercury

Charles M. Watson,[†] Daniel J. Dwyer,[†] Jeffrey C. Andle,[‡] Alice E. Bruce,[†] and Mitchell R. M. Bruce*[,†]

Department of Chemistry, University of Maine Orono, Maine 04469, and BIODE, Inc., 20 Freedom Parkway, Bangor, Maine 04401

The electrochemical deposition and stripping of mercury on gold surfaces was investigated to assess whether gold electrodes would return to mercury-free states after stripping analyses. X-ray photoelectron spectroscopy studies demonstrate the presence of mercury on gold foil electrodes that have undergone controlled-potential deposition procedures in Hg^{2+} solutions (10 nM−0.1 mM) followed by stripping and cleaning in mercury-free electrolyte. Results show that mercury is not completely removed electrochemically from the gold electrodes, even when the oxidizing potential is +2.5 V vs Ag/AgCl. Bulk electrolyses deposition and stripping procedures coupled with cold vapor atomic absorption spectroscopic analyses of solutions after deposition and stripping are also reported. Results suggest that the nature of the gold electrode is fundamentally altered by irreversible adsorption of mercury; that is, mercury is adsorbed during deposition and some of the mercury is retained even after stripping and cleaning. The implications and strategies for using stripping analysis and gold electrodes for the measurement of mercury under the experimental conditions employed in this study are discussed.

The utilization of electroanalytical techniques for the detection of aqueous mercury, either alone or in conjunction with such emerging technologies as piezoelectric sensors, offers promise for the development of sensors capable of remote quantification of mercury in the environment.[1-8] The gold electrode has been one of the electrodes of choice in electrochemical stripping analysis techniques for the detection of aqueous mercury. The techniques collectively termed stripping analysis include anodic stripping voltammetry, potentiometric stripping analysis, Osteryoung square-wave anodic stripping voltammetry, differential pulse stripping voltammetry, and constant-current stripping analysis.[9] One reason for the use of gold is its high affinity for mercury, which enhances the preconcentration effect.[10] A distinct advantage of using electrochemistry, over conventional methods to detect mercury, is its suitability for use in the field where on-site measurements are highly desirable or a necessity (i.e., with radioactive samples, down-hole well monitoring, or during remediation).

Stripping techniques utilizing gold electrodes have demonstrated high sensitivity with detection limits well below 1 ppb.[11-14] Repetitive use of any of these techniques necessitates a three-step cycle: preconcentration (deposition), measurement (stripping), and regeneration (cleaning). Some reports in the literature suggest that a relatively short "cleaning" step results in complete removal of all deposited mercury prior to the next measurement.[14-16] Repetitive mercury measurement studies, typically employing up to 20 measurement cycles, result in standard deviations below 5%, supporting the idea that mercury is removed from the electrode after each cleaning step. However, there is also evidence in the literature that the cleaning step may not result in a "fresh", analyte-free, gold surface. In the early 1980s, Johnson and co-workers reported that mercury accumulated on the electrode in cyclic voltammetry (CV) experiments and was not subsequently removed when the CV experiment was continued in fresh (mercury-free) electrolyte solution.[17]

In this investigation, we have set out to answer the question, is mercury retained on a gold electrode after a single controlled-potential deposition, stripping, and cleaning cycle? The experimental conditions used in this study were chosen to mimic situations where a field mercury electrode might be employed, e.g., for determination of mercury in natural freshwater with no added electrolyte. An investigation to answer a related question, whether mercury accumulates at a gold electrode after many deposition, stripping, and cleaning cycles, will be reported

[†] University of Maine.
[‡] BIODE, Inc.

(1) Andle, J.; Schweyer, M.; Munson, J.; Roderick, R.; McAllister, D.; French, L.; Vetelino, J.; Watson, C.; Foley, J.; Bruce, A.; Bruce, M. *UFFC Trans. Sens. Actuators* **1998**, *45*, 1408−1415.
(2) Evans, O.; McKee, G. *Analyst* **1988**, *113*(2), 243−6.
(3) Ho, M.; Guilbault, G.; Scheide, E. *Anal. Chim. Acta* **1981**, *130*(1), 141−7.
(4) Wu, Q.; Apte, S.; Batley, G.; Karl, C. *Anal. Chim. Acta* **1997**, *350*(1−2), 129−34.
(5) Svancara, I.; Matousek, M.; Sikora, E.; Schachl, K. *Electroanalysis* **1997**, *9*(11), 827−833.
(6) Viltchinskaia, E.; Zeigman, L.; Garcia, D.; Santos, P. *Electroanalysis* **1997**, *9*(8), 633−40.
(7) Korolczuk, M. *Fresenius' J. Anal. Chem.* **1997**, *357*(4), 389−91.
(8) Uhlig, A.; Schnakenberg, U.; Hintshce, R. *Electroanalysis* **1997**, *9*(2), 125−9.
(9) Dewald, H. D. In *Modern Techniques in Electroanalysis*; Vanysek, P., Ed.; Wiley: New York, 1996; pp 151−185.
(10) Zen, J.-M.; Chung, M.-J. *Anal. Chem.* **1995**, *67*, 3571−3577.
(11) Gil, E. P.; Ostapczuk, P. *Anal. Chim. Acta* **1994**, *293*, 55−64.
(12) Ostapczuk, P. *Anal. Chim. Acta* **1993**, *271*, 35−40.
(13) Wu, Q.; Apte, S. C.; Batley, G. E.; Bowles, K. C. *Anal. Chim. Acta* **1997**, *350*, 129−134.
(14) Rievaj, M.; Mesáros, S.; Bustin, D. *Collect. Czech. Chem. Commun.* **1993**, *58*, 2918−2923.
(15) Wang, J.; Larson, D.; Foster, N.; Armalis, S.; Lu, J.; Rongrong, X.; Olsen, K.; Zirino, A. *Anal. Chem.* **1995**, *67*, 1481−1485.
(16) Wang, J.; Tian, B.; Lu, J.; Wang, J.; Luo, D.; MacDonald, D. *Electoanalysis* **1998**, *10*, 399−402.
(17) Schadewald, L. A.; Linstrom, T. R.; Hussein, W.; Evenson, E. E.; Johnson, D. C. *J. Electrochem. Soc.* **1984**, *131*, 7.

10.1021/ac981312b CCC: $18.00
Published on Web 06/22/1999

separately. The justification for these investigations is based on the idea that if mercury is retained on a gold electrode, it would have a practical impact on the way stripping analysis is used to detect mercury. For example, would there be conditions when previously retained mercury is released during stripping? Would retained mercury alter the electrode composition enough to change the electrical properties of the electrode, such as the exchange current density, which is orders of magnitude different for gold and mercury?[18] Calculations on mercury suggest a metal–nonmetal transition in clusters at ~60 mercury atoms (i.e., a mercury cluster less than 60 atoms is nonmetallic).[19] Would limited surface coverage of mercury on gold effect calibration of the electrode? Finally, in field applications, the number of desirable reproducible cycles will be many times greater than the limited number that have been typically employed in laboratory studies. Thus, our studies were initiated to determine whether the cleaning step leaves the electrode in a state that can be predicted from cycle to cycle, the answer to which is critical for the success of any long-term repetitive electrochemical technique.

EXPERIMENTAL SECTION

Chemicals and Glassware. Water for all electrolyte and soaking solutions and for glassware rinsing was redistilled from a Barnstead NANOpure water purification system to a final conductivity of less than 0.1 μS cm^{-1}. All chemicals, unless otherwise noted, were Certified ACS Reagent Grade. The supporting electrolyte solutions (2.5 mM KCl/KNO_3, pH 3) were made daily by diluting a stock solution of either 1 M KCl or KNO_3 with water previously acidified to pH 3 with concentrated HCl or HNO_3. The pH of the electrolyte was stable during all electrochemical experiments. The concentration of the supporting electrolyte solution was chosen to limit interference from impurities and to mimic low electrolytic environmental conditions, where chloride ion concentrations normally range from a few to several hundred ppm in many natural water sources.[20] Ostapczuk et al. have shown that chloride ion concentrations between 2 and 20 mM were adequate and stable for mercury potentiometric stripping analysis experiments.[11,12] The electrolyte solution was sparged with nitrogen gas until just prior to transfer to the electrochemical cell. A 0.1 M $HgCl_2$ stock solution was made by dissolving $HgCl_2$ (Aldrich 99.999%) in 2% HNO_3. Mercuric chloride solutions of concentrations less than 1×10^{-4} M (20 000 ppm) were made fresh daily from this stock solution. Mercuric nitrate (Aldrich 99.99%) solutions were prepared and used in a similar manner. Mercury(II) atomic absorption standard solutions, 1–5 ppb, were made by diluting acidified 1004 ppm Hg^{2+} (VWR Certified Atomic Absorption Standard) to a 1 ppm solution, which was further diluted just prior to use with 2% HNO_3 (ACS Analytical Grade). A 10% $SnCl_2$ (ACS Analytical Grade) solution was diluted to 1.1% with 3% HCl (ACS Analytical Grade) to serve as the reducing agent in cold vapor atomic absorption (CVAA) analysis.

All glassware was rinsed several times with water and then soaked in 50% nitric acid for at least 24 h until just prior to use; whereupon, it was well rinsed again with water. All solution storage bottles were treated in the same manner.

Electrochemistry. The electrochemical cell, fabricated by Anderson Glass of New Hampshire, was composed of three chambers separated by porous glass frits. In all experiments, except as noted, the outer compartments contained a platinum wire auxiliary electrode and a Ag/AgCl reference electrode (BAS MF-2074: E° = 0.194 V vs NHE), respectively. The center compartment contained a gold foil working electrode cut from 0.1- and 0.5-mm gold foil (Aldrich 99.99%). The working electrodes had 0.25-mm gold wire spot welded to one side, providing a point for holding and for electrical contact. The surface area of the electrodes was controlled by coating the backside and most of the wire with a clear insulating butyl acetate polymer (Revlon No. 10).

The three-compartment design was chosen to prevent contamination of the auxiliary and reference electrodes, preventing them from becoming sources of mercury in sequential experiments. The mercury was additionally restricted to the central chamber by always maintaining a superior fluid level in the side chambers containing the reference and auxiliary electrodes. The success of this mercury containment scheme was established by CVAA analysis of the contents of the outer chambers, which confirmed that mercury concentrations were no higher than distilled water samples.

The applied potentials were controlled by using an EG&G model 273 potentiostat/galvanostat, EG&G's model 270 software, and a Micron 75-MHz Powerstation. The pH was monitored by using a Beckman Φ 11 pH meter with a Corning bulb-type pH ion-selective electrode. The water conductivity measurements were made with a YSI model 3200 conductivity meter using a YSI 3253 combination thermister conductivity cell.

Controlled-Potential Deposition, Stripping, and Cleaning Procedure. Before each controlled-potential deposition, stripping, and cleaning experiment, the electrodes underwent a blank deposition/stripping procedure in 18 mL of supporting electrolyte solution. The blank run was used to subtract the background current from the subsequent experiment with Hg^{2+} solution. After the blank run, the electrolyte solution was replaced with 18 mL of fresh electrolyte solution and the electrode was used for a mercury deposition and stripping experiment according to the following procedure.

A cathodic current was established at a constant potential of −0.3 V in a stirred aqueous electrolyte solution. After 150–600 s, a 20 μL to 1 mL aliquot of a mercuric chloride solution was injected into the central chamber. The deposition was allowed to continue for a specified period of time, whereupon, the experiment was interrupted and the gold working electrode was removed from the solution, while still at the set deposition potential. The deposition solution in the central chamber was collected for CVAA analysis. The electrode and the central chamber were rinsed with water and the rinsings were combined with the deposition solution for CVAA analysis. The gold electrode was reimmersed in another 18 mL of fresh electrolyte in the central chamber and the experiment (at −0.3 V) was allowed to continue for a period of 50–200 s. At this point, the potential was switched from a cathodic deposition potential to an anodic potential which ranged from +0.7 to +2.5 V. After an initial stripping event occurred (usually within

(18) Greef, R.; Peat, R.; Peter, L.; Pletcher, D.; Robinson, J. *Instrumental Methods in Electrochemistry*. Ellis Horwood Ltd.: Chichester, 1985; p 233.
(19) Jortner, J. In *Physics and Chemistry of Finite Systems: From Clusters to Crystals*; Jena, P., Khanna, S. N., Rao, B. K., Eds.; NATO ASI Series; Kluwer Academic Publishers: Dordecht, 1991, Chapter 1.
(20) *The NALCO Water Handbook*, 2nd ed.; Kremmer, F., Ed.; McGraw-Hill: New York, 1988.

seconds), the electrode was held at that potential to clean it. The total duration of the stripping and cleaning steps ranged from 500 to 4000 s. Just before the end of the prescribed stripping procedure, the experiment was stopped and the electrode was removed from the solution while still set at the oxidizing potential. The contents of the central chamber, along with solutions collected after rinsing several times, were then collected for CVAA analysis in the same manner as for the deposition solutions. After each experiment, the electrochemical cell was rinsed with water, and nitric acid was allowed to flow through the frits from the outside chambers to the central chamber. The cell was then thoroughly rinsed with water and electrolyte solution before the next experiment.

The gold electrodes were cleaned after each contact with mercury. The electrodes undergoing X-ray photoelectron spectroscopy (XPS) analysis were cleaned by argon plasma etching. The other electrodes were cleaned in the following manner: after rinsing with hot acetone to remove the polymer coating, they were heated to redness for 30 s in an air/gas flame, polished with 1.0-μm water-soluble diamond suspension (Buehler) on a Buehler Microcloth, rinsed with water, and boiled in nitric acid for at least 2 h, rinsed with water again, and finally heated at 400 °C in a ceramic crucible, with the polished surface exposed to air for at least 12 h. Thus cleaned, the clear polymer coating was applied to the electrodes followed by drying at 50 °C for at least 24 h. The electrodes were stored in a covered ceramic crucible.

Cyclic Voltammetry Procedure. The CV experiments were performed with all of the electrodes in separate chambers. Aliquots of the stock mercuric chloride solutions, 20 μL to 1 mL, were added to 18 mL of the supporting electrolyte solution in the central chamber once the starting potential was established. The solution was then stirred with a magnetic stirrer until 15 s before each CV run.

Cold Vapor Atomic Absorption Spectroscopy. The CVAA analysis was carried out on a Perkin-Elmer flow injection mercury hydride atomic absorption spectrometer (FIMS) equipped with an electrodeless discharge lamp. The spectrometer employs an absorption wavelength of 253.7 nm passing through a 0.7-nm slit. The sample volume was 500 μL, and the flow rate of the argon carrier gas (grade 5.0) was 100 mL/min. The mercury concentration was correlated to the absorption peak height with the Perkin-Elmer FIMS software. Immediately after collection, the deposition and stripping solutions were diluted with water and nitric acid to final concentrations of 1−5 ppb Hg^{2+} in 2% HNO_3. All samples were analyzed within 48 h of collection.

X-ray Photoelectron Spectroscopy. The XPS instrument was a prototype model with a differentially pumped X-ray source, fabricated by Leybold-Heraeus, that allows for XPS analysis of samples at relatively high pressures (1 mbar). All the spectra were recorded with magnesium Kα X-rays emanating from electron impact of a 20-mA emission current through an 11-kV voltage drop. The photoelectrons passed to the hemispherical energy analyzer, referenced to the Au $4f_{7/2}$ peak at 84.00 eV, through a 50-eV pass energy window. The pass energy was set at 100 eV when the electrode surfaces were analyzed for the presence of chloride, oxygen, residual mercury, or other species. The angle between the analyzer and the incident X-ray beam is 54.7° with the analyzer normal to the sample surface.

The argon (grade 5.0) plasma etching was conducted with a Leybold-Heraeus IQE-12/38 ion gun. The etching conditions were 1×10^{-4} mbar argon, 10 A ionization current, and 2250 V acceleration potential. The incident angle of the rastering plasma beam was 54.7° for the etching experiments, but for electrode cleaning, the surface was rotated into the plasma beam giving incident angles between −30 and 60°.

XPS Procedure. Electrodes were transported to the XPS laboratory in closed containers. Before an electrode sample was introduced into the high-vacuum system, a gold foil standard on the sample holder plate was analyzed for mercury contamination at a pass energy of 100 eV. If a mercury peak was observed in the XPS spectrum by scanning between binding energies from 95 to 110 eV, the gold foil was cleaned by argon plasma etching and then reanalyzed for mercury. At this point, the sample rod was removed from the XPS system and the gold electrode sample was placed on the holder plate on the side opposite of the gold foil standard. The sample rod was then reinserted into the XPS system and the gold electrode sample was pumped down, in an antechamber, to a pressure no greater than 1×10^{-7} mbar. This pumpdown time varied from 20 min to several hours (when left overnight). Once the pressure of 1×10^{-7} mbar was achieved, the sample was moved into the analysis chamber, where the XPS spectra were recorded at base pressures less than 5×10^{-9} mbar. After all the desired spectra on the gold sample were recorded, the sample rod was rotated 180° and the gold foil standard was reanalyzed for the presence of mercury to see whether contamination occurred during the time frame of the XPS experiment. No mercury peak was ever detected on the gold foil standard at this point. The gold foil standard and the electrode were then etched clean with argon plasma etching, usually for 30 min for each foil. After etching, the electrode was again analyzed for the presence of mercury and then immediately removed from the system and stored for another electrochemical experiment.

Safety. All waste solutions of concentrations greater than 20 ppb mercury were collected and stored for hazardous waste disposal pursuant EPA regulation 40CFR 261.24.

RESULTS AND DISCUSSION

The Latimer diagrams below indicate the formal oxidation potentials for mercury and gold involving their free cations as well as the potentials for the corresponding chloride complexes (in parentheses).[21-23] As illustrated in these diagrams and in eq 1,[24] mercury oxidation, either from Hg^0 or Hg_2^{2+}, occurs at potentials below 0.8 V (vs Ag/AgCl), whereas oxidation of gold generally requires higher potentials.

$$Hg^0 \underset{(+0.071)}{\overset{+0.600}{\longrightarrow}} Hg_2^{2+} \underset{(+0.333)}{\overset{+0.723}{\longrightarrow}} Hg^{2+}$$
$$\qquad\qquad +0.654$$

$$Au^0 \xrightarrow{+1.495} Au^+ \xrightarrow{+1.204} Au^{3+}$$
$$\qquad\qquad +1.301 \quad (+0.805)$$

$$Au_2O_3 + 6H^+ + 6e^- \rightleftharpoons 2Au + 3H_2O$$
$$E^\circ \approx 1.0\ V \qquad (Ag/AgCl) \quad (1)$$

Johnson and co-workers reported cyclic voltammetry studies of 0.1 mM Hg^{2+}/0.1 M $HClO_4$ aqueous solutions using a gold

rotating disk electrode (ω = 3600 rev min^{-1}, ϕ = 2.0 V min^{-1}).[17] Cycling between −0.0 and +1.6 V (vs SCE), they observed that mercury was readily reduced during each cathodic sweep and that three oxidation processes occurred on each anodic sweep at +0.4, +0.8, and +1.25 V. (An SCE reference electrode was used in their study and potentials are similar to the Ag/AgCl reference electrode.)[23] The first oxidation wave at +0.4 V was assigned as one-electron stripping of surface mercury, i.e., $Hg^0 \rightarrow Hg^{1+} + e^-$, while the second wave at +0.8 V was assigned as the stripping of mercury from the gold−mercury alloy. Interestingly, while the position and peak current of the first oxidation process remained fairly constant during 10 successive cyclic voltammetry scans, the oxidation signal at +0.8 V increased.

Cyclic Voltammetry Experiments. Linear potential sweep, cyclic voltammetry experiments on 0.5 mM Hg^{2+}/2.5 mM KCl aqueous solutions were performed to establish the potentials of mercury and gold oxidation in the three-compartment cell employed in this study. Cycling between −1.0 and +2.0 V (vs Ag/AgCl), a pattern almost identical to that reported by Johnson and co-workers was observed with some minor variations (Figure A, Supporting Information). On each anodic sweep, a shoulder was observed at ~+0.3 V (in comparison to the well-resolved peak observed at +0.4 V reported by Johnson and co-workers[17]) followed by peaks at about +0.55, +1.0, and +1.5 V. The additional oxidation wave observed at ~+1.5 V, due to the wider potential limit employed in our study, was assigned as oxidation of the gold electrode. Thus, the cyclic voltammetry investigation established that, upon each anodic sweep, oxidation occurred at about +0.3, +0.55, +1.1, and +1.5 V. The first two oxidations appear to involve mercury and the latter two gold. Cyclic voltammetry experiments were also run at a higher chloride concentration (1.0 M KCl). Although some shifts in redox potentials occurred (due to a decrease in *iR* drop), the same number and pattern of redox processes were observed as in the CV at 2.5 mM KCl. Higher mercury concentrations were also studied; under these conditions, deposition and stripping could be monitored visually by observing the silvering of the gold electrode.

In CV experiments using non-chloride-containing solutions, the mercury reduction peak shifted positively from about +0.05 to +0.35 V (compared to the chloride-containing solutions). The bulk mercury oxidation process, which occurs at +0.55 in chloride-containing solutions, shifted to +0.75 V. With our experimental setup, the oxidation of the gold electrode started at ~+0.90 V, a shift of 0.20 V to the negative compared to those in Cl^- solutions. Repeated CV cycling in 40 nM $Hg(NO_3)_2$ in 2.5 mM KNO_3 at pH 3 (pH adjusted with HNO_3) showed a rapid increase in the area of the mercury oxidation peaks vs those using chloride complexes. In addition, in nitrate solutions, the areas of the mercury oxidation peaks did not diminish significantly when the CV cycling was continued in flowing Hg-free electrolyte solution (40 mL min^{-1}) during a period of 25 min. What is apparent is that the electrochemical stripping efficiency is much better in chloride solutions than in nitrate solutions.

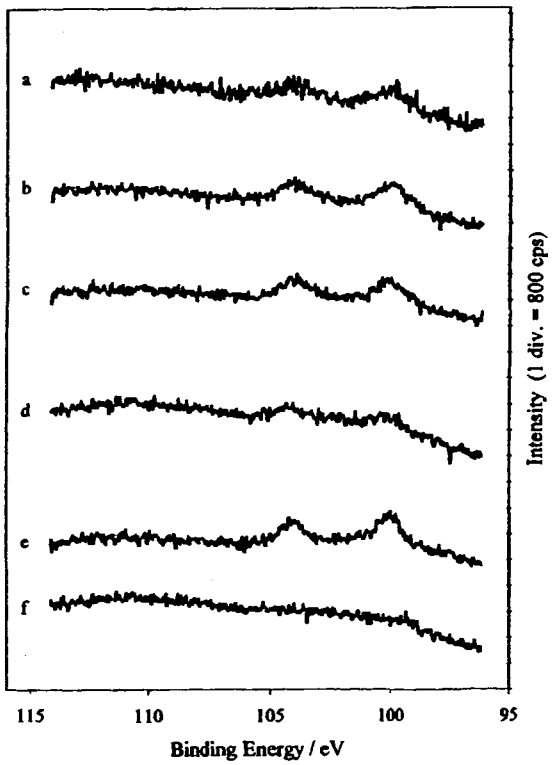

Figure 1. XPS spectra of 1-cm^2 Au foils after 150-s electrochemical deposition at −0.3 V in 0.1 mM Hg(II) followed by stripping for 600 s at (a) 2.5, (b) 1.9, (c) 1.5, (d) 1.1, and (e) 0.7 V vs Ag/AgCl. Spectrum f is the gold foil after argon plasma etching. Spectra were made with Mg Kα X-rays from 20 mA, 11 kV emission current, pressure <1 × 10^{-11} bar, 50 eV pass energy, and 20 scans.

Having established the potentials at which various oxidation processes occur in the three-compartment cell, the effects of mercury deposition, stripping, and cleaning of the gold foil electrode were studied using $HgCl_2$/KCl solutions. Deposition of mercury was accomplished by first introducing a cleaned 0.5-cm^2 gold working electrode into the central working electrode compartment. The potential of the electrode in a stirred, aqueous solution (2.5 mM KCl, pH 3) was then set to −0.3 V. After a current baseline was established, an aliquot of mercury chloride was injected into the central working electrode chamber, resulting in an initial 0.1 mM Hg^{2+} concentration. Deposition of mercury onto the gold foil electrode readily occurred at −0.3 V and was allowed to continue for 60 s. By switching to a positive potential between +0.7 and +2.5 V, deposited mercury was then stripped. The stripping step generally occurred within seconds after switching and was characterized by a large current peak that quickly returned to baseline. The electrode was held at the positive potential for a total of 600 s, 10 times longer than the deposition time, to ensure ample time for the electrode to be cleaned.

XPS Analysis. XPS analyses of gold foil electrodes are shown in Figure 1. The XPS spectra shown in Figure 1a−e each represent a separate experiment in which deposited mercury was stripped and cleaned at potentials ranging from +0.7 to +2.5 V, as indicated

(21) Vanysek, P. In *CRC Handbook of Chemistry and Physics*, 71st ed.; Lide, D. R., Ed.; CRC Press: Boca Raton, 1990−1991; Table 1, pp 8−16.
(22) Latimer, W. M. *The Oxidation States of the Elements and their Potentials in Aqueous Solutions*, 2nd ed.; Prentice-Hall: Englewood Cliffs, NJ, 1952.
(23) Mohamed, A. A.; Bruce, A. E.; Bruce, M. R. M. In *Organic Derivatives of Silver and Gold*; Patai, S., Rappaport, Z., Eds.; John Wiley & Sons: London, in press.
(24) Burke, L. D.; Nugent, P. F. *Gold Bull.* **1997**, *30*, 143−53.

in the figure. Figure 1f is an XPS spectrum of gold foil after argon plasma etching. Mercury is characterized by the doublet 4f photoelectron emissions occurring at 100 and 104 eV. Since the baseline noise is approximately the same intensity in each spectrum, the relative amounts of mercury can be qualitatively compared. No chloride or oxygen was detected by XPS on any electrode after electrochemical deposition or stripping. This indicates that calomel is not adsorbed on the electrode surface.

The most striking feature in Figure 1a–e is the presence of mercury on all of these gold foil surfaces. This is significant because it indicates a difficulty in electrochemically removing mercury from gold electrodes. Qualitatively, the amount of mercury remaining on the electrodes is lowest when the potential of +1.1 V is used to strip and clean it. Possible explanations for why the potential may effect removal of residual mercury are that, at high overvoltage (≥1.5 V), oxidation of the gold surface to gold oxide may provide a barrier against further oxidation of mercury,[17] while at +0.7 V, there may not be a significant driving force for oxidation and complete removal of mercury from the gold surface, due to underpotential deposition.[25,26] The experiment at +1.1 V may represent a potential that minimizes the formation of gold oxide as it is clear that, at this potential, mercury remains even after stripping and cleaning the electrode for a period 10 times longer than the deposition time.

Bulk Electrolysis Experiments. A series of bulk electrolysis experiments were run to gain insight into the fate of mercury during deposition and stripping. In the first set of experiments, Hg^{2+} was reduced at a gold foil electrode by applying a potential of −0.3 V for 30 min using initial Hg^{2+} concentrations ranging from 35 nM to 110 μM Hg^{2+}. After deposition, the solution was removed for analysis by CVAA. Then, fresh electrolyte was introduced into the working compartment and mercury was stripped off the electrode into solution by applying an oxidizing potential of +1.0 V for 30 min. The working compartment solution was then analyzed by CVAA. A representative set of amperograms of these experiments is provided in Supporting Information, Figure B.

As expected, there is a 1:1 relationship, with a high linear correlation coefficient (0.9997), between the amount of mercury stripped, as calculated from integrated charge during stripping assuming a two-electron oxidation process, and the amount of mercury found in solution after stripping, determined by CVAA analysis.[27,28] The micrograms of mercury stripped, as measured from the current and by CVAA analysis of the solution, respectively, are listed in pairs for six separate experiments: 0.009, 0.010; 0.18, 0.16; 0.34, 0.61; 1.5, 2.6; 8.6, 8.3; and 69, 64. This provides a confirmation of the utility of the stripping procedure using Faraday's law of electrolysis, which equates integrated charge with the amount of material undergoing a redox process during electrolysis. However, there was no such correlation (0.0853) between mercury deposition, as calculated from integrated charge during deposition, and the amount of mercury in solution after stripping, determined by CVAA analysis (or calculated from integrated charge during stripping). The micrograms of mercury stripped, as measured from deposition peak (current) and in solution after stripping, respectively, are listed in pairs for six separate experiments as follows: 2.9, 0.010; 57, 0.16; 9.3, 0.61; 27, 2.6; 15, 8.3; and 8.9, 64.

This was an unexpected result, because the baseline background current (from background processes such as reduction of water or trace amounts of oxygen) was clearly well established before mercury was injected into the working compartment. Subtraction of the background current from the sample deposition current should have resulted in a relatively good correlation if there were no changes in the nature of the electrode.

In general, the integrated charge during deposition (after subtracting out background current) predicted a much greater amount of mercury was deposited than subsequently was determined to be in solution after stripping. This led us to investigate whether a significant amount of mercury was diffusing into the electrode. Previous studies have suggested mercury atoms diffuse into gold when the coverage of mercury exceeds a monolayer.[17,25] To test this possibility, we performed argon plasma etching on two electrodes that had undergone 1 and 10 deposition, stripping, and cleaning cycles, respectively (deposition of 0.02 mM Hg^{2+} at −0.3 V for 60 s followed by stripping and cleaning for 600 s at +1.0 V). XPS monitoring was done concurrently with argon plasma etching. The etching rate for both electrodes was assumed to be the same because they were analyzed under the same conditions: 1×10^{-4} mbar argon, 10 A ionization current, and 2250 V acceleration potential. After establishing the presence of mercury by XPS, the etching was started. In the time required to run an additional XPS scan (60 s), the mercury peaks had disappeared. Although the sputtering rate has not been calibrated on the UHV system that we used, the etching depth is estimated to be ~50 ± 25 Å based on published etching rates.[29] This result demonstrates that mercury did not diffuse deeply into the gold at concentrations detectable by XPS.

One way to explain the discrepancy between the deposition and stripping integrated charges is to assume that a fundamental change to the electrode occurs during deposition. Figure 2 shows results from an experiment that was designed to explore this possibility. After a baseline was established at −0.3 V, a solution containing a total of 40 ng of Hg^{2+} was injected into the solution and deposition was allowed to occur for 50 s. Thereafter, the electrolyte solution was changed; i.e., all solution forms of mercury were removed. It is clear from Figure 2 that a new baseline was established. The overall effect of a similar change in baseline during a bulk electrolysis experiment would be to overestimate the amount of current involved in the mercury reduction process. This is, in general, exactly what is observed at low mercury concentrations. The baseline shift is consistent with a change in the nature of the electrode and suggests that a gold–mercury alloy electrode forms, which has electrochemical properties very different from that of a pure gold electrode. It is interesting to note that the response of the electrode is not always the same. At higher concentrations, the baseline shift actually reverses itself, compared to what is seen in Figure 2.

Table 1 summarizes mass balance data (determined by CVAA) from the bulk electrolysis experiments performed at six different mercury concentrations from 0.035 to 110 μM. For each experi-

(25) Li, J.; Abruña, H. *J. Phys. Chem. B* **1997**, *101*, 2907–2916.
(26) Sherwood, W.; Bruckenstein, S. *J. Electrochem. Soc.* **1978**, *125*, 1098–1102.
(27) Osteryoung, J.; Stojek, Z. *Anal. Chem.* **1988**, *60*, 131–141.
(28) Tokoro, R.; Tavares, M. *Anal. Lett.* **1986**, *19*, 2079–2094.
(29) Matsunami, L. N.; Yanamura, Y.; Itikawa, Y.; Itoh, N.; Kazumata, Y.; Miyagawa, S.; Morita, K.; Shimizu R.; Tawara, H. *At. Data Nucl. Data Tables* **1984**, *31*, 1.

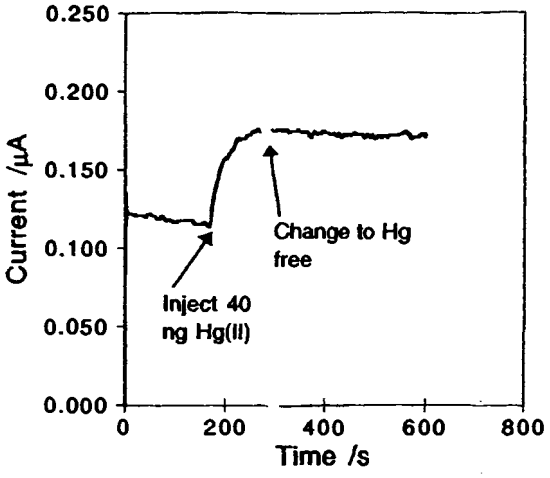

Figure 2. Amperogram before and after injection of 40 ng of Hg(II) in 18 mL of 2.5 mM KCl at pH 3 [1 × 10 $^{-6}$ M Hg(II)] after 200 s at −0.3 V vs Ag/AgCl. The break in the figure indicates the point at which the electrolyte solution was changed. Electrolysis was continued at −0.3 V in Hg(II)-free electrolyte.

Table 1. CVAA Determination of Hg (ng) in Deposition and Stripping Solutions

initial injection[a]	after deposition[b]	after stripping[c]	% recovery[d]
0.15	0.16	0.01	113
0.62	0.49	0.16	105
3.1	2.5	0.61	100
14	8.9	2.2	79
93	74	8.3	88
340	280	64	101

[a] Initial micrograms of Hg^{2+} injected into reaction chamber; final volume equaled 18 ± 0.5 mL. [b] Mercury remaining in solution after 30 min of deposition at −0.3 V. [c] Mercury in solution after stripping for 30 min at +1.0 V. [d] Percent of the mercury recovered calculated from the sum of columns 2 and 3, divided by column 1, times 100.

ment, the first column is the initial mass of mercury added to the cell. The second column is the mass of mercury in solution after deposition, and the third column is the mass of mercury in solution (starting with fresh electrolyte) after stripping and cleaning the electrode. The fourth column is the percentage of mercury recovered from solution calculated from the sum of the values in columns 2 and 3, divided by the value in column 1. Recovery averaged 98 ± 11%.

Comparison of the amount of mercury left in solution after each 30-min deposition (second column) to the amount initially added to the cell (first column) shows a significant amount of mercury remains in solution and is not deposited onto the electrode. As discussed above, it is difficult to establish the amount of mercury reduced due in part to the fundamental changes occurring at the electrode as electrolysis proceeds. However, with the exception that a different baseline is established after deposition is started, the current−time response during a 30-min bulk electrolysis experiment is typical for an electrochemical process that has gone nearly to completion (i.e., current levels out and thereafter remains unchanged). The fact that a significant amount of mercury remains in solution at the end of the deposition step suggests two possibilities; either the electrode becomes passivated during an electrolysis experiment or reduced mercury migrates into solution during the experiment. To test for passivation, an electrode used in a single 30-min deposition experiment using 4 μM Hg^{2+} solution was compared to an electrode used in five successive 30-min deposition experiments (each deposition started with fresh 4 μM Hg^{2+} solution). Although the charge passed in successive depositions was significantly diminished (Figure C, Supporting Information), the charge passed during stripping was more than 5 times (8.1 μC) that of the electrode used in the single deposition (1.3 μC). This suggests that passivation of the electrode does not occur. Migration of reduced mercury into solution remains a possibility and has been reported when dilute Hg^{2+} solutions were used to deposit mercury onto glassy carbon electrodes.[30]

Stripping Analysis of Mercury Using Gold Electrodes. As outlined in the introduction, gold electrodes offer many attractive features in stripping analysis of mercury. The present study, however, demonstrates that some of the mercury that is adsorbed during deposition is retained even after stripping and cleaning. While the concentration range of mercury used in this study was relatively high, preliminary data using mercury levels near the safe drinking water limits suggest that irreversible adsorption of mercury also occurs under these conditions.[31] Further, preliminary data also suggest that mercury accumulates on the electrode during successive cycling.[31] These results argue that, in long-term, repetitive, stripping analysis situations, the deposition, stripping, and adsorption processes need to be better understood and taken into account before the goal of developing a sensor capable of remote quantification of mercury in the environment is realized.

One attractive strategy that may be employed is to add a complimentary technique, such as a piezoelectric sensor.[1,32] The added sensor would be able to monitor mass changes at the electrode during deposition, stripping, and cleaning cycles. A piezoelectric sensor could be used to recalibrate the electrode after each stripping analysis cycle, thus overcoming some of the limitations of mercury buildup on an electrode. Another attractive feature of combining a piezoelectric sensor with electrochemical detection would be that it could offer additional ways to analyze the data. For example, mass-to-charge ratios could be used to identify analytes as they are removed from the electrode.

ACKNOWLEDGMENT

We thank Dr. Cliff Carlin for his helpful suggestions, Mike Handley and Tiffany Lindstrom, for their assistance with CVAA, and Nick Lecursi, for his assistance in the fabrication of the gold electrodes. This project has been financially supported by DOE Grant DE-FG02-94ER81717, BIODE Inc., and the University of Maine.

Received for review November 30, 1998. Accepted April 28, 1999.

AC981312B

(30) Yoshida, Z.; Kihara, S. *J. Electroanal. Chem.* **1979**, *95*, 159−168.

(31) Watson, C. M.; Dwyer, D. J.; Andle, J. C.; Bruce, A. E.; Bruce, M. R. M., unpublished results.

(32) Buttry, D. A.; Ward, M. D. *Chem. Rev.* **1992**, *92*, 1355−1379 and references therein.

APPENDIX F: PUBLISHED PAPER, IEEE SYMPOSIUM

1997 IEEE INTERNATIONAL FREQUENCY CONTROL SYMPOSIUM

Electrochemical Piezoelectric Sensors for Trace Ionic Contaminants

J. Andle, M. Schweyer, J. Munson, R. Roderick and D. McAllister, BIODE, Bangor, ME
L. French, and J. Vetelino, ECE Dept. & LaSST, U. Maine, Orono, ME
C. Watson, J. Foley, A. Bruce and M. Bruce, Dept. of Chemistry, U. Maine, Orono, ME

Abstract

Industrial processes, such as fossil fuel combustion and nuclear materials processing, have resulted in heavy metal contamination of soils and potentially of the surrounding groundwater. In particular, mercury contamination of groundwater is a serious threat to the ecosystem, cumulating in serious health problems for humans as well as wildlife. Monitoring of mercury contamination in groundwater requires a method of long-term verification. Sensors with lifetimes of months to years of operation without operator intervention are required. One sensor geometry, which is capable of detecting relevant concentrations of aqueous ionic contaminants, such as mercury, while withstanding typical environmental conditions, is the acoustic plate mode (APM) sensor. This piezoelectric sensor protects the electronics from the potentially corrosive aqueous fluid environment while providing a significant interaction with the fluid. Gold films are employed to accumulate the mercury via surface amalgamation. The added mass is measured as a change in the resonant frequency of the piezoelectric element. Electrochemical techniques are employed to impart selectivity, reversibility and to accelerate response kinetics.

Initial results indicate a sensitivity of approximately 2.4 ng/mL, which approaches the 2.0 ng/mL limit imposed by the safe drinking water act (SDWA). Research is underway to lower this detection limit to allow the sensor to meet the requirements of environmental sensing, wastewater monitoring and drinking water testing.

Introduction

The monitoring of trace ion contaminants in solution has many industrial applications. An example is the great deal of interest found relative to the detection of mercury in ground water [1]. A remote, *in situ* sensor, which is capable of selectively detecting mercury and other ionic contaminants, would provide many benefits. The continuous monitoring of environmental remediation efforts requires such a sensor, where transportation to laboratory based equipment is not feasible or cost effective.

There exist many methods to effectively analyze mercury and other heavy metal concentrations in solution, including cold vapor atomic adsorption (CVAA) [2], electrochemical quartz crystal microbalance (EQCM) techniques [3], and cyclic voltammetry techniques [4]. All of these methods have limitations in sensitivity or portability that prevent their use as the proposed sensor.

An alternative method to detect mercury in solution is the use of the shear horizontal acoustic plate mode (SHAPM) device. The SHAPM is a piezoelectric device that can detect changes in mass (among other things) as changes in velocity of the acoustic wave as the mass perturbs the surface. The advantage of the SHAPM to the QCM is the higher sensitivities obtainable. Previous results for ZX $LiNbO_3$ [5] and the temperature compensated –65° rotated Y-cut of quartz [6] SHAPM have found the SHAPM to be more sensitive than the QCM, but not sensitive enough to detect mercury levels imposed by the SDWA.

In order to increase the sensitivity of the SHAPM and to provide selectivity, electrochemical techniques have been incorporated into the SHAPM. The sensitivity is increased through the reduction and oxidation of mercury ions in a controllable fashion, and selectivity is introduced from the added variables of deposition and stripping potentials.

Theory

The choice of the piezoelectric device was based on several parameters. Since the measurements were to be performed in a fluid, only piezoelectric devices that generated predominantly shear acoustic waves could be used. This is because fluids do not propagate shear acoustic waves. Piezoelectric devices with predominately shear displacements are found in the shear horizontal surface acoustic wave (SH SAW), the QCM or thickness shear mode (TSM) device, the surface transverse wave (STW) device and the SHAPM device. Of these, the STW and the SHAPM devices appear to be the most promising [7]. Although the STW device can be used at higher frequencies and sensitivities, problems with packaging and isolation of the transducers from the fluid has yet to be solved for this application. The SHAPM is easily packaged and the electronics are completely isolated from the fluid as shown in Figure 1.

The SHAPM has acoustic waves generated from an RF signal applied to the input interdigital trans-

ducer (IDT). The shear acoustic wave is a standing wave through the thickness of the crystal, so perturbations can be detected on both sides of the piezoelectric plate. The back side of the plate is exposed to the fluid medium to isolate the IDTs from the fluid. The acoustic wave is converted back to an electrical signal at the output IDT.

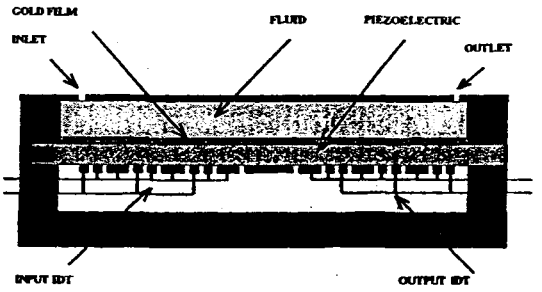

Figure 1. The packaged SHAPM consists of a piezoelectric plate, input and output IDTs, a gold film, fluid containment cell and a fluid solution.

Martin et al. [8] were the first to intentionally use the SHAPM device as a fluid phase sensor. An approximate model, based on an assumed isotropic substrate, provided significant insight into the operation of these devices. Biode has researched and compared the differences between Z-cut, X-propagating lithium niobate (ZX $LiNbO_3$) and various quartz substrates. The higher mass sensitivities of the ZX $LiNbO_3$ devices could not be employed due to the large temperature coefficient of frequency (TCF) of -70.8 ppm/°C. The family of rotated Y-cut (RYC) of quartz was mathematically searched for cuts of quartz which have a single dominant APM mode, adequate mass sensitivity and a low temperature coefficient of frequency [9]. The -65° RYC of quartz was found to satisfy these conditions, providing a single dominant mode, theoretical mass sensitivity of -0.4 ppm-mm^2/ng and a theoretical TCF approaching zero.

The incorporation of an electrochemical cell provides a method of reducing and oxidizing ions in solution upon a working electrode. A three-electrode electrochemical cell provides a method of controlling applied potentials to a working electrode while compensating for cell resistive losses, electric charge at the electrode-solution interface and dipole work functions in the solution. The three electrodes are referred to as the working, counter and reference electrodes. The counter electrode provides the potentials to the solution with respect to the working electrode. The control of the potential of the working electrode with respect to reference electrode is equivalent to controlling the energy of the electrons within the working electrode [10].

Standard reference electrodes are the saturated hydrogen electrode (SHE), the saturated calomel electrode (SCE) and the Ag-AgCl electrode. Essentially the reference electrode is a non-Faradic element or an element that has no charge transfer (zero current) over the operating range of the cell potentials.

The electrochemical cell is typically filled with an electrolyte, which lowers the potential drop of the cell. Driving the working electrode to more negative potentials raises the energy of the electrons. The electrons will eventually reach a level high enough to occupy vacant states on species in the electrolyte. The reduction current is the flow of electrons from electrode to solution. Energy of the electrons can be lowered by imposing a more positive potential to the working electrode, and at some point electrons on solutes in the electrolyte will find a more favorable energy on the electrode and will transfer there. The oxidation current is the flow of electrons from solution to the electrode.

It has been shown that different ionic contaminants have unique oxidation and reduction potentials [4]. This criterion enables the electrochemical cell to provide selectivity. The magnitude of the frequency shift of the SHAPM will provide the concentration of the solute. Therefore, the combination of the SHAPM with an electrochemical cell provides a portable sensor that can quantitatively detect trace ion contaminants and differentiate the different species in solution.

Experimental Setup

The design parameters for the SHAPM devices were engineered as fluid loaded devices operating around room temperature. The aluminum interdigital transducers were fabricated with standard photolithographic techniques. The mass sensitive film was a 1000 Å sputtered gold film. The electrochemical static fluid cell was mounted to the SHAPM using mechanical forces with a silicone gasket material to prohibit leakage. The cell was constructed from polycarbonate with feedthroughs for applying and measuring potentials to the working, counter and reference electrodes. Small inlet and outlet holes were in the fluid cell so that the electrolyte and measurand could be added and removed with standard pipettes. The SHAPM was mounted to an oscillator circuit to measure the oscillation frequency of the device.

The APM device was utilized as the feedback element of an oscillator. The oscillator was designed to require low power and have high stability. The amplifier chosen for the oscillator was the INA 12063 low noise amplifier. A potentiometer was placed in the circuit to control the overall gain of the

loop by limiting the current supplied to the amplifier. A variable capacitor was placed in the circuit to provide a tunable low pass filter to suppress harmonics and other modes of the piezoelectric device. A buffer amplifier was placed on the output of the circuit to prohibit interference and impedance loading of the measurement device to the oscillating loop. A simple emitter follower was employed as the buffer amplifier. The total power consumed by the oscillator for each SHAPM delay line was 100 mW. Note that the buffer draws half of the power of the oscillator circuit. Lowering the power dissipated by the buffer amplifier can further optimize the circuit.

The electrochemical cell was designed to ensure the volume of the fluid cell was 600 µL. The working electrode was the gold surface of the APM device. The counter and reference electrodes were 0.25 mm platinum wires. Standard reference electrodes could not be used due to the size limitations of the cell. Platinum was chosen for the electrodes because of its inherit inertness. A schematic of the electrochemical cell is shown in Figure 2.

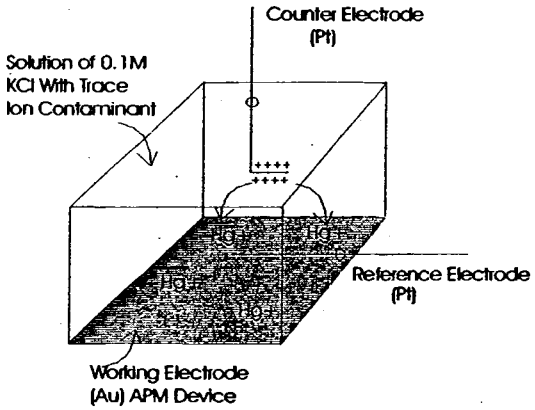

Figure 2. The electrochemical cell is mounted to the SHAPM device as a static cell. The potentials of the counter, reference and working electrodes provide the fluid kinetics and discriminate species in the electrolyte.

A 0.1 M potassium chloride (KCl) solution was used as the electrolyte. Previous attempts to use deionized water as the solution were unsatisfactory due to a large potential drop. The resistance of deionized water is approximately 18 MΩ. Groundwater typically has moderate electrolyte concentration, so no extra electrolytes are required to lower the cell resistance.

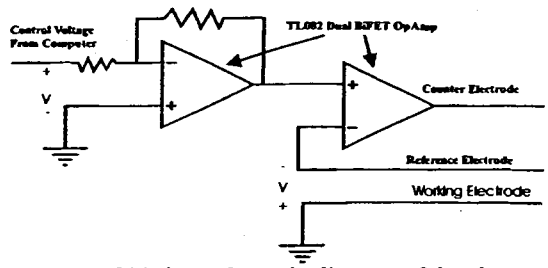

Figure 3. This is a schematic diagram of the electrochemistry circuit that provides the referenced potential to the working electrode.

A dual op-amp circuit was employed to reference the applied counter electrode voltage to the platinum reference electrode. Figure 3 is a circuit diagram of the electrochemical control circuit. The voltage applied to the first op-amp is inverted with no gain. The second op-amp provides the applied voltage between the working and the reference electrode, with the aforementioned inversion, because the reference electrode is a zero current element.

The sensor was setup as shown in Figure 4. Frequency was measured with a HP53131A frequency counter. The SHAPM devices were designed as dual delay line devices to compensate for changes in the fluid media, such as viscosity and density. The reference delay line is to be coated with a material that is inert to trace ionic materials. Self assembled monolayers (SAMs) are candidate materials for this application, but were not tested for initial responses to mercury. The frequencies of both bare delay lines were recorded with a computer employing HPIB communication between the software and the counter.

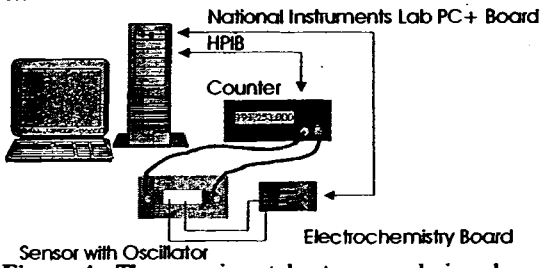

Figure 4. The experimental setup was designed using standard data acquisition techniques with a computer.

The temperature of the SHAPM was measured with a thermocouple, amplified with the AD597 thermocouple amplifier chip, and recorded with a National Instruments PC Plus data acquisition board. The data acquisition board also provided the cyclic voltage of the electrochemistry circuit and recorded the potential of the reference electrode to ensure the

board worked accurately. The potentials were ramped using software techniques with the acquisition board.

The SHAPM was measured for long time stability with the 0.1 M KCl solution with the applied electrochemistry potentials. Having satisfactorily noted that the SHAPM had no responses without any solute present, the SHAPM was dosed with 10 ng of mercury in solution. The response of the SHAPM was recorded for different cyclic potentials to observe the effect of the ramp rate of the potential and the minimum and maximum potentials reached.

Results

Results of the -65° RYC SHAPM device without an electrochemical cell are shown in Figure 5. The figure shows the difference frequency of the SHAPM with one side passivated with a hexadecyl mercaptan SAM. It is clearly seen that the difference frequency decreased 1.5 ppm with the addition of 10 ng of mercury, with a response time of 15 minutes. The volume of the fluid cell was 160 µL, yielding a concentration of 62.5 ng/mL of mercury in the fluid cell. The stability of the difference frequency of the device is measured to about 0.3 ppm, so the maximum sensitivity is about 12.5 ng/mL. This is comparable to prior results using the more sensitive but less stable $LiNbO_3$ device [5]. Additionally, the SHAPM requires regeneration with thermal or electrochemical techniques when the gold film is saturated, as seen with the second addition of mercury with no response.

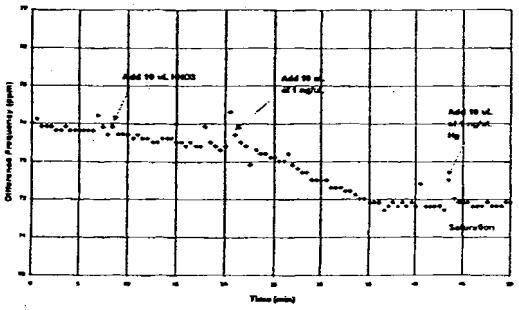

Figure 5. The SHAPM device has a 1.5 ppm difference frequency change with the addition of 10 ng of Hg. The mass sensitivity of SHAPM without electrochemistry is approximately 12.5 ng/mL.

The sensitivity and response time for the -65° RYC SHAPM was not acceptable for monitoring groundwater for concentrations in compliance with the SDWA. The electrochemical cell was attached to the SHAPM, but no passivation film was used. An experiment was run to ensure that no electrolytes affected the SHAPM at the applied electrochemical potentials. Figure 6 is the response of the SHAPM as the potentials are cycled from 0.6V to −1.5V, at a rate of 2 mV/s. Since there was no passivation film, both frequencies were monitored. Temperature of the fluid was measured with a type J thermocouple introduced into the fluid cell.

The results of the experiment show a slow frequency drift of the two delay line frequencies throughout the experiment. The temperature of the fluid in the electrochemical cell also slowly decreased during the experiment. There is a good correlation between the frequency drift and the temperature drift of approximately 5 ppm/°C. Previous experiments measuring the TCF of the -65° RYC SHAPM showed a TCF of 2 ppm/°C [9], but slight differences in metal thickness could easily change the TCF. Figure 6 has the temperature and the reference electrode potential on the same scale, so it appears that the temperature is constant, but expanding the scale shows the temperature effect clearly. The more important results of this experiment are the small responses of the frequencies that coincide with the electrochemical voltages. The 1.25 ppm spikes occur at consistent potentials throughout the experiment, but previous experiments did not show these spikes. It is the opinion of the authors that these spikes are from trace ions (i.e. lead) from the solder on the thermocouple, which was placed in the solution.

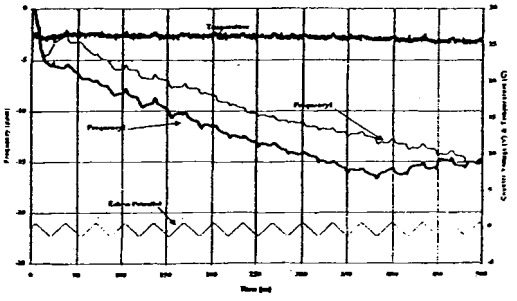

Figure 6. The two delay lines of the SHAPM have negligible response to electrochemical voltages with the absence of mercury ions.

The same device and solution from Figure 6 was used for a mercury test. Figure 7 shows the APM responses to additions of a "blank" (10 µL of KCl solution) and a mercury solution. (10 µL of 1 ng/µL mercury). The volume of the fluid cell is 600 µL, yielding a mercury solution in the fluid cell of 16.67 ng/mL.

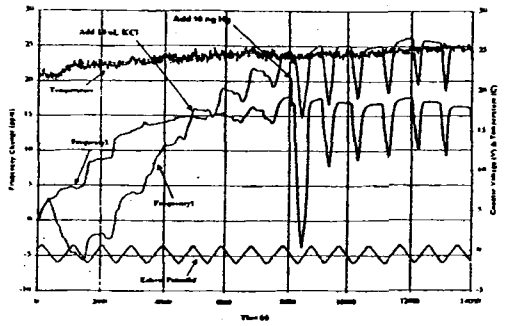

Figure 7. The oscillation frequencies of the SHAPM responded 7 ppm to 10 ng of Hg.

The oscillation frequencies of the two delay lines decrease about 7 ppm from nominal when the deposition potential is reached, and increase back to their original frequencies when the applied potential is large enough to strip the mercury from the gold electrode. The mercury is deposited at a lower potential than it is stripped. Unfortunately, the platinum reference electrode was not calibrated for the KCl solution against a standard reference electrode, so the potentials could not be compared with the potentials found in literature. Figure 8 is a graph of the oscillation frequency of one channel (frequency 2) plotted as a function of the applied potential.

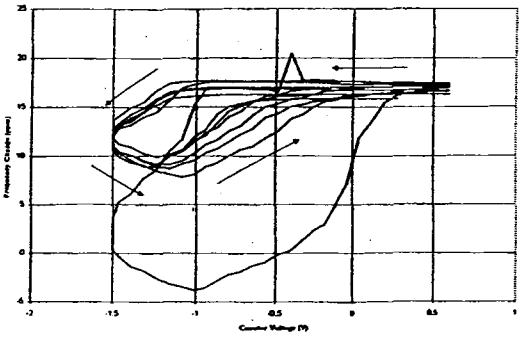

Figure 8. Oscillation frequency of quartz APM device as a function of counter voltage. Solution contains 16.62 ng/mL of elemental mercury.

The initial frequency spike is an artifact of introducing the mercury into the static cell solution. The initial device response is different from the subsequent voltage cycles for one of the two channels. The reason for this is not known by the authors and further experiments are required to understand this phenomena. This did not occur on the "identical" parallel channel.

The potential where the mercury is deposited and stripped occurs around 1.2 V referenced to the platinum reference electrode. Figure 8 demonstrates that the frequency begins decreasing at this potential and continues to decrease until the reduction potential is reached, where the frequency begins to increase to its original value. Subsequent voltammetry cycles exhibit the same frequency response. The measured response time of the APM when the proper potential is reached is about four minutes for both the deposition and stripping of mercury.

The active area of the gold film is approximately 20 mm^2, providing a surface density of 0.5 ng/mm^2. The predicted mass sensitivity of the device is –0.4 $ppm\text{-}mm^2/ng$ [9]. The predicted frequency shift for 10 ng of mercury is therefore -0.2 ppm. The 7 ppm frequency shift is 35 times the predicted frequency change. The large frequency change may be attributed to the acoustic energy trapping of the gold film, discrepancies between theoretical and actual acoustic displacements of -65° RYQ quartz, and viscoelastic changes of the gold film when mercury is absorbed. All these considerations could increase the response of the APM to absorbed trace ionic contaminants. Other effects that could increase the response of the SHAPM to the gold-mercury amalgamation are sited by Yang et al [11]. Their work shows gold clusters move into the amalgam, changing the structure of the gold film, which they detected using atomic force microscopy. The moving of the gold atoms could move the solution in contact with the film, which would yield a change in the SHAPM frequency.

Conclusions

The results indicate that the sensor is potentially capable of detecting nanogram quantities of mercury in milliliter volumes. Results obtained so far indicate a sensitivity of 2.4 ng/mL, which approaches the SDWA limit (2.0 ng/mL). The use of electrochemistry provides reversibility and potential selectivity of the sensor for many ionic contaminants.

With minor design improvements and proper packaging, the reported sensor should be capable of continuous field detection of trace ions. The size of the sensor provides easy implementation for "down well" analysis of remediation sites. Minor improvements in power requirements can offer continuous measurements from battery powered sensors.

Future Work

The experimental evaluation of the APM sensor for different ionic contaminants must be performed to confirm that the device is selective. Based on the work of Wang et al., the current sensor may be employed as the detector of several heavy metals simultaneously, including selenium, copper, and lead [4]. Incorporating neural networks into the sensor

could aid in the selectivity of the device, by measuring frequency shift versus applied potential. Finally, a microcontroller is being developed which will miniaturize the sensor circuitry for recording, interpreting, correcting and transmitting the sensor data.

Acknowledgements

The authors wish to acknowledge the support of the US Department of Energy under contract DE-FG02-94ER81717. J. Munson and R. Roderick were supported in part by a National Science Foundation Research Experience for Undergraduates (REU) program (EEC-9531738). The data and conclusions contained herein are the opinions of the authors and do not constitute the policy of the US Government.

References

1 U.S. Fish and Wildlife study reported in May 30, 1993 *Portland Sunday Telegram*, Guy Gannett Pub., Portland, ME. (Results from Terry Haines, US Fish & Wildlife Service).

2 D. H. Anderson, J. H. Evans, J. J. Murphy and W. W. White, "Determination of Mercury by a Combustion Technique Using Gold as a Collector", Anal. Chem. 43 (1971) 1511.

3 D. A. Buttry and M. D. Ward, "Measurement of Interfacial Processes at Electrode Surfaces with the Electrochemical Quartz Crystal Microbalance", Chem. Rev. 92 (1992) 1355-1379.

4 J. Wang et al., "Remote Electrochemical Sensor for Trace Metal Contaminants", Anal. Chem., 67 (1995) 1481-1485.

5 M. G. Schweyer, J. C. Andle, D. J. McAllister and J. F. Vetelino, "An Acoustic Plate Mode Sensor for Aqueous Mercury", Sensors and Actuators B 35-36 (1996) 170-175.

6 M. G. Schweyer, J. C. Andle, D. J. McAllister, L. A. French and J. F. Vetelino, "An Acoustic Plate Mode Sensor for Aqueous Mercury", IEEE Ultrasonics Symposium Proceedings, 1 (1996) 355-358.

7 J. C. Andle and J. F. Vetelino, "Acoustic Wave Based Biosensors", Invited paper, Sensors and Actuators A, 44-3 (1994) 167-176.

8 S. J. Martin, A. J. Ricco, T. M. Niemczyk and G. C. Frye, "Characterization of SH Acoustic Plate Mode Liquid Sensors", Sensors and Actuators, 20 (1989) 253-268, and ref. therein.

9 J. C. Andle, M. G. Schweyer, L. A. French and J. F. Vetelino, "Acoustic Plate Mode Properties of Rotated Y-Cut Quartz", IEEE Ultrasonic Symp. Proc., 2 (1996) 971-976.

10 A. J. Bard and L. R. Faulkner, Electrochemical Methods: Fundamentals and Applications, Wiley.

11 X. M. Yang, K. Tonami, L. A. Nagahara, K. Hashimoto, and A. Fujishima, "In-situ Observation of the Electrochemical Hg/Au Amalgam Process on an Au electrode Surface by Atomic Force Microscopy", Surface Science, 319 (1994) L17-L22.

APPENDIX G: PUBLISHED PAPER, DALTON

DALTON
FULL PAPER

Formation of separated *versus* contact ion pairs in alkali metal thiolates and selenolates

Scott Chadwick,[a] Ulrich Englich,[a] Karin Ruhlandt-Senge,*[a] Charles Watson,[b] Alice E. Bruce[b] and Mitchell R. M. Bruce*[b]

[a] *Department of Chemistry, 1-014 Center for Science and Technology, Syracuse University, Syracuse, NY 13244-4100, USA*
[b] *Department of Chemistry, University of Maine, Orono, ME 04469-5706, USA*

Received 24th January 2000, Accepted 27th April 2000
Published on the Web 14th June 2000

The solvation and ligation tendencies of alkali metal thiolates and selenolates in relation to metal and donors were investigated by synthesizing a family of target compounds, and analysing their structural features in solution and the solid state. The target compounds were synthesized utilizing hydrogen elimination, involving treatment of the chalcogenol with either sodium or potassium hydride in the presence of various donors. The separated ions were [Na(18-crown-6)(THF)$_2$][SMes*] **1**, (Mes* = 2,4,6-t$Bu_3C_6H_2$), [K(18-crown-6)(THF)$_2$][SMes*] **3**, and [K(18-crown-6)(THF)$_2$][SeMes*] **4**, and K(dibenzo-18-crown-6)(SMes*)·THF **2**, displayed potassium–sulfur contacts. Compounds **1**–**4** were characterized using X-ray crystallography, NMR and IR spectroscopy. Cyclic voltammetry studies were carried out on **1**–**3**, Na(dibenzo-18-crown-6)(SMes*) **5** and K(dibenzo-18-crown-6)(STrip)·THF **6** (Trip = 2,4,6-i$Pr_3C_6H_2$). A concentration dependent equilibrium reaction, which leads to an increase in free thiolate at higher concentrations, was observed for all complexes. NMR experiments using solutions of **5** (8.5 and 0.085 mM, THF-d_8) and trimethyl phosphate confirmed the presence of free thiolate at higher concentration.

Introduction

The concept of contact and separated ions was introduced as early as 1958 by Winstein and Robinson.[1] Since then numerous studies have been carried out, investigating the influence of cation, anion, solvent, and donors on the formation of these species. The majority of these studies focused on the investigation of organometallic compounds in conjunction with light alkali metals.[2] Many of the well studied species exhibit extended, delocalized π-systems, effectively stabilizing the negative charge residing on the carbon atom. In contrast, little work has been carried out to explore the structural chemistry of heteroatomic species, specifically those bearing a chalcogen atom.[3]

Since the ion association of the target compounds dictates the physical properties of the candidate molecules, the investigation of structural parameters in relation to metal, ligand, and donor is warranted. Critical factors in the formation of separated or contact ions are the Lewis base strength, size, and hapticity of the donor, the steric demand of the ligand, and its capacity for charge delocalization, in addition to the charge density of the metal center. The reduced capacity of simple, monodentate, heteroatomic ligands to delocalize electron density efficiently results in a reduced propensity to form separated species. Accordingly, only a small number of separated heteroatomic derivatives have been reported. Among those, pnicogen derivatives are most common, while chalcogen derivatives are more scarce.[3] To the best of our knowledge, only two structurally characterized alkali metal chalcogen derivatives have been reported [Li(12-crown-4)$_2$][SMes*][4] (Mes* = 2,4,6-t$Bu_3C_6H_2$) and [Li(12-crown-4)$_2$][TeSi($SiMe_3$)$_3$],[5] where crown ether was utilized to effect the cation–anion separation.

Our interest in the coordination chemistry of alkali metal chalcogenolates stems from their central role in organic and inorganic synthetic chemistry. One goal of our research program is to identify parameters affecting solution and solid state structural chemistry in families of alkali metal thiolates and selenolates. We report here a systematic study where the permutation of the metal and donor sheds light on the propensity of alkali metal centers to form contact or separated ions in the solid state. Described are the separated species [Na(18-crown-6)(THF)$_2$][SMes*] **1**, [K(18-crown-6)(THF)$_2$][SMes*] **3**, and [K(18-crown-6)(THF)$_2$][SeMes*] **4**, as well as K(dibenzo-18-crown-6)(SMes*)·THF **2**, displaying a bond between potassium and sulfur. Electrochemical studies were carried out to investigate whether contact or separated ions could be detected in solution since separated thiolates are expected to oxidize at lower potentials than those that form close contacts with alkali metals.

Results

Synthesis

Acid/base chemistry involving the reaction of sodium or potassium hydride with arene-thiol or -selenol was utilized for the synthesis of compounds **1**–**4** eqn. (1) where (A = Na or K; E = S

$$AH + HER + nD \longrightarrow A(ER)D_n + H_2 \qquad (1)$$

or Se; D = 18-crown-6, dibenzo-18-crown-6 or THF; R = 2,4,6-t$Bu_3C_6H_2$ or 2,4,6-i$Pr_3C_6H_2$). Hydrogen elimination reactions have been used successfully to prepare a variety of sodium and potassium chalcogenolates.[4–7] Generally, the reaction proceeds smoothly if the solubility of the alkali metal hydride is ensured by addition of a Lewis donor.

Crystallographic studies

Pertinent bond distances and angles for all compounds are given in Table 1, while Figs. 1–3 illustrate the structural principles displayed in compounds **1**–**4**. In each complex, geometrical data for the respective crown ether molecule and thiolate anion (bond distances and angles) were unexceptional

DOI: 10.1039/b000665n

Table 1 Selected bond distances (Å) and angles (°) for compounds 1–4

[Na(18-crown-6)(THF)$_2$][SMes*] 1					
Na(1)–O(1)	2.907(3)	Na(1)–O(4)	2.756(3)	Na(1)–O(7)	2.349(3)
Na(1)–O(2)	2.951(3)	Na(1)–O(5)	2.583(3)	Na(1)–O(8)	2.356(3)
Na(1)–O(3)	2.688(3)	Na(1)–O(6)	2.574(3)	S(1)–C(1)	1.761(3)
O(7)–Na(1)–O(8)	178.75(14)				
K(dibenzo-18-crown-6)(SMes*)·THF 2					
K(1)–S(1)	3.174(2)	K(1)–O(3)	2.767(4)	K(1)–O(6)	2.786(4)
K(1)–O(1)	2.815(4)	K(1)–O(4)	2.812(4)	S(1)–C(1)	1.773(5)
K(1)–O(2)	2.821(4)	K(1)–O(5)	2.826(4)		
K(1)–S(1)–C(1)	97.3(2)	S(1)–K(1)–O(4)	107.68(1)		
S(1)–K(1)–O(1)	96.00(1)	S(1)–K(1)–O(5)	93.64(1)		
S(1)–K(1)–O(2)	113.98(11)	S(1)–K(1)–O(6)	85.41(1)		
S(1)–K(1)–O(3)	116.46(1)				
[K(18-crown-6)(THF)$_2$][SMes*] 3					
K(1)–O(1)	2.819(5)	K(1)–O(4)	2.843(5)	K(1)–O(7)	2.744(8)
K(1)–O(2)	2.835(5)	K(1)–O(5)	2.740(5)	K(1)–O(8)	2.742(7)
K(1)–O(3)	2.730(6)	K(1)–O(6)	2.704(6)	S(1)–C(1)	1.742(7)
O(7)–K(1)–O(8)	172.1(3)				
[K(18-crown-6)(THF)$_2$][SeMes*] 4					
K(1)–O(1)	2.841(4)	K(1)–O(4)	2.852(3)	K(1)–O(7)	2.746(6)
K(1)–O(2)	2.837(4)	K(1)–O(5)	2.750(3)	K(1)–O(8)	2.763(5)
K(1)–O(3)	2.740(4)	K(1)–O(6)	2.717(4)	Se(1)–C(1)	1.930(4)
O(7)–K(1)–O(8)	172.8(2)				

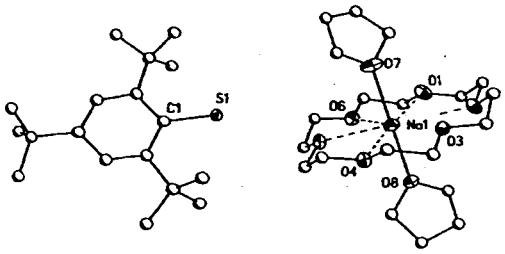

Fig. 1 Computer generated plot of compound 1 with anisotropic displacement parameters depicting 30% probability. The hydrogen atoms have been omitted for clarity.

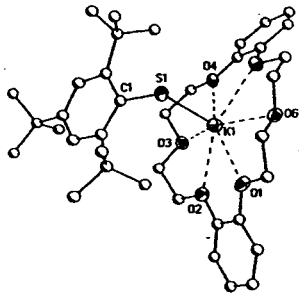

Fig. 2 Computer generated plot of compound 2. Details as in Fig. 1.

and can be found in greater detail in the deposited crystal structure data.

[Na(18-crown-6)(THF)$_2$][SMes*] 1. Compound 1 crystallizes with separated anions and cations, as illustrated in Fig. 1. The cation and anion are formally separated by a distance greater than 5.0 Å. Na(1) is eight-coordinate with six crown ether oxygen interactions and two coordinating THF molecules, oriented *trans* to one another, as evidenced by the O(7)–Na(1)–O(8) bond angle of 178.75(14)°. The Na(1)–O(crown) contacts are observed between 2.574(3) and 2.951(3) Å. The closest Na(1)–O bonding is seen for the coordinating THF molecules with values of 2.349(3) and 2.356(3) Å. In the thiolate anion the S(1)–C(1) bond length is observed at 1.761(3) Å.

K(dibenzo-18-crown-6)(SMes*)·THF 2. Compound 2, depicted in Fig. 2, crystallizes as a contact pair. K(1) is formally seven-coordinate with six crown ether contacts and one thiolato bond. The K(1)–S(1) bond distance is 3.174(2) Å, while the K(1)–O contacts range over 2.767(4)–2.826(4) Å. A narrow K(1)–S(1)–C(1) bond angle of 97.3(2)° leads to a subtle but marked orientation of the crown ether with respect to the thiolate. The S(1)–K(1)–O(3) bond angle is the widest (116.46(1)°), while the S(1)–K(1)–O(6) angle is accordingly compressed at 85.41(1)°. In the thiolate anion the S(1)–C(1) bond length is 1.773(5) Å.

[K(18-crown-6)(THF)$_2$][SMes*] 3. Compound 3 crystallizes as a separated ion pair. The overall structural motif of 3 is very similar to that of the sodium analog 1. In compound 3 the cation and anion are clearly non-interacting with a cation–anion separation of over 5.0 Å. K(1) is formally eight-coordinate with six crown ether contacts and two THF molecules, occupying *trans*-related axial coordination sites, with a O(7)–K(1)–O(8) bond angle of 172.1(3)°. The K(1)–O(crown) contacts fall in the range of 2.704(6)–2.843(5) Å, while the THF ligands interact with K(1) at 2.742(7) and 2.744(8) Å. In the arenethiolate, the S(1)–C(1) bond distance is observed at 1.742(7) Å.

[K(18-crown-6)(THF)$_2$][SeMes*] 4. Compound 4 is shown in Fig. 3. The overall structural features of 4 are very similar to those observed in 1 and 3, with a cation and anion separation of more than 5.0 Å. About the eight coordinate K(1), crown ether contacts range over 2.717(4)–2.852(3) Å, and the THF molecules interact at 2.746(6) and 2.763(5) Å. The *trans* orientation of the THF ligands is evidenced by the O(7)–K(1)–O(8) bond angle of 172.8(2)°. In the selenolate anion the Se(1)–C(1) bond distance is 1.930(4) Å.

Table 2 X-Ray ion-pairing and electrochemical parameters

Compound	X-Ray ion-pairing	Redox process (V)[a] I	II	III
1 [Na(18C6)(THF)$_2$][SMes*]	Separated	[b]	+0.24	[b]
2 [K(DB18C6)][SMes*]	Contact	−0.14	+0.25	+0.47[c]
3 [K(18C6)(THF)$_2$][SMes*]	Separated	−0.13	+0.32	[d]
5 [NaDB18C6)][SMes*]	Contact	−0.17	+0.25	+0.39[e]
6 [K(DB18C6)][STrip]	Contact	−0.07	+0.35	+0.46[f]

18C6 = 18-crown-6, DB = dibenzo. [a] Potential *vs.* Ag–AgCl. [b] Not measured. [c] $\Delta_{E_p - E_p} = 66$ mV. [d] At higher concentrations no peak was observed. [e] $\Delta_{E_p - E_p} = 144$ mV. [f] Irreversible.

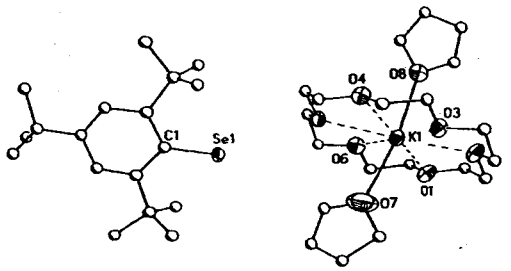

Fig. 3 Computer generated plot of compound 4. Details as in Fig. 1.

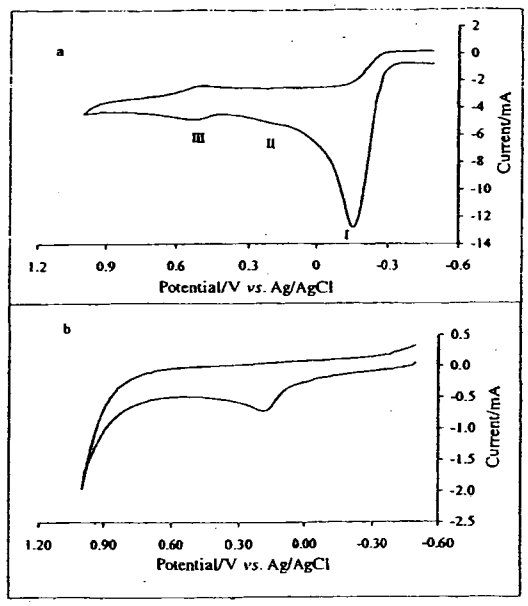

Fig. 4 Cyclic voltammograms of compound 2 at (a) 3.0 mM and at (b) 0.03 mM in 0.25 M NBu_4PF_6 in dry THF, using a 0.75 mm^2 platinum working electrode, platinum wire auxiliary electrode and a Ag–AgCl reference electrode with a scan rate of 0.1 V s^{-1}.

Cyclic voltammetry

The cyclic voltammograms of compounds **1**–**3**, Na(dibenzo-18-crown-6)(SMes*) **5**,[8] and K(dibenzo-18-crown-6)(STrip)·THF, **6** (Trip = 2,4,6-$iPr_3C_6H_2$)[6g] were studied using a polished platinum working electrode, a platinum wire auxiliary electrode, and a Ag–AgCl reference electrode (BAS M1520: 0.194 V *vs.* NHE) in THF with 0.25 M NBu_4PF_6 as supporting electrolyte. The redox data are summarized in Table 2.

Cyclic voltammetry (CV) experiments showed a dramatic effect of alkali metal thiolate concentration on the oxidation processes observed. This is illustrated in Fig. 4 for compound **2**, where CV trace (a) is for a solution that is approximately ten times more concentrated than that of trace (b) (*ca.* 3 and 0.3 mM respectively). At lower concentration only a single irreversible oxidation process occurs at *ca.* +0.2 V. At higher concentration two additional redox processes appear; an irreversible wave at *ca.* −0.15 V and a reversible or quasireversible wave at *ca.* +0.5 V (I and III respectively in Fig. 4a). The redox process I grows in at the expense of II as the concentration increases up to 5 mM. Above 5 mM no change in peak I occurs and the reaction can fully be reversed by diluting the solution with electrolyte. All of the complexes studied showed peaks corresponding to I at higher concentrations, but III was observed only for the dibenzo-18-crown-6 complexes.

Discussion

Over the last decade a small, but growing number of well characterized alkali metal chalcogenolates[4–12] has appeared in the literature. Importantly, all but two compounds have been shown by X-ray crystallography to exhibit interactions between the alkali metal cation and the Group VIB anion, namely [Li(12-crown-4)$_2$][SMes*][4] and [Li(12-crown-4)$_2$][TeSi(SiMe$_3$)$_3$],[5] where the combination of sterically demanding ligands and multidentate donor affected the cation–anion separation. Even though only limited structural work has been done, it is evident that ion separation commonly exists, specifically if bulky ligands are used in combination with multidentate donors, such as crown ethers.[13] Significantly, the formation of separated ions is often accompanied by drastic changes of physical properties, such as solubility or volatility, which can be utilized favorably in various applications.

Lithium thiolates have been intensively investigated.[6a,10] In contrast, much less is known about either (1) the heavy chalcogen congeners,[7b,11,12] or (2) the heavy alkali derivatives.[6] Remarkably, all but two of the structurally characterized alkali chalcogenolates display cation–anion interactions. In marked contrast, compounds **1**, **3** and **4** are the first structurally characterized sodium and potassium thiolates and selenolates displaying separated anions and cations. Moreover, compound **4** is a rare example of a well characterized heavy alkali metal selenolate.

The combination of a sterically encumbered thiolate or selenolate ligand with crown ether leads to contact or separated alkali-metal thiolates or selenolates. The cation–anion interaction in K(dibenzo-18-crown-6)(SMes*)·THF **2** is a result of the cup-shaped crown ether conformation in the solid state, facilitating the approach of the thiolate anion to the cation (see Fig. 2). A similar structural motif was observed in K(dibenzo-18-crown-6)(STrip)·THF **6**.[6g] Again, the cup shape of the crown ether allowed a close approach of the anion. The K–S bond length in **2** (3.174(2) Å) compares favorably with those of related potassium thiolates, such as the eight coordinate K(dibenzo-18-crown-6)(HMPA)SCPh$_3$ (3.216 Å)[6f] (HMPA = hexamethylphosphoramide), K(dibenzo-18-crown-6)(THF)(STrip) (3.202 Å),[6g] or the pseudo eight-coordinate K(dibenzo-18-crown-6)(C_6H_6)(SCPh$_3$) (3.135 Å, CN = 7 + arene), where a weak arene–metal interaction is filling the coordination void in the cup-shaped face of the crown ether.[6f]

The structural outcome changes dramatically if 18-crown-6 is employed, and the separated derivatives **1**, **3** and **4** are observed. The three compounds are structurally very similar, featuring eight-coordinate sodium (**1**) or potassium (**3**, **4**) cations with 18-crown-6 in the equatorial plane and two THF molecules in axial positions in addition to a separated thiolate (**1**, **3**) or selenolate (**4**) anion. The coordination of THF and 18-crown-6 about sodium or potassium has been recognized earlier as favorable for these metals.[14]

In contrast to the contact pair **2**, the almost planar solid-state conformation of 18-crown-6 prohibits the approach of the sterically demanding EMes* ligand (E = S or Se) to the cation, favoring the coordination of two THF donors. This result may be compared to that of K(18-crown-6)(TeTrip), displaying a cation–anion interaction of 3.499(1) Å.[7a] Apparently, the increased size of tellurium, as compared to sulfur or selenium, results in decreased effective ligand bulk, and the approach of the sterically encumbered tellurolate ligand becomes possible, despite the in-plane orientation of the crown ether. This result may also be compared with those for two magnesium thiolates, where the steric bulk of the ligand affected the formation of either contact or separated ions.[13c] Use of the sterically demanding SMes* in combination with 15-crown-5 and THF yielded the separated $[Mg(15\text{-crown-5})(THF)_2][SMes^*]_2$, while the smaller $SCPh_3$ anion forms bonds with magnesium, as observed in $Mg(15\text{-crown-5})(SCPh_3)_2$.

Cyclic voltammetry experiments and thiolate trapping studies

Cyclic voltammetry experiments were conducted on compounds **1–3**, **5**, and **6** to determine if a correlation exists between the oxidation potential of alkali metal thiolates and the nature of the solid state metal–sulfur interaction as revealed by crystallographic studies. Free thiolates, such as PhS^-, undergo oxidation near 0 V (*vs.* SCE), followed by a very fast dimerization step, with rate constants in the range of 2×10^8 to 2×10^{10} M^{-1} s^{-1}.[15,16] In contrast, thiolates bonded to metals usually oxidize at higher potentials and are thus 'protected' by coordination to a metal. For example, in linear phosphine gold(I) thiolate complexes an irreversible sulfur-based oxidation process is observed at potentials above +0.5 V (*vs.* SCE)[17] and a magnesium complex with bridging thiolates, $Mg(py)_3(\mu\text{-}SPh)_3\text{-}Mg(\mu\text{-}SPh)_3Mg(py)_3$, shows only an irreversible oxidation at +0.975 mV (*vs.* Ag–AgCl).[18]

As noted in the Results section, the concentration dependence of the cyclic voltammetry experiments is striking. Although this precludes making conclusions about a correlation between peak potential and the degree of ion pairing, it reveals a dynamic and complex process occurring in solution.[19] At low concentrations (0.1–0.3 mM) a single, irreversible wave is observed for all compounds studied. Although minor differences were observed in wave shape and potential, Fig. 4b (complex **2**) is representative of the data set. To consider what type of oxidation process is involved in wave II, it is useful to recognize that **2** is composed of three parts: (a) dibenzo-18-crown-6, (b) K^+, and (c) $[SMes^*]^-$. The oxidation of free dibenzo-18-crown-6 and alkali metal–dibenzo-18-crown-6 compounds has electrochemically been investigated by cyclic voltammetry.[20] No oxidation process is observed if the potential is kept below +1.5 V (*vs.* SCE).[16] These observations strongly suggest that peak II has a significant contribution from the SMes* ligand connected to the alkali metal cation. In comparison to $Au(PPh_3)(SC_6H_4CH_3\text{-}p)$, which oxidizes at +0.56 V (*vs.* SCE), **2** oxidizes at *ca.* +0.2 (*vs.* Ag–AgCl).[17] This is reasonable since the more covalently bound gold thiolate is expected better to 'protect' the thiolate ligand from oxidation.

At higher concentrations (0.5–17 mM) a significant change is observed in the wave shapes for all compounds studied. In Fig. 4a (complex **2**) a new irreversible oxidation process appears, labeled I. Savéant and co-workers investigated the potentials for the oxidation of *para*-substituted arenethiolates and found a linear correlation between oxidation potential and the Hammett σ coefficient of the *para* substituent group.[15] Extrapolation of their data,[21] using Hammett σ coefficients from Jaffé,[22] leads to an estimation of the oxidation potentials for $[SMes^*]^-$ and $[STrip]^-$ as −0.16 and −0.11 V (*vs.* SCE), respectively.[21,22] For all of the SMes* compounds studied, peak I occurred in the narrow range of -0.17 ± 0.03 V (*vs.* Ag–AgCl), suggesting that it represents the oxidation of "free" thiolate ligands in solution. Consistent with this are CV experiments on concentrated solutions of **6**, containing *i*-Pr rather than *t*-Bu substituents on the thiolate. These show peak I occurring at −0.07 V, *ca.* 80 mV more positive than peak I for **2**.

Further verification that separated thiolate forms at higher concentration was provided by thiolate trapping experiments using trimethyl phosphate.[23a] This reagent is rapidly demethylated by nucleophilic thiolates according to eqn. (2). An 8.5 mM

$$SR^- + (CH_3O)_3PO \longrightarrow CH_3SR + [(CH_3O)_2PO_2]^- \quad (2)$$

solution of compound **5** in THF-d_8 was treated with approximately 1 molar equivalent of $(CH_3O)_3PO$. The ^1H NMR spectrum, recorded within 4 minutes, showed a new peak at δ 2.1 which is assigned to the SCH_3 resonance, CH_3SMes^*.[23b] In contrast, a 0.085 mM solution of Na(dibenzo-18-crown-6)(SMes*) does not react with an excess of $(CH_3O)_3PO$ after 5 hours. These experiments are consistent with the cyclic voltammetry studies which suggest that separated thiolate is formed at higher concentrations.

A possible explanation for the unusual formation of separated ions at higher concentration [in contrast to the well established behavior of electrolytes where dissociation decreases as concentration increases] involves either additional solvation of the alkali metal crown ether thiolate compounds, or the establishment of an equilibrium where as the concentration is increased two or more complexes react with release of free thiolate. The mechanistic details are unknown at this time. However, at higher concentration most of the oxidation current originates in I and only a trace of process II is observed. (The peak current for I in Fig. 4a is about 20 times greater than II in Fig. 4b.) Thus, as the concentration is increased formation of separated thiolate is fairly complete by 5 mM.

Fig. 4(a) also shows a reversible or quasi-reversible redox couple labeled III at *ca.* +0.5 V. This couple appears in cyclic voltammograms of alkali metal thiolate compounds containing dibenzo-18-crown-6 ethers, but not for the 18-crown-6 compound tested (**3**), suggesting that III forms as a result of the redox reactivity of the dibenzo moiety.[20,24]

Observations and conclusions

The synthesis and characterization of a family of sodium and potassium thiolates and selenolates shows that small changes (use of 18-crown-6 instead of dibenzo-18-crown-6) affects the ion pairing in the solid state. The arguments seem to be mainly based on steric reasons: dibenzo-18-crown-6 adopts a cup-shaped arrangement, allowing the approach of the sterically demanding ligand. In contrast, 18-crown-6 exhibits an almost planar orientation, with consequent steric repulsion between the ligand and the crown ether, and ion separation with formation of $[A(18\text{-crown-6})(THF)_2][EMes^*]$ (A = Na or K; E = S or Se). Cyclic voltammetry experiments indicate that some degree of ion pairing occurs for all complexes in solution at low concentration. At higher concentrations, separated thiolate forms as a result of solvation processes or the establishment of an equilibrium where two or more complexes react with formation of free thiolate. The release of thiolate was confirmed for **5** by treating concentrated solutions of the alkali metal thiolate with $(CH_3O)_3PO$, a thiolate trapping reagent.

Experimental

General procedures

All reactions were performed under a purified nitrogen atmosphere by using modified Schlenk techniques and/or a dry box. n-Hexane and tetrahydrofuran (THF) for synthetic purposes were distilled prior to use from a Na/K alloy followed by two freeze–pump–thaw cycles. THF for electrochemical studies was

distilled over sodium–benzophenone. Trimethyl phosphate, $(CH_3O)_3PO$, was purchased from Aldrich and used as received. Commercially available 18-crown-6 was dissolved in freshly distilled diethyl ether and stirred with finely cut sodium metal for one day. After filtration from the metal, the crown was recrystallized at −20 °C and used as isolated. Dibenzo-18-crown-6 was kept at 50 °C in vacuum for several hours. Mineral oil suspensions of NaH and KH were each washed repeatedly with freshly distilled hexane and dried under vacuum. HSMes* and HSeMes* were prepared utilizing literature procedures.[17,25,26] Commercially available (98%) tetrabutylammonium hexafluorophosphate was used as received. ^1H and ^{13}C NMR spectra were recorded on Bruker DPX-300 and Varian Gemini 300 spectrometers, infrared spectra as Nujol mulls between KBr plates on a Perkin-Elmer PE 1600 FT-IR spectrometer. Elemental analysis was precluded by the high moisture sensitivity of the compounds reported. In addition, thiolates tend to give notoriously unreliable elemental analyses due to the formation of non-volatile metal sulfides.

Procedure for the synthesis of compounds 1–4

A 100 mL Schlenk flask was charged with NaH or KH, crown ether and HSMes*. Approximately 25 mL of THF were added, resulting in the evolution of H_2. The homogeneous reaction mixture was stirred at room temperature for one hour then filtered through a Celite padded frit.

[Na(18-crown-6)(THF)$_2$][SMes*] 1. 0.03 g (1.0 mmol) NaH, 0.26 g (1.0 mmol) 18-crown-6, 0.28 g (1.0 mmol) of HSMes*, 25 mL THF, and 5 mL hexane. Cooling to 0 °C for several days yielded colorless crystals in 27% yield (0.19 g). The white powder decomposed to a brown oil above 200 °C. ^1H NMR (THF-d_8): δ 6.90 (s, 2 H), 3.55 (s, 24 H), 1.73 (s, 18 H) and 1.20 (s, 9 H). ^{13}C-{^1H} NMR (THF-d_8): δ 159.49, 149.70, 135.11, 119.79, 70.93, 39.36, 35.02, 32.69 and 31.75. IR (cm^{-1}) (Nujol): 2934s, 1463s, 1377s, 1352s, 1283m, 1244m, 1210w, 1186w, 1111s, 1059m, 1044m, 969s, 914m, 874w, 846m, 758w, 722w and 616w.

K(dibenzo-18-crown-6)(SMes*)·THF 2. 0.04 g (1.0 mmol) KH, 0.36 g (1.0 mmol) dibenzo-18-crown-6, 0.28 g (1.0 mmol) HSMes*, and 20 mL THF. Pale tan solution, stirring at room temperature for one hour, heated briefly to reflux, immediate filtration through a Celite padded frit. Colorless crystals after cooling to 0 °C in 61% yield (0.48 g). The white powder decomposed to a brown oil above 220 °C. ^1H NMR (THF-d_8): δ 7.02 (s, 2 H), 6.95–6.84 (doublet m, 8 H), 4.13 (broad d, 8 H), 4.02 (broad d, 8 H), 1.72 (s, 18 H) and 1.25 (s, 9 H). ^{13}C-{^1H} NMR (THF-d_8): δ 156.40, 150.16, 148.41, 136.52, 127.72, 120.06, 111.92, 69.72, 68.22, 39.13, 34.93, 32.48 and 31.64. IR (cm^{-1}) (NaCl, Nujol): 2915s, 1592m, 1504s, 1455s, 1377s, 1340w, 1321m, 1284w, 1247s, 1209s, 1124s, 1066s, 944s, 914m, 871w, 854w, 775m and 748s.

[K(18-crown-6)(THF)$_2$][SMes*] 3. 0.04 g (1.0 mmol) KH, 0.26 g (1.0 mmol) 18-crown-6, 0.28 g (1.0 mmol) of HSMes*, and 20 mL of THF. Formation of a clear, pale tan mixture. Stirring for one hour at room temperature, brief heating, filtration through a Celite padded frit. Addition of 5 mL hexane, reduction of volume to 5 mL under vacuum. Cooling to 0 °C for several days yielded colorless crystals in 63% yield (0.46 g). The white powder decomposed to a light brown solid above 255 °C. ^1H NMR (THF-d_8): δ 6.95 (s, 2 H), 3.60 (s, 24 H), 1.76 (s, 18 H) and 1.22 (s, 9 H). ^{13}C-{^1H} NMR (THF-d_8): δ 157.50, 149.55, 135.82, 119.80, 71.09, 39.15, 34.88, 32.47, 31.71. IR (cm^{-1}) (Nujol): 2857s, 1591w, 1463s, 1376s, 1350s, 1283m, 1247m, 1155m, 1107s, 1045s, 965s, 838m, 722w, 618w, 530w and 492w.

[K(18-crown-6)(THF)$_2$][SeMes*] 4. 0.04 g (1.0 mmol) KH, 0.26 g (1.0 mmol) 18-crown-6, 0.33 g (1.0 mmol) freshly prepared HSeMes*, 20 mL THF, homogeneous yellow solution. Addition of 10 mL of hexane, reduction of volume under vacuum. Cooling to 0 °C, clear crystals within several days in 43% yield (0.33 g). The yellow powder decomposed to a brown solid above 230 °C. ^1H NMR (THF-d_8): δ 6.94 (s, 2 H), 3.55 (s, 24 H), 1.77 (s, 18 H) and 1.19 (s, 9 H). ^{13}C-{^1H} NMR (THF-d_8): δ 152.19, 146.58, 140.31, 119.91, 71.12, 40.12, 35.03, 32.47 and 32.25. IR (cm^{-1}) (Nujol): 3040w, 1585w, 1524w, 1462s, 1379s, 1344s, 1282s, 1248s, 1213m, 1110s, 1006s, 951s, 875m, 834s, 738s, 627w, 572w, 531w and 476w.

Electrochemical studies

In a VAC model HE-493 dry-box, 1 to 40 mg of crown ether metal thiolate was added to 6 mL of 0.25 M NBu_4PF_6 in THF. Cyclic voltammetry experiments were conducted on these solutions with an EG&G model 273 potentiostat/galvanostat interfaced with a Micron 75 MHz Powerstation using EG&G's m270 software. A 2 mm^2 platinum disc working electrode, polished with 1.0 μm water-soluble diamond suspension (Buehler) on a Buehler microcloth, with a 0.5 mm platinum wire coiled parallel to the working electrode at a distance of 4 mm and a Ag–AgCl reference electrode (BAS # MF 2063) were employed. The working electrode was polished between each experiment, and the other electrodes and the cell were rinsed thoroughly with distilled, dry THF. Cyclic voltammograms of ferrocene and the electrolyte solution were taken under the same conditions to assure that the cell was in working order.

Thiolate trapping studies

In the VAC model HE-493 dry-box, two solutions were prepared by dissolving 5 ± 1 mg (a) and a trace (b) of Na(dibenzo-18-crown-6)(SMes*), respectively, in 0.85 mL THF-d_8 (Aldrich 99.99% dry, sealed under nitrogen). The concentration of the first solution (a) was 8.5 mM. The concentration of the dilute solution (b) was estimated to be 0.085 mM on the basis of integration of the crown ether protons relative to an internal standard added to each tube. These solutions were transferred to 5 mm NMR tubes and sealed with rubber septa. In air, 10 μL trimethyl phosphate was diluted in 0.85 mL THF-d_8 to which 10 μL tetramethylsilane had been added. This resulted in a solution where 10 μL contained 1 μmol trimethyl phosphate (TMP). The tubes containing the crown ether complexes were removed from the dry-box and 60 and 10 μL of the TMP reagent solution were injected into the concentrated and dilute solutions, respectively. The ^1H NMR spectra were recorded within minutes.

X-Ray crystallographic studies

X-Ray quality crystals for all compounds were grown as described. The crystals were placed on the diffractometer as described earlier.[27] Data sets for compounds 2 and 4 were collected using a Rigaku AFC5S diffractometer equipped with a Molecular Structure Corporation low temperature device and graphite monochromated Mo-Kα radiation (λ = 0.71073 Å). Three standard reflections were measured every 150 and showed in both cases only statistical variation of the intensity (<1.5%). The intensities were corrected for Lorentz and polarization effects; extinction was disregarded. An absorption correction was applied using semi-empirical psi scans. The intensity data set for compound 1 was collected on a Siemens P4 diffractometer equipped with a locally modified Enraf Nonius low temperature device using graphite monochromated Mo-Kα radiation (λ = 0.71073 Å). Data for 3 were collected using a Siemens R3m/V rotating anode equipped with a locally modified Siemens LT 2 low temperature device, utilizing Ni-filtered Cu-Kα radiation (λ = 1.54178 Å). Absorption

Table 3 Crystallographic data for compounds **1–4**

Compound	1	2	3	4
Formula	$C_{38}H_{69}NaO_8S$	$C_{42}H_{61}KO_7S$	$C_{38}H_{69}KO_8S$	$C_{38}H_{69}KO_8Se$
M	708.98	749.07	725.09	771.99
Crystal system	Monoclinic	Triclinic	Monoclinic	Monoclinic
Space group	$P2_1/n$	$P\bar{1}$	$P2_1/n$	$P2(1)/n$
a/Å	10.598(3)	10.029(2)	10.680(5)	10.778(2)
b/Å	16.124(6)	13.819(3)	16.110(1)	16.129(3)
c/Å	24.430(8)	15.207(3)	24.857(1)	25.169(5)
α/°		92.41(3)		
β/°	92.41(3)	91.39(3)	92.72(4)	93.60(3)
γ/°		106.17(3)		
V/Å^3	4171(2)	2021.0(7)	4272(4)	4366.7(14)
Z	4	2	4	4
μ/mm^{-1}	0.133	0.231	1.897	0.998
T/K	126	213	213	213
Independent reflections	7768	4973	4865	7674
Observed reflections (>2σ)	4511	2775	3214	4424
$R1$, $wR2$ (all data)	0.1277, 0.1687	0.1509, 0.1945	0.1471, 0.2788	0.1350, 0.1578
(>2σ)	0.0654, 0.1332	0.0642, 0.1554	0.0999, 0.2416	0.0575, 0.1280

corrections for compounds **1** and **3** were performed with the program XABS2.[28] The crystal structures of all compounds were solved by direct methods and refined by full-matrix least squares on F^2 (SHELXL).[29] Hydrogen atoms were placed geometrically and refined using a riding model. All non-hydrogen atoms, with the exception of some disordered or restrained positions, were refined anisotropically. Disorder was handled by including split positions for the affected groups, and included the refinement of the respective occupancies. A set of restraints was applied to aid in the modeling. Crystallographic parameters for compounds **1–4** are summarized in Table 3.

CCDC reference number 186/1966.

See http://www.rsc.org/suppdata/dt/b0/b000665n/ for crystallographic files in .cif format.

Acknowledgements

This work was supported by Syracuse University, the University of Maine, the National Science Foundation (CHE-97-02246), and the Deutsche Forschungsgemeinschaft (Postdoctoral stipend for U. E.).

References

1 S. Winstein and G. C. Robinson, *J. Am. Chem. Soc.*, 1958, **80**, 169.
2 See for example: E. Weiss, *Angew. Chem., Int. Ed. Engl.*, 1993, **32**, 1501 and references therein.
3 P. P. Power, *Acc. Chem. Res.*, 1988, **21**, 147 and references therein; F. Pauer and P. P. Power, in *Lithium Chemistry, A Theoretical and Experimental Overview*, eds. A.-M. Sapse and P. v. R. Schleyer, Wiley, New York, 1995, p. 295.
4 K. Ruhlandt-Senge, U. Englich, M. O. Senge and S. Chadwick, *Inorg. Chem.*, 1996, **35**, 5820.
5 P. J. Bonasia, D. E. Gindelberger, B. O. Dabbousi and J. Arnold, *J. Am. Chem. Soc.*, 1992, **114**, 5209.
6 See for example: (*a*) S. Brooker, F. T. Edelmann, T. Kottke, H. W. Roesky, G. M. Sheldrick, D. Stalke and K. H. Whitmire, *J. Chem. Soc., Chem. Commun.*, 1991, 144; (*b*) A. M. Z. Slawin, J. Ward, D. J. Williams and D. Woollins, *J. Chem. Soc., Chem. Commun.*, 1994, 421; (*c*) D. J. Rose, Y. D. Chang, Q. Chen, P. B. Kettler and J. Zubieta, *Inorg. Chem.*, 1995, **34**, 3973; (*d*) M. Niemeyer and P. P. Power, *Inorg. Chem.*, 1996, **35**, 7264; (*e*) K. Ruhlandt-Senge and U. Englich, *Chem. Commun.*, 1996, 147; (*f*) S. Chadwick, U. Englich and K. Ruhlandt-Senge, *Organometallics*, 1997, **16**, 5792; (*g*) U. Englich, S. Chadwick and K. Ruhlandt-Senge, *Inorg. Chem.*, 1998, **37**, 283; (*h*) S. Chadwick and K. Ruhlandt-Senge, *Chem. Eur. J.*, 1998, **4**, 1768.
7 P. J. Bonasia and J. Arnold, (*a*) *J. Chem. Soc., Chem. Commun.*, 1990, 1299; (*b*) *J. Organomet. Chem.*, 1993, **449**, 147.
8 K. Chadwick and K. Ruhlandt-Senge, unpublished results.
9 See for example: Z. Hou and Y. Wakatsuki, *Chem. Eur. J.*, 1997, **3**, 1005; M. G. Stanton and M. R. Gagné, *J. Am. Chem. Soc.*, 1997, **119**, 5075; Z. Hou, A. Fujita, H. Yamazaki and Y. Wakatsuki, *J. Am. Chem. Soc.*, 1996, **118**, 2503; F. M. Mackenzie and R. E. Mulvey, *J. Am. Chem. Soc.*, 1996, **118**, 4721; K. W. Henderson, D. S. Walther and P. G. Williard, *J. Am. Chem. Soc.*, 1995, **117**, 8680; P. A. van der Schaaf, M. P. Hogerheide, D. M. Grove, A. L. Spek and G. van Koten, *J. Chem. Soc., Chem. Commun.*, 1992, 1703; M. Veith, *Chem. Rev.*, 1990, **90**, 3; K. G. Caulton and L. G. Hubert-Pfalzgraf, *Chem. Rev.*, 1990, **90**, 969.
10 Lithium thiolates: S. C. Ball, I. Cragg-Hine, M. G. Davidson, R. P. Davies, P. Raithby and R. Snaith, *Chem. Commun.*, 1996, 1581; S. C. Ball, I. Cragg-Hine, M. G. Davidson, R. P. Davies, A. J. Edwards, I. Lopez-Solera, P. R. Raithby and R. Snaith, *Angew. Chem., Int. Ed. Engl.*, 1995, **34**, 921; D. R. Armstrong, D. Barr, P. R. Raithby, R. Snaith, D. S. Wright and P. v. R. Schleyer, *Inorg. Chim. Acta*, 1991, **185**, 163; D. R. Armstrong, R. E. Mulvey, D. Barr, R. W. Porter, P. R. Raithby, T. R. E. Simpson, R. Snaith, D. S. Wright, K. Gregory and P. Mikulcik, *J. Chem. Soc., Dalton Trans.*, 1991, 765; D. Barr, P. R. Raithby, P. v. R. Schleyer, R. Snaith and D. S. Wright, *J. Chem. Soc., Chem. Commun.*, 1990, 643; D. R. Armstrong, R. E. Mulvey, D. Barr, R. Snaith, D. S. Wright, W. Clegg and S. M. Hodgson, *J. Organomet. Chem.*, 1989, **362**, C1; D. Barr, M. J. Doyle, R. E. Mulvey, R. P. Raithby, R. Snaith and D. S. Wright, *J. Chem. Soc., Chem. Commun.*, 1988, 145; D. R. Armstrong, A. J. Banister, W. Clegg and W. R. Gill, *J. Chem. Soc., Chem. Commun.*, 1986, 1672.
11 Lithium selenolates: (*a*) T. Nothegger, K. Wurst, M. Probst and F. Sladky, *Chem. Ber.*, 1997, **130**, 119; (*b*) D. V. Khasnis, M. Buretea, T. J. Emge and J. G. Brennan, *J. Chem. Soc., Dalton Trans.*, 1995, 45; (*c*) K. Flick, P. J. Bonasia, D. E. Gindelberger, J. E. B. Katari and D. Schwartz, *Acta Crystallogr., Sect. C*, 1994, **50**, 674; (*d*) K. Ruhlandt-Senge and P. P. Power, *Inorg. Chem.*, 1993, **32**, 4505; (*e*) W. W. Du Mont, S. Kubiniok, L. Lange, S. Pohl, W. Saak and I. Wagner, *Chem. Ber.*, 1991, **124**, 1315; (*f*) K. Ruhlandt-Senge and P. P. Power, *Inorg. Chem.*, 1991, **30**, 3683.
12 Lithium tellurolates: (*a*) P. J. Bonasia, V. Christou and J. Arnold, *J. Am. Chem. Soc.*, 1993, **115**, 6777; (*c*) P. J. Bonasia, D. E. Gindelberger, B. O. Dabbousi and J. Arnold, *J. Am. Chem. Soc.*, 1992, **114**, 5209; (*d*) G. Becker, K. W. Klinkhammer, S. Lartiges, P. Böttcher and W. Pohl, *Z. Anorg. Allg. Chem.*, 1992, **613**, 7; (*e*) G. Becker, K. W. Klinkhammer and W. Massa, *Z. Anorg. Allg. Chem.*, 1993, **619**, 628.
13 This was shown with the closely related alkaline-earth derivatives: (*a*) S. Chadwick, U. Englich, B. Noll and K. Ruhlandt-Senge, *Inorg. Chem.*, 1998, **37**, 4718; (*b*) S. Chadwick, U. Englich and K. Ruhlandt-Senge, *Chem. Commun.*, 1998, 2149; (*c*) S. Chadwick, U. Englich and K. Ruhlandt-Senge, *Inorg. Chem.*, 1999, **38**, 6289.
14 See for example, sodium compounds: L. M. Engelhard, W.-P. Leung, C. L. Raston and A. H. White, *J. Chem. Soc., Chem. Commun.*, 1983, 383; D. J. Darensbourg, C. G. Bauch and A. L. Rheingold, *Inorg. Chem.*, 1987, **26**, 977; H. Bock, T. Hauck, C. Näther and Z. Havlas, *Z. Naturforsch., Teil B*, 1994, **49**, 1012; D. R. Tueting, M. M. Olmstead and N. E. Schore, *Organometallics*, 1992, **11**, 2236; potassium compounds, T. A. Budzichowski, M. H. Chisholm, J. C. Huffmann and O. Eisenstein, *Angew. Chem., Int. Ed. Engl.*, 1994, **33**, 191; W. J. Gribsby and P. P. Power, *Chem. Eur. J.*, 1997, **3**, 368; F. Paul, F. Carmichael, C. Ricard and F. Mathey, *Angew. Chem., Int. Ed. Engl.*, 1996, **35**, 1125.

15 C. P. Andrieux, P. Hapiot, J. Pinson and J.-M. Savéant, *J. Am. Chem. Soc.*, 1993, **115**, 7783.
16 The SCE reference electrode is within 50 mV of the Ag–AgCl reference electrode used in this study. Thus these reference scales are very similar.
17 T. Jiang, G. Wei, C. Turmel, A. E. Bruce and M. R. M. Bruce, *Metal Based Drugs*, 1994, **1**, 419.
18 S. Chadwick, U. Englich, M. O. Senge, B. C. Noll and K. Ruhlandt-Senge, *Organometallics*, 1998, **17**, 3077; S. Chadwick, K. Ruhlandt-Senge, C. Watson, A. E. Bruce and M. R. M. Bruce, unpublished results.
19 Conductivity measurements were made as a function of concentration in an attempt to determine the extent of ion pairing. All complexes were weak electrolytes and molar conductivities were calculated to infinite dilution. The conductivity results, Λ_oS cm mol^{-1}, were as follows with the X-ray ion-pairing characterization in parentheses: [K(18C6)(THF)$_2$][SMes*] **3** (separated), 5.8×10^6; [K(DB18C6)][SMes*] **2** (contact), 4.0×10^6; [Na(DB18C6)][SMes*] **5** (contact), 3.4×10^6; [K(DB18C6)][STrip] **6** (contact), 3.4×10^6. This trend suggests a correlation between conductivity and ion pairing. However, the concentration dependent process complicated the measurements and we caution that more extensive measurements are needed before a correlation between conductivity and solution molecular structure can be considered valid.
20 V. Le Berre, L. Angely, N. Simonet-Gueguen and J. Simonet, *Nouv. J. Chim.*, 1985, **9**, 419; *J. Electroanal. Chem., Interfacial Electrochem.*, 1986, **206**, 115; C. Belloncle, P. Cauliez and J. Simonet, *J. Electroanal. Chem., Interfacial Electrochem.*, 1998, **444**, 101.
21 The extrapolation assumed that Hammett coefficients were additive.
22 H. H. Jaffé, *Chem. Rev.*, 1953, 191; C. Hansch and A. Leo, *Substituent Constants for Correlation Analysis in Chemistry and Biology*, Wiley, New York, 1979, pp. 1; M. T. Tribble and J. G. Traynham, *J. Am. Chem. Soc.*, 1969, **91**, 379; M. Charton, *J. Org. Chem.*, 1971, **36**, 266; *J. Am. Chem. Soc.*, 1969, **91**, 6649.
23 (*a*) J. J. Wilker, K. E. Wetterhahn and S. J. Lippard, *Inorg. Chem.*, 1997, **36**, 2079; (*b*) R. M. Silverstein, C. G. Bassler and T. C. Morill, *Spectrometric Identification of Organic Compounds*, 5th edn., John Wiley, New York, 1991.
24 Anodic polymerization of dibenzo-18-crown-6 and alkali metal–dibenzo-18-crown-6 compounds produces a reversible couple at *ca.* +1.0 V (see reference 20). Process III occurs *ca.* 500 mV lower than this, perhaps as a result of the presence of thiolate anions or radicals in solution. In addition, the current intensity of III did not increase when the CV experiment was allowed to continue for 50 cycles with stirring of the solution every fifth cycle, which suggests that if polymerization of dibenzo-18-crown-6 is responsible for III the polymer does not build up at the electrode surface.
25 J. M. A. Baas, H. van Bekkum, M. A. Hofnagel and B. M. Wepster, *Recl. Trav. Chim. Pays-Bas*, 1969, **88**, 1110; W. Rundel, *Chem. Ber.*, 1968, **101**, 2956.
26 W. W. Du Mont, S. Kubinock, L. Lange, S. Pohl, W. Saak and I. Wagner, *Chem. Ber.*, 1991, **124**, 1315.
27 H. Hope, *Prog. Inorg. Chem.*, 1994, **41**, 1.
28 S. R. Parkin, B. Moezzi and H. Hope, XABS2: An empirical absorption correction program, *J. Appl. Crystallogr.*, 1995, **28**, 53.
29 G. M. Sheldrick, SHELXTL PLUS, Program for crystal stucture solution and refinement, University of Göttingen, 1993.

BIOGRAPHY

Charles Martin Watson was born in Salmon, Idaho, of the United States of America, on February 14, 1965. From there the route has been circuitous. Before high school Charles never attended the same school more than two years in a row. He attended Flathead High School in Kalispell, MT, where he was quite active on the speech and debate team. During high school he worked as a mechanic and supported himself during his last year there 1982-83. After working as a hod carrier and mason for 2 years Charles went to Montana State University, in Bozeman, MT, where he earned his Bachelor of Science degree in Chemistry on December 15, 1990. At Montana State University Charles conducted natural products research with Dr. John H. Cardellina III and Dr. Larry L. Jackson. He also chaired the overseeing committee for the Student Health Service and produced and hosted part-time a weekly community issues "Talk Radio" program on KGLT 92 FM.

Charles joined the Peace Corps in June 1991, and spent two years teaching physics, chemistry and math at the College D'Enseignement Secondaire in Gamba, Gabon. Charles was also hired as a consultant to Shell Gabon in 1992 and 1993 to perform a laboratory audit of their "oil field chemistry" laboratory. After teaching in Gamba, Charles worked for the Gabonese Ministry of Education as a Didactic Counselor. During that time Charles compiled, designed and wrote a book of experiments, depicting the concepts in the French Physical Science Secondary Education Program using materials that could be found in the households and markets throughout Gabon. Charles was also a teacher trainer for the Ministry of Education until August 1995. It was in Gabon, where Charles met his wife, Armelle.

Charles' application to the University of Maine, Department of Chemistry's Doctoral Program was looked upon favorably in August 1995 — as there was an opening when a student belatedly withdrew — so he came to Orono, ME, a mere 10 days after leaving Gabon. Charles selected to work with Dr. Mitchell R. M. Bruce and Dr. Daniel J. Dwyer on the mercury gold research project featured in this thesis. As a graduate student Charles was active in the lab, the department and on campus. Charles presented his research at two National ACS conferences (1998, 1999) and two Gordon Research Conferences (Water and Surfaces: 1997; Electrodeposition, 1998). Charles organized the department graduate students to formally talk about their research, arranged for them to attend the Wesleyan Spring Colloquium in 1997. Charles was a member of graduate student government and was the President of the Association of Graduate Students in 1998/99. As president he developed and initiated a University-wide graduate research exposition. That activity continues to this day. Although very busy and productive as a graduate student in chemistry, Charles, wife and 9 month old daughter Lucinda, left the University of Maine in, July 1999, to attend medical school at the University of New England College of Osteopathic Medicine.

Three years, nine months and one more child later (Abbegael), Charles has completed the requirements for his Doctor of Osteopathy, medical degree. He is a 2nd Lieutenant in the US Army and will be a Captain in the general surgery residency program at William Beaumont Army Medical Center upon graduation in June 2003. Charles is now back at the University of Maine Department of Chemistry, for the completion and defense of his doctoral thesis. The following are a list of his publications:

Chadwick, Scott; Englich, Ulrich; Ruhlandt-Senge, Karin; Watson, Charles; Bruce, Alice E.; Bruce, Mitchell R. M.. Formation of separated versus contact ion pairs in alkali metal thiolates and selenolates. Dalton (2000), (13), 2167-2173.

Watson, Charles M.; Dwyer, Daniel J.; Andle, Jeffrey C.; Bruce, Alice E.; Bruce, Mitchell R. M.. Stripping Analyses of Mercury Using Gold Electrodes: Irreversible Adsorption of Mercury. Analytical Chemistry (1999), 71(15), 3181-3186.

French, Lester A.; Schweyer, Michael G.; Foley, Janet B.; Andle, Jeffrey C.; Watson, Charles; Bruce, Mitchell R. M.; Bruce, Alice E.; Vetelino, John F. Heavy metal detection combining stripping electrochemistry and piezoelectric sensor technology. Proceedings of SPIE-The International Society for Optical Engineering (1998), 3539(Chemical Microsensors and Applications), 161-169.

Andle, J.; Schweyer, M.; Munson, J.; Roderick, R.; Mcallister, D.; French, L.; Vetelino, J.; Watson, C.; Foley, J.; Bruce, A.; Bruce, M.. Electrochemical piezoelectric sensors for trace ionic contaminants. Proceedings of the IEEE International Frequency Control Symposium (1997), 51st 90-95.

Watson, Charles M. and Reddick, Lisa "Science Sans Labo", UNESCO, Libreville, 1994, 42 pp.

Watson, Charles M. and Davidson, Colin J., Sécurité dans la Manipulation des Produits Chimiques du Shell Gabon", Shell Gabon, Port Gentil, 1993, 121 pp.

Charles Martin Watson is a candidate for the Doctor of Philosophy degree in Chemistry from The University of Maine in May, 2003.